Ana Filipa Fernandes Vaz Portugal

Carbon Dioxide Removal from Anaesthetic Gas Circuits Using Absorbent Membrane Contactors

Dissertation presented for the degree of

Doctor of Philosophy in Chemical and Biological Engineering

by

University of Porto

Supervisors:

Adélio Miguel Magalhães Mendes

Fernão Domingos de Montenegro Baptista Malheiro de Magalhães

LEPAE – Chemical Engineering Department
Faculty of Engineering
University of Porto

Porto, February 2009

Acknowledgements

I would like to express my gratitude to the Portuguese Foundation for Science and Technology (FCT) for the PhD grant, reference SFRH/BD/16621/2004 and for the financial support through the project POCTI/EQU/45182/2002. I am also grateful to the European commission for the project Growth GRD1-2001-40257.

My acknowledgments go to my supervisors Prof. Adélio Mendes and Prof. Fernão de Magalhães for giving me the opportunity and conditions to perform the present work, for the scientific suggestions and recommendations and for the trust and encouragement.

I am grateful to everybody from the OOIP group, in the Netherlands for the hospitality, for the generosity on sharing their knowledge and for their skilled technical support. Special thanks to Peter and Prof. Geert Versteeg - your teachings were essential for the proceeding of this work. Thanks very much also to the true friends I made there which never hesitate to aid me whenever I needed!

My gratitude goes also to my colleagues from the lab for their help and contribution to the present work, for their support and, of course, for standing me singing or complaining during my experimental work.

I would like to expand this acknowledgement to the staff of LEPAE (spetially LEPAE/AMP) and of the Chemical Engineering department at FEUP for their kindness and assistance.

Thanks very much to the people from E319 for the counsels and encouragement and above all, for the good humour and friendship extended far beyond labour time... you provided the best working environment I could ever find!

Thanks to all my friends; those which helped me with fruitful discussions and recommendations, those with whom I've shared my PhD quotidian, and those which, even when not directly related to this task, made me keep the necessary confidence and

good mood to move further. Special thanks to Tiago and his family who was also my family during a significant part of this process.

For their unconditional support and for being so very special, I would like to acknowledge my family. Particularly, I thank my aunts Maria Luisa Portugal Basílio, on the subject “Carbon dioxide capture and sequestration”, Ana Portugal Crespo de Carvalho, on the subject “Anaesthesia”, and Ana Paula Vaz Fernandes, on the subject “How to deal with a PhD”.

Finally, always above all and above everything, thanks to my closest family: my Father, my Mother and André, for supporting, for believing, for being this amazing example that I am so proud of... for all possible reasons. Anything or any me would ever be possible without you!!!

Preface

The present work was carried out at the Laboratory of Processes, Environmental and Energy Engineering (LEPAE), in the Chemical Engineering Department of the Facu.lty of Engineering – University of Porto (FEUP), between 2003 and 2009, under the framework of the projects POCTI/EQU/45182/2002 (funded by the *Fundação para a Ciência e Tecnoologia*) and European Growth Project GRD1-2001-40257 – SpecSep (funded by the European Commission). This thesis contains different papers that were written and published or submitted for publication in international journals during the development of the PhD work.

Contents

Part III

Part IV

Figure Captions

Table Captions

Abstract

The present dissertation concerns the study of hollow fiber absorbent membrane contactors and their application for carbon dioxide removal from anaesthetic closed breathing circuits.

Carbon dioxide removal from closed anaesthetic circuits is currently achieved using canisters containing mixtures of alkali hydroxides. However, the volatile anaesthetics react exothermally with these absorbents, generating potentially harmful products such as carbon monoxide and compound A; besides, the exhausted canisters are contaminated hospital waste, dangerous and expensive to treat. This work proposes to contribute for the development of a safer and more environmentally friendly technology for carbon dioxide removal, based on membrane contactors using regenerable absorbent solutions. These solutions should be able to absorb carbon dioxide fast and reversibly when it is present in low concentrations (carbon dioxide concentration must be reduced from 5 to 0.5 % in an anaesthesia loop).

Although hollow fiber absorbent membrane contactors have been widely used and studied for carbon dioxide absorption purposes, there are two main difficulties that must be overcome to make them suitable for the suggested application. Firstly, dense membranes are necessary (instead of the porous membranes generally used in these devices) to avoid the transmission of pathogenic microorganisms from the breathing circuit to the absorbent solution. Additionally, new absorbent solutions need to be developed, since the ones commonly used (aqueous solutions of alkanolamines) undergo oxidative degradation in highly oxygenated environments, originating toxic compounds. The present dissertation is predominantly focussed on the latter problem.

Aqueous solutions of amino acid salts overcome some of the drawbacks associated to the use of alkanolamines. Among the available alkali salts of amino acids, potassium glycinate was chosen as a model for the subsequent studies, since glycine is the simplest amino acid and it has a relatively low cost. Additionally, the molecular structure of potassium glycinate indicates that high absorption kinetics towards carbon dioxide might be expected. Potassium salt of threonine was also studied for comparison and because its molecular structure envisioned better regeneration properties.

In order to estimate the diffusion coefficients of both carbon dioxide and amino acid salt, densities and viscosities of potassium glycinate and potassium threonate aqueous solutions were experimentally measured. The physical solubility of carbon dioxide in aqueous solution was determined based on the nitrous oxide analogy. Therefore, the solubility of this gas in aqueous solutions was experimentally obtained.

The kinetics of the reactions of carbon dioxide with potassium glycinate and potassium threonate were determined using a stirred reactor with a flat gas-liquid interface. The results were interpreted using the DeCoursey approach and an expression for the rate of absorption as a function of temperature and solution concentration was derived for each amino acid salt, based on the zwitterion reaction mechanism. It was observed that potassium glycinate absorbs carbon dioxide faster than potassium threonate and, for both amino acid salts, the absorption rate is strongly dependent on the solution ionic strength.

Solubility of carbon dioxide in potassium glycinate aqueous solutions was determined in a stirred reactor at different temperatures, amino acid salt concentrations and carbon dioxide partial pressures. Absorption equilibrium data was further interpreted using the Deshmukh-Mather and the Kent-Eisenberg models. For potassium threonate, the carbon dioxide solubility was also measured, but for a limited set of conditions. This amino acid salt showed lower absorption capacity than potassium glycinate.

A bi-dimensional model was developed to evaluate the carbon dioxide removal performance of a hollow fiber membrane contactor. The model considered potassium glycinate solutions as absorbents and a composite membrane, made of a porous support layer and a dense thin layer. Both co- and counter-current operations were analysed. The influence of some system parameters on the separation achieved was studied.

The use of hollow fiber absorbent membrane contactors with amino acid salt solutions was found to be suitable for carbon dioxide removal from closed anaesthetic breathing circuits.

Sumário

A presente dissertação versa sobre o estudo de contactores absorvedores de membranas de fibras ocas e sua aplicação na remoção de dióxido de carbono de circuitos anestésicos fechados.

A remoção de dióxido de carbono de circuitos anestésicos fechados é correntemente levada a cabo usando recipientes contendo misturas de hidróxidos alcalinos. No entanto, os compostos voláteis anestésicos reagem exotermicamente com estes absorventes formando produtos potencialmente perigosos como o monóxido de carbono e o composto A. Adicionalmente, depois de saturados, os recipientes são lixo sólido hospitalar contaminado que requer tratamentos caros e perigosos. Pretende-se que este trabalho contribua para o desenvolvimento de uma tecnologia mais segura e amiga do ambiente para a remoção de dióxido de carbono, baseada no uso de contactores de membrana com soluções absorventes recicláveis. Estas soluções devem conseguir remover o dióxido de carbono rápida e reversivelmente, quando este se encontra pouco concentrado na corrente gasosa (a concentração de dióxido de carbono deve ser reduzida de 5 para 0.5 % em cada ciclo anestésico).

Apesar dos contactores de membranas de fibras ocas terem sido vastamente estudados e utilizados com o propósito de absorver dióxido de carbono, duas limitações essenciais têm que ser ultrapassadas para que estes se tornem adequados para a aplicação sugerida. Em primeiro lugar, são necessárias membranas densas (em vez das membranas porosas habitualmente utilizadas nestas unidades) de modo a evitar a transmissão de micro organismos patogénicos do circuito respiratório para a solução absorvente. Adicionalmente, é necessário que novas soluções absorventes sejam desenvolvidas, uma vez que, as geralmente usadas (soluções aquosas de alcanolaminas) oxidam em ambientes muito oxigenados, originando compostos tóxicos. A presente dissertação foca-se predominantemente neste último problema.

As soluções aquosas de sais de aminoácidos superam algumas das limitações associadas ao uso de alcanolaminas. De entre os sais alcalinos de aminoácidos, o glicinato de potássio foi escolhido como modelo para um estudo mais aprofundado porque a glicina é o aminoácido mais simples e tem um custo relativamente baixo. Adicionalmente, a

estrutura molecular do glicinato de potássio indica que elevadas cinéticas de absorção do dióxido de carbono são espectáveis. O treonato de potássio foi também estudado para comparação e porque a sua estrutura molecular fazia prever maior regenerabilidade.

Com o propósito de estimar os coeficientes de difusão do dióxido de carbono e do sal de aminoácido, foram medidas experimentalmente a densidade e viscosidade de soluções aquosas de glicinato de potássio e treonato de potássio. A solubilidade física do dióxido de carbono nas soluções aquosas foi determinada através da analogia com o protóxido de azoto. Para tal, a solubilidade deste gás nas soluções aquosas foi obtida experimentalmente.

As cinéticas da reacção do dióxido de carbono com o glicinato de potássio e o treonato de potássio foram determinadas num reactor agitado com uma interface gás-líquido plana. Interpretaram-se os resultados através da aproximação de DeCoursey e, para cada sal de aminoácido, foi derivada uma expressão relacionando a velocidade de absorção com a temperatura e a concentração da solução, baseada no mecanismo de zwitterion. Observou-se que o glicinato de potássio absorve dióxido de carbono mais depressa do que o treonato de potássio e que, para ambos os sais, a velocidade de absorção é fortemente dependente da força iónica da solução.

A solubilidade do dióxido de carbono em soluções aquosas de glicinato de potássio foi medida num reactor agitado para diferentes temperaturas, concentrações de sal de aminoácido e pressões parciais de dióxido de carbono. Os resultados do equilíbrio de absorção foram seguidamente interpretados usando os modelos de Deshmukh-Mather e de Kent-Eisenberg. A solubilidade do dióxido de carbono em treonato de potássio foi também medida, mas para um conjunto de condições limitado. Este sal de aminoácido apresentou menor capacidade de absorção do dióxido de carbono que o glicinato de potássio.

Foi desenvolvido um modelo bidimensional para avaliar o desempenho na remoção de dióxido de carbono de um contactor de membranas de fibras ocas. No modelo, consideraram-se soluções de glicinato de potássio como absorventes e uma membrana compósita, constituída por uma camada de suporte poroso e uma fina camada densa.

Operações em co- e contra corrente foram analisadas. Estudou-se a influência de alguns parâmetros do sistema na separação conseguida.

Concluiu-se que os contactores absorvedores de membranas de fibras ocas são uma tecnologia viável para remover dióxido de carbono de circuitos anestésicos fechados.

Résumé

Ce travail se penche sur l'étude des contacteurs absorbeurs de membranes de fibres creuses et son application dans l'extraction du dioxyde de carbone dans les circuits fermés d'anesthésie.

L'extraction du dioxyde de carbone dans les circuits anesthésiques fermés est mise en œuvre à l'aide de récipients contenant des mélanges d'hydroxydes alcalins. Cependant, les composés volatiles anesthésiques ont une réaction exothermique avec ces absorbants provocant la formation des produits dangereux comme le monoxyde de carbone et le composant A. De plus, après saturation, les récipients utilisés se transforment en déchet toxique, qui demande un traitement cher et dangereux. L'objectif de cette étude est de contribuer au développent d'une technologie plus sécurisée et respectueuse de l'environnement pour l'extraction du dioxyde de carbone, basé sur l'utilisation des contacteurs de membrane avec des préparations d'absorbants recyclables. Ces préparations devront permettre d'extraire le dioxyde de carbone d'une façon rapide et réversible, lorsque le dioxyde de carbone est présent dans le gaz à faible concentrations (la concentration de dioxyde de carbone doit être réduite de 5 à 0.5% par cycle anesthésique).

Bien que les contacteurs de membranes de fibres vides aient déjà largement été étudiés et utilisés pour l'extraction du dioxyde de carbone, il reste deux principales contraintes à résoudre pour cette application. Premièrement, il est nécessaire d'utiliser des membranes denses (au lieu des membranes poreuses généralement utilisées dans ces outils) afin d'éviter la transmission de micro-organismes pathogènes du circuit de respiration aux préparations absorbantes. Deuxièmement, il reste à développer de nouvelles préparations absorbantes, vu que celles actuellement utilisées (solutions aqueuses d'alkanolamines) subissent une dégradation oxydative en milieu particulièrement oxygénés, provoquant l'apparition de composés toxiques. Cette étude se concentre principalement sur cette deuxième contrainte.

Des solutions de sels d'acides aminés permettent de dépasser les limites associées à l'utilisation des alkanolamines. Parmi les sels alcalins d'acides aminés disponibles, le

glycinate de potassium a été choisie comme modèle pour cette étude, car la glycine est l'acide aminé le plus simple et a un prix raisonnable. De plus, la structure du glycinate de potassium montre que l'on peut s'attendre à des cinétiques d'absorption du dioxyde de carbone élevées. Nous avons étudié également le sel de potassium de thréonine, pour comparaison d'une part, et du fait que sa structure moléculaire présentait de meilleurs propriétés de régénération.

Afin d'estimer les coefficients de diffusion aussi bien du dioxyde de carbone que des sels d'acides aminés, nous avons mesuré expérimentalement les densités et les viscosités du glycinate de potassium et du thréonate de potassium. Nous avons déterminé la solubilité physique du dioxyde de carbone en solution aqueuse par analogie avec le protoxyde d'azote. Ce faisant, la solubilité de ce gaz en solution aqueuse a été obtenu expérimentalement.

Nous avons déterminé les cinétiques de réaction du dioxyde de carbone avec le glycinate de potassium et le thréonate de potassium grâce à un réacteur à agitation avec une interface gaz-liquide. Les résultats ont été interprétés par une approche DeCoursey et, pour chacun des acides aminés, nous avons dérivé une équation mettant en relation la vitesse d'absorption en fonction de la température et de la concentration de la solution, en nous basant sur un mécanisme de réaction zwiterrienne. Nous avons observé que le glycinate de potassium absorbe le dioxyde de carbone plus rapidement que le thréonate de potassium, et que, pour les deux sels d'acides aminés, le taux d'absorption est particulièrement dépendant de la force ionique de la solution.

La solubilité du dioxyde de carbone dans une solution aqueuse de glycinate de potassium a été déterminée dan un réacteur à agitation à températures, concentrations d'acides aminés et pressions partielles de dioxyde de carbone différentes. Les données d'équilibre d'absorption ont été interprétées par les modèles de Deshmukh-Mather et de Kent-Eisenberg. Pour le thréonate de potassium, la solubilité du dioxyde de carbone a également été mesurée, mais avec des combinaisons de conditions limitées. Cet acide aminé a montré des capacités d'absorption plus faibles que le glycinate de potassium.

Un modèle bidimensionnel a été développé afin d'évaluer les performances d'extraction du dioxyde de carbone par un contacteur de membrane à fibres creuses. Ce modèle

prend en compte le glycinate de potassium en tant qu'absorbant et une membrane composite, obtenue par superposition de couches support poreuses et une fine couche dense. Nous avons analysé aussi bien les co- et contre-courants, ainsi que l'influence de certains systèmes de paramètres sur la séparation obtenue.

En conclusion, l'utilisation de contacteurs de membrane à fibres creuses avec des solutions de sels d'acides aminés s'est révélé être adaptée à l'extraction du dioxyde de carbone dans les circuits fermés de respiration d'anesthésie.

Part I

1. Introduction

The present dissertation aims to study a novel technology for carbon dioxide (CO_2) removal from anaesthetic closed breathing circuits. The viability of using hollow fiber absorbent membrane contactors for this application is analysed and new absorbent liquids are studied.

1.1. Anaesthesia

General anaesthesia is a technique to bring and keep the patient unconscious by the administrations of drugs which can be provided intravenously or by inhalation (Brandi, 2008; Pontes, 2006). General anaesthesia provides analgesia (absence of pain), amnesia (no memory), and muscle relaxation (Brandi, 2008). Apart from the heart, all the patient body muscles become relaxed and therefore breathing must be externally induced.

During general anaesthesia, the patient is continuously ventilated with a gaseous mixture typically composed of, approximately, 70 % carrier gas - usually nitrous oxide (N_2O) or air, 30 % oxygen (O_2) and 1 to 8 % volatile anaesthetic (Mendes, 2000; Pontes, 2006). The volatile anaesthetics currently used are halogenated compounds such as halothane, enflurane, isoflurane, desfluorane and sevofluorane being the latter two the most widely used nowadays (Pontes, 2006; Whalen et al., 2005).

The anaesthetic gas mixture can be delivered to the patient in open or closed breathing circuits and most of the anaesthetic machines can work using both circuits and switch between them. In the open breathing circuit, fresh gas is transferred to the patient and there is no recycling of the expired gases. This system results in high fresh gas flows - minimum of 5 $L \cdot min^{-1}$ (Dosch, 2004) – and it is commonly used for initializing the anaesthesia. Closed breathing circuit (also called low flow anaesthesia) consists in leading the expired air, containing the unused anaesthetic gases, back to the patient in the subsequent inhalation (Baum and Woehlck, 2003). Since the halogenated volatile anaesthetics are expensive substances, their waste must be kept as low as possible. In addition, N_2O and the halogenated compounds are potentially green house gases and their release into the atmosphere should be minimized (Dingley et al., 1999; Pontes,

2006). These reasons make the closed breathing circuit the desirable anaesthetic arrangement. However, the gaseous current coming out from the patient contains an excess of CO_2 (around 5 %) resulting from the patient breathing and an excess of N_2 (around 3 %) that was dissolved in the body tissues and is released during anaesthesia due to the lower N_2 concentration in the inhaled gas, that need to be removed and replaced by fresh anaesthetic gas before carry the mixture back again to the patient (Mendes, 2000). In routine clinical practice, the excess of N_2 is eliminated by periodically venting the system (Pontes, 2006; Reinelt et al., 2001) and the CO_2 removal is currently achieved using soda lime (a mixture of calcium, potassium and sodium hydroxides and water) or baralyme^{TM} (a mixture of calcium, potassium and octahydrated barium hydroxides) (Baum and Woehlck, 2003).

When Franz Kuhn first described a closed breathing circuit, in 1906, he raised concerns about the potential harmful products resulting from the reaction of the volatile anaesthetics with the CO_2 absorbent (Baum and Woehlck, 2003). Compounds used for anaesthesia substantially changed since then, however these concerns are still a reality nowadays (Baum and Woehlck, 2003; Fan et al., 2008; Knolle and Gilly, 2000; Whalen et al., 2005). Actually, all volatile anaesthetics react with conventional CO_2 absorbents when these become accidentally desiccated (Baum and Woehlck, 2003; Fan et al., 2008; Knolle and Gilly, 2000; Whalen et al., 2005). Even when CO_2 absorbents are properly hydrated undesirable products are eventually formed during long time surgeries (longer than four hours), although much less severe consequences are expected under this conditions (Baum and Woehlck, 2003; Fan et al., 2008).

The volatile anaesthetic sevofluorane reacts with soda lime, especially during low flow anaesthesia, generating, among others, the so called compound A - fluoromethyl-2,2-difluoro-1-(trifluoromethyl)vinyl ether) - a potentially nephrotoxic compound (Baum and Woehlck, 2003; Whalen et al., 2005). Carbon monoxide (CO) can be also generated, especially when desfluorane is used (Baum and Woehlck, 2003; Fan et al., 2008; Whalen et al., 2005). Besides the highly toxics compound A and CO, a number of other degradation products can be formed upon the contact of the volatile anaesthetic agents and the desiccated CO_2 absorbents. These include methanol and formaldehyde

and other flammable gases not yet identified (Baum and Woehlck, 2003; Marini et al., 2007). Considering the extreme heat produced in these reactions, there is a possibility of ignition of these gases during the anaesthesia (Baum and Woehlck, 2003). To overcome these drawbacks, a number of less reactive absorbents have been developed and some – including DragerSorb Free™, Amsorb™, LoFloSorb™ and Superia™ - present good results concerning the generation of harmful reaction products even under desiccation conditions (Baum and Woehlck, 2003; Marini et al., 2007; Murray et al., 1999; Struys et al., 2004). However, these less reactive absorbents enable lower utilization times than common soda lime, under comparable clinical conditions (Baum and Woehlck, 2003).

Besides the potentially harmful health effects, the environmental impact and the costs of using the present technology for CO_2 removal from anaesthetic gas circuits must be taken into account. The exhausted CO_2 absorbents are hospital solid waste, dangerous and expensive to treat (Mendes, 2000). Usually, one canister of 1.5 L of absorbent is enough to absorb CO_2 over one week. However, the exhaustion of the absorbent may occur before this period (Baum and Woehlck, 2003). For this reason, it would be desirable to replace common CO_2 absorbents by a safer but also cleaner technology.

Chemical absorption in liquid solutions is a proven and established technology to perform CO_2 separation from a variety of gas mixtures present in chemical process industry (Idem and Tontiwachwuthikul, 2006; Ma'mun et al., 2007). A wide number of studies related to the use of hollow fiber membrane contactors for CO_2 separation have been performed in the past few years (Al-Marzouqi et al., 2008; Kumar et al., 2002a; Li and Chen, 2005; Rangwala, 1996; Yan et al., 2007). The process showed promising results and is being implemented by several companies (Kumar, 2002).

In the present work the use of a hollow fiber absorbent membrane contactor for continuous CO_2 removal from anaesthetic gas circuits is proposed and its feasibility studied. The membrane material used is considered dense (non-porous) and highly permeable to CO_2, isolating the absorbent solution from the anaesthetic closed circuit. After going through the CO_2 absorption contactor, the absorbent solution is regenerated in another contactor and sent back to the absorption contactor.

1.2. Hollow Fiber Absorbent Membrane Contactors

A membrane contactor is a device to bring in contact two different phases, for mass transfer purposes, without dispersion of one phase into the other (Gabelman and Hwang, 1999).

Porous membrane modules for gas absorption have been explored and successfully used since 1975, when the technology was first proposed for blood oxygenators (Kumar, 2002) - nowadays, 99 % of the blood oxygenators sold in U. S. contain porous membranes (Wickramasinghe et al., 2005). Many other application can be find such as aeration of water in river and wastewater treatment plants, biological waste gas treatment, removal of volatile organic compounds from water, aeration of shear-sensitive cell cultures, aeration of reactors at high oxygen demand, removal of dissolved oxygen in ultrapure water production, gas exchange in artificial gills, CO_2 removal from industrial gaseous streams, etc. (Vladisavljevic, 1999).

Usually, in a gas-liquid hollow fiber membrane contactor, the liquid flows inside the fibers lumen and the gas flows in the shell (Li and Chen, 2005). The driving force for the mass transfer is the concentration gradient between gas and liquid phases (Kumar, 2002; Li and Chen, 2005) and the process of mass transfer includes the following steps: diffusion from the bulk of the gas to the outer membrane surface, diffusion trough the membrane, dissolution in the liquid and diffusion accompanied (or not) by chemical reaction in the liquid (Li and Chen, 2005).The selectivity is commonly provided by the liquid and the membrane works as an interface between two media, although is possible to use selective membranes (Li and Chen, 2005). A schematic representation of a hollow fiber in a gas liquid membrane contactor for CO_2 removal is shown in Figure 1.1.

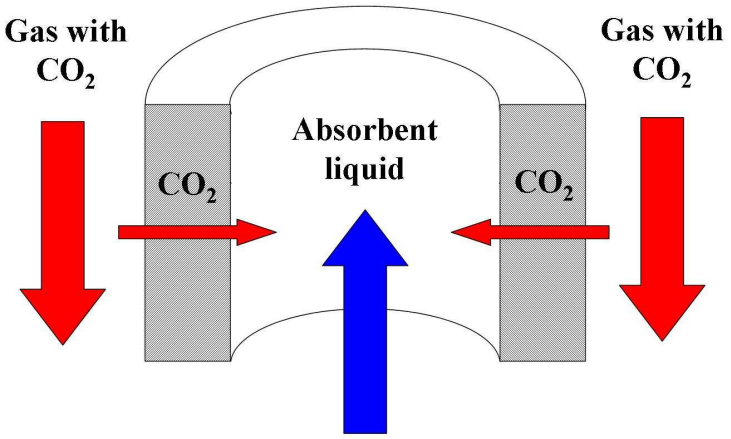

Figure 1.1 – Schematic representation of the CO_2 mass transfer in a hollow fiber.

Membrane contactors, and particularly hollow fiber membrane contactors, offer a number of advantages when compared to traditional gas/liquid contactor devices such as packed tower, spray tower, bubble column or venturi scrubber (among others) (Gabelman and Hwang, 1999; Kumar, 2002; Li and Chen, 2005; Rangwala, 1996):

- Much larger contact area per unit volume - hollow fiber membrane contactors can provide interfacial areas per unit volume around thirty times higher than other types of contactors. Besides, since the two fluids flow independently, this surface area does not depend on operational conditions such as the fluids flow rates.
- Because of the absence of interpenetration of the gaseous and liquid phases, these apparatus do not present operational limitations like flooding, channeling, entrainment, loading, weeping and foaming.
- Membrane modules can be linearly scaled up and, due to its modularity, different separation capacities can be achieved by simply changing the number of modules used and the contactor orientation is also not a matter of concern.
- Since membrane modules are compact, they are less energy consuming, and need lower volumes to achieve identical separations being very interesting in an economical point of view. They are also light on weight which makes them easy to be transported and used for offshore applications.
- Aseptic operation is much easier to achieve than with other types of contactors, which enables the process to be suitable for medical applications.

Hollow fiber membrane contactors have also some disadvantages (Gabelman and Hwang, 1999; Kumar, 2002; Li and Chen, 2005; Rangwala, 1996):

- Due to the small diameter of fibers, the liquid flow inside the fibers is usually laminar. As a consequence, the mass transfer coefficient is lower than in other types of contactors. The membrane itself also provides an additional resistance to the mass transfer.
- If the membranes to be used are porous, it must be assured that the pores are gas filled during the mass transfer process. If the membrane is wetted, the mass transfer is greatly penalized due to the presence of a stagnant liquid film in the membrane pores.
- Membranes are subject to fouling and they have a finite life time, which makes necessary to change the modules from time to time.
- There is pressure drop along the module.

The use of hollow fiber membrane contactors for CO_2 removal was first proposed by Zhang and Cussler (1985a, 1985b) (Li and Chen, 2005) and since then a lot of research on this particular application have been performed. This tremendous investment is due to the role of separating the CO_2 from flue gas for further sequestration (Idem and Tontiwachwuthikul, 2006; Metz et al., 2005). The climate change due to the greenhouse gases concentrations in the atmosphere is probably the most concerning environmental problem at the present. CO_2 is the greenhouse gas released in larger extend by anthropogenic action (Idem and Tontiwachwuthikul, 2006; UNFCCC, 2008) and its concentration in the atmosphere has risen by more than 30 % in the last 250 years (Hampe and Rudkevich, 2003). Most of the CO_2 emissions result from burning fossil fuels (mainly coal and natural gas) to produce energy (Hampe and Rudkevich, 2003; Metz et al., 2005) and the demand for energy is kept increasing in such a rate that replacing the use of fossil fuels by renewable and clean energy sources would take more time than we probably have to face this problem (CAETS, 1995). For this reason, there is a huge interest on the development of technologies to capture and storage CO_2 and absorption on reactive solutions is pointed out as one of the most promising ones (Favre, 2007). Relating to CO_2 and oxygen, the composition of the exhausted flue gas is very similar to that of the anaesthetic gas mixtures exhausted by the patient - namely, the molar fraction of CO_2 in the flue gas varies from 3 to 15 % and, in the exhausted anaesthetic mixture, it is around 5 %. For this reason, it should be kept in mind most of the research and analysis on the CO_2 removal from flue gas using absorbent hollow

fiber membrane contactors can be applied to the CO_2 removal from anaesthetic gas circuits. The opposite is also true: the progresses achieved on the CO_2 removal from anaesthetic gas circuits using hollow fiber membrane contactors will eventually find application on the flue gas treatment.

Generally, to model and to analyse the performance of the mass transfer between a gas and an absorbent liquid in a hollow fiber membrane contactor, the following information is required:

- The mass transfer coefficients of each component in the gas phase, which depend on the flow hydrodynamics - unlike the fiber lumen, the hydrodynamics in the shell side is usually difficult to describe. Several models have been proposed to describe gas flow in the shell side (Keshavarz et al., 2008), but usually gas phase mass transfer coefficients are experimentally obtained for the specific membrane module.
- The mass transfer coefficients trough the membrane, which depends on the membrane characteristics (material, porosity, etc) and is membrane specific - usually, the membranes used have high permeabilities and the resistance to mass transfer introduced by the membrane is negligible.
- The physical solubility of the components in the liquid.
- The diffusion coefficients of the gas components and the reactive species in the absorbent liquid – as mentioned before, the liquid flow inside the fiber lumen is usually laminar and bi-dimensional models for diffusion or diffusion/reaction are necessary to describe the mass transfer inside the liquid. Nevertheless, in some cases, especially for physical absorption, it is possible to estimate a mass transfer coefficient in the liquid; however the correlations used in these situations also require the previous knowledge of the diffusion coefficients and liquid physical properties such as density and viscosity.
- Information about the reaction kinetics and equilibrium between the absorbent reactive species and the reactive gases.

1.3. Selection of Liquid Absorbents for CO_2 Removal from Anaesthetic Gas Circuits

An absorbent solution to be used in a membrane contactor for CO_2 removal from anaesthetic circuits must verify the following requirements: biocompatibility, low vapour pressure (in order not to enter into the anaesthetic circuit), chemical and thermal stability and compatibility with the membrane contactor, i.e. do not originate the membrane swelling and, for porous membranes, do not wet the membrane pores. Besides, it should present fast absorption and desorption kinetics and high absorption capacity and it should be easily regenerable.

The absorbent solutions most widely used nowadays to separate CO_2 from gaseous mixtures in chemical industry are aqueous solutions of akanolamines and blends of alkanolamines (Idem and Tontiwachwuthikul, 2006). Alkanolamines have been extensively studied for CO_2 absorption purposes and their aqueous solutions characterized in detail concerning physical properties and reaction equilibrium and kinetics towards CO_2 (Austgen et al., 1989; Blauwhoff et al., 1984; Rochelle et al., 2001; Versteeg et al., 1996; Versteeg and Van Swaaij, 1988; Weiland et al., 1993). However, alkanolamines easily undergo oxidative degradation resulting in highly toxic degradation products and this degradation is far more extensive in oxygen rich environments (Goff and Rochelle, 2006; Holst et al., 2006; Kumar, 2002; Supap et al., 2006). Besides, alkanolamines are organic substances with surface tensions considerably lower than water and therefore they wet some commercially available membranes (Kumar, 2002). For these reasons, alkanolamines might not be suitable for CO_2 removal from anesthetic gas circuits and new absorbents, able to overcome these drawbacks need to be developed.

Amino acids (or, more precisely, alkali salts of amino acids[1]) are being studied as a possible alternative for alkanolamines (Feron and Jansen, 2002; Kumar et al., 2002b). Amino acids have the same reactive group towards CO_2 as alkanolamines and therefore

[1] Amino acids exist in solution as a zwitterion (with the amine group protonated) - $HOOC-R_1R_2R_3-N \leftrightarrow {}^{-}OOC-R_1R_2R_3-NH^{+}$. It is necessary to make it react with an alkali hydroxide (potassium hydroxide, for example) to enable it to react with CO_2.

they present equivalent equilibrium capacities and reaction kinetics (Holst et al., 2006; Kumar et al., 2003a; Kumar et al., 2003b). However, due to their ionic nature, amino acids present a number of advantages when compared to alkanolamines: they are much more resistant to oxidative degradation and more thermally stable, present lower volatilities (amino acids can be considered non volatile, so there is no loss of the active specie during the process and no transfer to the anaesthetic circuit) and their solutions have higher surface tensions (not wetting common and non expensive membranes) and have densities and viscosities similar to water (which means that no extra hydrodynamic concerns are introduced) (Feron and Jansen, 2002; Kumar et al., 2001; Kumar et al., 2002b). Nevertheless, amino acids present a couple of drawbacks: they are more expensive than alkanolamines and precipitation of the reaction products was observed during the absorption of CO_2 in their solutions (Hook, 1997; Kumar et al., 2003c; Majchrowicz et al., 2006). Precipitation is a severe limitation if porous membrane contactors are to be used because of possible blockage of membrane pores; even when non porous membranes are used, hydrodynamic problems can arise because of precipitation.

The general ability of an amino acid (or other amine based compound) to absorb CO_2 is determined by the molecular structure of the compound. There is a considerable amount of information in literature relating the molecular structure of CO_2 absorbents and reaction characteristics such as absorption kinetics, equilibrium capacity and regeneration extent (Caplow, 1968; Hook, 1997; Penny and Ritter, 1983; Sartori and Savage, 1983; Singh et al., 2007).

CO_2 reacts with aqueous solutions of primary or secondary amines forming carbamates, bicarbonates and carbonates (Caplow, 1968; Hook, 1997; Jensen et al., 1952). Generically, the stability of the carbamates formed influence the absorption as follows: amines which form stable carbamates react faster but present lower equilibrium capacities at loadings higher than 0.5 $mol_{CO_2} \cdot mol_{AmA}^{-1}$ (i.e. for the same loading, the CO_2 equilibrium pressure above the liquid is higher in solutions of this amines) and they are more difficult to regenerate than amines which form unstable carbamates (Hook, 1997; Park et al., 2003; Sartori and Savage, 1983). An amine is sterically

hindered when the amine group is connected to a secondary or terciary carbon, i.e. when the carbon adjacent to the amine group is substituted. Sterical hindrance is known to considerably reduce the carbamate stability (Sartori and Savage, 1983). Therefore, sterically hindered amines present generally higher absorption capacities at high loadings and show deeper desorption ability, but they exhibit lower absorption kinetics when compared to their non-sterically hindered equivalents. In the same way, secondary amines form less stable carbamates than primary amines. Singh et al. (2007) studied the influence of the chain length on the amines' absorption ability and concluded that increasing the chain length does not bring any advantage to the absorption equilibrium or to the absorption kinetics. Hook (1997) compared the regeneration achieved with amines containing a potassium carboxilate group $\left(CO_2^- K^+\right)$ (potassium amino acid salts) and a hydroxymethylen group $\left(HOCH_2\right)$ (amino alcohols) and concluded that the amino alcohols enable higher desorption levels and at higher rates than the corresponding amino acid salts.

Tertiary amines do not react directly with CO_2 to form carbamates. Instead, they act as a catalyst for the hydration of CO_2 to form bicarbonate (Bonenfant et al., 2003; Sartori and Savage, 1983). They are essentially slower absorbents than primary and secondary amines but enable high absorption capacities (Bonenfant et al., 2003). Tertiary alkanolamines are also easier to regenerate (Bonenfant et al., 2003; Derks et al., 2006). They are often used blended with other amines which act as rate promoters (Bishnoi and Rochelle, 2000; Derks et al., 2006).

1.4. Motivation and Outline of the Thesis

The doctoral work presented here arose in the context of the European Project entitled "Development of New Materials and Processes to Enhance Specialty Gas Separations" - SpecSep. The project concerned gas separations for medical applications and four partners were involved on the subject of CO_2 removal from anaesthetic gas streams and from life support applications using hollow fiber absorbent membrane contactors: LEPAE (Porto, Portugal), GKSS (Geesthacht, Germany), CSIC (Madrid, Spain) and Drager AG (Luebeck, Germany).

In the framework of the SpecSep European Project, LEPAE was in charge of characterizing different absorbents, focusing on the reaction kinetics and equilibrium towards CO_2. Both commercially available amino acids and amino acids synthesized by CSIC - Consejo Superior de Investigaciones Cientificas, Institute of Science and Technology of Polymers - were considered. Since laboratory synthesis of absorbents is an expensive and time consuming process and generally only a few grams can be produced in each batch, a lot of effort was put on the development of a fast and inexpensive methodology to analyze the performance of the absorbents using the lowest amount of substance possible. For the pre-screening of the absorbents, a setup similar to the ones used for the volumetric measurement of adsorption isotherms was used – this setup and methodology are described in detail by Santos et al. (2008). In addition, the solution was continuously stirred using a magnetic stirrer and the pressure decrease inside the absorbent tank was recorded during the entire absorption process. Uptake curves were drawn with the pressure decrease versus time. Using this method, only 10 mL of solution is spent for each experiment. Experiments were performed at 293 K.

During the SpecSep Project, the following commercially available amino acid salts were pre-screened: glycine, DL-alanine, beta-alanine, serine, threonine, isoleucine, DL-valine, piperazine-2-carboxilic acid, proline, arginine, gamma-aminobutyric acid, ornithine, taurine, creatine and histidine. The biocompatibility of the absorbents was checked based on values of oral LD50 reported in the safety data sheets of the compounds. LD50 (lethal dose 50 %) is a measure of the toxicity of a compound which is an important indicator of its biocompatibility. Glycine, isoleucine, proline, arginine, ornithine, taurine and histidine present values of oral LD50 in rats between 5000 and 15 000, which means that they are practically non toxic (CCOHS, 2008). No information about LD50 is available for the other compounds. Concerning hazardous information, only arginine is irritant. Nine new and non-commercially available absorbents synthesised by CSIC were also pre-screened using the described methodology.

All the absorbents studied proved to be able to absorb CO_2 at significant rates and absorption capacities. Nevertheless, the method used was not able to accurately differentiate them. A more precise and quantitative analysis require time consuming

experiments and larger amounts of these substances. Since, unlike alkanolamines, there is little information in literature about the CO_2 absorption in amino acid salt solutions, the potassium salt of the simplest amino acid (glycine) was selected for this more extensive characterization. However, the molecular structure of potassium glycinate, a primary and non-sterically hindered amino acid, makes it expectable to be difficult to regenerate. Given the considerations made in section 1.3, potassium threonate is likely to overcome this problem and at the same time to have acceptable reaction kinetics (this is clarified in Chapter 3). For this reason, this compound was also selected for further characterization.

The structural formulas of the amino acids glycine and trheonine are presented in Table 1.1.

Table 1.1 - Structural formulas of the amino acids characterized in the present dissertation.

Glycine	Threonine
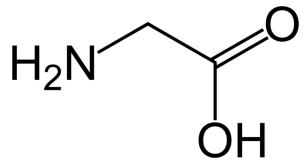	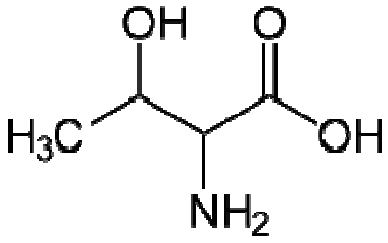

The present dissertation is organized as follows.

In Part II, the selected amino acids salts are characterized for CO_2 absorption purposes: potassium glycinate (Chapter 2) and potassium threonate (Chapter 3). Physical properties of their aqueous solutions, including density, viscosity and CO_2 physical solubility are determined at different temperatures and amino acid salt concentrations. Reaction kinetics towards CO_2 is also measured at different temperature and concentration conditions.

Part III (Chapter 4) reports the study of the CO_2 absorption equilibrium in amino acid salt solutions. Absorption equilibrium in potassium glycinate is measured at different

temperatures and amino acid salt concentrations. The equilibrium absorption capacity of potassium threonate is also determined for one condition of concentration and temperature and compared to the results for potassium glycinate.

In Part IV (Chapter 5), a bi-dimensional model to describe the membrane contactor process under study is proposed. The performance of the hollow fiber membrane contactor using potassium glycinate solutions is analysed (based on the physical, kinetics and equilibrium data determined in the previous chapters). The influence of the system parameters on the separation achieved is discussed and a contactor design and a set of operating conditions are suggested.

Finally, in Part V (Chapter 6), the main conclusions are summarised and suggestions for future work are presented.

Further details on the experimental setups used along this work are presented in Appendix A.

1.5. References

Al-Marzouqi, M. H., El-Naas, M. H., Marzouk, S. A. M., Al-Zarooni, M. A., Abdullatif, N. and Faiz, R. (2008). "Modeling of CO_2 absorption in membrane contactors." Separation and Purification Technology, 59(3), 286-293.

Austgen, D. M., Rochelle, G. T., Peng, X. and Chen, C. C. (1989). "Model of Vapor Liquid Equilibria for Aqueous Acid Gas Alkanolamine Systems Using the Electrolyte Nrtl Equation." Industrial & Engineering Chemistry Research, 28(7), 1060-1073.

Baum, J. A. and Woehlck, H. J. (2003). "Interaction of inhalational anaesthetics with CO_2 absorbents " Best Practice and Research Clinical Anaesthesiology, 17(1), 63-76.

Bishnoi, S. and Rochelle, G. T. (2000). "Absorption of carbon dioxide into aqueous piperazine: reaction kinetics, mass transfer and solubility." Chemical Engineering Science, 55(22), 5531-5543.

Blauwhoff, P. M. M., Versteeg, G. F. and Vanswaaij, W. P. M. (1984). "A Study on the Reaction between CO_2 and Alkanolamines in Aqueous-Solutions." Chemical Engineering Science, 39(2), 207-225.

Bonenfant, D., Mimeault, M. and Hausler, R. (2003). "Determination of the structural features of distinct amines important for the absorption of CO_2 and regeneration in aqueous solution." Industrial & Engineering Chemistry Research, 42(14), 3179-3184.

Brandi, L. S. (2008). "Anesthesia - Information for patients - http://www.brandianestesia.it/." Retrieved October, 2008, 2008.

CAETS (1995). The Role of Technology in Environmentally Sustainable Development. Kiruna, Sweden, Council of Academies of Engineering and Technological Sciences.

Caplow, M. (1968). "Kinetics of carbamate formation and breakdown." Journal of the American Chemical Society, 90(24), 6795-6803.

CCOHS. (2008). "What is an LD50 and LC50? - http://www.ccohs.ca." Retrieved October, 2008, 2008.

Derks, P. W. J., Kleingeld, T., van Aken, C., Hogendoom, J. A. and Versteeg, G. F. (2006). "Kinetics of absorption of carbon dioxide in aqueous piperazine solutions." Chemical Engineering Science, 61(20), 6837-6854.

Dingley, J., Ivanova-Stoilova, T. M., Grundler, S. and Wall, T. (1999). "Xenon: recent developments." Anaesthesia, 54(4), 335-346.

Dosch, M. P. (2004). "The Anesthesia Gas Machine - http://www.udmercy.edu." Retrieved October, 2008, 2008.

Fan, S. Z., Lin, Y. W., Chang, W. S. and Tang, C. S. (2008). "An evaluation of the contributions by fresh gas flow rate, carbon dioxide concentration and desflurane partial pressure to carbon monoxide concentration during low fresh gas flows to a circle anaesthetic breathing system." European Journal of Anaesthesiology, 25(8), 620-626.

Favre, E. (2007). "Carbon dioxide recovery from post-combustion processes: Can gas permeation membranes compete with absorption?" Journal of Membrane Science, 294(1-2), 50-59.

Feron, P. and Jansen, A. (2002). "CO_2 separation with polyolefin membrane contactors and dedicated absorption liquids: performances and prospects." Separation and Purification Technology, 27(3), 231-242.

Gabelman, A. and Hwang, S. (1999). "Hollow fiber membrane contactors." Journal of Membrane Science, 159(1-2), 61-106.

Goff, G. S. and Rochelle, G. T. (2006). "Oxidation inhibitors for copper and iron catalyzed degradation of monoethanolamine in CO_2 capture processes." Industrial & Engineering Chemistry Research, 45(8), 2513-2521.

Hampe, E. M. and Rudkevich, D. M. (2003). "Exploring reversible reactions between CO_2 and amines." Tetrahedron, 59(48), 9619-9625.

Holst, J., Politiek, P. P., Niederer, J. P. M. and Versteeg, G. F. (2006). "CO_2 capture from flue gas using amino acid salt solutions". GHGT-8, NTNU VIDERE, Pav. A, Dragvoll, NO-7491 Trondheim, Norway.

Hook, R. J. (1997). "An investigation of some sterically hindered amines as potential carbon dioxide scrubbing compounds." Industrial & Engineering Chemistry Research, 36(5), 1779-1790.

Idem, R. and Tontiwachwuthikul, P. (2006). "Preface for the special issue on the capture of carbon dioxide from industrial sources: Technological developments and future opportunities." Industrial & Engineering Chemistry Research, 45(8), 2413-2413.

Jensen, A., Jensen, J. B. and Faurholt, C. (1952). "Studies on Carbamates .6. The Carbamate of Glycine." Acta Chemica Scandinavica, 6(3), 395-397.

Keshavarz, P., Ayatollahi, S. and Fathikalajahi, J. (2008). "Mathematical modeling of gas–liquid membrane contactors using random distribution of fibers." Journal of Membrane Science, 325, 98–108.

Knolle, E. and Gilly, H. (2000). "Absorption of carbon dioxide by dry soda lime decreases carbon monoxide formation from isoflurane degradation." Anesthesia and Analgesia, 91(2), 446-451.

Kumar, P., Hogendoorn, J., Feron, P. and Versteeg, G. (2001). "Density, viscosity, solubility, and diffusivity of N_2O in aqueous amino acid salt solutions." Journal of Chemical and Engineering Data, 46(6), 1357-1361.

Kumar, P., Hogendoorn, J., Feron, P. and Versteeg, G. (2002a). "New absorption liquids for the removal of CO_2 from dilute gas streams using membrane contactors." Chemical Engineering Science, 57(9), 1639-1651.

Kumar, P., Hogendoorn, J., Timmer, S., Feron, P. and Versteeg, G. (2003a). "Equilibrium solubility of CO_2 in aqueous potassium taurate solutions: Part 2. Experimental VLE data and model." Industrial & Engineering Chemistry Research, 42(12), 2841-2852.

Kumar, P., Hogendoorn, J., Versteeg, G. and Feron, P. (2003b). "Kinetics of the reaction of CO_2 with aqueous potassium salt of taurine and glycine." American Institute of Chemical Engineers Journal, 49(1), 203-213.

Kumar, P. S. (2002). "Development and design of membrane gas absorption processes". Enschede, University of Twente.

Kumar, P. S., Hogendoorn, J. A., Feron, P. H. M. and Versteeg, G. F. (2002b). "New absorption liquids for the removal of CO_2 from dilute gas streams using membrane contactors." Chemical Engineering Science, 57(9), 1639-1651.

Kumar, P. S., Hogendoorn, J. A., Feron, P. H. M. and Versteeg, G. F. (2003c). "Equilibrium solubility of CO_2 in aqueous potassium taurate solutions: Part 1. Crystallization in carbon dioxide loaded aqueous salt solutions of amino acids." Industrial & Engineering Chemistry Research, 42(12), 2832-2840.

Li, J. L. and Chen, B. H. (2005). "Review Of CO_2 absorption using chemical solvents in hollow fiber membrane contactors." Separation and Purification Technology, 41(2), 109-122.

Ma'mun, S., Svendsen, H. F., Hoff, K. A. and Juliussen, O. (2007). "Selection of new absorbents for carbon dioxide capture." Energy Conversion and Management, 48(1), 251-258.

Majchrowicz, M., Niederer, J. P. M., Velders, A. H. and Versteeg, G. F. (2006). "Precipitation in amino acid salt CO_2 absorption systems". GHGT-8 NTNU VIDERE, Pav. A, Dragvoll, NO-7491 Trondheim, Norway.

Marini, F., Bellugi, I., Gambi, D., Pacenti, M., Dugheri, S., Focardi, L. and Tulli, G. (2007). "Compound A, formaldehyde and methanol concentrations during low-flow sevoflurane anaesthesia: comparison of three carbon dioxide absorbers." Acta Anaesthesiologica Scandinavica, 51(5), 625-632.

Mendes, A. M. M. (2000). "Development of an adsorption/membrane based system for carbon dioxide, nitrogen and spur gases removal from a nitrous oxide and xenon anaesthetic closed loop." Acp-Applied Cardiopulmonary Pathophysiology, 9(2), 156-163.

Metz, B., Davidson, O., Coninck, H. d., Loos, M. and Meyer, L. (2005). IPCC Special Report on Carbon Dioxide Capture and Storage. C. U. Press. Cambridge, New York, Melbourne, Madrid, Cape Town, Singapore, São Paulo, Intergovernmental Panel on Climate Change.

Murray, J. M., Renfrew, C. W., Bedi, A., McCrystal, C. B., Jones, D. S. and Fee, J. P. H. (1999). "Amsorb - A new carbon dioxide absorbent for use in anesthetic breathing systems." Anesthesiology, 91(5), 1342-1348.

Park, J. Y., Yoon, S. J. and Lee, H. (2003). "Effect of steric hindrance on carbon dioxide absorption into new amine solutions: Thermodynamic and spectroscopic verification through solubility and NMR analysis." Environmental Science & Technology, 37(8), 1670-1675.

Penny, D. E. and Ritter, T. J. (1983). "Kinetic-Study of the Reaction between Carbon-Dioxide and Primary Amines." Journal of the Chemical Society-Faraday Transactions I, 79, 2103-2109.

Pontes, S. L. d. R. (2006). "Removal of carbon dioxide and nitrogen from a xenon based closed-circuit anaesthetic system". Porto, Porto.

Rangwala, H. A. (1996). "Absorption of carbon dioxide into aqueous solutions using hollow fiber membrane contactors." Journal of Membrane Science, 112(2), 229-240.

Reinelt, H., Marx, T., Schirmer, U. and Schmidt, M. (2001). "Xenon expenditure and nitrogen accumulation in closed-circuit anaesthesia." Anaesthesia, 56(4), 309-311.

Rochelle, G. T., Bishnoi, S., Chi, S., Dang, H. and Santos, J. (2001). Research needs for CO_2 capture from flue gas by aqueous absorption/stripping. U. S. D. o. E.-F. E. T. Center. Pittsburg, U. S. Department of Energy - Federal Energy Technology Center: 60.

Santos, J. C., Magalhaes, F. D. and Mendes, A. (2008). "Contamination of zeolites used in oxygen production by PSA: Effects of water and carbon dioxide." Industrial & Engineering Chemistry Research, 47(16), 6197-6203.

Sartori, G. and Savage, D. W. (1983). "Sterically Hindered Amines for CO_2 Removal from Gases." Industrial & Engineering Chemistry Fundamentals, 22(2), 239-249.

Singh, P., Nierderer, J. P. M. and Versteeg, G. F. (2007). "Structure and activity relationships for amine based CO_2 absorbents - I." International Journal of Greenhouse Gas Control, 1(1), 5-10.

Struys, M. M. R. F., Bouche, M. P. L. A., Rolly, G., Vandevivere, Y. D. I., Dyzers, D., Goeteyn, W., Versichelen, L. F. M., Van Bocxlaer, J. F. P. and Mortier, E. P. (2004). "Production of compound A and carbon monoxide in circle systems: an in vitro comparison of two carbon dioxide absorbents." Anaesthesia, 59(6), 584-589.

Supap, T., Idem, R., Tontiwachwuthikul, P. and Saiwan, C. (2006). "Analysis of monoethanolamine and its oxidative degradation products during CO_2 absorption from flue gases: A comparative study of GC-MS, HPLC-RID, and CE-DAD analytical techniques and possible optimum combinations." Industrial & Engineering Chemistry Research, 45(8), 2437-2451.

UNFCCC (2008). United Nations Framework Convention on Climate change, http://unfccc.int.

Versteeg, G. F., Van Dijck, L. A. J. and Van Swaaij, W. P. M. (1996). "On the kinetics between CO_2 and alkanolamines both in aqueous and non-aqueous solutions. An overview." Chemical Engineering Communications, 144, 113-158.

Versteeg, G. F. and Van Swaaij, W. P. M. (1988). "Solubility and Diffusivity of Acid Gases (CO_2, N_2O) in Aqueous Alkanolamine Solutions." Journal of Chemical and Engineering Data, 33(1), 29-34.

Vladisavljevic, G. T. (1999). "Use of polysulfone hollow fibers for bubbleless membrane oxygenation/deoxygenation of water." Separation and Purification Technology, 17(1), 1-10.

Weiland, R. H., Chakravarty, T. and Mather, A. E. (1993). "Solubility of Carbon-Dioxide and Hydrogen-Sulfide in Aqueous Alkanolamines." Industrial & Engineering Chemistry Research, 32(7), 1419-1430.

Whalen, F. X., Bacon, D. R. and Smith, H. M. (2005). "Inhaled anesthetics: an historical overview." Best Practice Research Clinical Anaesthesiology, 19(3), 323-330.

Wickramasinghe, S. R., Han, B., Garcia, J. D. and Specht, R. (2005). "Microporous membrane blood oxygenators." American Institute of Chemical Engineers Journal, 51(2), 656-670.

Yan, S. P., Fang, M. X., Zhang, W. F., Wang, S. Y., Xu, Z. K., Luo, Z. Y. and Cen, K. F. (2007). "Experimental study on the separation of CO_2 from flue gas using hollow fiber membrane contactors without wetting." Fuel Processing Technology, 88(5), 501-511.

Zhang, Q. and Cussler, E. L. (1985a). "Microporous Hollow Fibers for Gas-Absorption .1. Mass-Transfer in the Liquid." Journal of Membrane Science, 23(3), 321-332.

Zhang, Q. and Cussler, E. L. (1985b). "Microporous Hollow Fibers for Gas-Absorption .2. Mass-Transfer across the Membrane." Journal of Membrane Science, 23(3), 333-345.

Part II

2. Characterization of potassium glycinate for carbon dioxide absorption purposes[1]

Abstract

Aqueous solutions of potassium glycinate were characterized for carbon dioxide absorption purposes. Density and viscosity of these solutions, with concentrations ranging from 0.1 to 3 M, were determined at temperatures from 293 to 313 K. Diffusivity of CO_2 in solution was estimated applying the modified Stokes-Einstein relation. Solubilities of N_2O at the same temperatures and concentrations were measured and the ion specific parameter based on the Schumpe's model was determined for the glycinate anion; the solubilities of CO_2 in these solutions were then computed.

The reaction kinetics of CO_2 in the aqueous solution of potassium glycinate was determined at 293, 298 and 303 K using a stirred cell reactor. The results were interpreted using the DeCoursey equation for the calculation of the enhancement factor. The rate of absorption as a function of the temperature and solution concentration for the conditions studied was found to be given by the following expression: $-r_{CO_2} = 2.42\times10^{16}\exp\left(\frac{-8544}{T}\right)\exp\left(0.44C_S\right)C_S C_{CO_2}$.

[1] Portugal, A. F.; Derks, P. W. J.; Versteeg, G. F.; Magalhães, F. D.; Mendes, A., "Characterization of potassium glycinate for carbon dioxide absorption purposes", Chem. Eng. Sci., 2007, 62(23), 6534 – 6547

2.1. Introduction

The carbon dioxide removal from closed anesthetic loops is currently achieved using soda lime canisters (a mixture of calcium, potassium and sodium hydroxides) which is an unsafe technique (Mendes, 2000). The use of dehydrated soda lime is associated to explosions due to the hydrogen formation and excessive heating during the reaction with carbon dioxide. Soda lime can also originate toxic compounds resulting from the reaction with some halogenated anesthetics (Whalen et al., 2005). Because of that and because exhausted soda lime canisters are a hospital solid waste, this outdated system needs to be replaced by a safer technology. A possible candidate is the use of absorption membrane contactors. This strategy presents various advantages. The use of a dense highly permeable membrane isolates the absorption system from the anesthetic loop and the absorption solution can be regenerated after contacting with carbon dioxide. However, the absorbent should have a suitable carbon dioxide absorption kinetics and capacity, negligible vapor pressure, high chemical and thermal stability and should be harmless to the patient.

Mostly as a consequence of the Kyoto protocol, the new stringent environmental regulations towards the emission of acidic gases raised concern about carbon dioxide capture and storage In the last decades, hollow fiber membrane contactors have been studied using absorbent aqueous solutions such as alkanolamines or blends of alkanolamines for the selective removal of acid gases like H_2S and CO_2 from a variety of industrial and natural gas streams (Al-Juaied and Rochelle, 2006; Kumar et al., 2003c). However, for applications in highly oxygenated environments, such as flue gas treatment, life support systems or anesthetic gas circuits, alkanolamines might not be of interest since they undergo oxidative degradation (Goff and Rochelle, 2006; Kumar et al., 2003c; Supap et al., 2006). Amino acids are now being studied as a possible alternative for alkanolamines (Feron and Jansen, 2002). Although being more expensive, a few advantages make amino acids attractive like being generally more stable to oxidative degradation and presenting lower volatilities while showing similar absorption kinetics and capacities in comparison to alkanolamine solutions (Kumar et al., 2003b). Moreover, amino acids aqueous solutions have higher surface tensions and the viscosities are very similar to water's. If membrane contactors are to be used, it is

important to consider that the membrane materials should be compatible with the absorption liquid. A liquid with higher surface tension and lower corrosiveness will make possible the efficient use of cheaper and commercially available membranes, economically improving the process (Kumar et al., 2003a).

Despite of rising interest, few studies have been performed so far on amino acids as carbon dioxide absorbents. TNO Environment Energy and Process Innovation has been developing a process for carbon dioxide removal from flue gas process based on the use of amino acids and salts (Feron and Jansen, 2002). Kumar and co-workers studied in detail the absorption of carbon dioxide in potassium salts of taurine and briefly analyzed glycine (Kumar et al., 2001, 2002, 2003a, 2003b, 2003c). Holst et al. (2006) compared the apparent absorption rate constants of CO_2 with different amino acid salt solutions and concluded that they were comparable with alkanolamines. Recently Lee et al. studied the physical properties and the absorption kinetics of sodium glycinate as an absorbent of carbon dioxide (Lee et al., 2005, 2006, 2007; Song et al., 2006). However, the data available in literature is still too limited to permit a suitable design and optimization of processes using amino acid absorbents.

After a pre-screening of a set of different amino acid salts, potassium glycinate presented several interesting properties, such as very good thermal stability and fast apparent reaction rate towards carbon dioxide. Besides, it is commercially available and relatively cheap. For these reasons, it was selected for characterization as a carbon dioxide absorbent in the present work. This includes the determination of the densities and viscosities of aqueous solutions with concentrations between 0.1 to 3 M and temperatures from 293 to 313 K. The solubility of N_2O in potassium glycinate solutions was also measured and the absorption kinetics of carbon dioxide in potassium glycinate solutions obtained.

2.2. Zwitterion Reaction Mechanism

The zwitterion mechanism, originally proposed by Caplow (1968) is generally applied to model the carbon dioxide absorption in amino acid aqueous solutions. According to the zwitterion mechanism, CO_2 reacts with the amino acid salt (potassium glycinate in

the present case) forming a zwitterion that is subsequently deprotonated by a base present in solution.

Formation of the potassium glycinate zwitterion

$$H_2N-CH_2-COO^-K^+ + CO_2 \underset{k_{-1}}{\overset{k_2}{\rightleftharpoons}} {}^-OOC^+H_2N-CH_2-COO^-K^+ \quad (1)$$

Removal of a proton by a base

$${}^-OOC^+H_2N-CH_2-COO^-K^+ + B_i \underset{k_{-B}}{\overset{k_B}{\rightleftharpoons}} {}^-OOCHN-CH_2-COO^-K^+ + B_iH^+ \quad (2)$$

where B_i are the bases present in solution able to deprotonate the zwitterion. In amino acid salt solutions, these bases are H_2O, OH^- and the amino acid salt $H_2NCH_2COO^-K^+$ (Blauwhoff et al., 1984).

Assuming quasi steady-state condition for the zwitterion concentration and since the second proton transfer step can be considered irreversible, the overall reaction rate, $-r_{CO_2}$, can then be obtained:

$$-r_{CO_2} = \frac{k_2}{1+\dfrac{k_{-1}}{\sum_i k_{B_i} c_{B_i}}} C_S C_{CO_2} \quad (3)$$

where C_S is the concentration of the amino acid salt and C_{CO_2} is the concentration of carbon dioxide in the liquid. Limiting conditions lead to simplified reaction rate expressions that are well described in literature (Derks et al., 2006; Kumar et al., 2003c).

During the absorption, carbon dioxide reacts also with the hydroxide ions present in solution:

$$CO_2 + OH^- \xrightarrow{k_{OH}} HCO_3^- \quad (4)$$

Taking reaction (4) into account, the overall reaction rate (3) becomes:

$$-r_{CO_2} = \left(\frac{k_2}{1 + \frac{k_{-1}}{\sum_i k_{B_i} C_{B_i}}} C_S + k_{OH^-} C_{OH^-} \right) C_{CO_2} \tag{5}$$

However, as potassium glycinate is a weak base, the contribution of reaction (4) to the overall reaction kinetics can be considered negligible as well as the contribution of OH^- to the deprotonation of the zwitterion (Kumar et al., 2003c). The overall rate of reaction of CO_2 with potassium glycinate therefore becomes:

$$-r_{CO_2} = \frac{k_2 C_S C_{CO_2}}{1 + \frac{1}{\left(k_{H_2O}/k_{-1}\right) C_{H_2O} + \left(k_{AmA}/k_{-1}\right) C_S}} \tag{6}$$

Primary amines such as monoethanolamine (MEA) usually react with CO_2 following a second order reaction kinetics, which means that the deprotonation of the zwiteterion is relatively fast when compared to the reversion rate of CO_2 and the amine ($\frac{k_{-1}}{\sum_i k_{B_i} c_{B_i}} << 1$). Equation (6) is then reduced to:

$$-r_{CO_2} = k_2 C_S C_{CO_2} \tag{7}$$

A thermodynamically sound model for the calculation of the kinetic constant should be expressed in terms of activities rather than concentrations (Haubrock et al., 2005). However, such a model would require the knowledge of a number of parameters including equilibrium data that are not available. To account for the solution non-idealities it is common to use a semi empirical model which relates the kinetic constant to the solution ionic strength (Cullinane and Rochelle, 2006):

$$k_{eff} = k \exp(bI) \tag{8}$$

where k_{eff} is the effective kinetic constant, corrected for the solution ionic strength, b is a constant and I is the ionic strength given by $I = \frac{1}{2} \sum C_i z_i^2$, where C_i and z_i are respectively the molar concentration and the charge of ion i in solution. This model is not thermodynamically sound and cannot be extrapolated for different ions present in solution since all the solution non-idealities are lumped in the effective kinetic constant,

k_{eff} ; however it is generally sufficient to represent the experimental data of a single absorption system (Haubrock et al., 2005).

2.3. Mass Transfer

The absorption of a pure gas (carbon dioxide in the present work) into a lean reactive liquid (potassium glycinate solution) is described by the following equation (Danckwerts, 1970)

$$N_{CO_2} = E \cdot k_L \frac{P_{CO_2}}{H_{CO_2}} A \tag{9}$$

where N_{CO_2} is the molar flow of CO_2 entering the liquid, k_L is the physical mass transfer coefficient, P_{CO_2} is the CO_2 partial pressure in the gas phase, H_{CO_2} is the Henry constant of CO_2 in solution, A is the interfacial area between the gas and the liquid phases and E is the enhancement factor. The enhancement factor represents the ratio between the rate of absorption in the presence of the chemical reaction and the physical rate of absorption. When the reaction rate is sufficiently high, the reaction occurs entirely in the liquid film and not in the liquid bulk and the absorption rate can be divided into three main regimes depending on the dimensionless Hatta number:

$$Ha = \frac{\sqrt{k_{ov} D_{CO_2}}}{k_L} \tag{10}$$

where k_{ov} is the overall reaction kinetic constant ($k_{ov} = -r_{CO_2} / C_{CO_2}$) and D_{CO_2} is the diffusion coefficient of CO_2 in solution.

Fast pseudo-first order (PFO) reaction regime can be assumed if the following criterion is fulfilled (Danckwerts, 1970):

$$3 < Ha << E_\infty \tag{11}$$

In this case, the processes of diffusion and reaction occur in parallel in the liquid film. The enhancement factor can be considered equal to the Hatta number and the gas absorption rate becomes, therefore, independent of the physical mass transfer coefficient. The infinite enhancement factor, E_∞, corresponds to a situation of

instantaneous reaction and can be estimated, according to the penetration theory, by the following equation (Danckwerts, 1970; Higbie, 1935):

$$E_\infty = \sqrt{\frac{D_{CO_2}}{D_S}} + \frac{C_S}{\nu_{CO_2} \frac{P_{CO_2}}{H_{CO_2}}} \sqrt{\frac{D_S}{D_{CO_2}}} \tag{12}$$

where D_S is the amino acid salt diffusion coefficient and ν_{CO_2} is the stoichiometric coefficient. The instantaneous reaction regime can be considered when $E_\infty << Ha$.

Between the limiting situations of fast pseudo-first order and instantaneous reaction regime, there is the intermediate regime. According to DeCoursey, the enhancement factor in the intermediate regime can be approximated as a function of the Hatta number and the infinite enhancement factor (DeCoursey, 1974; Van Swaaij and Versteeg, 1992):

$$E = -\frac{Ha^2}{2(E_\infty - 1)} + \sqrt{\frac{Ha^4}{4(E_\infty - 1)^2} + \frac{E_\infty \cdot Ha^2}{E_\infty - 1} + 1} \tag{13}$$

Since carbon dioxide reacts with the amino acid salt solution, the physical properties such as physical solubility and diffusivity cannot be directly measured and need to be estimated indirectly by analogy with a non-reactive gas with similar properties. Typically, N_2O is the gas used for this purpose because it has a very similar molecular configuration, volume and electronic structure and it does not react with the absorbent solution (Laddha et al., 1981).

Since the amino acid salt solutions are ionic, the so called N_2O analogy cannot be directly applied to estimate the solubility of CO_2 in these solutions. Schumpe proposed a model to describe the solubility of gases in ionic solutions, which takes into account the salting out effect observed in electrolyte solutions (Schumpe, 1993; Weisenberger and Schumpe, 1996). This model enables a reliable estimation of the solubility of CO_2 in electrolyte solutions.

The diffusion coefficient is usually difficult to accurately determine and requires time consuming experiments. Many authors studied the dependence of the diffusion

coefficient on the temperature and on the concentration of the absorbent solution and concluded that it can be related to the solution viscosity, η, through a modified Stokes-Einstein equation (Brilman et al., 2001; Joosten and Danckwerts, 1972; Kumar et al., 2001; Versteeg and Van Swaaij, 1988).

$$D\eta^{\alpha} = \text{constant} \tag{14}$$

where α is a constant that depends on the pair gas/solution.

2.4. Experimental

Chemicals

Since the amino acid exists in solution with the amine group protonated, it is necessary to make it react with a hydroxide salt to deprotonate the amine group enabling it to react with carbon dioxide. The potassium glycinate aqueous solutions were prepared by adding to the amino acid an equimolar amount of potassium hydroxide in a volumetric flask with distilled and deionised water. The concentrations of the solutions were verified by a standard potentiometric titration with 1N HCl solution.

Density and Viscosity

The density of the solutions was measured using a commercial density meter (DMA 58, anton Paar GmbH).

Viscosities of potassium glycinate solutions were determined experimentally using a standard Cannon-Fenske viscosimeter.

N_2O solubility

The procedure adopted to measure the solubility of N_2O in the amino acid salt solutions is described in detail by Derks et al. (2005) and will only be briefly summarized here. The set-up used is composed of two vessels with calibrated volumes; one for storing the nitrous oxide and the other for the absorbent solution which is magnetically stirred. A known volume of solution is transferred to the absorbent vessel

and degassed by applying vacuum. The vapour equilibrium is allowed to be reached at a given temperature; the vapour pressure, P_{vapor}, is then recorded. The gas vessel is filled with N_2O. A certain amount of N_2O is allowed to enter the absorbent vessel and the initial pressure, P_{init}, is recorded. The stirrer is then switched on and the solution equilibrium is allowed to be established. The final pressure, P_{eq}, is recorded as well as the temperature, T_{init}. The temperature is then set to a different value, T, with the help of the thermostatic bath and a new equilibrium state is established. The amount of absorbed gas is calculated applying the ideal gas law. The Henry coefficient for N_2O, H_{N_2O}, is then computed from the following equation:

$$H_{N_2O}(T) = \frac{\left[P_{eq}(T) - P_{vapour}(T)\right]}{\frac{\left[P_{init} - P_{vapour}(T_{init})\right]}{T_{init}} - \frac{\left[P_{eq}(T) - P_{vapour}(T)\right]}{T}} \left(\frac{V_L}{RV_g}\right) \tag{15}$$

where V_g and V_L are respectively the volume of gas and liquid in the absorbent vessel and R is the universal gas constant.

The solution vapour pressure at each temperature is estimated by the following relation:

$$P_{vapour}(T) = x_{H_2O} P_{H_2O}^{pure}(T) \tag{16}$$

where x_{H_2O} is the molar fraction of water in solution. The vapour pressure as a function of the absolute temperature, $P_{H_2O}^{pure}(T)$, is obtained from the Antoine equation (Poling et al., 2001).

The experimental solubility of N_2O as a function of the temperature is hence obtained using the same sample. The volume of liquid as a function of temperature and the amino acid molar fraction are obtained using the density and the mass of solution.

Kinetic Measurements

The experiments were performed in a stirred cell reactor with a smooth gas-liquid interface, with an interfacial area of $6.490 \times 10^{-3} \text{m}^2$, operating batchwise with respect to the liquid phase and semi-continuously with respect to the gas phase. The set-up and

procedure are described in detail by Derks et al. (2006) and will be only briefly summarized here. The stirred cell reactor is connected to a calibrated gas vessel filled with pure carbon dioxide by means of a pressure controller (Brooks, model 5866, 0-500 mbar, 0.5 FS precision). A fresh potassium glycinate solution, previously degassed by applying vacuum, is transferred into the stirred reactor. Subsequently, after the vapour-liquid equilibrium is attained at a given temperature, the gas phase pressure inside the stirred reactor is recorded, P_{vapour}. One begins the experiment by letting the carbon dioxide to flow from the gas vessel into the stirred cell reactor. During the experiment the pressure inside the stirred cell reactor is kept constant, P_{sc}, using the pressure controller, and the flow of absorbed carbon dioxide is computed following the pressure decrease inside the gas vessel. A sketch of the unit is presented in Figure 2.1.

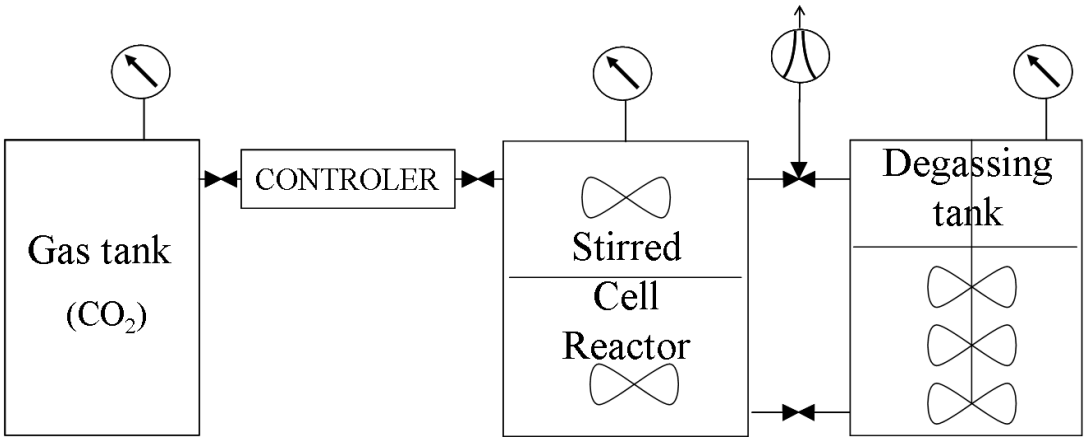

Figure 2.1 – Simplified scheme of the experimental set-up.

The flow of absorbed carbon dioxide in the stirred reactor, $N_{CO_2,sc}$, is given by equation (9) and P_{CO_2} is the carbon dioxide partial pressure in the stirred cell ($P_{CO_2} = P_{sc} - P_{vapour}$). In the gas vessel, by simply applying the ideal gas law, the flow of CO_2 is given by:

$$N_{CO_2,gv} = \frac{V_{gv}}{RT}\frac{dP_{gv}}{dt} \tag{17}$$

where $\frac{dP_{gv}}{dt}$ is the pressure decrease rate in the gas vessel and V_{gv} is the volume of the gas vessel.

$$N_{CO_2,gv} = N_{CO_2,sc} \tag{18}$$

If fast pseudo-first order regime is fulfilled, it is possible to determine experimentally the overall reaction kinetic constant, k_{ov}, knowing H_{CO_2} and D_{CO_2}. When pseudo-first order is considered, the carbon dioxide flow into the reactor tank is given by:

$$\frac{V_{gv}}{RT}\frac{dP_{gv}}{dt} = \sqrt{k_{ov} D_{CO_2}}\,\frac{P_{CO_2,sc}}{H_{CO_2}}\,A \tag{19}$$

However, to decide the operating conditions that lead to fast pseudo-first order reaction regime, it is necessary to calculate Ha, which implies the previous knowledge of k_{ov}. For experiments performed at a given temperature, absorbent concentration and stirring speed, the Hatta number is constant. Changing the partial pressure of carbon dioxide inside the reactor, one changes the infinite enhancement factor and, consequently, the ratio between Ha and E_∞, which means that the absorption regime changes. By lowering the carbon dioxide partial pressure at constant Ha, the ratio between the flow and the partial pressure of carbon dioxide becomes eventually constant, that is the value of N_{CO_2}/P_{CO_2} becomes independent of P_{CO_2}. Under these conditions it is very probable that the pseudo-first order reaction regime is attained. Plotting N_{CO_2} as a function of P_{CO_2} at the fast pseudo-first order regime, the slope of this curve is related with k_{ov} at a given temperature and amino acid concentration. Figure 2.2 shows experimental values of N_{CO_2} as a function of the partial pressure of carbon dioxide. The slope of the fitted line is related with k_{ov} through equation (19).

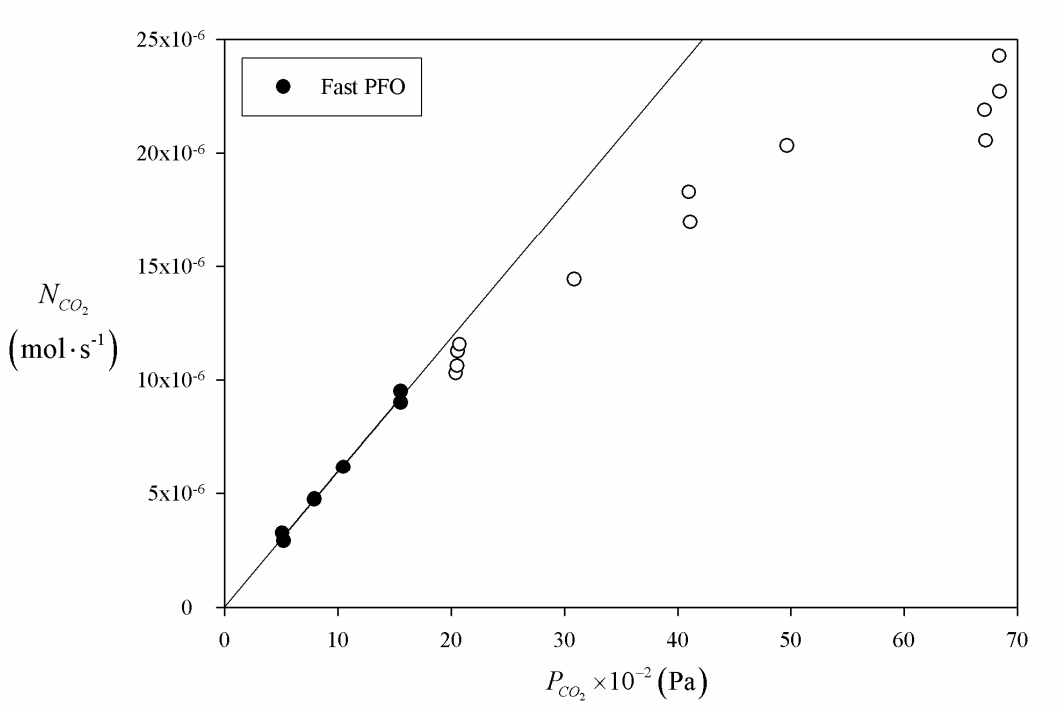

Figure 2.2 - N_{CO_2} as a function of P_{CO_2} at 298 K for a potassium glycinate concentration of 0.587 M.

For higher carbon dioxide partial pressures, still at constant Ha, the flow of carbon dioxide into the liquid (absorption) depends not only on the overall kinetic constant but also on the diffusivity ratio of carbon dioxide and absorbent, D_{CO_2}/D_S. For sufficiently high partial pressures, the instantaneous reaction regime is reached when the enhancement factor becomes independent on the overall kinetic constant.

2.5. Results and discussion

Densities of potassium glycinate aqueous solutions with concentrations from 0.1 to 3 M and temperatures from 273 to 313 K were determined and are presented in Table 2.1.

Table 2.2 – Densities of potassium glycinate solutions - $\rho\left(\mathrm{kg\cdot m^{-3}}\right)$

$C_S\,(\mathrm{M})$ \ $T\,(\mathrm{K})$	293	298	303	313
0	998.29	997.13	995.71	992.25
0.102	1004.37	1003.06	1001.59	997.28
0.296	1015.97	1014.56	1013.00	1001.77
0.594	1033.28	1031.69	1030.02	1025.15
1.003	1056.57	1054.81	1052.98	1047.94
1.992	1112.29	1110.13	1108.01	1102.34
2.984	1163.85	1161.44	1159.07	1150.37

The experimental solubility of N_2O in potassium glycinate solutions is given in Table 2.2 and Figure 2.3.

Table 3.2 - Experimental Henry constants of N_2O in potassium glycinate solutions.

$C_S\,(\mathrm{M})$	$T\,(\mathrm{K})$	$H_{N_2O}\left(\mathrm{Pa\,m^3\,mol^{-1}}\right)$	$C_S\,(\mathrm{M})$	$T\,(\mathrm{K})$	$H_{N_2O}\left(\mathrm{Pa\,m^3\,mol^{-1}}\right)$
0.102	293.2	3640	1.003	293.9	4718
0.102	297.4	4086	1.003	298.3	5368
0.102	298.5	4196	1.003	298.7	5301
0.102	303.1	4719	1.003	303.0	5991
0.296	293.1	3908	1.003	303.4	5854
0.296	293.3	3861	1.003	312.4	7252
0.296	293.4	3876	1.992	293.1	6017
0.296	293.5	3830	1.992	293.2	6140
0.296	298.0	4369	1.992	293.6	6112
0.296	298.2	4455	1.992	293.8	6024
0.296	303.3	4995	1.992	298.1	6711
0.296	311.9	6094	1.992	298.4	6974
0.594	293.4	4241	1.992	302.9	7753
0.594	293.7	4235	1.992	303.0	7519
0.594	298.3	4856	1.992	312.0	9315
0.594	302.2	5375	2.984	293.2	7694
0.594	312.0	6782	2.984	293.3	7621
1.003	293.0	4683	2.984	298.5	8545
1.003	293.1	4539	2.984	303.1	9305
1.003	293.3	4626			

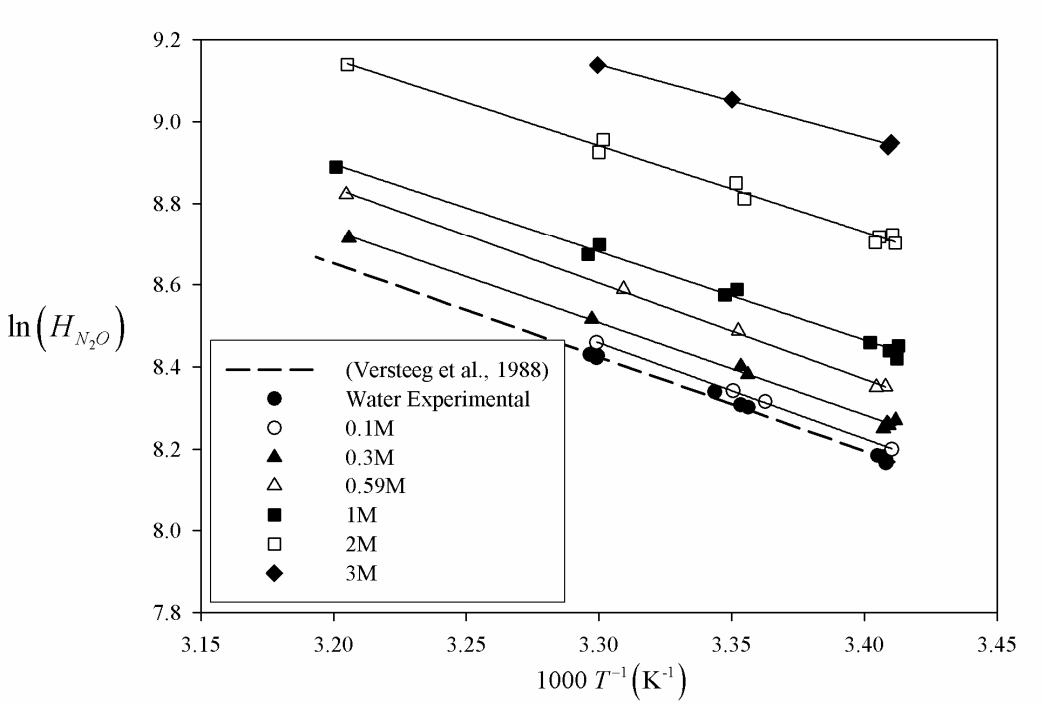

Figure 2.3 – Experimental Henry constants of N_2O in water and in potassium glycinate solutions as a function of temperature. Comparison with the solubility in water determined by Versteeg and Van Swaaij (1988).

The same experimental method was also used to obtain the solubility of N_2O in water and results compared with the ones by Versteeg and Van Swaaij (1988). It was verified that they agree within 2% relative error.

The solubility data of N_2O in potassium glycinate was fitted using the Sechenov relation:

$$\log\left(\frac{H_{N_2O}}{H_{N_2O,w}}\right) = K \cdot C_s \tag{20}$$

where H_{N_2O} and $H_{N_2O,w}$ are respectively the Henry constants of N_2O in the amino acid salt solution and in water. For each concentration and temperature, averaged values of H_{N_2O} were used. For each temperature, the computed Sechenov constants, K, failing the t-test were rejected based on a 5% confidence limit.

For a single salt, Weisenberger and Schumpe (1996) proposed the following model to predict the Sechenov's constant, K:

$$K = \sum \left(h_i + h_G \right) n_i \tag{21}$$

where h_i and h_G are the ion and gas specific parameters and n_i is the valency number of the ion. In the present work, $n_{Gly^-} = 1$ and $n_{K^+} = 1$ and the Sechenov constant becomes:

$$K_{N_2O} = \left(h_{Gly^-} + h_{N_2O} \right) + \left(h_{K^+} + h_{N_2O} \right) \tag{22}$$

Values of parameters h_{K^+} and h_{N_2O} for the cation and the gas respectively, are reported in literature (Weisenberger and Schumpe, 1996). These values, together with the experimental Sechenov's constant, K_{N_2O}, were used to calculate the anion specific parameter, h_{Gly^-}. The values of Sechenov's constant as well as the specific parameters of gas and cation and the calculated value of the anion parameter are given in Table 2.4.

Table 2.4 – Sechenov's constants for solubility of N_2O in aqueous potassium glycinate solutions.

$T\,(\mathrm{K})$	$K_{N_2O}\left(\mathrm{dm^3 mol^{-1}}\right)$	$h_{N_2O}\left(\mathrm{dm^3 mol^{-1}}\right)$	$h_{K^+}\left(\mathrm{dm^3 mol^{-1}}\right)$	$h_{Gly^-}\left(\mathrm{dm^3 mol^{-1}}\right)$
293	0.115	-0.0061	0.0922	0.0352
298	0.116	-0.0085	0.0922	0.0408
303	0.112	-0.0109	0.0922	0.0417
313	0.102	-0.0157	0.0922	0.0409

Parameters h_{K^+} and h_{Gly^-} are expected to be essentially constant with the temperature (Weisenberger and Schumpe, 1996). The values obtained for h_{Gly^-} show, however, slight temperature dependence. The average h_{Gly^-} over the temperature range is 0.0397. Taking the values of solubility in water reported by Versteeg and Van Swaaij (1988), the anion parameter h_{Gly^-} obtained by Kumar et al. (2001) is 0.0413 at 295 K which is in agreement with the present work. The value of the anion specific parameter h_{Gly^-} along with the CO_2 specific parameter, h_{CO_2}, determined by Weisenberger and Schumpe (1996) enables to predict the Sechenov's constant of CO_2 in potassium glycinate solutions, K_{CO_2}, and subsequently its physical solubility.

Table 2.5 – Sechenov's constants for solubility of CO_2 in aqueous potassium glycinate solutions.

$T\,(\mathrm{K})$	$h_{CO_2}\,(\mathrm{dm^3 mol^{-1}})$	$K_{CO_2}\,(\mathrm{dm^3 mol^{-1}})$
293	-0.0155	0.101
298	-0.0172	0.097
303	-0.0189	0.094
313	-0.0223	0.087

The computed physical solubility of carbon dioxide in potassium glycinate solutions is given in Table 2.6.

Table 2.6 – Henry constants of CO_2 in potassium glycinate solutions computed based on the Sechenov's model - $H_{CO_2}\,(\mathrm{Pa\,m^3\,mol^{-1}})$.

$C_S\,(\mathrm{M})$ \ $T\,(\mathrm{K})$	293	298	303	313
0.10	2710	3044	3405	4217
0.30	2839	3183	3556	4390
0.59	3036	3397	3787	4653
1.0	3340	3725	4138	5053
2.0	4212	4662	5139	6179
3.0	5313	5835	6382	7554

Viscosities of potassium glycinate solutions were determined experimentally and the Stokes-Einstein relation was used to estimate the diffusion coefficient of N_2O. Versteeg and Van Swaaij (1988) obtained parameter α of the Stokes-Einstein relation from experimental values of the diffusion coefficient of N_2O in several alkanolamines aqueous solutions. These authors proposed $\alpha = 0.8$, while Brilman et al. (2001) concluded that the ionic strength of the salt solutions does not influence the diffusion coefficient. For these reasons, in the present work it is assumed $\alpha = 0.8$ for estimating of the diffusion coefficient of N_2O in potassium glycinate solutions. Kumar et al. (2001) studied the diffusivity of N_2O in amino acid salts aqueous solutions and found $\alpha = 0.74$ for potassium taurate. The differences in the calculated diffusivities using one or the other value for α are lower than 5%, which is within the general experimental error for the determination of diffusion coefficients.

The diffusion coefficient of CO_2 in solution is determined using the so called $N_2O : CO_2$ analogy (Gubbins et al., 1966):

$$\frac{D_{N_2O}}{D_{N_2O,w}} = \frac{D_{CO_2}}{D_{CO_2,w}} \tag{23}$$

The values of the diffusivity of nitrous oxide and carbon dioxide in water were obtained from the literature (Versteeg and Van Swaaij, 1988). The results of the experimentally determined viscosities are given in Table 2.7 along with calculated diffusion coefficients of N_2O and CO_2.

Table 2.7 – Viscosity and diffusivity of N_2O and CO_2 in potassium glycinate solutions.

$C_S\,(\mathrm{M})$	$T\,(\mathrm{K})$	$\eta\times10^3\left(\mathrm{kg\cdot m^{-1}\cdot s^{-1}}\right)$	$D_{N_2O}\times10^9\left(\mathrm{m^2\cdot s^{-1}}\right)$	$D_{CO_2}\times10^9\left(\mathrm{m^2\cdot s^{-1}}\right)$
0.102	293	1.030	1.52	1.67
	298	0.914	1.75	1.89
	303	0.819	1.99	2.12
	313	0.666	2.57	2.66
0.296	293	1.075	1.47	1.61
	298	0.962	1.68	1.81
	303	0.851	1.93	2.06
	313	0.693	2.49	2.58
0.594	293	1.148	1.40	1.53
	298	1.020	1.60	1.73
	303	0.909	1.8	1.95
	313	0.746	2.35	2.43
1.003	293	1.263	1.30	1.42
	298	1.136	1.47	1.58
	303	1.008	1.69	1.80
	313	0.826	2.16	2.24
1.992	293	1.620	1.06	1.16
	298	1.449	1.21	1.30
	303	1.287	1.39	1.48
	313	1.070	1.76	1.82
2.984	293	2.109	0.86	0.94
	298	1.861	0.99	1.07
	303	1.677	1.12	1.20
	313	1.363	1.45	1.50

Overall Kinetic Constants

The overall kinetic constants of the carbon dioxide absorption in potassium glycinate aqueous solutions were calculated using the described methodology for a potassium glycinate concentration from 0.1 to 3 M and at 293, 298 and 303 K.

Table 2.8 shows the overall kinetic constants of carbon dioxide absorption obtained at the potassium glycinate concentrations and temperatures employed. Only the experimental values of N_{CO_2} as a function of P_{CO_2} considered to be in the fast pseudo-first reaction order regime were used for that calculation. The complete set of kinetic results is shown in Appendix.

Table 2.8 – Experimental values of the overall kinetic constant assuming pseudo-first order behaviour.

	$\text{Slope} \cdot 10^7 \left(\text{mol} \cdot \text{mbar}^{-1} \cdot \text{s}^{-1}\right)$			$k_{ov} \left(\text{s}^{-1}\right)$		
$T\,(\text{K})$ / $C_S\,(\text{M})$	293	298	303	293	298	303
0.0994	---	2.51	---	---	732	---
0.299	4.44	4.38	5.19	2340	2540	3930
0.587	4.30	5.94	7.37	2640	5590	9490
0.999	7.09	8.83	9.40	9390	16200	20000
1.984	7.92	9.55	12.7	22800	36100	68000
3.005	---	10.7	---	---	86300	---

One must now verify if inequality (11), corresponding to the pseudo-first order reaction criterion, is fulfilled. The Hatta numbers and the infinite enhancement factors were then calculated for each experimental condition. However, to calculate the Hatta number one needs to determine the physical mass transfer coefficient, k_L - see equation (10), and to calculate the infinite enhancement factors one needs to determine the diffusion coefficient of potassium glycinate in solution, D_S - see equation (12).

The physical mass transfer coefficient, k_L, was calculated using the empirical expression referred by Versteeg et al. (1987):

$$\text{Sh} = c_2 \, \text{Re}^{c_3} \, \text{Sc}^{c_4} \tag{24}$$

where Sh, Re and Sc are respectively the Sherwood, Reynolds and Schmidt dimensionless numbers defined as:

$$\mathrm{Sh} = \frac{k_L \cdot d_S}{D_{CO_2}} \tag{25}$$

$$\mathrm{Re} = \frac{\left(d_S\right)^2 N \rho}{\eta} \tag{26}$$

$$\mathrm{Sc} = \frac{\eta}{\rho \cdot D_{CO_2}} \tag{27}$$

where d_S and N are respectively the characteristic dimension and the speed of the stirrer which are, in the present case, $d_S = 9.09 \times 10^{-2}\,\mathrm{m}$ and $N = 108\,\mathrm{min}^{-1}$. The constants c_2, c_3 and c_4 were determined experimentally performing absorption experiments of CO_2 in water at different temperatures and they show to be within the usual values for this kind of systems (Versteeg et al., 1987).

$$\mathrm{Sh} = 0.1018 \cdot \mathrm{Re}^{0.7279}\,\mathrm{Sc}^{0.4076} \tag{28}$$

It was verified that all computed Ha were much higher than 3 and therefore the first part of the inequality (11) is confirmed.

The diffusion coefficient of potassium glycinate in solution, D_S, was computed assuming that it follows the modified Stokes-Einstein relation (14) with $\alpha = 0.6$ (Versteeg and Van Swaaij, 1988). To estimate the diffusion coefficient of the salt at infinite dilution, D_S^0, the Nernst equation for the diffusion in electrolyte solutions was applied (Poling et al., 2001):

$$D_S^0 = \frac{RT\left[\left(1/z_+\right) + \left(1/z_-\right)\right]}{F^2\left[\left(1/\lambda_+^0\right) + \left(1/\lambda_-^0\right)\right]} \tag{29}$$

where F is the Faraday constant, z_+ and z_- are the valencies of the cation and anion respectively and λ_+^0 and λ_-^0 are the ionic conductances of the cation and anion respectively at infinite dilution. Values of λ_+^0 at each temperature was calculated based on the work of Fell and Hutchiso (1971). λ_-^0 at 298 K was obtained from Miyamoto and Schmidt (1933) and it was assumed that it depends on the temperature in the same way

as λ_{+}^{0}. The computed diffusion coefficient of potassium glycinate in solutions, D_S, are shown in Table 2.9.

Table 2.9 – Computed values of D_S used to calculate E_∞ - $D_S \times 10^{10}\left(\mathrm{m^2 \cdot s^{-1}}\right)$.

$C_S\,(\mathrm{M})$ \ $T\,(\mathrm{K})$	293	298	303
0.0994	---	11.2	---
0.299	8.56	10.8	13.3
0.587	8.23	10.5	12.8
0.999	7.77	9.80	12.0
1.984	6.69	8.47	10.4
3.005	---	7.29	---

The Hatta number, Ha, along with the minimum value of E_∞ (corresponding to the higher pressure used for computing k_{ov} assuming the pseudo-first order) are given in Table 2.10 for the absorbent concentrations and temperatures studied.

Table 2.10 - Ha and minimum values of E_∞ used for computing k_{ov} assuming PFO.

	Ha			E_∞		
$C_S\,(\mathrm{M})$ \ $T\,(\mathrm{K})$	293	298	303	293	298	303
0.0994	---	38.5	---	---	182	---
0.299	73.1	72.9	86.2	316	477	713
0.587	79.4	110	137	437	500	776
0.999	154	194	205	748	937	1460
1.984	261	314	410	1930	2430	3710
3.005	---	528	----	---	4400	---

Fast pseudo-first order regime can only be ensured for ratios between E_∞ and Ha close to 10. For this reason, the DeCoursey relation was applied and new values for k_{ov} were calculated by minimizing the sum of the square residues between the experimental carbon dioxide absorption flow and the flow calculated by applying the DeCoursey equation. These values are given in Table 2.11.

Table 2.11 - Experimental values of the overall kinetic constants of potassium glycinate calculated using the DeCoursey equation - $k_{ov}\left(\mathrm{s}^{-1}\right)$.

$C_S\,(\mathrm{M})$ \ $T\,(\mathrm{K})$	293	298	303
0.0994	---	881	---
0.299	2860	2710	4360
0.587	3130	6420	11000
0.999	11500	19600	22000
1.984	24200	38600	69800
3.005	---	93900	---

The deviation of the enhancement factor determined experimentally and the one calculated based on the DeCoursey equation is presented in Figure 2.4.

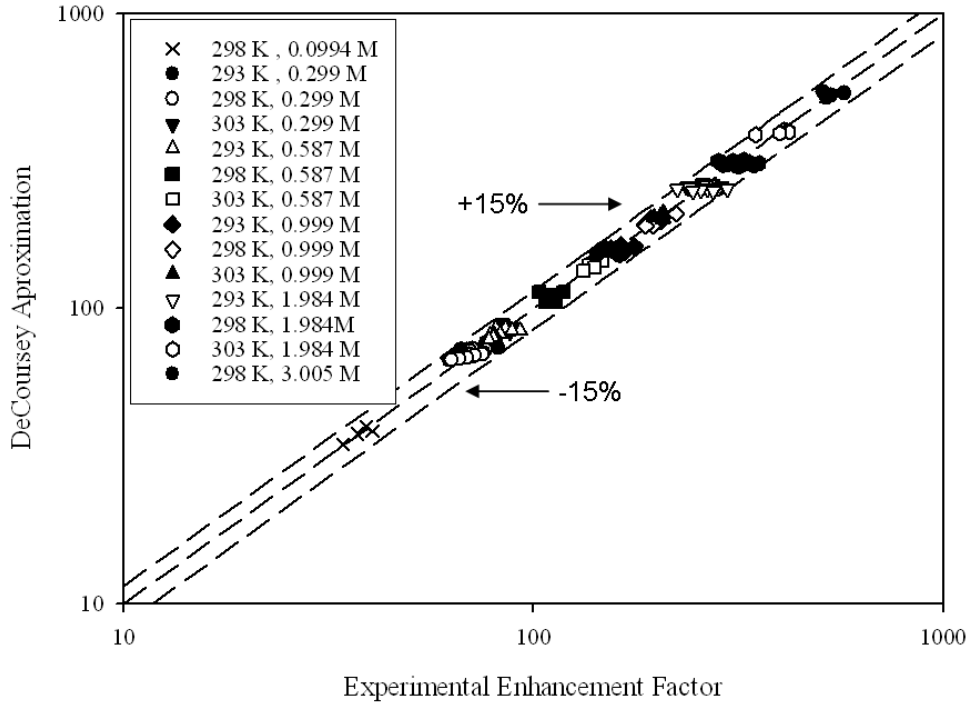

Figure 2.4 – Parity plot of experimental enhancement factor and the DeCoursey approximation.

Since all the experiments were performed at very low loadings, the only ions contributing to the ionic strength of the solutions are potassium cation and glycinate anion, both monovalent species ($z^2 = 1$) and thus $I = C_S$. Combining equation (7) with (8), the absorption rate of CO_2 becomes:

$$-r_{CO_2} = k_2 C_S \exp\left(bC_S\right) C_{CO_2} \tag{30}$$

In addition, assuming that the kinetic constant obeys the Arrhenius equation:

$$k_2 = k_{2,0} \cdot \exp\left(\frac{A}{T}\right) \tag{31}$$

Plotting k_{ov} as a function of C_S it is possible to perform a global fitting to the experimental results for all temperatures and concentrations considered, in order to obtain the kinetic parameters $k_{2,0}$, A and b. The resulting expression for computation of the overall kinetic constant as a function of temperature and amino acid salt concentration, obtained by minimizing the sum of the relative residues squared is (with C_S expressed in mol dm^{-3}):

$$k_{ov} = 2.42\times10^{16} \exp\left(\frac{-8544}{T}\right)\exp\left(0.44C_S\right)C_S \qquad \text{s}^{-1} \tag{32}$$

where a coefficient of determination of 0.991 was obtained.

The zwitterion mechanism constants, k_2, $\left(k_{H_2O}/k_{-1}\right)$ and $\left(k_{AmA}/k_{-1}\right)$, were also fitted using the same procedure but not accounting to the solution ionic strength: $k_2 = 2.81\times10^{13} \exp\left(\frac{-5800}{T}\right) \text{M}^{-1}\cdot\text{s}^{-1}$; $\left(k_{H_2O}/k_{-1}\right) = 1.05\times10^{-1} \exp\left(\frac{-1265}{T}\right) \text{M}^{-1}$ and $\left(k_{AmA}/k_{-1}\right) = 4.89\times10^{6} \exp\left(\frac{-5307}{T}\right)\text{M}^{-1}$, where a coefficient of determination of 0.956 was obtained. Both fittings are shown in Figures 2.5 and 2.6. Although the first model fits better the experimental results (smaller sum of squared residues), generally both models are in agreement with the experimental results for concentrations up to 3 M. It is however noticeable that above this concentration it is no longer possible to neglect the non-idealities of the solution. The second model has 6 fitting parameters while the first has just 3. The second model has a large number of fitting parameters and over fitting can easily occur. It is very difficult in such circumstances to identify if the non-idealities play or not a significant role. The simpler first model becomes then more attractive in the present work.

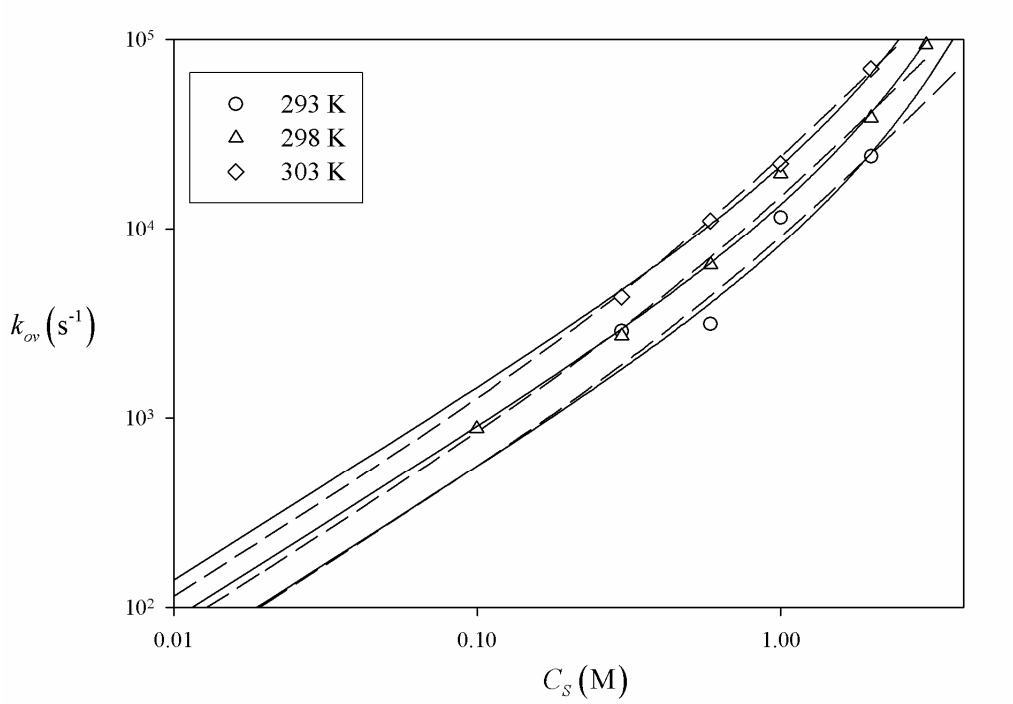

Figure 2.5 – Overall absorption kinetic constant as a function of potassium glycinate concentration and for different temperatures: experimental values and model lines. Solid lines correspond to the model that takes into account the ionic strength and dashed lines to the zwitterion model.

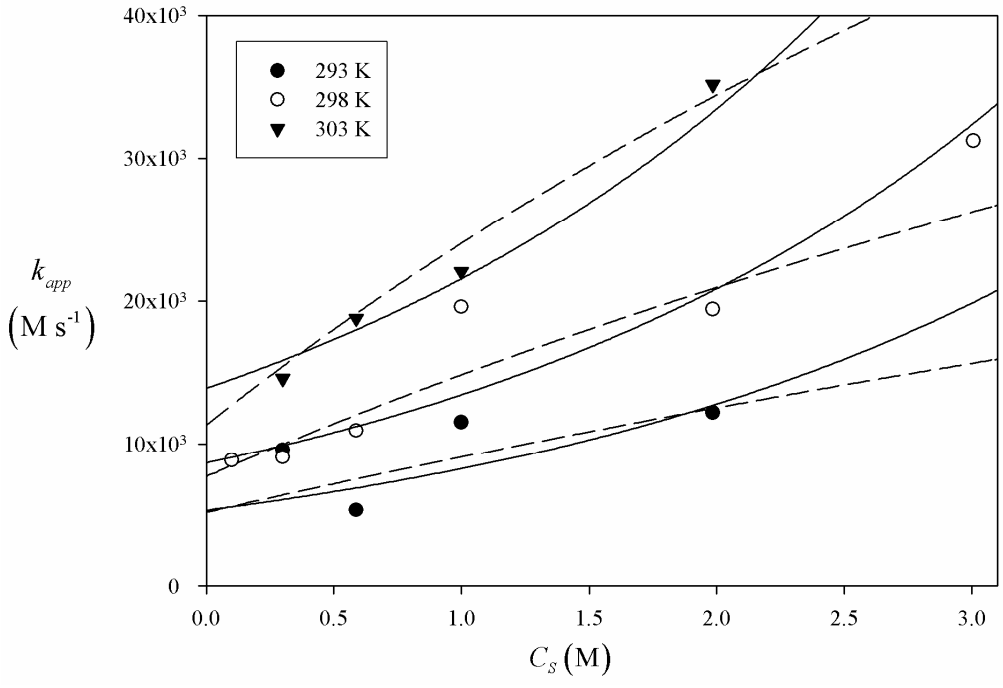

Figure 2.6 - Apparent absorption kinetic constants as a function of potassium glycinate concentration and at different temperatures: experimental values and model lines. Solid lines correspond to the model that takes into account the ionic strength and dashed lines to the zwitterion model.

The values of k_{ov} obtained are in good agreement with the work of Kumar et al. (2003c) for low concentrations but deviate for higher concentrations. This is possibly due to the effect of the ionic strength not being taken into account in Kumar's work. On the other hand, the results of the present work are quite different from the ones by Lee et al. (2007). Those authors mention apparent kinetic constants for carbon dioxide absorption in aqueous sodium glycinate solutions about two orders of magnitude lower. However, a careful analysis of that work shows that the kinetic measurements were performed far from the fast pseudo-first order reaction regime, since in some cases E_∞ was even lower than Ha.

It is common to relate the kinetic constant of reaction, k_2, with the pK_a of the aminoacid salt by means of a Brønsted plot. Penny and Ritter (1983) determined the kinetic constant and the pK_a of several amino acids (including glycinate anion) and alkanolamines. The values of k_2 determined in the present work deviate less than 30% (relative error) from the Brønsted plot based on the work from Penny and Ritter (1983) in the entire temperature range. Figure 2.7 presents the Brønsted plot of Penny and Ritter (1983) along with the results from this work.

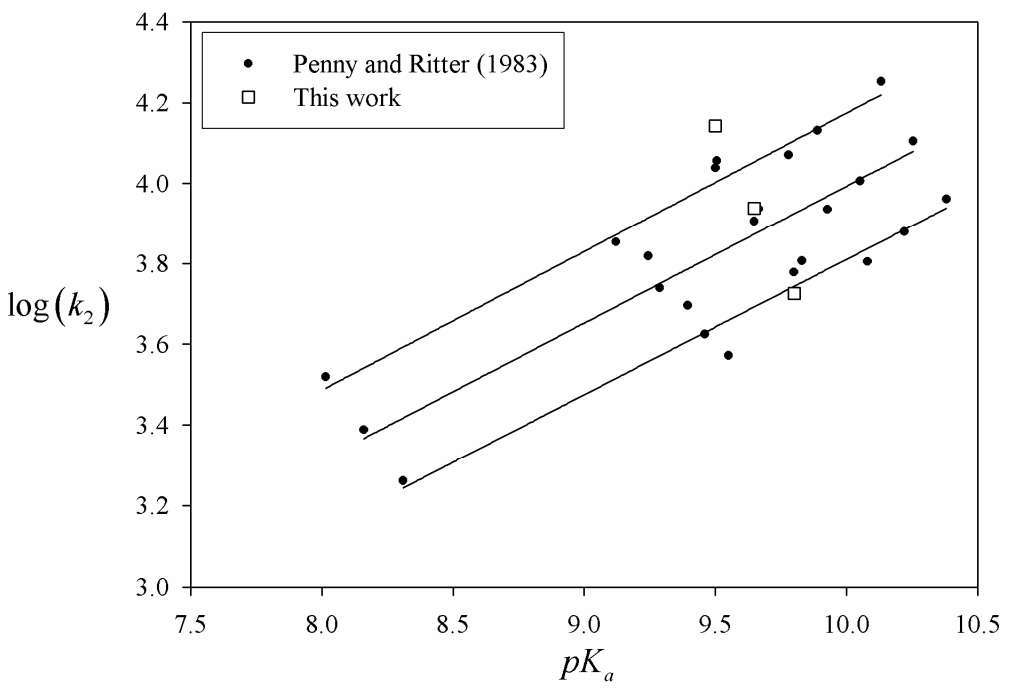

Figure 2.7 - Brønsted plot of Penny and Ritter (1983) at 293, 298 and 303 K – Comparison with the present work.

2.6. Conclusions

Density and viscosity of potassium glycinate aqueous solutions ranging from 0.1 and 3 M and at temperatures between 273 and 313 K were obtained. The diffusion coefficient of N_2O in solution was estimated using a modified Stokes-Einstein relation and the CO_2 diffusion coefficient in solution was estimated using the so called $N_2O:CO_2$ analogy (Gubbins et al., 1966).

The solubility of N_2O in the potassium glycinate solutions was experimentally determined. The salting out effect of the salt concentration in the solubility showed to be well described by the Sechenov equation. The specific parameter of the glycinate anion, based on the Schumpe model (Schumpe, 1993), was calculated ($h_{Gly^-} = 0.0397\,\text{mol dm}^{-3}$) and the solubility of CO_2 in solution was then estimated.

The rate of reaction of CO_2 with potassium glycinate was determined in a stirred cell reactor operating in semi-continuous mode. Two approaches were used to obtain the relevant parameters of the model. Since the conditions for fast pseudo-first order reaction regime were apparently not fulfilled, the DeCoursey equation was employed to calculate the enhancement factor. The results indicate that the reaction kinetics significantly depend on the ionic strength of the solution. The apparent rate of reaction is in line with the Brønsted plot based on the work from Penny and Ritter (1983). The obtained overall kinetic constants point out that potassium glycinate is a fast absorbent when compared with other absorbents, namely with MEA, which shows an overall kinetic constant at 298 K for a 1 M solution of 5920 s^{-1} (Glasscock et al., 1991) against the value of 13400 s^{-1} obtained in the present work for potassium glycinate at the same concentration and temperature conditions. In the future, these results will be applied in the design and optimization of a membrane contactor to be used for carbon dioxide removal from anesthetic gas streams.

2.7. Nomenclature

A Gas-liquid interfacial area, m^2

C	Concentration, M or $\mathrm{mol \cdot m^{-3}}$
D	Diffusion coefficient, $\mathrm{m^2 \cdot s^{-1}}$
d_S	Stirrer diameter, m
E	Enhancement factor, dimensionless
E_∞	Infinite enhancement factor, dimensionless
F	Faraday constant, 96500 $\mathrm{C \cdot mol^{-1}}$
Ha	Hatta number, dimensionless
h	Ion and gas specific constants in the Shumpe equation, $\mathrm{m^3 \cdot mol^{-1}}$
H	Henry coefficient, $\mathrm{Pa \cdot mol \cdot m^{-3}}$
I	Ionic strength of the solution, $\mathrm{mol \cdot dm^{-3}}$
J_{CO_2}	Carbon dioxide absorption flux, $\mathrm{mol \cdot m^{-2} \cdot s^{-1}}$
K	Sechenov constant, $\mathrm{dm^3 \cdot mol^{-1}}$
k_{-1}	Zwitterion kinetic constant of the reverse reaction, $\mathrm{s^{-1}}$
k_2	Zwitterion kinetic constant of the reaction, $\mathrm{M^{-1} \cdot s^{-1}}$
k_{AmA}	Zwitterion deprotonation rate constant for amino acid, $\mathrm{M^{-1} \cdot s^{-1}}$
k_{app}	Apparent rate constant defined as: $k_{app} = k_{ov} / C_S$, $\mathrm{M^{-1} \cdot s^{-1}}$
k_{B_i}	Zwitterion mechanism deprotonation rate constant by base, $\mathrm{M^{-1} \cdot s^{-1}}$
k_{H_2O}	Zwitterion mechanism deprotonation rate constant for water, $\mathrm{M^{-1} \cdot s^{-1}}$
k_L	Liquid phase physical mass transfer coefficient, $\mathrm{m \cdot s^{-1}}$
k_{OH^-}	Reaction rate constant with hydroxide ion $\mathrm{M^{-1} \cdot s^{-1}}$
k_{ov}	Overall kinetic constant, $\mathrm{s^{-1}}$
N	Stirrer speed, rps
N_{CO_2}	Carbon dioxide absorption flow, $\mathrm{mol \cdot s^{-1}}$
n_i	Valency number of the ions
P_{CO_2}	Carbon dioxide partial pressure, Pa
$-r_{CO_2}$	Rate of reaction, $\mathrm{mol \cdot m^{-3} \cdot s^{-1}}$
R	Universal gas constant, 8.314 $\mathrm{J \cdot mol^{-1} \cdot K^{-1}}$
Re	Reynolds number, dimensionless

Sh	Sherwood number, dimensionless
Sc	Schmidt number, dimensionless
T	Temperature, K
V	Volume, m^3
x	Molar fraction, $mol \cdot mol^{-1}$
z_+, z_-	Valencies of the cation and anion

Greek symbols

α	Constant from the modified Stokes-Einstein equation
$\alpha_{máx}$	Maximum loading achieved in one experiment, $mol_{CO_2} \cdot mol_S^{-1}$
ν_S	Stoichiometric coefficient
η	Solution viscosity, $kg \cdot m^{-1} \cdot s^{-1}$
ρ	Solution density, $kg \cdot m^{-3}$
λ_+^0, λ_-^0	Ionic conductances of the cation and anion at infinite dilution, $cm^2 \cdot \Omega^{-1}$

Subscripts

CO_2	Carbon dioxide
eff	Effective (after correcting for the ionic strength)
eq	Equilibrium
final	Final
g	Gas phase
Gly^-	Glycinate anion
gv	Gas vessel
K^+	Potassium cation
init	Initial
L	Liquid phase
MEA	Monoethanolamine
N_2O	Nitrous oxide
S	Amino acid salt
sc	Stirred cell
w	Water

2.8. References

Al-Juaied, M. and Rochelle, G. T. (2006). "Absorption of CO_2 in aqueous diglycolamine." Industrial & Engineering Chemistry Research, 45(8), 2473-2482.

Blauwhoff, P. M. M., Versteeg, G. F., et al. (1984). "A Study on the Reaction between CO_2 and Alkanolamines in Aqueous-Solutions." Chemical Engineering Science, 39(2), 207-225.

Brilman, D. W. F., Van Swaaij, W. P. M., et al. (2001). "Diffusion coefficient and solubility of isobutene and trans-2-butene in aqueous sulfuric acid solutions." Journal of Chemical and Engineering Data, 46(5), 1130-1135.

Caplow, M. (1968). "Kinetics of carbamate formation and breakdown." Journal of the American Chemical Society, 90(24), 6795-6803.

Cullinane, J. T. and Rochelle, G. T. (2006). "Kinetics of carbon dioxide absorption into aqueous potassium carbonate and piperazine." Industrial & Engineering Chemistry Research, 45(8), 2531-2545.

Danckwerts, P. (1970). "Gas-Liquid Reactions", McGraw-Hill Book Company.

Decoursey W. J. (1974). "Absorption with Chemical-Reaction - Development of a New Relation for Danckwerts Model." Chemical Engineering Science, 29(9), 1867-1872.

Derks, P., Hogendoorn, K., et al. (2005). "Solubility of N_2O in and density, viscosity, and surface tension of aqueous piperazine solutions." Journal of Chemical and Engineering Data, 50(6), 1947-1950.

Derks, P. W. J., Kleingeld, T., et al. (2006). "Kinetics of absorption of carbon dioxide in aqueous piperazine solutions." Chemical Engineering Science, 61(20), 6837-6854.

Fell, C. J. D. and Hutchiso, H. P. (1971). "Diffusion Coefficients for Sodium and Potassium Chlorides in Water at Elevated Temperatures." Journal of Chemical and Engineering Data, 16(4), 427-429.

Feron, P. and Jansen, A. (2002). "CO_2 separation with polyolefin membrane contactors and dedicated absorption liquids: performances and prospects." Separation and Purification Technology, 27(3), 231-242.

Glasscock, D. A., Critchfield, J. E., et al. (1991). "CO_2 Absorption desorption in mixtures of methyldiethanolamine with monoethanolamine or diethanolamine." Chemical Engineering Science, 46(11), 2829-2845.

Goff, G. S. and Rochelle, G. T. (2006). "Oxidation inhibitors for copper and iron catalyzed degradation of monoethanolamine in CO_2 capture processes." Industrial & Engineering Chemistry Research, 45(8), 2513-2521.

Gubbins, K. E., Bhatia, K. K., et al. (1966). "Diffusion of Gases in Electrolytic Solutions." American Institute of Chemical Engineers Journal, 12(3), 548-552.

Haubrock, J., Hogendoorn, J. A., et al. (2005). "The applicability of activities in kinetic expressions: a more fundamental approach to represent the kinetics of the system CO_2-OH- in terms of activities." International Journal of Chemical Reactor Engineering 3.

Higbie, R. (1935). "The rate of absorption of a pure gas into a still liquid during a short time of exposure." Transactions of the American Institute of Chemical Engineers, 31, 365–389.

Holst, J., Politiek, P., et al. (2006). "CO_2 capture from flue gas using amino acid salt solutions" GHGT-8 Proceedings.

Joosten, G. E. H. and Danckwerts, P. V. (1972). "Solubility and diffusivity of nitrous-oxide in equimolar potassium carbonate - potassium bicarbonate solutions at 25 ºC and 1 atm." Journal of Chemical and Engineering Data, 17(4), 452-454.

Kumar, P., Hogendoorn, J., et al. (2001). "Density, viscosity, solubility, and diffusivity of N_2O in aqueous amino acid salt solutions." Journal of Chemical and Engineering Data, 46(6), 1357-1361.

Kumar, P., Hogendoorn, J., et al. (2002). "New absorption liquids for the removal of CO_2 from dilute gas streams using membrane contactors." Chemical Engineering Science, 57(9), 1639-1651.

Kumar, P., Hogendoorn, J., et al. (2003a). "Equilibrium solubility of CO_2 in aqueous potassium taurate solutions: Part 1. Crystallization in carbon dioxide loaded aqueous salt solutions of amino acids." Industrial & Engineering Chemistry Research, 42(12), 2832-2840.

Kumar, P., Hogendoorn, J., et al. (2003b). "Equilibrium solubility of CO_2 in aqueous potassium taurate solutions: Part 2. Experimental VLE data and model." Industrial & Engineering Chemistry Research, 42(12), 2841-2852.

Kumar, P., Hogendoorn, J., et al. (2003c). "Kinetics of the reaction of CO_2 with aqueous potassium salt of taurine and glycine." American Institute of Chemical Engineers Journal, 49(1), 203-213.

Laddha, S. S., Diaz, J. M., et al. (1981). "The N_2O Analogy - the Solubilities of CO_2 and N_2O in Aqueous-Solutions of Organic-Compounds." Chemical Engineering Science, 36(1), 228-229.

Lee, S., Choi, S., et al. (2005). "Physical properties of aqueous sodium glycinate solution as an absorbent for carbon dioxide removal." Journal of Chemical and Engineering Data, 50(5), 1773-1776.

Lee, S., Song, H. J., et al. (2007). "Kinetics of CO_2 absorption in aqueous sodium glycinate solutions." Industrial & Engineering Chemistry Research, 46(5), 1578-1583.

Lee, S., Song, H. J., et al. (2006). "Physical solubility and diffusivity of N_2O and CO_2 in aqueous sodium glycinate solutions." Journal of Chemical and Engineering Data, 51(2), 504-509.

Mendes, A. M. M. (2000). "Development of an adsorption/membrane based system for carbon dioxide, nitrogen and spur gases removal from a nitrous oxide and xenon anaesthetic closed loop." Acp-Applied Cardiopulmonary Pathophysiology, 9(2), 156-163.

Miyamoto, S. and Schmidt, C. L. A. (1933). "Transference and conductivity studies on solutions of certain proteins and amino acids with special reference to the formation of complex ions between the alkaline earth elements and certain proteins." Journal of Biological Chemistry, 99(2), 335.

Penny, D. E. and Ritter, T. J. (1983). "Kinetic-Study of the Reaction between Carbon-Dioxide and Primary Amines." Journal of the Chemical Society-Faraday Transactions I, 79, 2103-2109.

Poling, B. E., Prausnitz, J. M., et al. (2001). "The Properties of Gases and Liquids". McGraw-Hill Book Company

Schumpe, A. (1993). "The Estimation of Gas Solubilities in Salt-Solutions." Chemical Engineering Science, 48(1), 153-158.

Song, H. J., Lee, S., et al. (2006). "Solubilities of carbon dioxide in aqueous solutions of sodium glycinate." Fluid Phase Equilibria, 246(1-2), 1-5.

Supap, T., Idem, R., et al. (2006). "Analysis of monoethanolamine and its oxidative degradation products during CO_2 absorption from flue gases: A comparative study of GC-MS, HPLC-RID, and CE-DAD analytical techniques and possible optimum combinations." Industrial & Engineering Chemistry Research, 45(8), 2437-2451.

Van Swaaij, W. P. M. and Versteeg, G. F. (1992). "Mass-Transfer Accompanied with Complex Reversible Chemical-Reactions in Gas-Liquid Systems - an Overview." Chemical Engineering Science, 47(13-14), 3181-3195.

Versteeg, G. F., Blauwhoff, P. M. M., et al. (1987). "The Effect of Diffusivity on Gas-Liquid Mass-Transfer in Stirred Vessels - Experiments at Atmospheric and Elevated Pressures." Chemical Engineering Science, 42(5), 1103-1119.

Versteeg, G. F. and Van Swaaij, W. P. M. (1988). "Solubility and Diffusivity of Acid Gases (CO_2, N_2O) in Aqueous Alkanolamine Solutions." Journal of Chemical and Engineering Data, 33(1), 29-34.

Weisenberger, S. and Schumpe, A. (1996). "Estimation of gas solubilities in salt solutions at temperatures from 273 K to 363 K." American Institute of Chemical Engineers Journal, 42(1), 298-300.

Whalen, F. X., Bacon, D. R., et al. (2005). "Inhaled anesthetics: an historical overview." Best Practice Research Clinical Anaesthesiology, 19(3), 323-330.

2.A. Experimental kinetic data

Values of the carbon dioxide flux, J_{CO_2}, as a function of the carbon dioxide partial pressure for all temperatures and potassium glycinate concentrations studied are presented in Tables 2.A1-2.A14.

All the experiments began with fresh solution. The maximum loading reached at the end of each experiment, $\alpha_{máx}$, is also shown.

The values used to calculate k_{ov} considering pseudo first order reaction regime and using the DeCoursey approach are marked respectively with ^{PFO} and ^{DeCo}. Since at high carbon dioxide partial pressures, the overall kinetic constant plays a minor role on the enhancement factor and the values of D_{CO_2} and D_S are estimated, only experiments at low partial pressures were used to calculate k_{ov} even when the DeCoursey approach was used.

Table 2.A1 – Kinetic data of the reaction of CO_2 with potassium glycinate at 0.0994 M and 298 K.

$P_{CO_2} \times 10^{-2}$ (Pa)	$J_{CO_2} \times 10^4$ $\left(\mathrm{mol \cdot s^{-1} \cdot m^{-2}}\right)$	$\alpha_{máx}$ $\left(\mathrm{mol_{CO_2} \cdot mol^{-1}_{AmA}}\right)$	$P_{CO_2} \times 10^{-2}$ (Pa)	$J_{CO_2} \times 10^4$ $\left(\mathrm{mol \cdot s^{-1} \cdot m^{-2}}\right)$	$\alpha_{máx}$ $\left(\mathrm{mol_{CO_2} \cdot mol^{-1}_{AmA}}\right)$
3.42 PFO/DeCo	1.34	0.010	16.50 DeCo	4.78	0.037
5.05 PFO/DeCo	2.05	0.015	21.65 DeCo	5.31	0.042
6.43 PFO/DeCo	2.40	0.017	31.54 DeCo	6.52	0.054
11.44 DeCo	3.94	0.029	52.11 DeCo	7.65	0.068

Table 2.A2 - Kinetic data of the reaction of CO_2 with potassium glycinate at 0.299 M and 293 K

$P_{CO_2} \times 10^{-2}$ (Pa)	$J_{CO_2} \times 10^4$ $\left(\mathrm{mol \cdot s^{-1} \cdot m^{-2}}\right)$	$\alpha_{máx}$ $\left(\mathrm{mol_{CO_2} \cdot mol^{-1}_{AmA}}\right)$	$P_{CO_2} \times 10^{-2}$ (Pa)	$J_{CO_2} \times 10^4$ $\left(\mathrm{mol \cdot s^{-1} \cdot m^{-2}}\right)$	$\alpha_{máx}$ $\left(\mathrm{mol_{CO_2} \cdot mol^{-1}_{AmA}}\right)$
4.71 PFO/DeCo	3.36	0.008	12.57 DeCo	8.35	0.019
5.66 PFO/DeCo	4.27	0.010	14.60 DeCo	8.49	0.020
6.27 PFO/DeCo	4.57	0.011	19.84	10.0	0.023
6.76 PFO/DeCo	4.92	0.012	24.81	12.4	0.019
7.28 PFO/DeCo	5.58	0.013	34.73	15.2	0.023
8.28 PFO/DeCo	5.34	0.013	40.05	16.2	0.038
8.85 PFO/DeCo	5.48	0.013	44.87	16.1	0.039
9.84 PFO/DeCo	6.38	0.015	54.97	16.8	0.023

Table 2.A3 - Kinetic data of the reaction of CO_2 with potassium glycinate at 0.299 M and 298 K

$P_{CO_2} \times 10^{-2}$ (Pa)	$J_{CO_2} \times 10^4$ $\left(\text{mol} \cdot \text{s}^{-1} \cdot \text{m}^{-2}\right)$	$\alpha_{máx}$ $\left(\text{mol}_{CO_2} \cdot \text{mol}_{AmA}^{-1}\right)$	$P_{CO_2} \times 10^{-2}$ (Pa)	$J_{CO_2} \times 10^4$ $\left(\text{mol} \cdot \text{s}^{-1} \cdot \text{m}^{-2}\right)$	$\alpha_{máx}$ $\left(\text{mol}_{CO_2} \cdot \text{mol}_{AmA}^{-1}\right)$
2.71 PFO/DeCo	1.78	0.004	9.76 DeCo	5.80	0.013
3.52 PFO/DeCo	2.50	0.002	9.82 DeCo	6.27	0.015
4.77 PFO/DeCo	3.09	0.007	10.56 DeCo	6.44	0.015
5.89 PFO/DeCo	4.14	0.010	11.66 DeCo	6.79	0.016
6.71 PFO/DeCo	4.33	0.010	16.71	9.02	0.021
7.18 PFO/DeCo	4.99	0.012	26.66	13.3	0.031
7.74 PFO/DeCo	5.16	0.012	41.96	16.3	0.040
8.82 DeCo	5.55	0.013			

Table 2.A4 - Kinetic data of the reaction of CO_2 with potassium glycinate at 0.299 M and 303 K

$P_{CO_2} \times 10^{-2}$ (Pa)	$J_{CO_2} \times 10^4$ $\left(\text{mol} \cdot \text{s}^{-1} \cdot \text{m}^{-2}\right)$	$\alpha_{máx}$ $\left(\text{mol}_{CO_2} \cdot \text{mol}_{AmA}^{-1}\right)$	$P_{CO_2} \times 10^{-2}$ (Pa)	$J_{CO_2} \times 10^4$ $\left(\text{mol} \cdot \text{s}^{-1} \cdot \text{m}^{-2}\right)$	$\alpha_{máx}$ $\left(\text{mol}_{CO_2} \cdot \text{mol}_{AmA}^{-1}\right)$
2.10 PFO/DeCo	1.64	0.004	11.34 DeCo	8.62	0.021
3.94 PFO/DeCo	3.12	0.007	16.37	11.6	0.027
5.22 PFO/DeCo	4.36	0.010	31.74	17.3	0.040
6.00 PFO/DeCo	4.66	0.010	56.62	21.2	0.051
8.17 DeCo	6.62	0.015			

Table 2.A5 - Kinetic data of the reaction of CO_2 with potassium glycinate at 0.587 M and 293 K

$P_{CO_2} \times 10^{-2}$ (Pa)	$J_{CO_2} \times 10^4$ $\left(\text{mol} \cdot \text{s}^{-1} \cdot \text{m}^{-2}\right)$	$\alpha_{máx}$ $\left(\text{mol}_{CO_2} \cdot \text{mol}_{AmA}^{-1}\right)$	$P_{CO_2} \times 10^{-2}$ (Pa)	$J_{CO_2} \times 10^4$ $\left(\text{mol} \cdot \text{s}^{-1} \cdot \text{m}^{-2}\right)$	$\alpha_{máx}$ $\left(\text{mol}_{CO_2} \cdot \text{mol}_{AmA}^{-1}\right)$
2.16 PFO/DeCo	1.54	0.002	12.19 PFO/DeCo	8.11	0.010
2.22 PFO/DeCo	1.50	0.002	15.00 PFO/DeCo	9.67	0.007
4.43 PFO/DeCo	3.43	0.004	15.00 PFO/DeCo	9.73	0.008
4.46 PFO/DeCo	3.29	0.004	23.75	13.5	0.013
7.62 PFO/DeCo	5.28	0.006	24.79	13.5	0.011
9.47 PFO/DeCo	6.26	0.006	24.85	13.5	0.013
9.51 PFO/DeCo	6.38	0.009	35.42	19.4	0.015
10.12 PFO/DeCo	6.62	0.009	45.50	22.7	0.018
12.06 PFO/DeCo	8.10	0.010	62.55	26.7	0.020

Table 2.A6 - Kinetic data of the reaction of CO_2 with potassium glycinate at 0.587 M and 298 K

$P_{CO_2} \times 10^{-2}$ (Pa)	$J_{CO_2} \times 10^4$ $\left(\text{mol} \cdot \text{s}^{-1} \cdot \text{m}^{-2}\right)$	α_{max} $\left(\text{mol}_{CO_2} \cdot \text{mol}_{AmA}^{-1}\right)$	$P_{CO_2} \times 10^{-2}$ (Pa)	$J_{CO_2} \times 10^4$ $\left(\text{mol} \cdot \text{s}^{-1} \cdot \text{m}^{-2}\right)$	α_{max} $\left(\text{mol}_{CO_2} \cdot \text{mol}_{AmA}^{-1}\right)$
5.08 PFO/DeCo	5.01	0.003	20.57	17.4	0.011
5.22 PFO/DeCo	4.49	0.005	20.75	17.8	0.010
7.91 PFO/DeCo	7.26	0.008	30.88	22.2	0.016
7.94 PFO/DeCo	7.32	0.008	41.00	28.2	0.016
10.48 PFO/DeCo	9.47	0.007	41.11	26.2	0.017
10.51 PFO/DeCo	9.50	0.006	49.65	31.3	0.018
15.54 PFO/DeCo	13.9	0.008	67.11	33.7	0.034
15.55 PFO/DeCo	14.7	0.008	67.20	31.7	0.022
20.41	15.9	0.009	68.41	37.4	0.026
20.53	16.4	0.010	68.44	35.0	0.021

Table 2.A7 - Kinetic data of the reaction of CO_2 with potassium glycinate at 0.587 M and 303 K

$P_{CO_2} \times 10^{-2}$ (Pa)	$J_{CO_2} \times 10^4$ $\left(\mathrm{mol \cdot s^{-1} \cdot m^{-2}}\right)$	α_{max} $\left(\mathrm{mol_{CO_2} \cdot mol^{-1}_{AmA}}\right)$	$P_{CO_2} \times 10^{-2}$ (Pa)	$J_{CO_2} \times 10^4$ $\left(\mathrm{mol \cdot s^{-1} \cdot m^{-2}}\right)$	α_{max} $\left(\mathrm{mol_{CO_2} \cdot mol^{-1}_{AmA}}\right)$
2.50 PFO/DeCo	3.06	0.003	11.61 PFO/DeCo	12.8	0.014
4.58 PFO/DeCo	5.35	0.006	16.95	16.5	0.021
6.60 PFO/DeCo	7.52	0.008	31.56	26.0	0.025
8.52 PFO/DeCo	10.0	0.011	56.87	36.7	0.022

Table 2.A8 - Kinetic data of the reaction of CO_2 with potassium glycinate at 0.999 M and 293 K

$P_{CO_2} \times 10^{-2}$ (Pa)	$J_{CO_2} \times 10^4$ $\left(\mathrm{mol \cdot s^{-1} \cdot m^{-2}}\right)$	α_{max} $\left(\mathrm{mol_{CO_2} \cdot mol^{-1}_{AmA}}\right)$	$P_{CO_2} \times 10^{-2}$ (Pa)	$J_{CO_2} \times 10^4$ $\left(\mathrm{mol \cdot s^{-1} \cdot m^{-2}}\right)$	α_{max} $\left(\mathrm{mol_{CO_2} \cdot mol^{-1}_{AmA}}\right)$
5.42 PFO/DeCo	6.26	0.004	15.46 PFO/DeCo	17.4	0.012
7.06 PFO/DeCo	8.82	0.006	16.54 PFO/DeCo	19.0	0.013
10.37 PFO/DeCo	11.3	0.008	20.42	18.8	0.012
10.43 PFO/DeCo	11.0	0.007	20.48	18.9	0.011
12.27 PFO/DeCo	13.9	0.009	25.59	25.6	0.017
13.61 PFO/DeCo	13.8	0.010	35.30	32.3	0.018
13.86 PFO/DeCo	16.3	0.010	45.53	37.7	0.017
15.23 PFO/DeCo	17.2	0.011	55.70	42.1	0.017
15.42 PFO/DeCo	15.8	0.010			

Table 2.A9 - Kinetic data of the reaction of CO_2 with potassium glycinate at 0.999 M and 298 K

$P_{CO_2} \times 10^{-2}$ (Pa)	$J_{CO_2} \times 10^4$ $\left(\mathrm{mol \cdot s^{-1} \cdot m^{-2}}\right)$	α_{max} $\left(\mathrm{mol_{CO_2} \cdot mol^{-1}_{AmA}}\right)$	$P_{CO_2} \times 10^{-2}$ (Pa)	$J_{CO_2} \times 10^4$ $\left(\mathrm{mol \cdot s^{-1} \cdot m^{-2}}\right)$	α_{max} $\left(\mathrm{mol_{CO_2} \cdot mol^{-1}_{AmA}}\right)$
2.53 PFO/DeCo	3.95	0.002	15.64 PFO/DeCo	20.6	0.013
7.74 PFO/DeCo	10.5	0.006	17.59	22.5	0.015
9.15 PFO/DeCo	12.7	0.009	17.62	23.2	0.010
9.33 PFO/DeCo	12.8	0.008	22.64	25.2	0.013
10.62 PFO/DeCo	15.2	0.010	27.52	28.0	0.017
11.08 PFO/DeCo	15.2	0.010	32.98	32.7	0.017
12.68 PFO/DeCo	17.6	0.011	55.02	43.4	0.016
13.78 PFO/DeCo	18.1	0.011	67.09	48.8	0.015
15.26 PFO/DeCo	20.9	0.014			

Table 2.A10 - Kinetic data of the reaction of CO_2 with potassium glycinate at 0.999 M and 303 K.

$P_{CO_2} \times 10^{-2}$ (Pa)	$J_{CO_2} \times 10^4$ $\left(\mathrm{mol \cdot s^{-1} \cdot m^{-2}}\right)$	α_{max} $\left(\mathrm{mol_{CO_2} \cdot mol^{-1}_{AmA}}\right)$	$P_{CO_2} \times 10^{-2}$ (Pa)	$J_{CO_2} \times 10^4$ $\left(\mathrm{mol \cdot s^{-1} \cdot m^{-2}}\right)$	α_{max} $\left(\mathrm{mol_{CO_2} \cdot mol^{-1}_{AmA}}\right)$
3.42 PFO/DeCo	4.99	0.003	10.54 PFO/DeCo	15.5	0.010
5.23 PFO/DeCo	7.68	0.005	11.59 PFO/DeCo	16.9	0.011
6.94 PFO/DeCo	10.0	0.007	17.70	24.7	0.016
8.59 PFO/DeCo	11.9	0.007	27.91	34.7	0.016
9.23 PFO/DeCo	13.4	0.009	57.65	54.7	0.020

Table 2.A11 - Kinetic data of the reaction of CO_2 with potassium glycinate at 1.984 M and 293 K.

$P_{CO_2} \times 10^{-2}$ (Pa)	$J_{CO_2} \times 10^{4}$ $\left(\mathrm{mol \cdot s^{-1} \cdot m^{-2}}\right)$	α_{max} $\left(\mathrm{mol_{CO_2} \cdot mol^{-1}_{AmA}}\right)$	$P_{CO_2} \times 10^{-2}$ (Pa)	$J_{CO_2} \times 10^{4}$ $\left(\mathrm{mol \cdot s^{-1} \cdot m^{-2}}\right)$	α_{max} $\left(\mathrm{mol_{CO_2} \cdot mol^{-1}_{AmA}}\right)$
2.77 PFO/DeCo	3.35	0.001	15.16 PFO/DeCo	19.6	0.006
4.76 PFO/DeCo	6.11	0.002	15.51 PFO/DeCo	18.6	0.006
6.74 PFO/DeCo	8.33	0.003	16.07 PFO/DeCo	18.4	0.006
7.71 PFO/DeCo	9.33	0.003	16.47 PFO/DeCo	21.2	0.006
8.31 PFO/DeCo	9.23	0.004	21.75	20.4	0.007
8.61 PFO/DeCo	11.6	0.004	21.78	19.8	0.007
8.74 PFO/DeCo	9.67	0.003	24.81	24.2	0.008
10.49 PFO/DeCo	13.9	0.004	25.00	24.1	0.008
10.78 PFO/DeCo	12.4	0.004	26.84	27.4	0.009
10.81 PFO/DeCo	12.1	0.004	36.88	35.0	0.009
12.56 PFO/DeCo	15.7	0.005	47.01	40.2	0.007
13.07 PFO/DeCo	18.2	0.006	57.00	47.9	0.008
13.26 PFO/DeCo	13.9	0.005	77.29	55.9	0.010

Table 2.A12 - Kinetic data of the reaction of CO_2 with potassium glycinate at 1.984 M and 298 K.

$P_{CO_2} \times 10^{-2}$ (Pa)	$J_{CO_2} \times 10^4$ $\left(\mathrm{mol \cdot s^{-1} \cdot m^{-2}}\right)$	α_{max} $\left(\mathrm{mol_{CO_2} \cdot mol^{-1}_{AmA}}\right)$	$P_{CO_2} \times 10^{-2}$ (Pa)	$J_{CO_2} \times 10^4$ $\left(\mathrm{mol \cdot s^{-1} \cdot m^{-2}}\right)$	α_{max} $\left(\mathrm{mol_{CO_2} \cdot mol^{-1}_{AmA}}\right)$
3.34 PFO/DeCo	5.12	0.001	13.53 PFO/DeCo	21.9	0.006
5.20 PFO/DeCo	7.51	0.002	14.33 PFO/DeCo	21.5	0.007
5.28 PFO/DeCo	7.01	0.002	15.36 PFO/DeCo	22.9	0.007
8.37 PFO/DeCo	13.3	0.004	17.34	27.3	0.007
9.31 PFO/DeCo	15.5	0.005	17.50	29.4	0.008
10.06 PFO/DeCo	13.8	0.005	19.42	29.4	0.008
10.24 PFO/DeCo	14.4	0.003	19.47	28.0	0.009
11.09 PFO/DeCo	16.6	0.005	21.52	26.8	0.008
11.30 PFO/DeCo	15.8	0.005	24.52	30.3	0.007
11.32 PFO/DeCo	15.3	0.005	29.47	33.9	0.007
12.52 PFO/DeCo	17.1	0.005	49.46	52.5	0.008
12.54 PFO/DeCo	18.5	0.005	69.86	66.3	0.007
13.42 PFO/DeCo	19.6	0.006			

Table 2.A13 - Kinetic data of the reaction of CO_2 with potassium glycinate at 1.984 M and 303 K.

$P_{CO_2} \times 10^{-2}$ (Pa)	$J_{CO_2} \times 10^4$ $\left(\mathrm{mol \cdot s^{-1} \cdot m^{-2}}\right)$	α_{max} $\left(\mathrm{mol_{CO_2} \cdot mol^{-1}_{AmA}}\right)$	$P_{CO_2} \times 10^{-2}$ (Pa)	$J_{CO_2} \times 10^4$ $\left(\mathrm{mol \cdot s^{-1} \cdot m^{-2}}\right)$	α_{max} $\left(\mathrm{mol_{CO_2} \cdot mol^{-1}_{AmA}}\right)$
5.44 PFO/DeCo	10.6	0.003	11.52 PFO/DeCo	21.9	0.007
7.44 PFO/DeCo	14.8	0.005	14.34 DeCo	23.8	0.008
9.51 PFO/DeCo	19.1	0.006			

Table 2.A14 - Kinetic data of the reaction of CO_2 with potassium glycinate at 3.005 M and 298 K.

$P_{CO_2} \times 10^{-2}$ (Pa)	$J_{CO_2} \times 10^{4}$ $\left(\mathrm{mol \cdot s^{-1} \cdot m^{-2}}\right)$	α_{max} $\left(\mathrm{mol_{CO_2} \cdot mol_{AmA}^{-1}}\right)$	$P_{CO_2} \times 10^{-2}$ (Pa)	$J_{CO_2} \times 10^{4}$ $\left(\mathrm{mol \cdot s^{-1} \cdot m^{-2}}\right)$	α_{max} $\left(\mathrm{mol_{CO_2} \cdot mol_{AmA}^{-1}}\right)$
$3.43^{\mathrm{PFO/DeCo}}$	5.45	0.001	21.61	35.6	0.007
$6.37^{\mathrm{PFO/DeCo}}$	11.4	0.003	26.49	38.4	0.008
$11.44^{\mathrm{PFO/DeCo}}$	19.0	0.004	31.32	44.1	0.006
$16.46^{\mathrm{PFO/DeCo}}$	26.7	0.005	51.45	60.3	0.005

3. Carbon dioxide absorption kinetics in potassium threonate[1]

Abstract

The absorption of carbon dioxide in potassium threonate aqueous solutions is studied at concentrations ranging from 0.1 to 3 M and temperatures from 293 to 313 K. This study includes experimental density, viscosity, solubility of N_2O and absorption kinetics of CO_2 (using a stirred cell reactor) data obtained for the various potassium threonate solutions. The diffusion coefficients of CO_2 and potassium threonate in the absorption solutions are estimated using a modified Stokes-Einstein relation. N_2O solubility is interpreted using the Schumpe (1993) model and CO_2 physical solubility estimated. Physical absorption experiments were performed in the stirred cell in order to determine the physical mass transfer coefficients. The kinetics results are interpreted using both the pseudo-first order and the DeCoursey approaches. It was concluded that CO_2 absorption in the aqueous potassium threonate solutions is well represented by $-r_{CO_2} = 4.13\times10^{8} \exp\left(\frac{-3580}{T}\right) C_S \exp\left(0.90\, C_S\right) C_{CO_2}$.

[1] Portugal, A. F.; Magalhães, F. D.; Mendes, A., "Carbon dioxide absorption kinetics in potassium threonate", Chem. Eng. Sci, 2008, 63(13), 3493-3503

3.1. Introduction

The constant emissions of CO_2 (due to the burning of fossil fuels, coal and natural gas) have originated the rise of atmospheric concentrations to such values that the earth's natural absorption processes have become inefficient (Hampe and Rudkevich, 2003). For this reason, several technologies for the capture of CO_2 are being continuously developed, especially in the last years, as a consequence of the stringent environmental regulations stated on the Kyoto protocol (Granite and O'Brien, 2005; Idem and Tontiwachwuthikul, 2006; Yan et al., 2007). Among these, the absorption of CO_2 in alkanolamines is, at present, the most widely used technology in the chemical industry (Holst et al., 2006; Idem and Tontiwachwuthikul, 2006). However, alkanolamines easily degrade, especially in oxygenated environments, making necessary the development of new absorbents for gas mixtures with significant oxygen concentrations, namely for flue gas, life support systems and anesthetic gas circuits (Goff and Rochelle, 2006; Holst et al., 2006; Hook, 1997; Mendes, 2000; Portugal et al., 2007; Supap et al., 2006).

Amino acids (or, more precisely, alkali salts of amino acids) have the same functional group as alkanolamines (presenting therefore similar capacities and reaction rates with CO_2) and are much more stable in the presence of oxygen (Holst et al., 2006; Kumar et al., 2003c). Besides, due to the ionic nature of the solutions, they present lower volatilities and higher surface tensions (Kumar et al., 2002). Nevertheless, precipitation of the reaction products was observed during the absorption of CO_2 in several absorbent solutions based on amino acids (Hook, 1997; Kumar et al., 2003a). Commercially, amino acids are being used mainly as promoters of the absorption of carbon dioxide in carbonate-bicarbonate solutions (Jeffreys and Bull, 1964; Kohl and Nielsen, 1997). Companies including Giammarco Vetrocoke, BASF, TNO and Exxon use amino acids in their CO_2 removal absorption liquids (Feron and Jansen, 2002; Kumar et al., 2003c). Although the use of amino acids is becoming an attractive option, data about the absorption of CO_2 in their solutions is still scarce. The present work aims to contribute for the characterization and understanding of amino acid salt solutions (namely, aqueous solutions of potassium threonate) as CO_2 absorbents.

The general ability of an amine based compound to absorb CO_2 is related to its molecular structure (Caplow, 1968; Hook, 1997; Penny and Ritter, 1983; Sartori and Savage, 1983; Singh et al., 2007). Potassium threonate, shown in Figure 3.1, is a relatively small amino acid salt, which makes it expectable to present better absorption equilibrium and kinetics than bigger molecules (Singh et al., 2007); it is a primary amine containing both potassium carboxylate and alcohol groups in its structure. It is sterically hindered, but the α carbon (carbon adjacent to the amine group) is only mono-substituted. It is expected to have the properties of the sterically hindered amines (high capacity and relatively easy regeneration) (Hook, 1997; Sartori and Savage, 1983) and simultaneously, since it is a primary amine and the α carbon is only mono-substituted, it is likely to absorb CO_2 at a reasonable rate, without precipitation at low loadings (Hook, 1997). It is also expected to combine the properties conferred by the potassium carboxylate group - good oxidation stability, low volatility and high surface tension – with the good regeneration properties conferred by the alcohol group (Hook, 1997). For these reasons along with the fact of not being harmful for the health, it was selected for being characterized for carbon dioxide absorption.

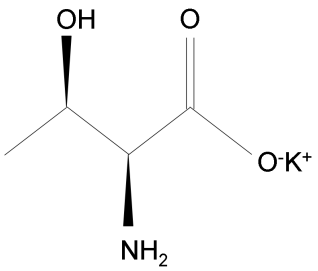

Figure 3.1 - Chemical structure of potassium threonate.

3.2. Reaction Mechanism

Generally it is accepted that the absorption of CO_2 in amine based compounds with a primary or secondary amine group occurs according to the so-called zwitterion mechanism (Caplow, 1968; Derks et al., 2006; Kumar et al., 2003c; Portugal et al., 2007), being the overall reaction rate, $-r_{CO_2}$, given by:

$$-r_{CO_2} = \frac{k_2}{1+\frac{k_{-1}}{\sum_i k_{B_i} C_{B_i}}} C_S C_{CO_2} \quad (1)$$

where k_2, k_{-1} and k_{B_i} are the zwitterion mechanism kinetic constants, C_S is the concentration of the amino acid salt, C_{CO_2} is the concentration of carbon dioxide in the liquid and C_{B_i} are the concentrations of the bases that can deprotonate the zwitterion - H_2O, OH^- and the amine itself (R_1R_2NH) (Blauwhoff et al., 1984). However, since potassium threonate is a weak base - $pK_A = 9.100$ at 25 ºC (Perrin, 1965) - the contribution of OH^- to the deprotonation of the zwitterion can be neglected (Kumar et al., 2003c) as well as the parallel reaction of CO_2 with OH^- to form bicarbonate. Additionally, in primary amines such as monoethanolamine (MEA) and potassium glycinate usually the deprotonation of the zwitterion is relatively fast when compared to the rate of the reverse reaction (Derks et al., 2006; Kumar et al., 2003c; Portugal et al., 2007) and therefore, equation (1) is simplified to a second order reaction kinetics:

$$-r_{CO_2} = k_2 C_S C_{CO_2} \quad (2)$$

To be thermodynamically consistent, the CO_2 absorption rate should be expressed in terms of activities rather than concentrations (Haubrock et al., 2007). However, for the purposes of the present work – to describe the absorption in a single absorption system – it is enough to account for the solution non-idealities by means of the semi-empirical equation (8) (Cullinane and Rochelle, 2006):

$$k_{eff} = k \exp(bI) \quad (3)$$

where k_{eff} is the effective kinetic constant, corrected by the ionic strength of the solution, b is a constant and I is the ionic strength given by $I = \frac{1}{2}\sum C_i z_i^2$, where C_i and z_i are respectively the molar concentration and the charge of ion i in solution.

3.3. Mass Transfer

The absorption of CO_2 into lean potassium threonate solutions can be described by the following equation (Danckwerts, 1970):

$$N_{CO_2} = E\, k_L \frac{P_{CO_2}}{H_{CO_2}} A \tag{4}$$

where N_{CO_2} is the molar flow of CO_2 crossing the liquid surface with interfacial area A, k_L is the physical mass transfer coefficient, P_{CO_2} is the CO_2 partial pressure and H_{CO_2} is the Henry constant of CO_2 in solution. The enhancement factor, E, is the ratio between the amount of gas absorbed in the reactive liquid and the amount that would be absorbed if no reaction took place. The enhancement factor is a function of the Hatta number, Ha, and the infinite enhancement factor, E_∞ (Danckwerts, 1970; Derks et al., 2006). The dimensionless Hatta number is defined as:

$$Ha = \frac{\sqrt{k_{ov} D_{CO_2}}}{k_L} \tag{5}$$

where k_{ov} is the overall reaction kinetic constant ($k_{ov} = -r_{CO_2} / C_{CO_2}$) and D_{CO_2} is the diffusion coefficient of CO_2 in solution. According to the penetration theory (Higbie, 1935), the infinite enhancement factor can be estimated by the following equation:

$$E_\infty = \sqrt{\frac{D_{CO_2}}{D_S}} + \frac{C_S \times 10^3}{\nu_S \frac{P_{CO_2}}{H_{CO_2}}} \sqrt{\frac{D_S}{D_{CO_2}}} \tag{6}$$

where D_S is the amino acid salt diffusion coefficient and ν_S is the stoichiometric coefficient. Factor 10^3 is there to convert $\mathrm{mol \cdot dm^{-3}}$ (M) into $\mathrm{mol \cdot m^{-3}}$.

If Ha is sufficiently lower than E_∞, fast pseudo-first order (PFO) reaction regime can be assumed (Danckwerts, 1970; Derks et al., 2006; Portugal et al., 2007):

$$3 < Ha < \sim 0.1 E_\infty \tag{7}$$

In this case, diffusion and reaction occur in parallel in the liquid film. The enhancement factor can be considered equal to the Hatta number and the gas absorption rate becomes, therefore, independent of the physical mass transfer coefficient.

If $E_\infty << Ha$, instantaneous reaction regime can be considered and $E = E_\infty$. In this situation, the enhancement to the mass transfer is determined by the diffusion of the reactants and do not depend on the reaction kinetic constant.

Between the limiting situations of fast pseudo-first order and instantaneous reaction regime, there is the intermediate regime. According to DeCoursey, the enhancement factor in the intermediate regime can be approximated as a function of the Hatta number and the infinite enhancement factor (DeCoursey, 1974; Van Swaaij and Versteeg, 1992):

$$E = -\frac{Ha^2}{2(E_\infty - 1)} + \sqrt{\frac{Ha^4}{4(E_\infty - 1)^2} + \frac{E_\infty Ha^2}{E_\infty - 1} + 1} \tag{8}$$

3.4. Physical Properties

Since CO_2 reacts with potassium threonate, its physical solubility and diffusivity in solution need to be measured indirectly using a non-reactive gas with similar properties, usually N_2O (Joosten and Danckwerts, 1972; Laddha et al., 1981).

Amino acid salt solutions are ionic in nature. For this reason, a "salting out" effect needs to be taken into account when interpreting the solubility data of gases in these solutions. At moderately high salt concentrations, this effect can be accounted for using the Sechenov relation:

$$\log\left(\frac{H}{H_w}\right) = K \cdot C_S \tag{9}$$

where H and H_w are respectively the Henry constants of the gas in the amino acid salt solution and in water and K is the Sechenov constant, which can be calculated by equation (12) (Schumpe, 1993; Weisenberger and Schumpe, 1996):

$$K = \sum (h_i + h_G) n_i \tag{10}$$

where h_i and h_G are the ion and gas specific parameters and n_i is the valency number of the ion.

It is generally accepted that the diffusion coefficient of a diffusant in solution can be related to the solution viscosity, η, through modified Stokes-Einstein equation (Brilman

et al., 2001; Joosten and Danckwerts, 1972; Kumar et al., 2001; Versteeg and Van Swaaij, 1988):

$$D\eta^{\alpha} = \text{constant} \tag{11}$$

where α is a constant that depends on the pair diffusant/solvent.

It can be considered $\alpha = 0.8$ to estimate the diffusion coefficient of N_2O in the aqueous solutions of potassium threonate (Versteeg and Van Swaaij, 1988; Joosten and Danckwerts, 1972; Brilman et al., 2001) and $\alpha = 0.6$ to estimate the diffusion coefficient of the amino acid salt in solutions (Versteeg and Van Swaaij, 1988; Snijder et al., 1993).

Gubbins et al. (1966) found that the ratio of the diffusivity of a gas in an electrolyte solution to the diffusivity of the same gas in water does not vary significantly with the nature of the diffusant. Therefore, it is reasonable to use the so-called N_2O analogy to estimate the diffusion coefficient of CO_2 in solutions.

$$\frac{D_{N_2O}}{D_{N_2O,w}} = \frac{D_{CO_2}}{D_{CO_2,w}} \tag{12}$$

To estimate the diffusion coefficient of the salt at infinite dilution, D_S^0, the Nernst equation for the diffusion in electrolyte solutions can be applied (Poling et al., 2001):

$$D_S^0 = \frac{RT\left[\left(1/z_+\right)+\left(1/z_-\right)\right]}{F^2\left[\left(1/\lambda_+^0\right)+\left(1/\lambda_-^0\right)\right]} \tag{13}$$

where F is the Faraday constant, z_+ and z_- are the valencies of the cation and anion respectively and λ_+^0 and λ_-^0 are the ionic conductances of the cation and anion respectively at infinite dilution.

The physical mass transfer coefficient, k_L, is related to the pair gas/solution and to the apparatus where the mass transfer takes place through the empirical expression referred by Versteeg et al. (1987):

$$\text{Sh} = c_2\,\text{Re}^{c_3}\,\text{Sc}^{c_4} \tag{14}$$

where Sh, Re and Sc are respectively the Sherwood, Reynolds and Schmidt dimensionless numbers and the constants c_2, c_3 and c_4 depend on the specific apparatus. Performing experiments with a known and non-reactive gas/fluid pair (for example CO_2/water or N_2O/solution) at different temperatures and stirring speeds, it is possible to determine the constants of equation (14) and consequently, to estimate the k_L of a given reactive system.

3.5. Experimental

Chemicals

The potassium threonate aqueous solutions were prepared by adding to the amino acid an equimolar amount of potassium hydroxide (KOH) in a volumetric flask filled up with distilled and deionised water. It is important to notice that before the addition of KOH, the amino acid exists in solution as a zwitterion (with the amine group protonated). The addition of potassium hydroxide to form the potassium carboxylate group will deprotonate the amine group enabling it to react with carbon dioxide (Kumar et al., 2003c).

Density and Viscosity

Densities of potassium threonate solutions at 293, 298, 303 and 313 K were determined using hydrometers series M100, ranges 1.000 to 1.100 and 1.100 to 1.200 ± 0.002 $g \cdot ml^{-1}$.

Viscosities of the solutions of potassium threonate were determined using a standard Cannon-Fenske viscosimeter.

N_2O solubility

The procedure adopted to measure the solubility of N_2O in the amino acid salt solutions is described in detail by Derks et al. (2005) and Portugal et al. (2007). The set-up used is composed of two vessels with calibrated volumes; one for storing the N_2O and the other for the absorbent solution, which is magnetically stirred. A known volume of degassed solution is transferred to the absorbent vessel and the solution vapour pressure, P_{vapour}, recorded (pressure sensor from Druck, PMP4000, 0-350 mbar, accuracy: 0.08% FS). A certain amount of N_2O is allowed to enter the absorbent tank from the gas vessel and the initial pressure, P_0, recorded. The stirrer is then switched on and the solution equilibrium is allowed to be established (the final pressure, P_{eq}, is recorded as well as the temperature, T_0). The temperature is then set to a different value, T, and a new equilibrium state is obtained; this procedure is repeated for the temperatures at which the solubility is to be determined. The solution is weighed at the end of the experiment. The amount of absorbed gas is calculated applying the ideal gas law and the Henry coefficient for N_2O, H_{N_2O}, is computed from the equation:

$$H_{N_2O}(T) = \frac{\left[P_{eq}(T) - P_{vapour}(T)\right]}{\frac{\left[P_0 - P_{vapour}(T_0)\right]}{T_0} - \frac{\left[P_{eq}(T) - P_{vapour}(T)\right]}{T}} \left(\frac{RV_L}{V_G}\right) \tag{15}$$

where V_G and V_L are respectively the volume of gas and liquid in the absorbent vessel and R is the universal gas constant. The solution vapour pressure at each temperature is estimated by the following relation:

$$P_{vapour}(T) = x_{H_2O} P_{H_2O}^{pure}(T) \tag{16}$$

where x_{H_2O} is the molar fraction of water in solution. The water vapour pressure as a function of the absolute temperature, $P_{H_2O}^{pure}(T)$, is obtained from the Antoine equation (Poling et al., 2001).

Kinetic measurements

The experiments were performed in a stirred cell reactor with a smooth gas-liquid interface operating batchwise with respect to the liquid phase and semi-continuously

with respect to the gas phase. Although experiments were performed in a different set-up (much smaller – liquid volume: 50 cm^3, reactor diameter: 3.87 cm, stirrer diameter: 2 cm), the followed procedure is the same of the one described by Derks et al. (2006) and Portugal et al. (2007) and will be only briefly summarized here. Before starting the experiment, the vapour-liquid equilibrium of the fresh solution of potassium threonate, previously degassed, is established in the absorbent vessel and the vapour pressure, P_{vapour}, recorded (pressure sensor from Druck, PMP4000, 0-350 mbar, accuracy: 0.08% FS). During the experiment, the pressure inside the stirred reactor is kept constant, P_{SC}, using a pressure controller (Bronkhorst, P602-C, 0-200 mbar, accuracy: 0.5% FS) while CO_2 from the gas vessel (filled with pure CO_2) is being fed to it. All CO_2 that is being absorbed in the stirred cell comes from the gas vessel and therefore the flow of absorbed CO_2 can be computed following the pressure decrease inside the gas vessel, $\frac{dP_{GV}}{dt}$, (pressure sensor from Druck, PMP4000, 0-2 bar, accuracy: 0.08% FS). Since the CO_2 absorption inside the stirred cell reactor is described by equation (9), after replacing N_{CO_2} by the pressure derivative and noticing that $P_{CO_2} = P_{SC} - P_{vapour}$, one obtains the following expression:

$$\frac{V_{GV}}{RT}\frac{dP_{GV}}{dt} = E\,k_L\,\frac{P_{SC} - P_{vapour}}{H_{CO_2}}\,A \qquad (17)$$

where V_{GV} is the volume of the gas vessel. Finally, the experimental kinetic constant can be extracted from the computed enhancement factor, depending on the absorption reaction regime.

Figure 3.2 shows a sketch of the experimental setup.

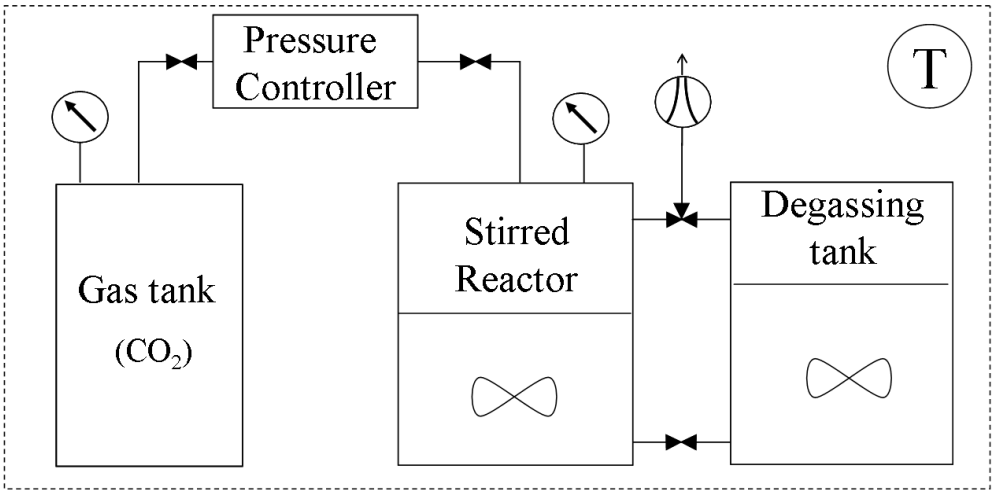

Figure 3.2 – Experimental set-up sketch.

Physical mass transfer coefficient

The physical mass transfer coefficient, necessary for equation (17), was obtained from experimental data of CO_2 absorption in water (at different temperatures) and N_2O in water and in potassium threonate solutions; the experimental set-up shown in Figure 3.2 was used. At a given temperature, a known volume of degassed water or absorbent solution is placed in the stirred reactor, the vapour-liquid equilibrium allowed to be established and the vapour pressure, P_{vapour}, recorded. Then, a certain amount of CO_2 or N_2O is admitted in the reactor, while the stirrer is switched off, and the initial pressure, P_0, recorded. The stirrer is then switched on, at a given stirring speed, and the pressure history inside the reactor recorded. The procedure is repeated for different stirring speeds given that a smooth gas-liquid interface is ensured. Only physical absorption takes place, since the gas/liquid pairs are non-reactive (pairs CO_2/water and N_2O/absorbent aqueous solutions); for this reason, equation (9) becomes:

$$N_{CO_2} = \frac{V_G}{RT}\frac{dP_{CO_2}}{dt} = k_L A\left(\frac{P_{CO_2}}{H_{CO_2}} - C_{CO_2}\right) \tag{18}$$

where C_{CO_2} is the absorbed gas concentration and V_G is the volume of gas above the liquid in the stirred reactor. Performing a mass balance to the stirred reactor one obtains:

$C_{CO_2} = \frac{\left(P_{0,CO_2} - P_{CO_2}\right)}{RT}\frac{V_G}{V_L}$ where $P_{0,CO_2} = P_0 - P_{vapour}$. Solving equation (18), it becomes:

$$\ln\left(\frac{\left(\frac{RT}{H_{CO_2}}V_L+V_G\right)\frac{P_{CO_2}}{P_{0,CO_2}}-V_G}{\frac{RT}{H_{CO_2}}V_L}\right)=-k_L A\left(\frac{RT}{H_{CO_2}V_G}+\frac{1}{V_L}\right)t \qquad (19)$$

Note that equation (19) derived for the CO_2 physical absorption is also valid for N_2O.

3.6. Results and Discussion

Density and viscosity

Densities and viscosities of potassium threonate solutions at temperatures from 273 to 313 K and concentrations from 0.1 to 3.0 M were determined and are presented in Table 3.1.

N_2O and CO_2 solubility

The experimental solubility of N_2O and CO_2 in water was experimentally determined and it is given in Table 3.2. Although the Henry coefficients values obtained for N_2O are in line with the ones reported in literature (Abu-Arabi et al., 2001), the values for carbon dioxide in water are slightly below to what is reported by Abu-Arabi et al. (2001).

The experimental solubility of N_2O in potassium threonate solutions is given in Table 3.2.

The results were interpreted using equation (9) and are presented graphically in Figure 3.3.

Table 3.1 – Densities and viscosities of potassium threonate solutions.

C_S (M) \ T (K)	293		298		303		313	
	ρ $(\mathrm{kg \cdot m^{-3}})$	$\eta \times 10^3$ $(\mathrm{kg \cdot m^{-1} \cdot s^{-1}})$	ρ $(\mathrm{kg \cdot m^{-3}})$	$\eta \times 10^3$ $(\mathrm{kg \cdot m^{-1} \cdot s^{-1}})$	ρ $(\mathrm{kg \cdot m^{-3}})$	$\eta \times 10^3$ $(\mathrm{kg \cdot m^{-1} \cdot s^{-1}})$	ρ $(\mathrm{kg \cdot m^{-3}})$	$\eta \times 10^3$ $(\mathrm{kg \cdot m^{-1} \cdot s^{-1}})$
0.1	1006	1.036	1004	0.929	1003	0.830	1000	0.683
0.3	1020	1.126	1018	1.007	1017	0.899	1014	0.785
0.6	1040	1.254	1038	1.146	1037	1.024	1034	0.888
1.0	1067	1.541	1065	1.355	1064	1.216	1061	1.080
2.0	1132	2.555	1131	2.276	1129	1.991	1125	1.577
3.0	1192	5.116	1190	3.984	1188	3.409	1184	2.827

Table 3.2 - Henry constants of N_2O and CO_2 in water and in potassium threonate solutions. All values are experimental except for CO_2 in potassium threonate solutions that were computed based on Sechenov's model - $H\,(\mathrm{Pa \cdot m^3 \cdot mol^{-1}})$.

C_S (M) \ T (K)	293		298		303		313	
	N_2O	CO_2	N_2O	CO_2	N_2O	CO_2	N_2O	CO_2
Water	3357	2442	3831	2771	4353	3132	5551	3953
0.1	3490	2520	3980	2854	4519	3219	5755	4048
0.3	3735	2683	4235	3026	4781	3400	6025	4244
0.6	4201	2949	4748	3305	5345	3691	6697	4557
1.0	4844	3344	5418	3717	6037	4119	7419	5009
2.0	6842	4578	7499	4987	8194	5418	9700	6349
3.0	9782	6268	10326	6690	10880	7126	12019	8046

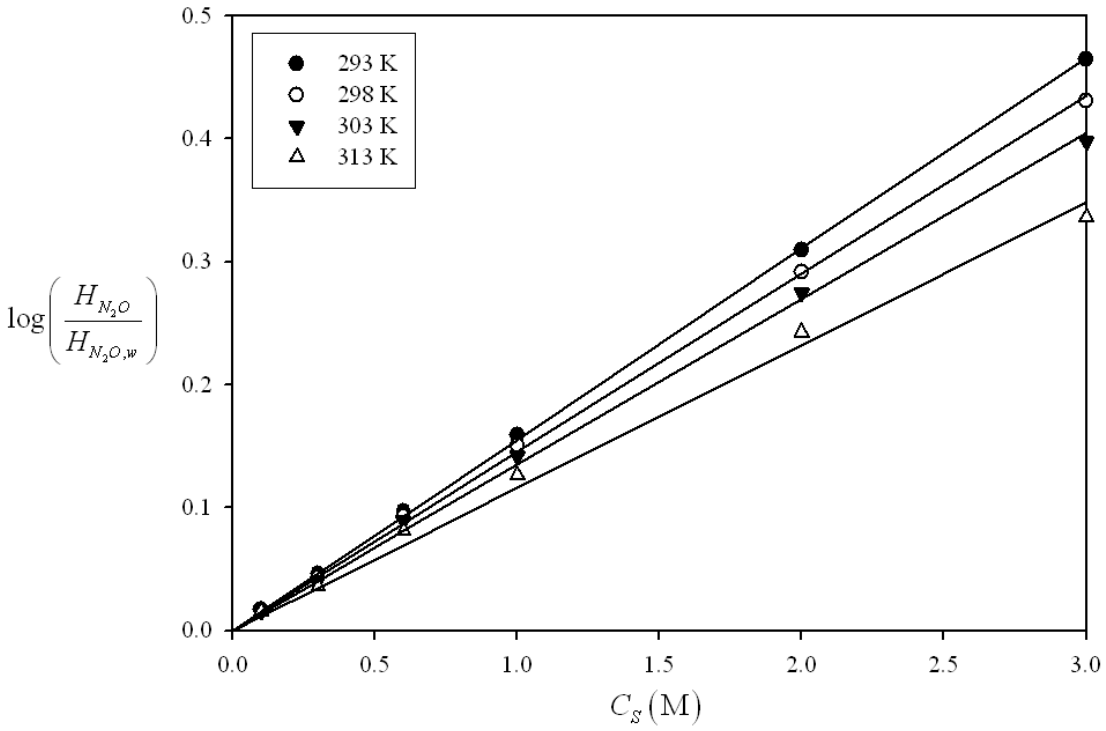

Figure 3.3 – Sechenov plots of the N_2O solubility in potassium threonate solutions.

The specific parameters of Schumpe model for the cation and the gas (respectively, h_{K^+} and h_{N_2O}) were taken from the work by Weisenberger and Schumpe (1996). These, along with the Sechenov constants, enable to calculate the anion specific parameter, h_{Th^-}, according to equation (10). Weisenberger and Schumpe (1996) also report the CO_2 specific parameter, h_{CO_2}, which allows to calculate the Sechenov constants and consequently the Henry coefficients of CO_2 in potassium threonate solutions. The computed values of the Sechenov constants and the specific parameters of Schumpe model are presented in Table 3.3. Figure 3.4 shows the computed anion specific parameter as a function of the temperature.

Table 3.3 – Sechenov constants and specific parameters of Schumpe model for the solubility of N_2O and CO_2 in potassium threonate solutions.

T (K)	K_{N_2O} $\left(\mathrm{dm^3 \cdot mol^{-1}}\right)$	h_{N_2O} * $\left(\mathrm{dm^3 \cdot mol^{-1}}\right)$	h_{K^+} * $\left(\mathrm{dm^3 \cdot mol^{-1}}\right)$	h_{Th^-} $\left(\mathrm{dm^3 \cdot mol^{-1}}\right)$	h_{CO_2} * $\left(\mathrm{dm^3 \cdot mol^{-1}}\right)$	K_{CO_2} $\left(\mathrm{dm^3 \cdot mol^{-1}}\right)$
293	0.155	-0.0061	0.0922	0.0753	-0.0155	0.136
298	0.145	-0.0085		0.0698	-0.0172	0.128
303	0.135	-0.0109		0.0646	-0.0189	0.119
313	0.116	-0.0157		0.0552	-0.0223	0.103

* - Values taken from Weisenberger and Schumpe (1996)

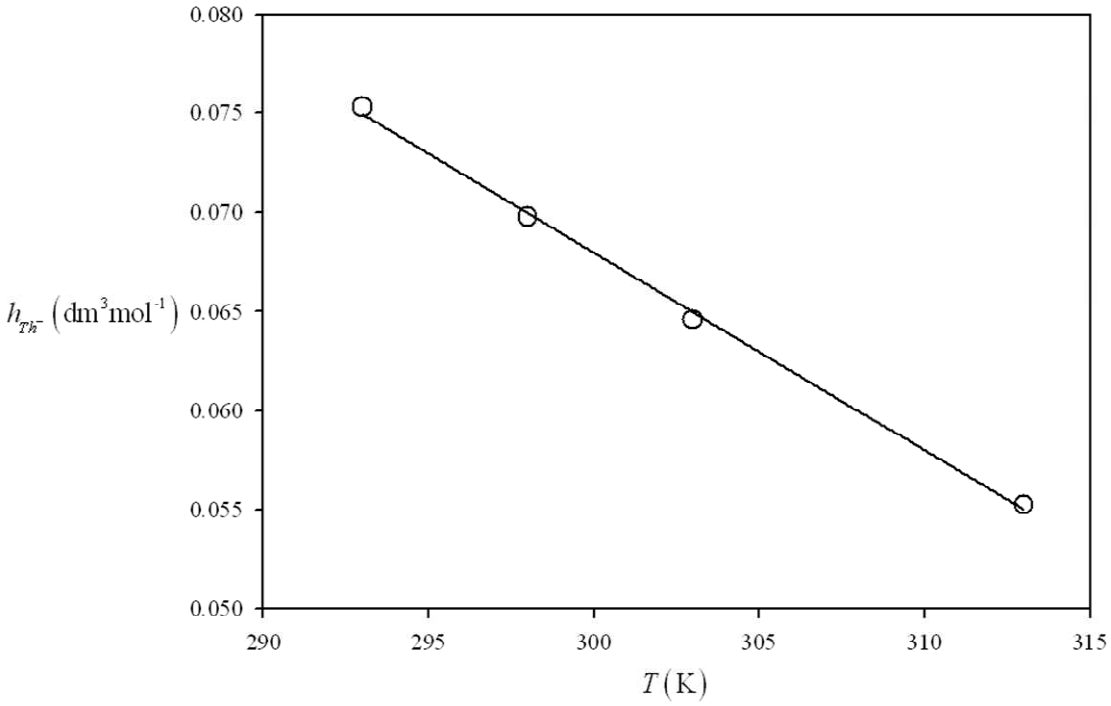

Figure 3.4 – Threonate anion specific parameter as a function of temperature.

It was expected the ion specific parameters to be constant with temperature (Weisenberger and Schumpe, 1996), however h_{Th^-} clearly decreases with temperature $\left(h_{Th^-} = 0.368 - 9.98\times10^{-4}T\right)$, as it is shown in Table 3.3 and Figure 3.4. For this reason, instead of taking the mean value of h_{Th^-} (0.0662 $\mathrm{dm^3 \cdot mol^{-1}}$) to calculate the CO_2 solubility, K_{CO_2} was computed for each temperature by the following expression: $K_{CO_2} = K_{N_2O} - 2h_{N_2O} + 2h_{CO_2}$; results are presented in Table 3.3. The computed Henry coefficients of CO_2 in potassium threonate solutions are shown in Table 3.2.

Gas and ion diffusion coefficients

To estimate the diffusion coefficient of N_2O and CO_2 in potassium threonate solutions, equations (14) (with $\alpha = 0.8$) and (12) were applied. Results are presented in Table 3.4. The diffusion coefficients of potassium threonate in potassium threonate solutions were estimated using the Stokes-Einstein relation – equation (14) – with $\alpha = 0.6$ and the Nernst equation – equation (13). The ionic conductance at infinite dilution of the cation K^+, λ_+^0, as a function of temperature was computed based on the work by Fell and Hutchiso (1971). The ionic conductance of the threonate anion at 298 K was linearly interpolated using values of λ_-^0 available in literature for similar anions with molar masses respectively lower and higher than the threonate anion: glycinate and aspartate (Miyamoto and Schmidt, 1933). The temperature dependence was assumed to be linear and equal to the one of aspartate, being λ_-^0 at 273 K of aspartate obtained from the work by Hoskins et al. (1930). Table 3.4 presents the computed diffusion coefficients of potassium threonate in the potassium threonate solutions.

Table 3.4 - Diffusion coefficient of N_2O, CO_2 and potassium threonate in potassium threonate solutions computed based on the Stokes-Einstein relation - $D \times 10^{10} \left(\mathrm{m}^2 \cdot \mathrm{s}^{-1} \right)$

$C_S \left(\mathrm{M} \right)$	N_2O	CO_2	Potassium threonate	N_2O	CO_2	Potassium threonate
	293 K			298 K		
0.1	15.2	16.6	9.47	17.3	18.6	10.6
0.3	14.2	15.6	9.01	16.2	17.5	10.1
0.6	13.0	14.3	8.44	14.6	15.7	9.35
1.0	11.0	12.1	7.46	12.8	13.8	8.45
2.0	7.37	8.07	5.51	8.42	9.09	6.19
3.0	4.23	4.63	3.63	5.38	5.81	4.43
	303 K			313 K		
0.1	19.7	21.0	11.8	25.2	26.1	14.4
0.3	18.5	19.7	11.3	22.5	23.4	13.2
0.6	16.7	17.7	10.4	20.4	21.2	12.3
1.0	14.5	15.4	9.42	17.4	18.1	10.9
2.0	9.79	10.4	7.01	12.9	13.4	8.72
3.0	6.36	6.77	5.08	8.08	8.38	6.14

Physical mass transfer coefficient

The physical mass transfer coefficient of CO_2 in water was determined for the studied temperatures and for stirring speeds ranging from 75 to 200 rpm. Physical mass transfer coefficients of N_2O in water and in solutions of 1 M and 3 M were measured at $N = 200$ rpm and 298 K. Equation (14) was fitted to the experimental data and it was verified that the constants are within the usual values for stirred cell reactors (Versteeg et al., 1987):

$$\mathrm{Sh} = 6.33\times10^{-2}\,\mathrm{Re}^{0.778}\,\mathrm{Sc}^{0.390} \qquad (20)$$

The experimental and predicted k_L values differ less than 7 %. Since the physical properties of the solutions are known, it is possible to extrapolate the value of k_L for the potassium threonate solutions using equation (20). These values are presented in Table 3.5.

Table 3.5 - Physical mass transfer coefficient of CO_2 in potassium threonate solutions, computed based on equation (20) - $k_L \times 10^6 \left(\mathrm{m \cdot s^{-1}}\right)$

$C_S\,(\mathrm{M})$ \ $T\,(\mathrm{K})$	293	298	303	313
0.1	17.1	19.1	21.4	26.4
0.3	16.0	17.9	20.1	23.5
0.6	14.6	16.1	18.0	21.2
1.0	12.3	14.0	15.7	18.0
2.0	8.09	9.10	10.4	13.2
3.0	4.49	5.68	6.62	8.10

Kinetic Measurements

The experimental carbon dioxide flux data, J_{CO_2}, as a function of the carbon dioxide partial pressure, P_{CO_2}, for all temperatures and potassium threonate concentrations studied are presented in appendix.

The carbon dioxide absorption performance of potassium threonate at 1 M and 298 K was compared to the absorption performance of a primary and a secondary amines – potassium glycinate and diethanolamine (DEA), respectively – obtained using the same set-up and method. Results, shown in Figure 3.5, confirm that although potassium threonate absorbs slower than potassium glycinate, it is faster than DEA. Looking to the pK_A values, this was an expected result since $pK_{A,DEA} = 8.883 < pK_{A,Th^-} = 9.100 < pK_{A,Gly^-} = 9.7775$ and since DEA has a secondary amine group while potassium glycinate has a non-sterically hindered primary amine group. This result also confirms that potassium threonate is able to absorb CO_2 at a considerable rate.

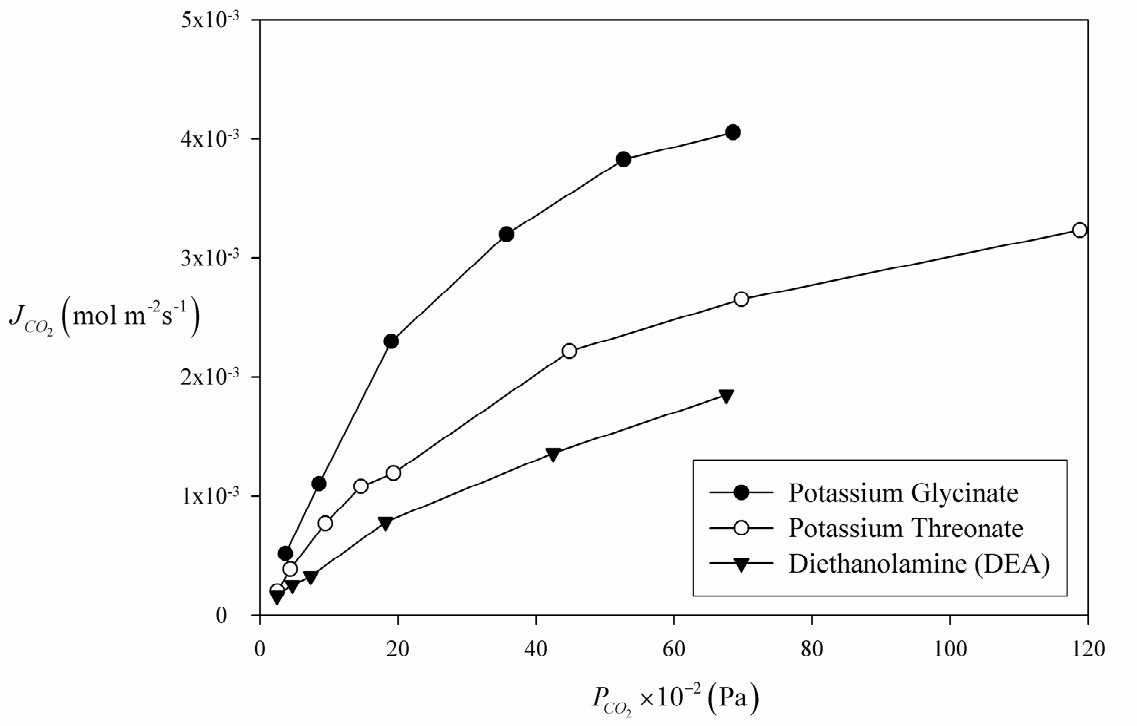

Figure 3.5 – Comparison of CO_2 absorption flux in potassium threonate, potassium glycinate and diethanolamine (DEA) solutions at 1 M and 298 K (all measurements were performed in the setup presented in Figure 3.2).

The results presented in the appendix were treated using both the pseudo-first order assumption and equation (8) (DeCoursey, 1974) to obtain the overall kinetic constant. For the pseudo-first order approach, only experiments that obey condition (11) ($E_\infty / Ha > 10$) were taken into account, while for the DeCoursey approach only

experiments at carbon dioxide partial pressures lower than 20 mbar were used. Such low partial pressure range was chosen because this is when, within the DeCoursey model, the overall kinetic constant is obtained with higher precision, mainly due to the uncertainty of the CO_2 and potassium threonate diffusivity coefficients. Results of both approaches are presented in Table 3.6. The overall kinetic constants computed using both methods are in agreement within a 20% difference (which corresponds to a maximum deviation of 10% in the Ha values). This difference is very acceptable taking into consideration that experiments at low partial pressures can be strongly affected by experimental errors: CO_2 partial pressures vary from values close to the solution vapour pressure (in the range of tens of mbar) to values in the same order of magnitude as the pressure equipment accuracy (in the range of tenths of mbar). For this reason, it was decided to use the results obtained by the DeCoursey approach for further analysis, since they were obtained using more experimental values, therefore reducing the associated experimental error.

Table 3.6 – Experimental overall kinetic constants using the PFO and the DeCoursey (DC) approaches - $k_{ov}\left(\mathrm{s}^{-1}\right)$.

$T\left(\mathrm{K}\right)$ / $C_S\left(\mathrm{M}\right)$	293		298		303		313	
	PFO	DC	PFO	DC	PFO	DC	PFO	DC
0.1	305	251	238	246	254	306	---	
0.3	773	824	986	1010	1240	1320	---	
0.6	2220	2380	2430	2620	4280	4420	---	
1.0	3920	4560	7610	7090	5790	7090	11 400	11 100
2.0	22 600	23 200	27 300	27 800	39 800	45 500	---	
3.0	---		139 000	120 000	---		---	

It can be considered that at low loadings, the only ions present in solution are potassium cation and threonate anion, both monovalent ($z^2=1$). Hence, $I=C_S$ and combining equations (7) and (8), it can be written:

$$k_{ov}=-r_{CO_2}/C_{CO_2}=k_2 C_S \exp\left(b\,C_S\right) \tag{21}$$

Assuming that the kinetic constant follows the Arrhenius law, it is possible to make an overall fit for all the temperatures and concentrations:

$$k_{ov} = k_{2,0} \exp\left(\frac{A}{T}\right) C_S \exp\left(b\, C_S\right) \tag{22}$$

The resulting fit, Equation (23), was obtained by minimizing the sum of the relative residues and it is shown in Figures 3.6 and 3.7 along with the experimental results.

$$k_{ov} = 4.13\times10^{8} \exp\left(\frac{-3580}{T}\right) C_S \exp\left(0.90\, I\right) \tag{23}$$

Penny and Ritter (1983) and Versteeg et al. (1996) suggested that the rate of CO_2 absorption in amines is related to the amine pK_A. The kinetic constants, k_2, were compared with the Brønsted plots drew by these authors; pK_A values of threonate as a function of temperature were extracted from Perrin (1965). They were found to be considerably lower than the expected and the discrepancy increases with temperature. One possible explanation for this is the molecular configuration. Although the amine group is not connected to a tertiary carbon, potassium threonate is sterically hindered due to the hydroxyethylene group connected to the α carbon. This may confer instability to the carbamate formed, hence decreasing the absorption rate. AMP, which is a primary sterically hindered amine (with the α carbon dimethylated), diverges even more from the referred Brønsted plots – $pK_{A,AMP} = 9.72$ (Perrin, 1965), $k_{2,AMP} = 555\ \mathrm{dm^3 \cdot mol^{-1} \cdot s^{-1}}$ (Saha et al., 1995), both at 298 K – supporting this hypothesis.

Usually, the effect of the ionic strength on the reaction kinetic constant is much lower than $b = 0.9$ (Cullinane and Rochelle, 2006; Portugal et al., 2007). To confirm the obtained value for *b*, it was prepared a 1 M potassium threonate solution with the ionic strength modified by adding $NaCl$ up to 1 M (I = 2 M) and obtained the corresponding overall kinetic constant. The obtained overall kinetic constant, at 298 K, was $k_{ov} = 14\,900\ \mathrm{s^{-1}}$, as shown in Figure 3.7. This value is in agreement with the proposed model given by equation (23). Nevertheless, it must be taken into account that the overall kinetic constants were extracted based on computed values of the CO_2 diffusion coefficients - hence any uncertainty on these values affects significantly the final results.

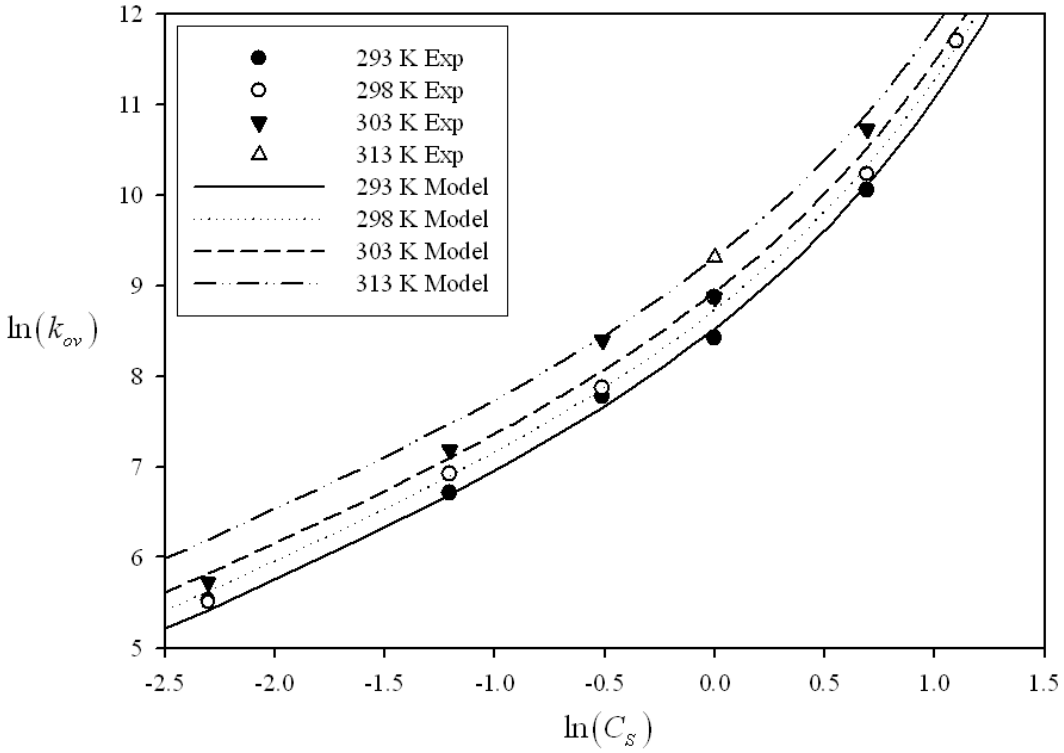

Figure 3.6 – Logarithmic plot of the overall absorption kinetic constant as a function of the potassium threonate concentration - Experimental values and model curves.

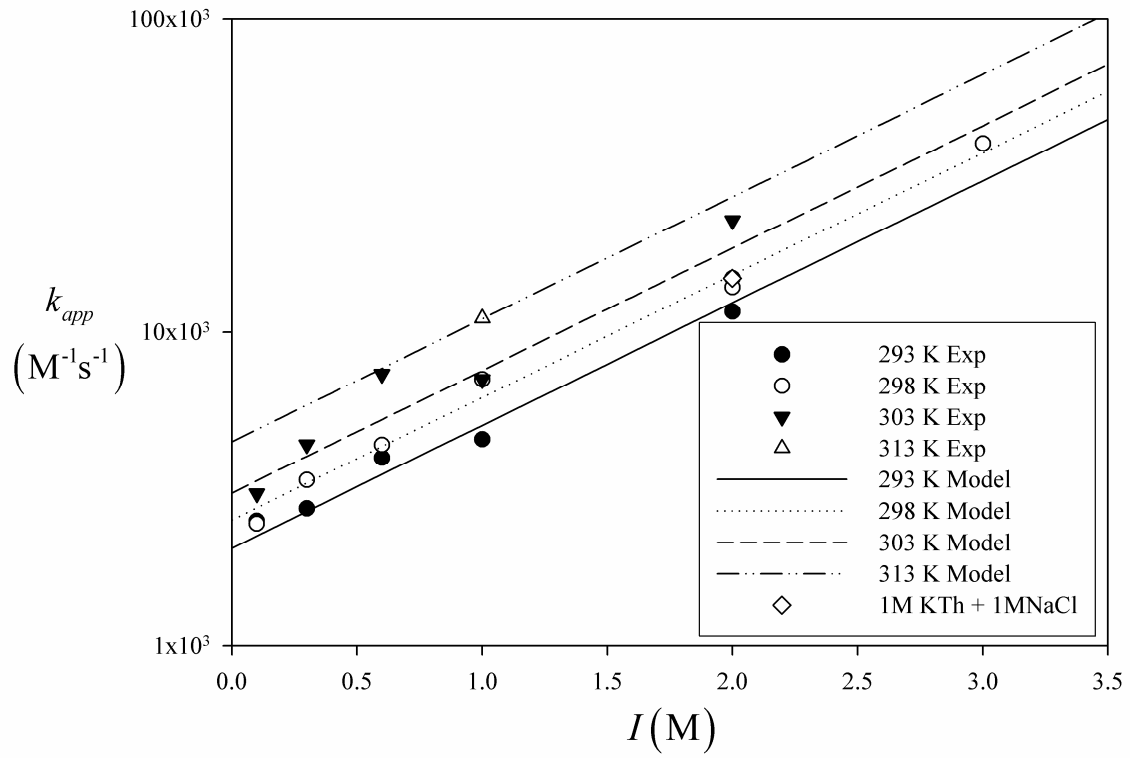

Figure 3.7 – Semi-log plot of the apparent absorption kinetic constant, $k_{app} = k_{ov}/C_S$, as a function of the solution ionic strength - Experimental values and model curves.

3.7. Conclusions

Potassium threonate was characterized for carbon dioxide absorption. Densities and viscosities of aqueous solutions with concentrations from 0.1 to 3 M at 293, 298, 303 and 313 K were determined. The solubility of N_2O in these solutions was measured at the same temperatures. The results were treated using the Schumpe model (Schumpe, 1993). Threonate specific parameter was found to vary linearly with temperature - $h_{Th^-} = 0.368 - 9.98\times10^{-4}T$. Physical solubility of CO_2 in solutions was then computed.

Diffusion coefficients of N_2O and CO_2 were estimated using a modified Stokes-Einstein relation and the N_2O analogy. Diffusion coefficient of potassium threonate at infinite dilution was estimated using the Nernst equation for the diffusion in electrolyte solutions and the diffusion of the ions in solutions was estimated applying modified Stokes-Einstein relation.

The physical mass transfer coefficient of N_2O and CO_2 in water and of N_2O in solutions was measured and its dependence on the system physical properties for the used absorption reactor obtained $\left(\mathrm{Sh} = 6.33\times10^{-2}\,\mathrm{Re}^{0.778}\,\mathrm{Sc}^{0.390}\right)$.

Kinetic measurements were performed in a stirred cell reactor operating semi-continuously. It was verified experimentally that the CO_2 absorption rate in potassium threonate solutions are within the rates found for other amines. Nevertheless, the computed kinetic constants do not follow the Brønsted plot proposed by Penny and Ritter (1983) and by Versteeg et al. (1996). This has to do with the molecular configuration, which is likely to originate unstable carbamates, thus favoring the equilibrium and regeneration but penalizing the kinetics.

Since the absorption overall kinetics depends directly on the CO_2 diffusivity, a more accurate determination of this parameter in potassium threonate solutions will improve the accuracy of the absorption overall kinetics. Further studies of potassium threonate as a carbon dioxide absorbent should consider the absorption equilibrium and regeneration.

3.8. Nomenclature

A	Gas-liquid interfacial area, m^2
C_{B_i}	Concentrations of the bases that can deprotonate the zwitterion, M
C_{CO_2}	Absorbed gas concentration, $mol \cdot m^{-3}$
C_S	Amino acid salt concentration, M
D	Diffusion coefficient, $m^2 \cdot s^{-1}$
d_S	Stirrer diameter, m
E	Enhancement factor, dimensionless
E_∞	Infinite enhancement factor, dimensionless
F	Faraday constant, 96500 $C \cdot mol^{-1}$
Ha	Hatta number, dimensionless
h	Ion and gas specific constants in the Shumpe equation, $m^3 \cdot mol^{-1}$
H	Henry coefficient, $Pa \cdot mol \cdot m^{-3}$
I	Ionic strength of the solution, $mol \cdot dm^{-3}$
J_{CO_2}	Carbon dioxide absorption flux, $mol \cdot m^{-2} \cdot s^{-1}$
K	Sechenov constant, $dm^3 \cdot mol^{-1}$
k_{-1}	Zwitterion kinetic constant of the reverse reaction, s^{-1}
k_2	Zwitterion kinetic constant of the reaction, $M^{-1} \cdot s^{-1}$
k_{app}	Apparent rate constant defined as: $k_{app} = k_{ov} / C_S$, $M^{-1} \cdot s^{-1}$
k_{B_i}	Zwitterion mechanism deprotonation rate constant by base, $M^{-1} \cdot s^{-1}$
k_L	Liquid phase physical mass transfer coefficient, $m \cdot s^{-1}$
k_{ov}	Overall kinetic constant, s^{-1}
N	Stirrer speed, rps
N_{CO_2}	Carbon dioxide absorption flow, $mol \cdot s^{-1}$
n_i	Valency number of the ions
P_{CO_2}	Carbon dioxide partial pressure, Pa
PFO	Pseudo-first order reaction regime

$-r_{CO_2}$	Rate of reaction, $\text{mol}\cdot\text{m}^{-3}\cdot\text{s}^{-1}$
R	Universal gas constant, 8.314 $\text{J}\cdot\text{mol}^{-1}\cdot\text{K}^{-1}$
Re	Reynolds number, $\text{Re}=\frac{(d_S)^2 N\rho}{\eta}$, dimensionless
Sh	Sherwood number, $\text{Sh}=\frac{k_L d_S}{D_{CO_2}}$, dimensionless
Sc	Schmidt number, $\text{Sc}=\frac{\eta}{\rho D_{CO_2}}$, dimensionless
T	Temperature, K
V	Volume, m^3
x	Molar fraction, $\text{mol}\cdot\text{mol}^{-1}$
z_+, z_-	Valencies of the cation and anion

Greek symbols

α	Constant from the modified Stokes-Einstein equation
$\alpha_{máx}$	Maximum loading achieved in one experiment, $\text{mol}_{CO_2}\cdot\text{mol}_S^{-1}$
ν_S	Stoichiometric coefficient
η	Solution viscosity, $\text{kg}\cdot\text{m}^{-1}\cdot\text{s}^{-1}$
ρ	Solution density, $\text{kg}\cdot\text{m}^{-3}$
λ_+^0, λ_-^0	Ionic conductances of the cation and anion at infinite dilution, $\text{cm}^2\cdot\Omega^{-1}$

Subscripts

0	Initial
CO_2	Carbon dioxide
DEA	Diethanolamine
eff	Effective (after correcting for the ionic strength)
eq	Equilibrium
final	Final
G	Gas phase
GV	Gas vessel
K^+	Potassium cation

L	Liquid phase
N_2O	Nitrous oxide
S	Amino acid salt
SC	Stirred cell
Th^-	Threonate anion
w	Water

3.9. References

Abu-Arabi, M. K., Al-Jarrah, A. M., et al. (2001). "Physical Solubility and Diffusivity of CO_2 in aqueous Diethanolamine Solutions". Journal of Chemical and Engineering Data, 46(3), 516-521.

Blauwhoff, P. M. M., Versteeg, G. F., et al. (1984). "A Study on the Reaction between CO_2 and Alkanolamines in Aqueous-Solutions". Chemical Engineering Science, 39(2), 207-225.

Brilman, D. W. F., van Swaaij, W. P. M., et al. (2001). "Diffusion coefficient and solubility of isobutene and trans-2-butene in aqueous sulfuric acid solutions". Journal of Chemical and Engineering Data, 46(5), 1130-1135.

Caplow, M. (1968). "Kinetics of carbamate formation and breakdown". Journal of the American Chemical Society, 90(24), 6795-6803.

Cullinane, J. T. and Rochelle, G. T. (2006). "Kinetics of carbon dioxide absorption into aqueous potassium carbonate and piperazine". Industrial & Engineering Chemistry Research, 45(8), 2531-2545.

Danckwerts, P. (1970). "Gas-Liquid Reactions". McGraw-Hill Book Company.

Decoursey, W. J. (1974). "Absorption with Chemical-Reaction - Development of a New Relation for Danckwerts Model". Chemical Engineering Science, 29(9), 1867-1872.

Derks, P. W., Hogendoorn, K. J., et al. (2005). "Solubility of N_2O in and density, viscosity, and surface tension of aqueous piperazine solutions". Journal of Chemical and Engineering Data, 50(6), 1947-1950.

Derks, P. W. J., Kleingeld, T., et al. (2006). "Kinetics of absorption of carbon dioxide in aqueous piperazine solutions". Chemical Engineering Science, 61(20), 6837-6854.

Fell, C. J. D. and Hutchiso, H. P. (1971). "Diffusion Coefficients for Sodium and Potassium Chlorides in Water at Elevated Temperatures". Journal of Chemical and Engineering Data, 16(4): 427-429.

Feron, P. and Jansen, A. (2002). "CO_2 separation with polyolefin membrane contactors and dedicated absorption liquids: performances and prospects". Separation and Purification Technology, 27(3), 231-242.

Goff, G. S. and Rochelle, G. T. (2006). "Oxidation inhibitors for copper and iron catalyzed degradation of monoethanolamine in CO_2 capture processes". Industrial & Engineering Chemistry Research, 45(8), 2513-2521.

Granite, E. J. and O'Brien, T. (2005). "Review of novel methods for carbon dioxide separation from flue and fuel gases". Fuel Processing Technology, 86(14-15), 1423-1434.

Gubbins, K. E., Bhatia, K. K., et al. (1966). "Diffusion of Gases in Electrolytic Solutions". American Institute of Chemical Engineers Journal, 12(3), 548.

Hampe, E. M. and Rudkevich, D. M. (2003). "Exploring reversible reactions between CO_2 and amines". Tetrahedron, 59(48), 9619-9625.

Haubrock, J., Hogendoorn, J. A., et al. (2007). "The applicability of activities in kinetic expressions: a more fundamental approach to represent the kinetics of the system CO_2-OH^- in terms of activities". Chemical Engineering Science, 62(21), 5753-5769.

Higbie, R. (1935). "The rate of absorption of a pure gas into a still liquid during a short time of exposure". Transactions of the American Institute of Chemical Engineers, 31, 365–389.

Holst, J., Politiek, P. P., et al. (2006). "CO_2 capture from flue gas using amino acid salt solutions". GHGT-8 proceedings, Norway.

Hook, R. J. (1997). "An investigation of some sterically hindered amines as potential carbon dioxide scrubbing compounds". Industrial & Engineering Chemistry Research, 36(5), 1779-1790.

Hoskins, W. M., Randall, M., et al. (1930). "The conductance and activity coefficients of glutamic and aspartic acids and their monosodium salts". Journal of Biological Chemistry, 88(1), 215-239.

Idem, R. and Tontiwachwuthikul, P. (2006). "Preface for the special issue on the capture of carbon dioxide from industrial sources: Technological developments and future opportunities". Industrial & Engineering Chemistry Research, 45(8), 2413-2413.

Jeffreys, G. V. and Bull, A. F. (1964). "The effect of glycine additive on the rate of absorption of carbon dioxide in sodium glycinate solutions". Transactions of the Institution of Chemical Engineers and the Chemical Engineer, 42, 118-125.

Jensen, A., Jensen, J. B., et al. (1952). "Studies on Carbamates .6. The Carbamate of Glycine". Acta Chemica Scandinavica, 6(3), 395-397.

Joosten, G. E. H. and Danckwerts, P. V. (1972). "Solubility and Diffusivity of Nitrous-Oxide in Equimolar Potassium Carbonate-Potassium Bicarbonate Solutions at 25 ºC and 1 Atm". Journal of Chemical and Engineering Data, 17(4), 452.

Kohl, A. L. and Nielsen, R. B. (1997). "Gas Purification". Houston: Gulf Publishing Company.

Kumar, P., Hogendoorn, J., et al. (2001). "Density, viscosity, solubility, and diffusivity of N_2O in aqueous amino acid salt solutions". Journal of Chemical and Engineering Data, 46(6), 1357-1361.

Kumar, P., Hogendoorn, J., et al. (2003a). "Equilibrium solubility of CO_2 in aqueous potassium taurate solutions: Part 1. Crystallization in carbon dioxide loaded aqueous salt solutions of amino acids". Industrial & Engineering Chemistry Research, 42(12), 2832-2840.

Kumar, P., Hogendoorn, J., et al. (2003b). "Equilibrium solubility of CO_2 in aqueous potassium taurate solutions: Part 2. Experimental VLE data and model". Industrial & Engineering Chemistry Research 42(12), 2841-2852.

Kumar, P., Hogendoorn, J., et al. (2003c). "Kinetics of the reaction of CO_2 with aqueous potassium salt of taurine and glycine". American Institute of Chemical Engineers Journal, 49(1), 203-213.

Kumar, P. S., Hogendoorn, J. A., et al. (2002). "New absorption liquids for the removal of CO_2 from dilute gas streams using membrane contactors". Chemical Engineering Science, 57(9), 1639-1651.

Laddha, S. S., Diaz, J. M., et al. (1981). "The N_2O Analogy - the Solubilities of CO_2 and N_2O in Aqueous-Solutions of Organic-Compounds". Chemical Engineering Science, 36(1), 228-229.

Mendes, A. M. M. (2000). "Development of an adsorption/membrane based system for carbon dioxide, nitrogen and spur gases removal from a nitrous oxide and xenon anaesthetic closed loop". Applied Cardiopulmonary Pathophysiology, 9(2), 156-163.

Miyamoto, S. and Schmidt, C. L. A. (1933). "Transference and conductivity studies on solutions of certain proteins and amino acids with special reference to the formation of complex ions between the alkaline earth elements and certain proteins". Journal of Biological Chemistry, 99(2), 335-358.

Penny, D. E. and Ritter, T. J. (1983). "Kinetic-Study of the Reaction between Carbon-Dioxide and Primary Amines". Journal of the Chemical Society-Faraday Transactions I, 79, 2103-2109.

Perrin, D. (1965). "Dissociation Constants of Organic Bases in Aqueous Solutions". Butterworth, London.

Poling, B. E., Prausnitz, J. M., et al. (2001). "The Properties of Gases and Liquids". McGraw-Hill International Editions.

Portugal, A. F., Derks, P. W. J., et al. (2007). "Characterization of potassium glycinate for carbon dioxide absorption purposes". Chemical Engineering Science, 62(23), 6534-6547.

Saha, A. K., Bandyopadhyay, S. S., et al. (1995). "Kinetics of Absorption of CO_2 into Aqueous-Solutions of 2-Amino-2-Methyl-1-Propanol". Chemical Engineering Science, 50(22), 3587-3598.

Sartori, G. and Savage, D. W. (1983). "Sterically Hindered Amines for CO_2 Removal from Gases". Industrial & Engineering Chemistry Fundamentals, 22(2), 239-249.

Schumpe, A. (1993). "The Estimation of Gas Solubilities in Salt-Solutions". Chemical Engineering Science, 48(1), 153-158.

Singh, P., Nierderer, J. P. M., et al. (2007). "Structure and activity relationships for amine based CO_2 absorbents". International Journal of Greenhouse Gas Control, 1(1), 5-10.

Snijder, E. D., Teriele, M. J. M., et al. (1993). "Diffusion-Coefficients of Several Aqueous Alkanolamine Solutions". Journal of Chemical and Engineering Data, 38(3), 475-480.

Supap, T., Idem, R., et al. (2006). "Analysis of monoethanolamine and its oxidative degradation products during CO_2 absorption from flue gases: A comparative study of GC-MS, HPLC-RID, and CE-DAD analytical techniques and possible optimum combinations". Industrial & Engineering Chemistry Research, 45(8), 2437-2451.

Van Swaaij, W. P. M. and Versteeg, G. F. (1992). "Mass-Transfer Accompanied with Complex Reversible Chemical-Reactions in Gas-Liquid Systems - an Overview". Chemical Engineering Science, 47(13-14), 3181-3195.

Versteeg, G. F., Blauwhoff, P. M. M., et al. (1987). "The Effect of Diffusivity on Gas-Liquid Mass-Transfer in Stirred Vessels - Experiments at Atmospheric and Elevated Pressures". Chemical Engineering Science, 42(5), 1103-1119.

Versteeg, G. F., Van Dijck, L. A. J., et al. (1996). "On the kinetics between CO_2 and alkanolamines both in aqueous and non-aqueous solutions. An overview". Chemical Engineering Communications, 144, 113-158.

Versteeg, G. F. and Van Swaaij, W. P. M. (1988). "Solubility and Diffusivity of Acid Gases (CO_2, N_2O) in Aqueous Alkanolamine Solutions". Journal of Chemical and Engineering Data, 33(1), 29-34.

Weisenberger, S. and Schumpe, A. (1996). "Estimation of gas solubilities in salt solutions at temperatures from 273 K to 363 K". American Institute of Chemical Engineers Journal, 42(1), 298-300.

Yan, S. P., Fang, M. X., et al. (2007). "Experimental study on the separation of CO_2 from flue gas using hollow fiber membrane contactors without wetting". Fuel Processing Technology, 88(5), 501-511.

3.A. Experimental kinetic data

The experimental CO_2 flux in aqueous potassium threonate solutions, J_{CO_2}, as a function of the CO_2 partial pressure for all the concentrations and temperatures studied is presented in Tables 3.A1 to 3.A6 along with he maximum loading reached at the end of each experiment, α_{max}. All experiments started with fresh solutions.

Table 3.A1 – Flux of CO_2 in 3 M potassium threonate solutions as a function of the CO_2 partial pressure, at 298 K.

$P_{CO_2} \times 10^{-2}\,(\mathrm{Pa})$	$J_{CO_2} \times 10^{4}\,(\mathrm{mol \cdot s^{-1} \cdot m^{-2}})$	$\alpha_{máx}\,(\mathrm{mol_{CO_2} \cdot mol_S^{-1}})$
0.98	1.42	0.00067
2.62	3.41	0.0016
3.37	4.59	0.0021
7.97	8.02	0.0052
9.98	10.1	0.0067
18.8	16.0	0.0074
24.0	17.9	0.0089
48.8	26.3	0.013
73.0	29.1	0.014

Table 3.A2 – Flux of CO_2 in 0.1 M potassium threonate solutions as a function of the CO_2 partial pressure, at 293, 298 and 303 K.

293 K			298 K			303 K		
$P_{CO_2} \times 10^{-2}$ (Pa)	$J_{CO_2} \times 10^{4}$ $\left(\mathrm{mol \cdot s^{-1} \cdot m^{-2}}\right)$	α_{max} $\left(\mathrm{mol_{CO_2} \cdot mol_S^{-1}}\right)$	$P_{CO_2} \times 10^{-2}$ (Pa)	$J_{CO_2} \times 10^{4}$ $\left(\mathrm{mol \cdot s^{-1} \cdot m^{-2}}\right)$	α_{max} $\left(\mathrm{mol_{CO_2} \cdot mol_S^{-1}}\right)$	$P_{CO_2} \times 10^{-2}$ (Pa)	$J_{CO_2} \times 10^{4}$ $\left(\mathrm{mol \cdot s^{-1} \cdot m^{-2}}\right)$	α_{max} $\left(\mathrm{mol_{CO_2} \cdot mol_S^{-1}}\right)$
1.70	0.481	0.0059	1.57	0.312	0.0047	1.05	0.260	0.0036
3.52	0.921	0.012	2.06	0.522	0.0073	2.32	0.516	0.0073
6.22	1.62	0.021	4.14	0.973	0.017	3.84	1.03	0.021
10.7	1.76	0.041	6.97	1.52	0.020	7.48	1.64	0.026
12.7	2.02	0.044	12.5	2.29	0.029	20.0	3.26	0.038
15.8	2.31	0.042	17.0	2.79	0.043	32.0	4.20	0.048
26.3	2.95	0.035	42.4	4.17	0.051	57.5	5.06	0.049
51.2	4.15	0.045	68.5	4.86	0.064	106	5.63	0.091
75.8	4.01	0.054						

Table 3.A3 – Flux of CO_2 in 0.3 M potassium threonate solutions as a function of the CO_2 partial pressure, at 293, 298 and 303 K.

293 K			298 K			303 K		
$P_{CO_2} \times 10^{-2}$ (Pa)	$J_{CO_2} \times 10^{4}$ $\left(\mathrm{mol \cdot s^{-1} \cdot m^{-2}}\right)$	α_{max} $\left(\mathrm{mol_{CO_2} \cdot mol_S^{-1}}\right)$	$P_{CO_2} \times 10^{-2}$ (Pa)	$J_{CO_2} \times 10^{4}$ $\left(\mathrm{mol \cdot s^{-1} \cdot m^{-2}}\right)$	α_{max} $\left(\mathrm{mol_{CO_2} \cdot mol_S^{-1}}\right)$	$P_{CO_2} \times 10^{-2}$ (Pa)	$J_{CO_2} \times 10^{4}$ $\left(\mathrm{mol \cdot s^{-1} \cdot m^{-2}}\right)$	α_{max} $\left(\mathrm{mol_{CO_2} \cdot mol_S^{-1}}\right)$
2.83	1.14	0.0051	2.43	1.13	0.0073	2.35	1.05	0.0078
3.73	1.54	0.0087	4.07	1.72	0.0094	4.64	2.15	0.015
5.57	2.31	0.011	7.10	2.86	0.018	7.69	3.38	0.017
15.6	5.11	0.025	12.5	4.58	0.023	20.3	6.80	0.046
25.6	6.94	0.031	17.8	6.01	0.032	32.5	9.69	0.048
50.5	9.35	0.043	42.0	9.52	0.044	57.1	12.3	0.060
75.5	10.3	0.048	67.3	11.8	0.064			

Table 3.A4 – Flux of CO_2 in 0.6 M potassium threonate solutions as a function of the CO_2 partial pressure, at 293, 298 and 303 K.

293 K			298 K			303 K		
$P_{CO_2} \times 10^{-2}$ (Pa)	$J_{CO_2} \times 10^{4}$ $(\mathrm{mol \cdot s^{-1} \cdot m^{-2}})$	α_{max} $(\mathrm{mol_{CO_2} \cdot mol_S^{-1}})$	$P_{CO_2} \times 10^{-2}$ (Pa)	$J_{CO_2} \times 10^{4}$ $(\mathrm{mol \cdot s^{-1} \cdot m^{-2}})$	α_{max} $(\mathrm{mol_{CO_2} \cdot mol_S^{-1}})$	$P_{CO_2} \times 10^{-2}$ (Pa)	$J_{CO_2} \times 10^{4}$ $(\mathrm{mol \cdot s^{-1} \cdot m^{-2}})$	α_{max} $(\mathrm{mol_{CO_2} \cdot mol_S^{-1}})$
2.36	1.45	0.0037	3.68	2.09	0.0070	2.26	1.68	0.0075
3.27	2.06	0.0051	4.41	2.68	0.0088	4.33	3.23	0.012
3.91	2.42	0.0060	7.79	4.85	0.016	7.64	5.79	0.015
5.60	3.27	0.0081	12.9	6.95	0.023	19.7	10.8	0.038
15.5	7.70	0.019	17.8	9.03	0.028	32.9	15.7	0.042
25.6	10.9	0.027	43.4	16.4	0.042	57.5	20.3	0.052
75.3	18.1	0.045	68.2	20.3	0.048			

Table 3.A5 – Flux of CO_2 in 2 M potassium threonate solutions as a function of the CO_2 partial pressure, at 293, 298 and 303 K.

293 K			298 K			303 K		
$P_{CO_2} \times 10^{-2}$ (Pa)	$J_{CO_2} \times 10^{4}$ $(\mathrm{mol \cdot s^{-1} \cdot m^{-2}})$	α_{max} $(\mathrm{mol_{CO_2} \cdot mol_S^{-1}})$	$P_{CO_2} \times 10^{-2}$ (Pa)	$J_{CO_2} \times 10^{4}$ $(\mathrm{mol \cdot s^{-1} \cdot m^{-2}})$	α_{max} $(\mathrm{mol_{CO_2} \cdot mol_S^{-1}})$	$P_{CO_2} \times 10^{-2}$ (Pa)	$J_{CO_2} \times 10^{4}$ $(\mathrm{mol \cdot s^{-1} \cdot m^{-2}})$	α_{max} $(\mathrm{mol_{CO_2} \cdot mol_S^{-1}})$
3.12	2.82	0.0023	2.39	2.71	0.0030	2.49	3.18	0.0045
5.15	5.08	0.0043	5.21	5.06	0.0052	6.19	7.27	0.0057
7.45	6.81	0.0053	10.1	8.45	0.0087	11.5	13.5	0.0099
17.6	13.3	0.010	16.2	13.7	0.011	24.1	20.4	0.015
27.9	18.4	0.013	20.9	16.8	0.013	36.2	29.5	0.021
52.7	25.9	0.016	45.8	27.8	0.016	60.8	36.1	0.017
77.6	30.9	0.019	70.7	36.5	0.019			

Table 3.A6 – Flux of CO_2 in 1 M potassium threonate solutions as a function of the CO_2 partial pressure, at 293, 298, 303 and 313 K.

293 K			298 K		
$P_{CO_2} \times 10^{-2}$ (Pa)	$J_{CO_2} \times 10^{4}$ $(\mathrm{mol \cdot s^{-1} \cdot m^{-2}})$	α_{max} $(\mathrm{mol_{CO_2} \cdot mol_S^{-1}})$	$P_{CO_2} \times 10^{-2}$ (Pa)	$J_{CO_2} \times 10^{4}$ $(\mathrm{mol \cdot s^{-1} \cdot m^{-2}})$	α_{max} $(\mathrm{mol_{CO_2} \cdot mol_S^{-1}})$
2.55	1.88	0.0027	2.49	2.03	0.0047
4.16	2.93	0.0042	4.35	3.87	0.0083
5.60	3.90	0.0055	9.44	7.71	0.012
7.87	4.76	0.0070	14.6	10.8	0.016
11.6	7.38	0.011	19.3	11.9	0.017
16.7	9.87	0.015	44.8	22.2	0.032
27.0	13.9	0.020	69.7	26.5	0.038
52.0	20.9	0.032	119	32.3	0.038
76.7	23.6	0.035			
303 K			313 K		
$P_{CO_2} \times 10^{-2}$ (Pa)	$J_{CO_2} \times 10^{4}$ $(\mathrm{mol \cdot s^{-1} \cdot m^{-2}})$	α_{max} $(\mathrm{mol_{CO_2} \cdot mol_S^{-1}})$	$P_{CO_2} \times 10^{-2}$ (Pa)	$J_{CO_2} \times 10^{4}$ $(\mathrm{mol \cdot s^{-1} \cdot m^{-2}})$	α_{max} $(\mathrm{mol_{CO_2} \cdot mol_S^{-1}})$
2.02	1.80	0.0031	2.36	2.14	0.0024
2.86	2.77	0.0053	8.75	7.15	0.011
4.10	2.30	0.0066	32.7	22.0	0.032
5.17	3.90	0.0070			
5.87	4.15	0.0066			
10.4	8.12	0.016			
22.5	16.2	0.023			
36.8	20.6	0.031			
60.7	27.2	0.041			
110	35.6	0.036			

Part III

4. Solubility of carbon dioxide in aqueous solutions of amino acid salts[1]

Abstract

The solubility of CO_2 in aqueous solutions of potassium glycinate was measured in a stirred reactor, at temperatures from 293 to 351 K, for amino acid salt concentrations ranging between 0.1 and 3.0 M and CO_2 partial pressures up to 6×10^4 Pa. CO_2 solubility in potassium threonate 1.0 M was also measured at 313 K. It was observed that amino acid salt solutions can be very interesting for CO_2 absorption purposes since they present considerably high absorption capacities. Nevertheless, CO_2 solubility in these solutions does not change significantly for temperatures between 293 and 323 K, which can be a draw back concerning the absorbent regeneration.

Potassium glycinate solubility data were interpreted using the thermodynamically sound model proposed by Deshmukh and Mather (1981) and the empirical Kent and Eisenberg (1976) model.

[1] Portugal, A. F.; Sousa, J. L.; Magalhães, F. D.; Mendes, A., "Solubility of carbon dioxide in aqueous solutions of amino acid salts", Chem. Eng. Sci., DOI: 10.1016/j.ces.2009.01.036

4.1. Introduction

The climate change due to the rising greenhouse gases concentrations in the atmosphere became an unquestionable problem nowadays (Idem and Tontiwachwuthikul, 2006; IEA, 2008; UNFCCC, 2008). Since the Kyoto protocol, in December 1997, several stringent environmental regulations are being proposed and recently (in January 2008) the European Council (EC) stated as a key target to reduce 20 % greenhouse gases emissions by 2020 (EC, 2008; Gibbins and Chalmers, 2008). Among the greenhouse gases, carbon dioxide (CO_2) is the one released in larger extent by human activity (Idem and Tontiwachwuthikul, 2006; UNFCCC, 2008), hence, much effort is being put on the development of technologies for CO_2 capture and storage. Three basic processes can be applied for capturing CO_2 from flue gases: oxyfuel combustion, pre-combustion, and post-combustion (Idem and Tontiwachwuthikul, 2006; Metz et al., 2005). Although apparently less efficient than pre- and oxyfuel combustion, post-combustion seems to be the best solution to meet the exigent EC emission targets, because it can be easily retrofitted to already existing equipment and power plants (Favre, 2007; Gibbins and Chalmers, 2008).

Chemical absorption in liquid solutions is a proven technology for CO_2 removal from a variety of gas streams and it is considered the best available technology for post-combustion flue gas treatment (Favre, 2007; Gibbins and Chalmers, 2008; Idem and Tontiwachwuthikul, 2006). Nevertheless, the absorbent solutions commonly used (alkanolamine solutions) undergo oxidative degradation, so they might not be suitable for the specified separation due the high oxygen concentrations present in flue gas (Goff and Rochelle, 2006; Hook, 1997; Supap et al., 2006). Because of their higher stability in the presence of oxygen, growing interest is being given to amino acid salts solutions. Amino acid salts are more resistant to oxidative degradation, have negligible volatilities and their aqueous solution present viscosities and surface tensions similar to water (Holst et al., 2006; Kumar et al., 2002; Kumar et al., 2003c; Portugal et al., 2007). Additionally, they react with CO_2 in the same way as alkanolamines, presenting therefore comparable absorption kinetics and equilibrium capacities (Hook, 1997; Kumar et al., 2003b; Kumar et al., 2003c; Portugal et al., 2007; Portugal et al., 2008; Song et al., 2006). Nevertheless,

precipitation of reaction products was observed during the absorption of CO_2 in aqueous solutions of amino acids salts (Hook, 1997; Kumar et al., 2003a).

Although amino acids are used for CO_2 absorption in a number of industrial solutions (Feron and Jansen, 2002; Kumar et al., 2003c), very few data are available in literature for these systems. In the present work, the absorption capacity of potassium glycinate towards CO_2 is determined at different temperatures, using potassium glycinate aqueous solutions with initial concentrations ranging from 0.1 to 3.0 $mol \cdot dm^{-3}$ and for CO_2 partial pressures up to 6×10^4 Pa. The absorption capacity of a solution of potassium threonate, 1.0 $mol \cdot dm^{-3}$, at 313 K was also measured for the same pressure range.

Several models are available in literature for representing the vapour – liquid equilibrium in the CO_2 – amines – water systems. They are basically divided into three types:

- Empirical models such as Kent and Eisenberg (1976) model, where the non-idealities of the system are lumped in the equilibrium constants. Despite its simplicity, the Kent-Eisenberg model has been successfully applied to a number of CO_2 absorption systems (Aroua and Salleh, 2004; Li and Shen, 1993; Park et al., 2002; Tontiwachwuthikul et al., 1991) and has demonstrated to predict fairly well the system behaviour for loadings between 0.2 and 0.7 $mol_{CO_2} \cdot mol^{-1}_{Amine}$ (Kumar et al., 2003b; Weiland et al., 1993).

- Models based on the excess Gibbs energy, in which a term to account for the electrostatic forces due to the presence of ions in solution is added to the molecular Gibbs energy models. Examples of this approach are the Deshmukh and Mather (1981) method, the electrolyte-NRTL model of Chen and Evans (1986) and the models developed by Austgen et al. (1989) and Clegg and Pitzer (1992).

- Models using an equation of state (EoS) to describe both liquid and vapour phases. A term to account for the ionic interactions is also added to the molecular EoS. Applications of the EoS models to CO_2 absorption systems are quite recent.

Further details and applications can be found in the work of Fürst and Renon (1993), Vallee et al. (1999), Li and Fürst (2000), Derks et al. (2005) and Huttenhuis et al. (2008).

In the present work, two models are considered: the empirical Kent and Eisenberg (1976) and the Deshmukh and Mather (1981). The model developed by Deshmukh and Mather (1981) is thermodynamically sound and reasonably simple when compared to other electrolyte-NRTL and EoS models. It considers the long-range electrostatic interactions and short-range Van der Walls interactions between the chemical species to describe the system non-idealities and is used with success to represent acid gases – amines – water systems (Benamor and Aroua, 2005; Kumar et al., 2003b; Weiland et al., 1993; HajiSulaiman et al., 1996; Liu et al., 1999; Ma'mun et al., 2006; Rascol et al., 1996; Tobiesen et al., 2008).

4.2. Modelling

Amino acid salts containing a primary amine group (such as potassium glycinate and potassium threonate) react with CO_2 according to the following equilibrium reactions (where $R \equiv CH_2COO^-$, for potassium glycinate):

Carbamate hydrolysis

$$RNHCOO^- + H_2O \rightleftarrows RNH_2 + HCO_3^- \quad (1)$$

Amine deprotonation

$$RNH_3^+ \rightleftarrows RNH_2 + H^+ \quad (2)$$

Bicarbonate formation

$$CO_2 + H_2O \rightleftarrows HCO_3^- + H^+ \quad (3)$$

Carbonate formation

$$HCO_3^- \rightleftarrows CO_3^{2-} + H^+ \quad (4)$$

Water auto-ionization

$$H_2O \rightleftarrows OH^- + H^+ \tag{5}$$

The reaction kinetically dominant in the absorption system is the direct reaction between CO_2 and the amino acid salt to form a carbamate and the protonated amino acid:

Direct reaction between CO_2 and *the amino acid salt*

$$2RNH_2 + CO_2 \rightleftarrows RNH_3^+ + RNHCOO^- \tag{6}$$

However, reaction (6) can be written as a combination of the independent reactions (1), (2) and (3) (Kumar et al., 2003b).

The equilibrium constants, K, of the above independent reactions can be expressed as follows:

$$K_{carb} = \frac{\left[RNH_2\right]\left[HCO_3^-\right]}{\left[RNHCOO^-\right]} \frac{\gamma_{RNH_2}\gamma_{HCO_3^-}}{a_w \gamma_{RNHCOO^-}} \tag{7}$$

$$K_{AmA} = \frac{\left[RNH_2\right]\left[H^+\right]}{\left[RNH_3^+\right]} \frac{\gamma_{RNH_2}\gamma_{H^+}}{\gamma_{RNH_3^+}} \tag{8}$$

$$K_{CO_2} = \frac{\left[HCO_3^-\right]\left[H^+\right]}{\left[CO_2\right]} \frac{\gamma_{HCO_3^-}\gamma_{H^+}}{a_w \gamma_{CO_2}} \tag{9}$$

$$K_{HCO_3^-} = \frac{\left[CO_3^{2-}\right]\left[H^+\right]}{\left[HCO_3^-\right]} \frac{\gamma_{CO_3^{2-}}\gamma_{H^+}}{\gamma_{HCO_3^-}} \tag{10}$$

$$K_w = \left[OH^-\right]\left[H^+\right] \frac{\gamma_{OH^-}\gamma_{H^+}}{a_w} \tag{11}$$

where $\left[i\right]$ are the molar concentrations of species i in the liquid phase, γ_i are the respective activity coefficients and a_w is the water activity. The equilibrium constant of reaction (6) is given by (Kumar et al., 2003b):

$$K_{ov} = \frac{K_{CO_2}}{K_{AmA} K_{carb}} \tag{12}$$

Additionally to the equilibrium constants, the following mass conservation and charge balance equations must be verified:

Amine mass balance

$$\left[RNH_2\right]_0 = \left[RNH_2\right] + \left[RNHCOO^-\right] + \left[RNH_3^+\right] \quad (13)$$

CO_2 mass balance

$$\alpha\left[RNH_2\right]_0 = \left[CO_2\right] + \left[RNHCOO^-\right] + \left[HCO_3^-\right] + \left[CO_3^{2-}\right] \quad (14)$$

where α is the loading: moles of CO_2 absorbed per mole of amino acid salt initially in solution.

Charges balance

For amino acid salts, R is charged and, therefore, RNH_2 is a mono-valent anion, $RNHCOO^-$ is bivalent and RNH_3^+ is neutral. The charge balance becomes then:

$$\left[K^+\right] + \left[H^+\right] = \left[RNH_2\right] + 2\left[RNHCOO^-\right] + \left[HCO_3^-\right] + 2\left[CO_3^{2-}\right] + \left[OH^-\right] \quad (15)$$

Since the pressure range considered is always lower than 1×10^5 Pa, the vapour phase can be considered ideal (Smith et al., 1996) and the vapour-liquid equilibrium is described by the Henry Law:

$$P_{CO_2} = H_{CO_2}\left[CO_2\right] \quad (16)$$

where P_{CO_2} is the CO_2 partial pressure and H_{CO_2} is the Henry coefficient of CO_2 in potassium glycinate solutions, obtained experimentally in a previous work (Portugal et al., 2007).

To account for the liquid non-idealities, the Deshmukh-Mather method (Deshmukh and Mather, 1981) can be applied. The Deshmukh-Mather method uses the following equation, originally proposed by Guggenheim (1935), to calculate the activity coefficients:

$$\ln\gamma_i = \frac{-2.303Az_i^2\sqrt{I}}{1+Ba\sqrt{I}} + 2\sum_{j\neq solvent}\beta_{i,j}\left[j\right] \quad (17)$$

The first term of equation (17) accounts for the long-range interactions between species and is based on the Debye-Hückel theory. The solution ionic strength, I, is defined as:

$$I = \frac{1}{2}\sum_j [j] z_j^2 \tag{18}$$

where z_j is the ion charge and $[j]$ is the molar concentration of species *j*. The Debye-Hückel limiting slope, A, and the parameter B depend on the temperature, T, and on the dielectric constant of the solvent, ε, as follows (Kumar et al., 2003b):

$$A = 1.825\times10^6 \left(\varepsilon T\right)^{-3/2} \tag{19}$$

$$B = 50.3\left(\varepsilon T\right)^{-1/2} \tag{20}$$

The dielectric constant of the solvent (water) is given by $\varepsilon = 80 - 0.4\left(T - 293\right)$ (Knowlton, 1941). Parameter a roughly corresponds to the effective size of the hydrated ions (Weiland et al., 1993). The second term of equation (17) accounts for the short-range interactions between molecular and ionic solutes by means of the adjustable binary interaction parameters, $\beta_{i,j}$.

In the present absorption system, the following 10 species are present in solution: H_2O, CO_2, HCO_3^-, CO_3^{2-}, RNH_2, K^+, RNH_3^+, $RNHCOO^-$, H^+ and OH^-. Excluding the solvent (H_2O), there are still 9 species which short range interactions are to be taken into account. This leads to 36 binary interaction parameters, $\beta_{i,j}$, resulting in an intractable problem. To make it manageable, Weiland et al. (1993) proposed the following assumptions that reduce the number of binary interaction parameters needed to be fit:

- All interactions between like charged ions are neglected;
- All self-interactions of molecular species are neglected, except for the molecular amine (in the present case, the protonated amine: RNH_3^+);
- All interactions with water and its self-ionization products (H^+ and OH^-) are neglected;
- All interactions with CO_2 and CO_3^{2-} are neglected.

The number of interaction parameters is consequently reduced to 8:

$RNH_3 - HCO_3^-$, $RNH_3^+ - RNH_3^+$, $K^+ - HCO_3^-$, $K^+ - RNH_2$, $RNH_3^+ - RNH_2$, $K^+ - RNH_3^+$, $K^+ - RNHCOO^-$ and $RNH_3^+ - RNHCOO^-$.

Instead, Kent and Eisenberg (1976) considered the liquid phase non-idealities lumped in the equilibrium constants. In their model, the equilibrium constants are only functions of the species concentrations (γ_i=1) and K_{carb} and K_{AmA} are used as fitting parameters. Therefore, the equilibrium constants K_{carb} and K_{AmA} obtained by this method are apparent constants.

4.3. Experimental

The aqueous solutions of the amino acid salts were prepared by adding to the amino acid an equimolar amount of potassium hydroxide (KOH) in a volumetric flask filled up with distilled and deionized water. The concentrations of the solutions were checked by titration with a standard solution of *HCl* 1 M.

The set-up used to determine the solubility of CO_2 is shown in Figure 4.1. It is composed of two vessels with calibrated volumes, one for storing the CO_2 (237.04 mL) and the other for the absorbent solution (110.56 mL), which is magnetically stirred. The temperature, T, is controlled by means of an in-house developed thermostatic closet and a thermostatic bath that controls the jacket temperature of the absorbent reactor.

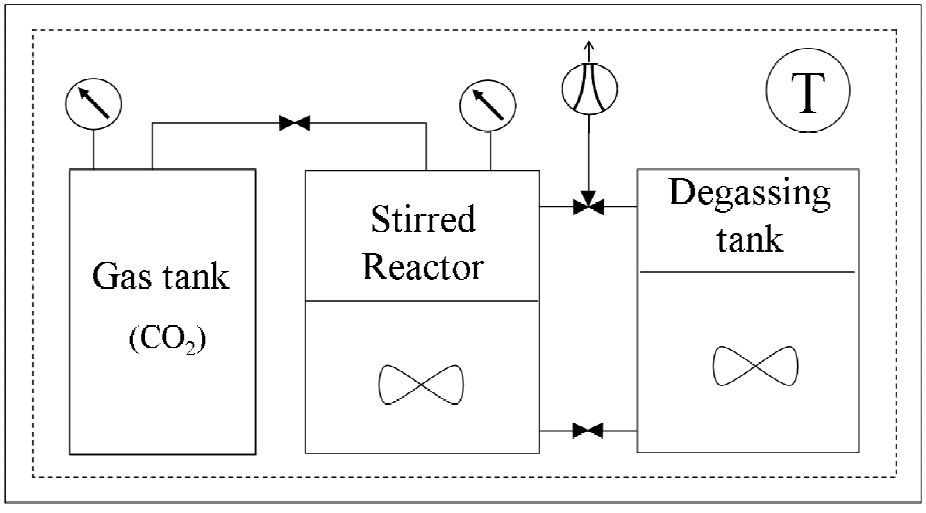

Figure 4.1 - Experimental set-up sketch.

Using a setup with lower dimensions than usually found in the literature (Derks et al., 2005) allows for the use of small quantities of the amino acid salt solutions, even though it implies larger relative errors in the determination of the equilibrium loadings (estimated to be lower than 10 %).

A known volume (about 50 mL) of fresh solution of amino acid salt, V_{sol}, previously degassed is transferred to the absorbent vessel. The vapour-liquid equilibrium is established and the vapour pressure, P_{vapour}, recorded (pressure sensor from Druck, PMP4000; accuracy: $\pm 0.28\times10^{2}$ Pa). On the meantime, the gas vessel is filled with CO_2 and the pressure recorded, $P^{k}_{CO_2,\,0}$ (pressure sensor from Druck, PMP4000; accuracy: $\pm 1.6\times10^{2}$ Pa); pressure inside the gas vessel is always lower than 3×10^{5} Pa. After that, a certain amount of CO_2 is transferred from the gas vessel to the absorbent vessel and the pressure inside the gas vessel is again recorded, $P^{k}_{CO_2,\,fin}$. Once the equilibrium is attained (this happens when the pressure becomes constant inside the absorbent vessel) the pressure of the absorbent vessel is recorded, P^{k}_{eq}. More CO_2 is then admitted from the gas vessel into the absorbent vessel and a new equilibrium value is achieved. It is assumed that the solution vapor pressure does not change with loading and the amount of CO_2 absorbed is computed from the ideal gas law:

$$n^{k}_{CO_2,\,add} = n^{k-1}_{CO_2,\,add} + \frac{P^{k}_{CO_2,\,0} - P^{k}_{CO_2,\,fin}}{RT} V_{GV} \tag{21}$$

$$n^{k}_{CO_2,\,abs} = n^{k}_{CO_2,\,add} - \frac{P^{k}_{eq} - P_{vapour}}{RT}\left(V_{AV} - V_{sol}\right) \tag{22}$$

where V_{GV} and V_{AV} are respectively the volumes of the gas and absorbent vessels. For amino acid salt concentrations higher than the ones used in the present work, the assumption of constant vapor pressure might become unrealistic for loadings higher than 0.5 $\mathrm{mol_{CO_2}\cdot mol_S^{-1}}$, because of the change on the liquid composition.

The loading, α_k, corresponding to each CO_2 partial pressure $\left(P^{k}_{CO_2,eq} = P^{k}_{eq} - P_{vapour}\right)$ is then calculated:

$$\alpha_k = \frac{n^{k}_{CO_2,\,abs} \big/ V_{sol}}{\left[RNH_2\right]_0} \tag{23}$$

Sub and super scripts k denote the experimental stage.

The small size of the setup used (stirred reactor: 110.56 mL, liquid volume ≈ 50 mL and gas vessel: 237.04 mL) enables the characterization of the amino acid salt solutions using small quantities of reactant within an error that should be smaller than 10 %.

4.4. Results and Discussion

Experimental method validation

Before and after measuring the solubility of CO_2 in potassium glycinate, the set up was tested with 2.5 M aqueous solution of monoethanolamine (MEA) and the results compared with the ones reported in literature (Jones et al., 1959; Lee et al., 1974; Lee et al., 1976; Shen and Li, 1992) – please see Figure 4.2. Experimental values of the solubility of CO_2 in MEA solutions are presented in Table 4.1.

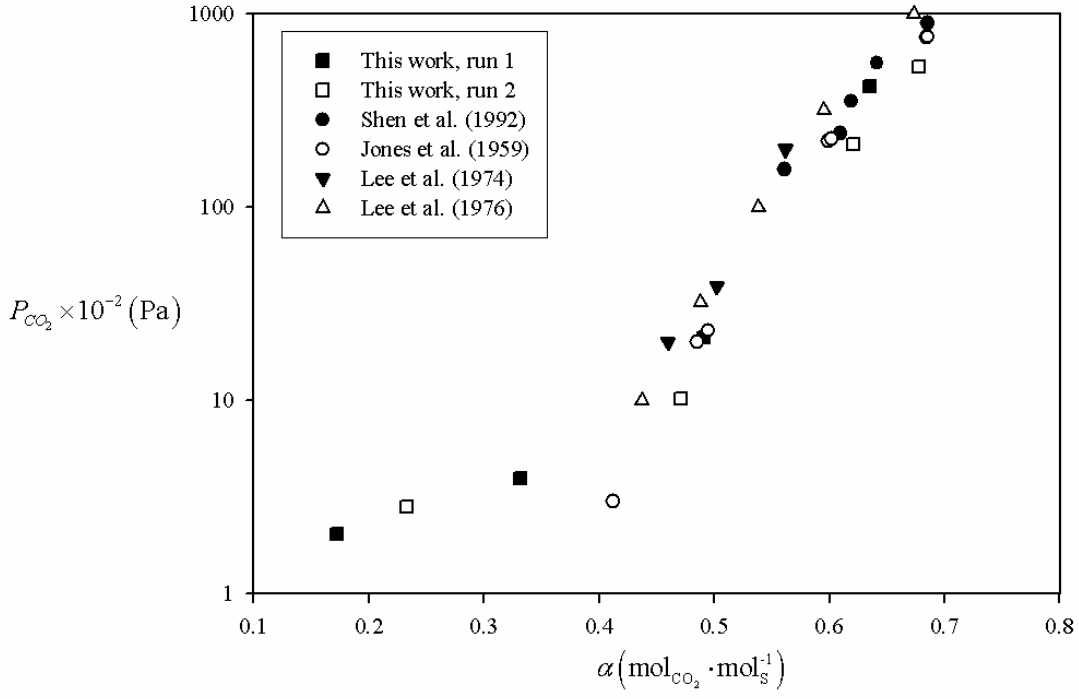

Figure 4.2 – Semi-log plot of the solubility of CO_2 in aqueous solutions of MEA 2.5 M, at 313 K - comparison with results from literature.

Table 4.1 - Solubility of CO_2 in aqueous solutions of MEA 2.5 M.

Run 1 - C_{MEA} = 2.51 M		Run 2 - C_{MEA} = 2.43 M	
$P_{CO_2} \times 10^{-2}$ (Pa)	α $\left(\text{mol}_{CO_2} \cdot \text{mol}_S^{-1}\right)$	$P_{CO_2} \times 10^{-2}$ (Pa)	$\alpha\left(\text{mol}_{CO_2} \cdot \text{mol}_S^{-1}\right)$
2.03	0.173	2.82	0.233
3.95	0.331	10.2	0.471
21.1	0.491	211	0.621
414	0.635	628	0.678

CO_2 solubility in potassium glycinate

The experimental values of the solubility of CO_2 in the potassium glycinate solutions are shown in Tables 4.2 to 4.4. The results for CO_2 solubility in a 1.0 $\text{mol} \cdot \text{dm}^{-3}$ potassium glycinate solution are presented in Figure 4.3 and Figure 4.4 shows the results for a 3.0 $\text{mol} \cdot \text{dm}^{-3}$ solution.

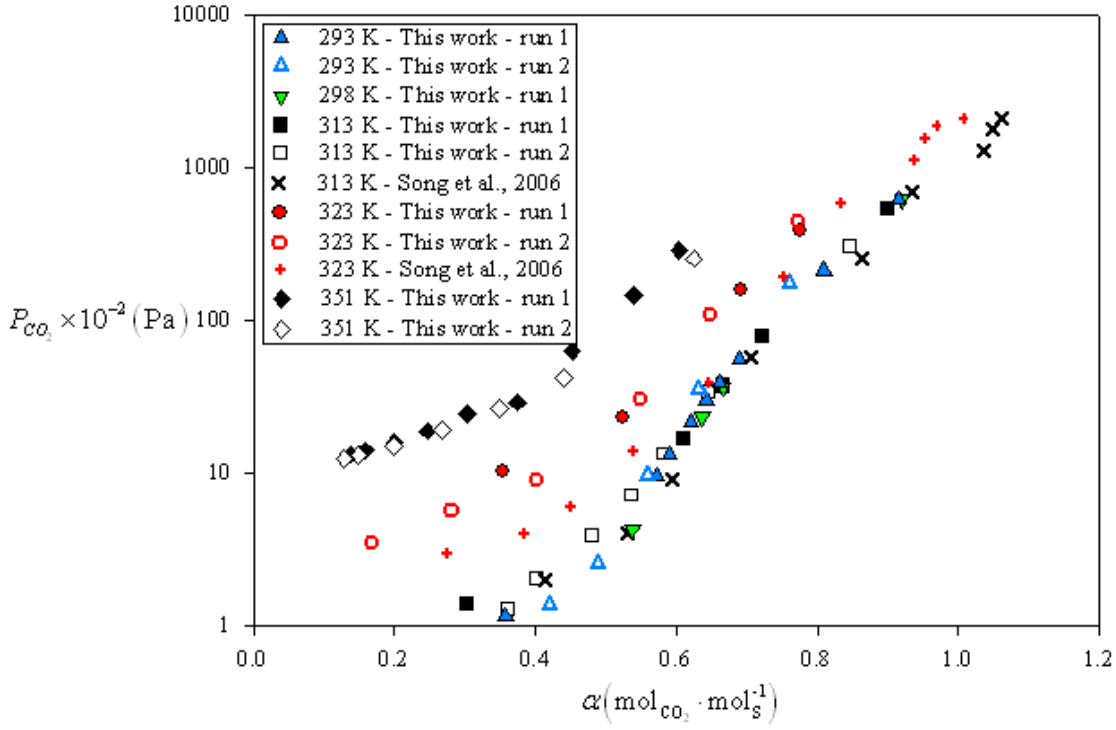

Figure 4.3 – Semi-log plot of the experimental solubility of CO_2 in aqueous solutions of potassium glycinate, 1.0 $\text{mol} \cdot \text{dm}^{-3}$ - comparison with the results from Song et al. (2006) for an aqueous solution of sodium glycinate 1.06 $\text{mol} \cdot \text{dm}^{-3}$, at 313 and 323 K.

Table 4.2 - Experimental solubility of CO_2 in aqueous solutions of potassium glycinate 0.1 M.

293 K		303 K		313 K		323 K	
$P_{CO_2} \times 10^{-2}$ (Pa)	α $\left(\mathrm{mol}_{CO_2} \cdot \mathrm{mol}_S^{-1}\right)$	$P_{CO_2} \times 10^{-2}$ (Pa)	α $\left(\mathrm{mol}_{CO_2} \cdot \mathrm{mol}_S^{-1}\right)$	$P_{CO_2} \times 10^{-2}$ (Pa)	α $\left(\mathrm{mol}_{CO_2} \cdot \mathrm{mol}_S^{-1}\right)$	$P_{CO_2} \times 10^{-2}$ (Pa)	α $\left(\mathrm{mol}_{CO_2} \cdot \mathrm{mol}_S^{-1}\right)$
0.85 Run 1	0.332	0.89 Run 1	0.318	0.54 Run 1	0.213	6.20 Run 1	0.650
2.55 Run 1	0.607	4.60 Run 1	0.728	1.57 Run 1	0.428	83.2 Run 1	1.096
18.7 Run 1	0.867	90.88 Run 1	1.129	4.09 Run 1	0.620	388 Run 1	1.289
71.4 Run 1	0.958	4.02 Run 2	0.692	16.52 Run 1	0.864	3.10 Run 2	0.471
639 Run 1	1.209	6.93 Run 2	0.778	60.47 Run 1	1.044	32.2 Run 2	0.953
6.88 Run 2	0.740	12.9 Run 2	0.868	208.46 Run 1	1.179	361 Run 2	1.294
396 Run 2	1.071	23.3 Run 2	0.949	624.47 Run 1	1.320	5.30 Run 3	0.462
40.7 Run 3	1.002	572 Run 2	1.357			16.1 Run 3	0.794
448 Run 3	1.205					112 Run 3	1.152
						310 Run 3	1.309

Table 4.3 – Experimental solubility of CO_2 in aqueous solutions of potassium glycinate 1.0 M.

293 K		298 K		313 K		323 K		351 K	
$P_{CO_2} \times 10^{-2}$ (Pa)	α $\left(\mathrm{mol_{CO_2} \cdot mol_S^{-1}}\right)$	$P_{CO_2} \times 10^{-2}$ (Pa)	α $\left(\mathrm{mol_{CO_2} \cdot mol_S^{-1}}\right)$	$P_{CO_2} \times 10^{-2}$ (Pa)	α $\left(\mathrm{mol_{CO_2} \cdot mol_S^{-1}}\right)$	$P_{CO_2} \times 10^{-2}$ (Pa)	α $\left(\mathrm{mol_{CO_2} \cdot mol_S^{-1}}\right)$	$P_{CO_2} \times 10^{-2}$ (Pa)	α $\left(\mathrm{mol_{CO_2} \cdot mol_S^{-1}}\right)$
1.15 [Run 1]	0.358	0.95 [Run 1]	0.349	1.40 [Run 1]	0.302	10.3 [Run 1]	0.353	13.2 [Run 1]	0.137
9.54 [Run 1]	0.572	4.28 [Run 1]	0.538	17.0 [Run 1]	0.610	23.1 [Run 1]	0.524	14.0 [Run 1]	0.159
13.1 [Run 1]	0.590	23.2 [Run 1]	0.637	37.5 [Run 1]	0.665	158 [Run 1]	0.692	15.7 [Run 1]	0.200
21.5 [Run 1]	0.621	36.2 [Run 1]	0.666	79.6 [Run 1]	0.721	389 [Run 1]	0.776	18.7 [Run 1]	0.247
29.8 [Run 1]	0.643	616 [Run 1]	0.920	547 [Run 1]	0.899	3.45 [Run 2]	0.169	24.1 [Run 1]	0.303
38.8 [Run 1]	0.661			1.30 [Run 2]	0.360	5.60 [Run 2]	0.282	28.9 [Run 1]	0.375
55.5 [Run 1]	0.689			2.02 [Run 2]	0.400	8.90 [Run 2]	0.403	62.5 [Run 1]	0.452
211 [Run 1]	0.810			3.87 [Run 2]	0.479	30.1 [Run 2]	0.550	146 [Run 1]	0.539
617 [Run 1]	0.915			7.18 [Run 2]	0.535	108 [Run 2]	0.649	288 [Run 1]	0.604
0.37 [Run 2]	0.172			13.4 [Run 2]	0.582	437 [Run 2]	0.773	12.3 [Run 2]	0.129
1.34 [Run 2]	0.420			34.4 [Run 2]	0.645			13.0 [Run 2]	0.150
2.54 [Run 2]	0.490			305 [Run 2]	0.846			15.0 [Run 2]	0.200
9.62 [Run 2]	0.559							19.0 [Run 2]	0.268
34.6 [Run 2]	0.632							26.5 [Run 2]	0.349
174 [Run 2]	0.761							41.5 [Run 2]	0.441
								253 [Run 2]	0.625

Table 4.4 – Experimental solubility of CO_2 in aqueous solutions of potassium glycinate 3.0 M.

293 K		303 K		313 K		323 K	
$P_{CO_2} \times 10^{-2}$ (Pa)	α $\left(\mathrm{mol}_{CO_2} \cdot \mathrm{mol}_S^{-1}\right)$	$P_{CO_2} \times 10^{-2}$ (Pa)	α $\left(\mathrm{mol}_{CO_2} \cdot \mathrm{mol}_S^{-1}\right)$	$P_{CO_2} \times 10^{-2}$ (Pa)	α $\left(\mathrm{mol}_{CO_2} \cdot \mathrm{mol}_S^{-1}\right)$	$P_{CO_2} \times 10^{-2}$ (Pa)	α $\left(\mathrm{mol}_{CO_2} \cdot \mathrm{mol}_S^{-1}\right)$
1.61 Run 1	0.069	1.61 Run 1	0.075	3.73 Run 1	0.185	2.70 Run 1	0.088
1.90 Run 1	0.103	2.29 Run 1	0.131	8.23 Run 1	0.375	5.10 Run 1	0.144
2.59 Run 1	0.164	3.49 Run 1	0.190	10.3 Run 1	0.446	7.70 Run 1	0.213
3.25 Run 1	0.228	4.34 Run 1	0.228	24.9 Run 1	0.559	9.80 Run 1	0.283
4.60 Run 1	0.292	5.74 Run 1	0.255	1.94 Run 2	0.130	17.8 Run 1	0.363
8.27 Run 1	0.358	8.39 Run 1	0.293	5.34 Run 2	0.260	23.7 Run 1	0.438
10.2 Run 1	0.426	9.94 Run 1	0.327	8.09 Run 2	0.386	60.5 Run 1	0.532
14.9 Run 1	0.489	11.1 Run 1	0.361	15.6 Run 2	0.517	135 Run 1	0.572
45.0 Run 1	0.548	12.0 Run 1	0.394	188 Run 2	0.633	350 Run 1	0.620
168 Run 1	0.617	13.6 Run 1	0.437	326 Run 2	0.664		
330 Run 1	0.661	19.3 Run 1	0.475				
		29.4 Run 1	0.505				
		53.6 Run 1	0.536				
		152 Run 1	0.588				
		381 Run 1	0.645				

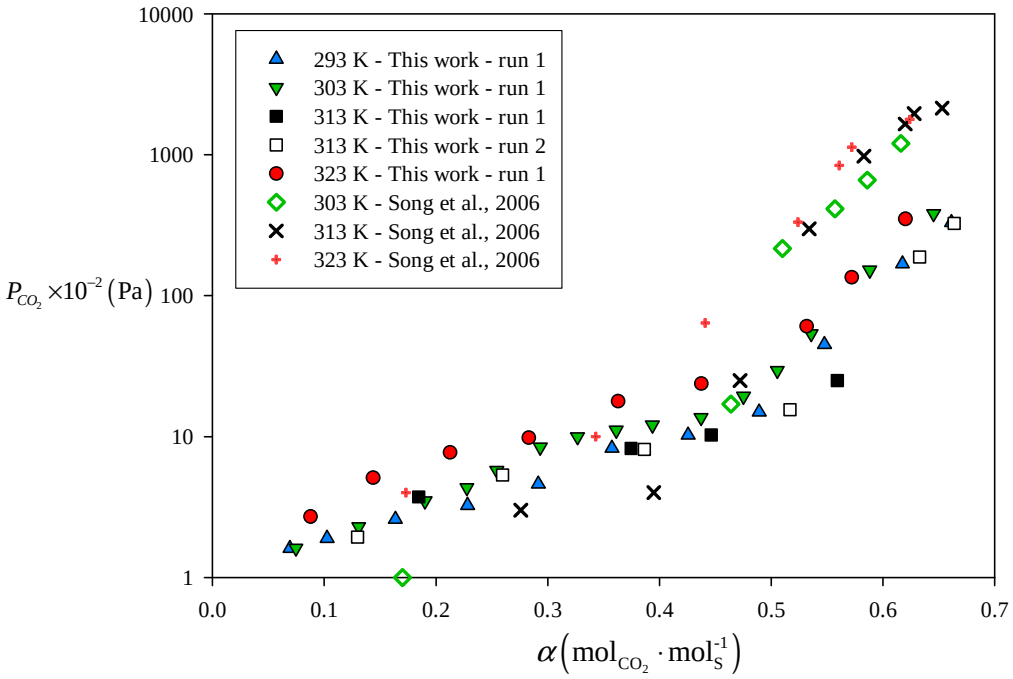

Figure 4.4 – Semi-log plot of the experimental solubility of CO_2 in 3.0 M aqueous solutions of potassium glycinate - comparison with the results from Song et al. (2006) for an aqueous solution of sodium glycinate 3.09 M, at 303, 313 and 323 K.

Surprisingly, no noticeable difference in the CO_2 solubility was observed for temperatures between 293 and 313 K. This behaviour is unusual in the absorption of acid-gases in amine based solutions (Benamor and Aroua, 2005; Derks et al., 2005; Ma'mun et al., 2006; Shen and Li, 1992). Only above 323 K differences start to be noticeable and at 351 K there is a clear reduction on the solution absorption capacity. The same trend was observed for the 3.0 M solutions and, for 0.1 M solutions, there were no differences on the absorption capacity in the entire temperature range studied.

The measured CO_2 solubility in 1.0 M potassium glycinate solutions does not differ significantly from the data obtained by Song et al. (2006) for sodium glycinate 1.06 M, at 313 and 323 K. Indeed, it should be expected that the absorption capacity of sodium glycinate is similar to the potassium glycinate aqueous solution used in this work. Contrarily to the results at 1.0 M, the absorption capacities determined at 3.0 M are not in line with the results that Song et al. (2006) obtained for sodium glycinate. This can be due to the difference in the salt cation. Although it is the glycinate anion that reacts with CO_2, the salt cation may start playing a significant role on the process at solution

concentrations as high as 3.0 M by modifying the ionic character of the solution. According to the Guggenheim Equation (17), differences between the short-range interactions of K^+ (from potassium glycinate) and Na^+ (from sodium glycinate) with the other ions present in solution would become more noticeable at higher concentrations.

At high amino acid salt concentrations and high loadings, precipitation of reaction products was observed by Hook (1997) and Kumar et al. (2003a). The latter authors concluded that, most likely, the precipitate corresponds to the zwitterionic form of the amino acid (RNH_3^+). They also found a relationship between the critical loading (the loading at which reaction products start to precipitate), α_{crit}, and the solubility of the zwitterionic form of the amino acid in solution, S:

$$\alpha_{crit} = \frac{S}{[RNH_2]_0} \tag{24}$$

Although precipitation was not visually detected during the absorption experiments in the present work, the critical loading at 3.0 M concentrations was computed using the solubility data of glycine in water obtained by Ferreira et al. (2004). The minimum critical loading computed was 0.868 (corresponding to the temperature of 293 K) which is above the maximum experimental loading at that temperature (0.661). This result confirms that precipitation was unlikely to occur. Crystallization of the reaction product RNH_3^+ would increase the amount of CO_2 absorbed (and therefore the solution capacity) due to the concentration decrease of this reaction product in the liquid phase (Kumar et al., 2003a).

The effect of the amino acid salt concentration on the absorbent solution capacity at 313 K is shown in Figure 4.5. The loading is shown as a function of the CO_2 equilibrium partial pressure in linear scale. As expected, the loading for a given CO_2 partial pressure decreases with increasing amino acid salt concentration. The same trend was observed for the other temperatures studied. The CO_2 absorption capacity of potassium glycinate at 313 K was compared to MEA at the same temperature. It was verified that, at that temperature, potassium glycinate absorbs more than MEA, which is one of the most widely used CO_2 absorbents nowadays.

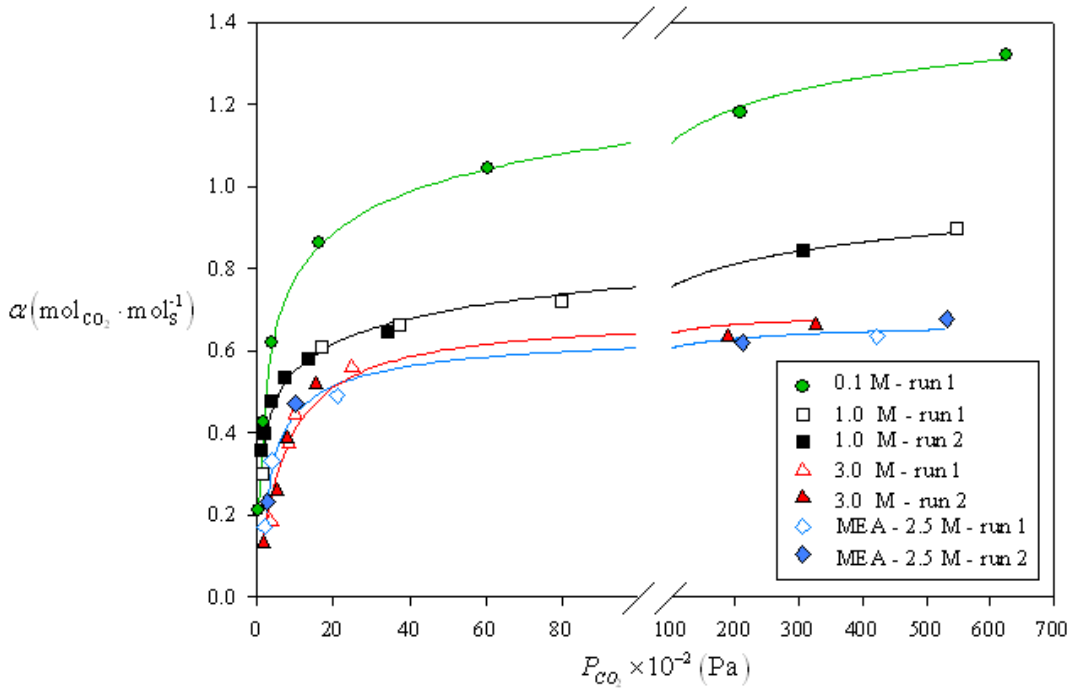

Figure 4.5 - Solution loading as a function of the CO_2 equilibrium partial pressure in aqueous solutions of potassium glycinate at 313 K - comparison with MEA at 2.5 M. Solid lines are provided to make the figure clearer and do not correspond to theoretical model results.

CO_2 solubility in potassium threonate

The absorption capacity of a 1.0 M potassium threonate solution, at 313 K, was also measured and it is shown in Table 4.5 and Figure 4.6.

Table 4.5 – Experimental solubility of CO_2 in aqueous solutions of potassium threonate 1.0 M and 313 K.

$P_{CO_2}\times10^{-2}$ (Pa)	α $\left(\mathrm{mol_{CO_2}}\cdot\mathrm{mol_S^{-1}}\right)$
1.03 Run 1	0.092
2.28 Run 1	0.188
4.68 Run 1	0.292
8.78 Run 1	0.384
24.5 Run 1	0.479
62.5 Run 1	0.572
190 Run 1	0.674
420 Run 1	0.753

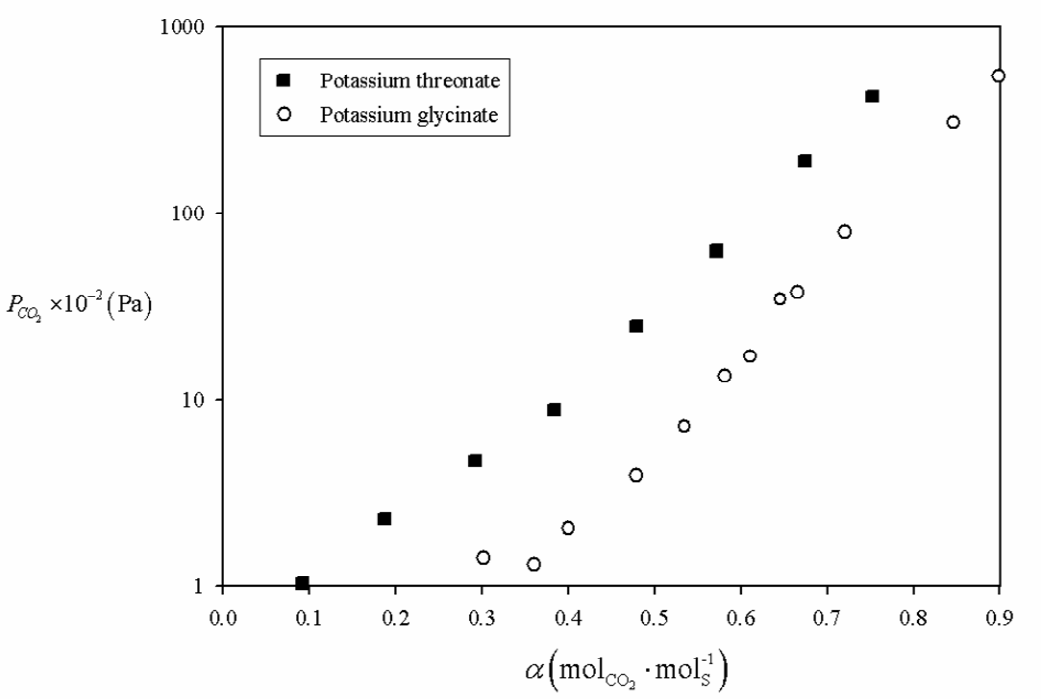

Figure 4.6 - Semi-log plot of the experimental solubility of CO_2 in aqueous solutions of potassium threonate and potassium glycinate with concentrations 1.0 M at 313 K.

Comparing the absorption capacity of both amino acid salts at the same solution concentration, potassium glycinate presents a higher absorption capacity. Threonate has a deprotonation equilibrium constant, K_{AmA}, higher than glycinate (Perrin, 1965). Additionally, the amine group is sterically hindered (Portugal et al., 2008), which makes the carbamate ($RNHCOO^-$) formed less stable and consequently, K_{carb} is expected to be higher (although no values were found in literature for this equilibrium constant).

It is generally accepted that amines that form unstable carbamates (high K_{carb}) present higher absorption capacities towards CO_2 (Baek et al., 2000; Hook, 1997; Li and Chang, 1994; Seo and Hong, 1996). However, this is only true at high CO_2 partial pressures (Park et al., 2003; Sartori and Savage, 1983; Tontiwachwuthikul et al., 1991). On the other hand, increasing K_{AmA} causes a decrease in loading for the entire pressure range (Sartori and Savage, 1983).

To clarify how the solution absorption capacities are influenced by the equilibrium constants K_{AmA} and K_{carb}, the effect of changing these constants by a factor of 10 was

checked by simulation, using the Kent and Eisenberg model. The K_{AmA} and K_{carb} values reported in literature for glycinate (Jensen et al., 1952; Perrin, 1965) – see Table 4.6 – were used as reference. Results are shown in Figures 4.7 and 4.8.

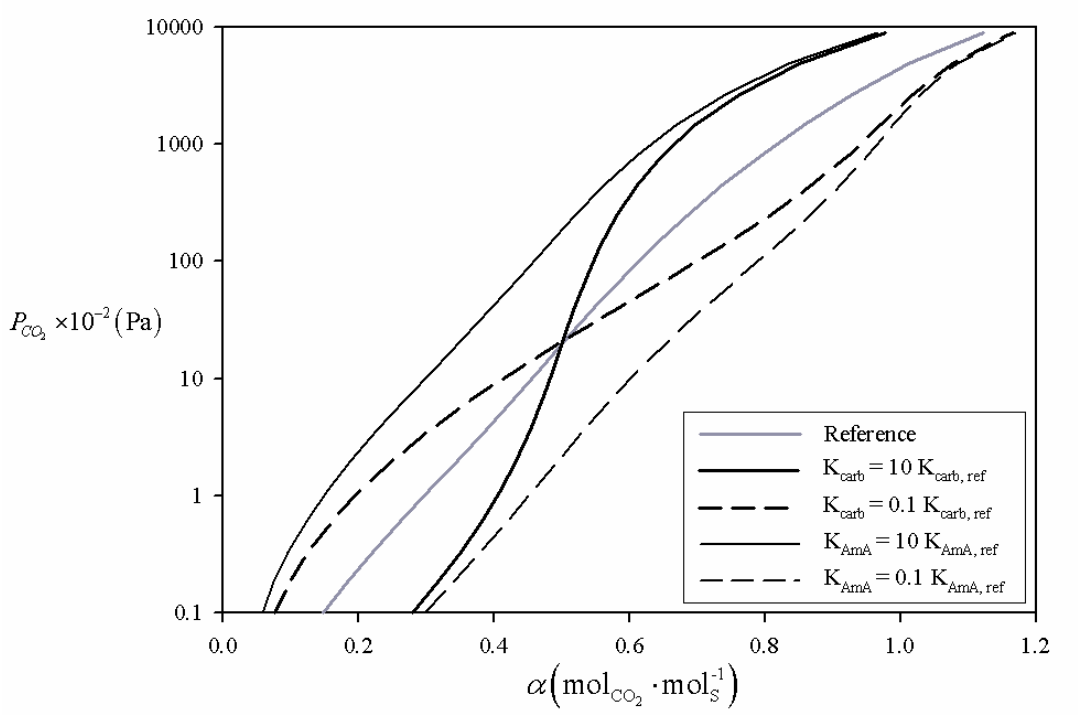

Figure 4.7 – Effect of changing the carbamate hydrolysis and amine deprotonation equilibrium constants independently on the predicted P_{CO_2} versus loading curves.

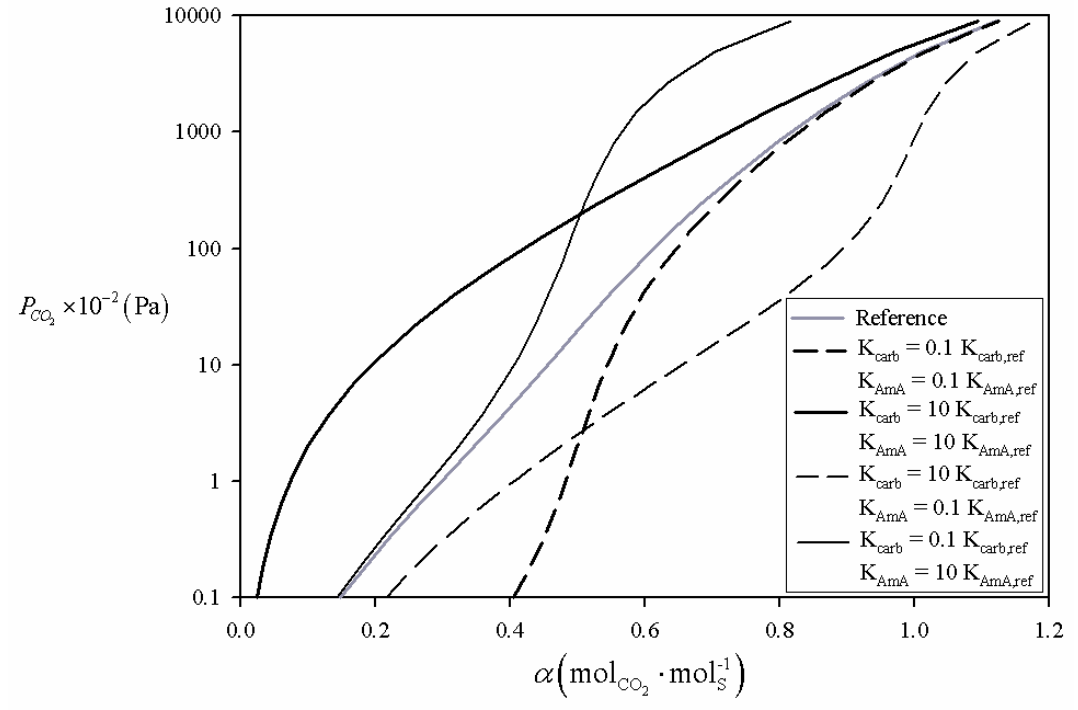

Figure 4.8 – Effect of changing the carbamate hydrolysis and amine deprotonation equilibrium constants simultaneously on the predicted P_{CO_2} versus loading curves.

The simulated results confirm that increasing K_{carb} alone leads to a mixed effect, depending on the pressure range considered, as seen in Figure 4.7. On the other hand, the simultaneous increase of both equilibrium constants, K_{AmA} and K_{carb}, causes a decrease in loading for the entire pressure range, which is in agreement with what is experimentally observed in the present work. A more complete analysis would require knowledge of the carbamate hydrolysis equilibrium constant for threonate. Additionally, ionic interactions must be considered in these systems and, since threonate and glycinate anions are different in size and configuration, it is expectable that these interactions will be different in each case.

Modelling

To model the CO_2 absorption equilibrium in potassium glycinate solution, using the Deshmukh-Mather method (Deshmukh and Mather, 1981), equilibrium constants of reactions (1) to (5) and the Henry coefficient of CO_2 in solutions need to be defined. Table 4.6 shows the values of the equilibrium constants and Henry coefficient and respective literature sources.

Table 4.6 – Equilibrium constants of reactions (1) to (5) and Henry coefficient of CO_2 in potassium glycinate solutions.

$\log\left(\frac{H_{CO_2}}{H_{CO_2,w}}\right) = K\left[RNH_2\right]_0$		
$K = \frac{62.183098}{T} - 0.111175$	$\left(\mathrm{M^{-1}}\right)$	Portugal et al., 2007
$H_{CO_2,w} = \frac{\exp\left(-2044/T\right)}{3.54\times10^{-7}}$	$\left(\mathrm{Pa\ mol^{-1}m^3}\right)$	Versteeg and Van Swaaij, 1988
$K_{carb} = \exp\left(\frac{-2767.18}{T} + 6.10312\right)$	$\left(\mathrm{M}\right)$	Jensen et al., 1952
$K_{AmA} = \exp\left(-0.000237956T^2 + 0.202203T - 61.6499\right)$	$\left(\mathrm{M}\right)$	Perrin, 1965
$K_{CO_2} = \exp\left(-\frac{12092.1}{T} - 36.7816\ln T + 235.482\right)$	$\left(\mathrm{M}\right)$	Benamor and Aroua, 2005
$K_{HCO_3^-} = \exp\left(-\frac{12431.7}{T} - 35.4819\ln T + 220.067\right)$	$\left(\mathrm{M}\right)$	Benamor and Aroua, 2005
$K_w = \exp\left(-\frac{13445.9}{T} - 2.4773\ln T + 140.932\right)$	$\left(\mathrm{M^2}\right)$	Benamor and Aroua, 2005

Kielland (1937) summarized the effective size of a set of hydrated ions, including the ions existent in the studied system, except for the carbamate of glycine. Values of parameter a, based on Kielland's work are shown in Table 4.7.

Table 4.7 – Effective size of the hydrated ions, based on the work by Kielland (1937).

Ion	H^+	OH^-	HCO_3^-	CO_3^{2-}	RNH_2	K^+	$RNHCOO^-$
Parameter a	9	3.5	4	4.5	4.5	3	5 (estimated)

Kumar et al. (2003b) noticed that the ionic strength of the amino acid salt solutions do not change significantly during CO_2 absorption. For this reason, the long-range interactions, LR_{Ki}, between ions will depend essentially on the solution initial concentration - $I \simeq [RNH_2]_0$ - and can be directly computed. Concerning the short-range binary interactions, in reality, when substituting the activity coefficients on the calculation of the equilibrium constants, only six independent parameters can be fitted:

$$K_{carb} = \frac{[RNH_2][HCO_3^-]}{[RNHCOO^-]} LR_{Kcarb} \exp\left[2\left(p_1[RNH_3^+] + p_2[K^+]\right)\right] \quad (25)$$

$$K_{AmA} = \frac{[RNH_2][H^+]}{[RNH_3^+]} LR_{KAmA} \exp\left[2\begin{pmatrix} p_3[RNH_3^+] + p_4[K^+] - p_5[RNH_2] \\ -(p_5 - p_1)[RNHCOO^-] \end{pmatrix}\right] \quad (26)$$

$$K_{CO_2} = \frac{[HCO_3^-][H^+]}{[CO_2]} LR_{KCO2} \exp\left(2 p_6 [K^+]\right) \quad (27)$$

$$K_{HCO_3^-} = \frac{[CO_3^{2-}][H^+]}{[HCO_3^-]} LR_{KHCO3} \exp\left(-2 p_6 [K^+]\right) \quad (28)$$

$$K_w = [OH^-][H^+] LR_{Kw} \quad (29)$$

where the model parameters p_1 to p_6 are defined as:

$$
\begin{aligned}
p_1 &= \left(\beta_{RNH_3^+,\,RNH_2} - \beta_{RNH_3^+,\,RNHCOO^-}\right) \\
p_2 &= \left(\beta_{RNH_2,\,K^+} + \beta_{HCO_3^-,\,K^+} - \beta_{RNHCOO^-,\,K^+}\right) \\
p_3 &= \left(\beta_{RNH_3^+,\,RNH_2} - \beta_{RNH_3^+,\,RNH_3^+}\right) \\
p_4 &= \left(\beta_{RNH_2,\,K^+} - \beta_{RNH_3^+,\,K^+}\right) \\
p_5 &= \beta_{RNH_3^+,\,RNH_2} \\
p_6 &= \beta_{HCO_3^-,\,K^+}
\end{aligned}
\tag{30}
$$

For each P_{CO_2}, the set of eight equations (1 vapour-liquid equilibrium equation, 5 reaction equilibrium constants and 2 mass balances) can be reduced to only 1 equation in terms of the hydrogen ion concentration, $\left[H^+\right]$:

$$
\begin{aligned}
&\left[RNH_2\right]_0 + \left[H^+\right] - \frac{\left[RNH_2\right]_0 \left[H^+\right]}{\frac{1}{K'_{AmA}}\left[H^+\right]^2 + \left[H^+\right] + \frac{K'_{CO_2}}{K'_{carb}}\left(P_{CO_2}/H_{CO_2}\right)} \\
&- \frac{K'_W}{\left[H^+\right]} - \frac{K'_{CO_2}\left(P_{CO_2}/H_{CO_2}\right)}{\left[H^+\right]} - \frac{2K'_{HCO_3^-}K'_{CO_2}\left(P_{CO_2}/H_{CO_2}\right)}{\left[H^+\right]^2} \\
&- \frac{2\left[RNH_2\right]_0 K'_{CO_2}\left(P_{CO_2}/H_{CO_2}\right)}{\frac{K'_{carb}}{K'_{AmA}}\left[H^+\right]^2 + K'_{carb}\left[H^+\right] + K'_{CO_2}\left(P_{CO_2}/H_{CO_2}\right)} = 0
\end{aligned}
\tag{31}
$$

where K'_i are the equilibrium constants expressed in terms of molar concentrations - $K'_i = \frac{K_i}{LR_{Ki} \cdot SR_{Ki}}$ and SR_{Ki} denote the short-range interactions term. The correspondent loading, α_{mod}, is computed using equation (14).

A global fit to all temperatures and concentrations was performed. The objective function to be minimized was:

$$
F_{obj} = \sum \left| \frac{\alpha_{\mathrm{exp}} - \alpha_{\mathrm{mod}}}{\alpha_{\mathrm{exp}}} \right| \tag{32}
$$

The fitted parameters are presented in Table 4.8.

Table 4.8 – Model parameters fitted for the system potassium glycinate-water-CO_2

p_1	p_2	p_3	p_4	p_5	p_6
0.230	-0.877	0.0115	0.351	0.419	0.125

Unlike other amines or amino acids, the amine deprotonation equilibrium constant of glycine, K_{AmA}, found in literature seem to be very established and several authors determined it with agreeing results – results summarized by Perrin (1965). However, the equilibrium constant for the carbamate hydrolysis, K_{carb}, available in the literature is rather old (Jensen et al., 1952). The simple approach from Kent and Eisenberg (1976) was also fit considering that:

$$\ln K_{carb} = K_0 + \frac{A}{T} \tag{33}$$

The same data range and objective function were used. The values of K_0 and A obtained were, respectively, -4.786 and 1792 K^{-1}.

Results obtained with both models for the temperature of 293 K are presented in Figure 4.9 and Figure 4.10 shows the parity plot of the predicted and experimental loadings of CO_2 in solution for all analysed data.

Figure 4.11 shows the species concentrations as a function of loading, obtained with the Deskmukh-Mather model, for a 1.0 M solution at 313 K as a function of the loading. Similar trends were obtained for all studied temperatures and initial amino acid salt concentrations.

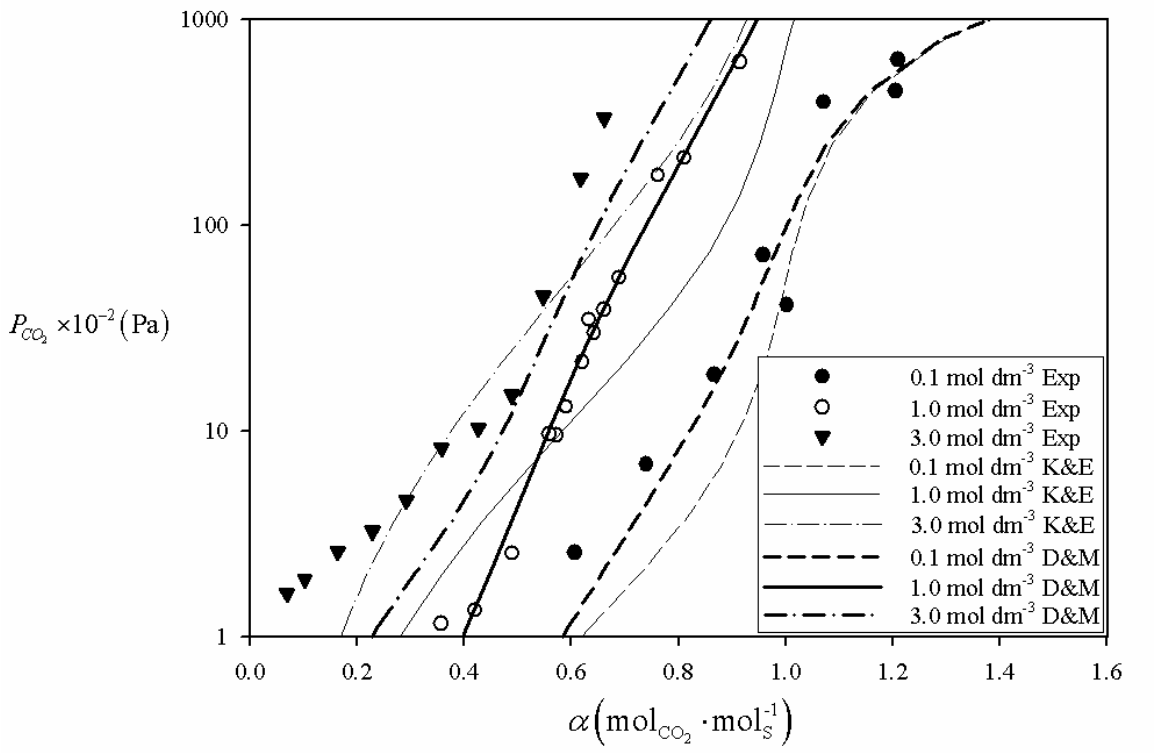

Figure 4.9 – Solubility of CO_2 in potassium glycinate solutions at 293 K – experimental values and model curves.

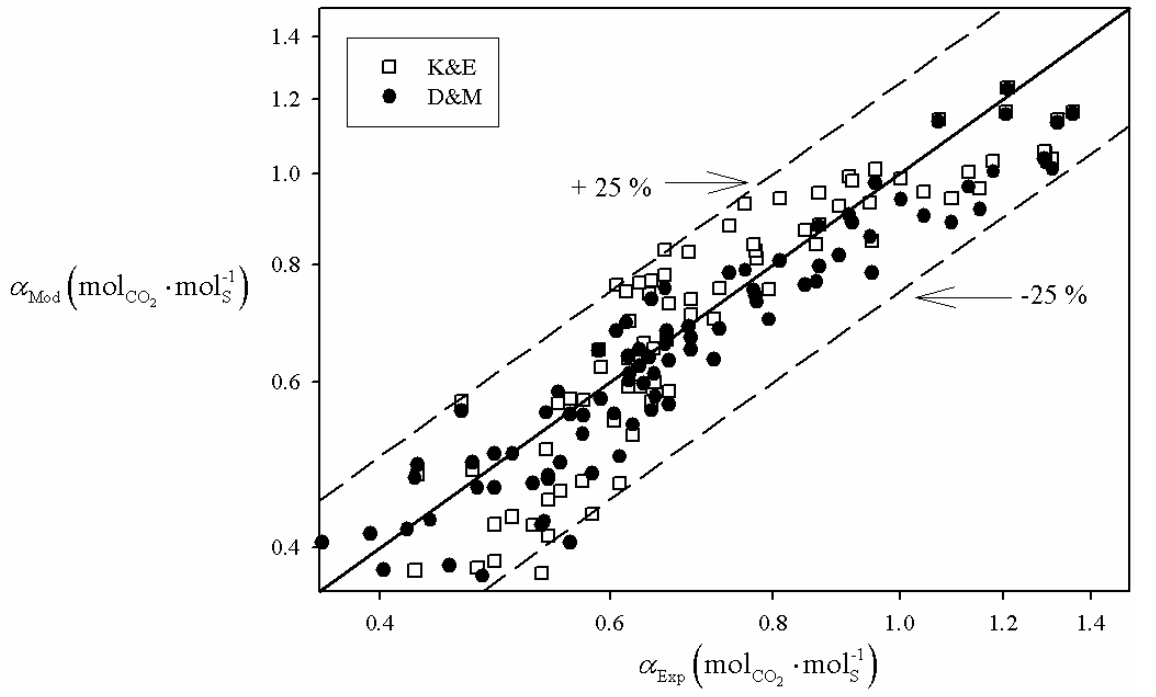

Figure 4.10 – Parity plot of the predicted and experimental loadings of CO_2 in solution for all data analysed.

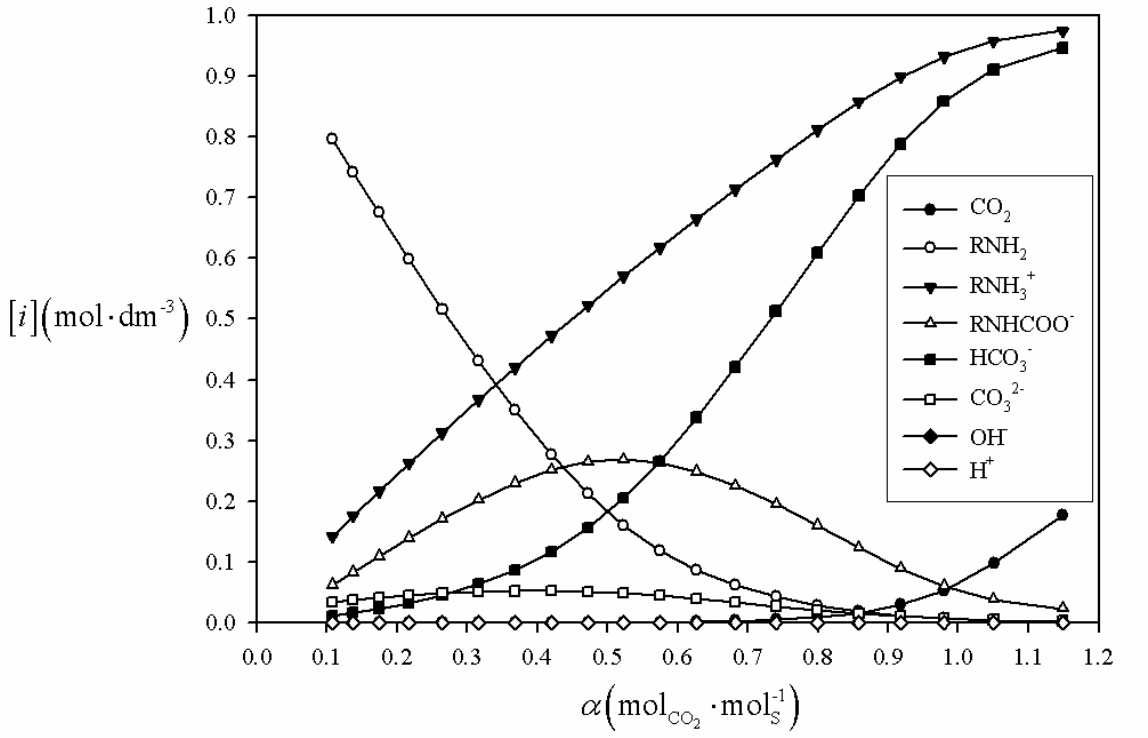

Figure 4.11 – Species concentrations as a function of loading for a potassium glycinate solution, 1.0 M, at 313 K obtained using the Deskmukh-Mather model. Note that points are not experimental data but simulation results.

The average relative deviations presented by the Deskmukh-Mather (D&M) and the Kent and Eisenberg (K&E) models are respectively 22 and 20 %. The error distribution is shown in Figure 4.10. Apparently, the D&M is able to describe better the experimental trends, although the K&E shows a lower average deviation. Globally, both models show similar accuracies which is surprising since the D&M has 6 fitting parameters against the 2 from the K&E model.

Even though the relative deviations may be considered acceptable, Figure 4.9 clearly shows that both fits can still be considerably improved. Several authors (Benamor and Aroua, 2005; Ermatchkov et al., 2006; Ma'mun et al., 2006) considered in their regressions various interaction parameters that were neglected in the present work (including interactions with CO_2 and CO_3^{2-}). The species concentrations as a function of loading shown in Figure 4.11 suggests that, in fact, CO_3^{2-} can be playing a role in the absorption process and that CO_2 concentration can become significant for very high loadings. However, their concentrations are relatively low, for the loadings considered,

when compared to the other species in solution. Benamor and Aroua (2005) and Ermatchkov et al. (2006) also suggest that the short-range interactions between ions are temperature dependent. Nevertheless, regressing more than 6 parameters from the presented data set would lead to unreliable results. For this reason, obtaining the carbamate hydrolysis equilibrium constant, K_{carb}, as well as some of the binary interaction parameters, $\beta_{i,j}$, independently would be a way to improve the prediction results. Experiments at higher temperatures are also recommended.

4.5. Conclusions

The solubility of CO_2 in potassium glycinate and potassium threonate solutions was measured. The amino acid salts shown absorption capacities in the same order of magnitude as MEA.

At moderately low temperatures – between 293 and 323 K – no difference was noticed in the CO_2 solubility at different temperatures. However, increasing temperature to about 351 K, the CO_2 solubility decreases considerably. Experimental data at higher temperatures will be very important to understand the dependence of CO_2 solubility on temperature. The temperature at which the solution needs to be heated to efficiently desorb CO_2 will define the amount of energy required for absorbent regeneration, which will be determinant for the economical viability of the global process.

As observed for other amine based compounds (Benamor and Aroua, 2005; Kumar et al., 2003b; Song et al., 2006), CO_2 solubility in potassium glycinate solutions (expressed in terms of loading) decreases with increasing potassium glycinate concentration.

CO_2 solubility in a 1.0 M potassium threonate solution at 313 K was also measured and compared to potassium glycinate. The trend observed experimentally was qualitatively confirmed by simulation. However, for a quantitative analysis, the carbamate hydrolysis equilibrium constant of threonate needs to be determined and binary interactions between ions should be considered.

CO_2 solubility in the potassium glycinate solutions was interpreted using the Deshmukh-Mather thermodynamically sound model and the empirical Kent-Eisenberg model. Although the average deviations between predicted and experimental loadings are lower than 22 % for both models, the predictions can still be significantly improved. With this purpose, it is suggested to determine independently the carbamate hydrolysis equilibrium constant, K_{carb}, and some of the binary interaction parameters, $\beta_{i,j}$.

4.6. Nomenclature

[ ]	Concentration, M
A	Debye-Hückel limiting slope
a	Parameter corresponding to the effective size of hydrated ions, Å
a_w	Water activity
B	Parameter of equation (17)
H	Henry coefficient, $\mathrm{Pa \cdot mol^{-1} \cdot m^3}$
I	Ionic strength of the solution, $\mathrm{mol \cdot dm^{-3}}$
k	Experimental stage
K	Equilibrium constants, expressed in terms of molarity
LR	Long-range interactions
n	Number of moles, mol
p	Model parameters
P_{CO_2}	Carbon dioxide partial pressure, Pa
R	Universal gas constant, $\mathrm{J \cdot mol^{-1} \cdot K^{-1}}$
S	Solubility, M
SR	Short-range interactions
T	Temperature, K
V	Volume, $\mathrm{m^3}$
z	Ion charge

Greek symbols

α	Loading, $\mathrm{mol_{CO_2} \cdot mol_S^{-1}}$
$\beta_{i,j}$	Short range interaction parameters

ε	Dielectric constant of water, K^{-1}
γ	Activity coefficient
Subscripts	
0	Initial
abs	Absorbed
add	Added
AV	Absorbent vessel
eq	Equilibrium
Exp	Experimental
fin	Final
GV	Gas vessel
Mod	Model
S	Amino acid salt
SC	Stirred cell
sol	Solution
w	Water

4.7. References

Aroua, M. K. and Salleh, R. M. (2004). "Solubility of CO_2 in aqueous piperazine and its modeling using the Kent-Eisenberg approach." Chemical Engineering & Technology, 27(1), 65-70.

Austgen, D. M., Rochelle, G. T., Peng, X. and Chen, C. C. (1989). "Model of Vapor Liquid Equilibria for Aqueous Acid Gas Alkanolamine Systems Using the Electrolyte NRTL Equation." Industrial & Engineering Chemistry Research, 28(7), 1060-1073.

Baek, J.-I., Yoon, J.-H. and Eum, H.-M. (2000). "Prediction of equilibrium solubility of carbon dioxide in aqueous 2-amino-2-methyl-1,3-propanediol solutions." Korean Journal of Chemical Engineering, 17(4), 484-487.

Benamor, A. and Aroua, M. K., (2005). "Modeling of CO_2 solubility and carbamate concentration in DEA, MDEA and their mixtures using the Deshmukh-Mather model." Fluid Phase Equilibria, 231(2), 150-162.

Chen, C. C. and Evans, L. B., (1986). "A Local Composition Model for the Excess Gibbs Energy of Aqueous-Electrolyte Systems." American Institute of Chemical Engineers Journal, 32(3), 444-454.

Clegg, S. L. and Pitzer, K. S. (1992). "Thermodynamics of Multicomponent, Miscible, Ionic-Solutions - Generalized Equations for Symmetrical Electrolytes." Journal of Physical Chemistry, 96(8), 3513-3520.

Clegg, S. L., Pitzer, K. S. and Brimblecombe, P. (1992). "Thermodynamics of multicomponent, miscible, ionic-solutions .2. Mixtures including unsymmetrical electrolytes." Journal of Physical Chemistry, 96(23), 9470-9479.

Derks, P. W. J., Dijkstra, H. B. S., et al., (2005). "Solubility of carbon dioxide in aqueous piperazine solutions." American Institute of Chemical Engineers Journal, 51(8), 2311-2327.

Deshmukh, R. D. and Mather, A. E., (1981). "A Mathematical-Model for Equilibrium Solubility of Hydrogen-Sulfide and Carbon-Dioxide in Aqueous Alkanolamine Solutions." Chemical Engineering Science, 36(2), 355-362.

EC (2008). "Communication from the Commission to the European Parliament, The Council, The European Economic and Social Committee and The Committee of the Regions - 20 20 by 2020 Europe's climate change opportunity." E. Commission, Commission of the European Communities.

Ermatchkov, V., Kamps, A. P. S., et al., (2006). "Solubility of carbon dioxide in aqueous solutions of piperazine in the low gas loading region." Journal of Chemical and Engineering Data, 51(5), 1788-1796.

Favre, E., (2007). "Carbon dioxide recovery from post-combustion processes: Can gas permeation membranes compete with absorption?" Journal of Membrane Science, 294(1-2), 50-59.

Feron, P. H. M. and Jansen, A. E. (2002). "CO_2 separation with polyolefin membrane contactors and dedicated absorption liquids: performances and prospects." Separation and Purification Technology, 27(3), 231-242.

Ferreira, L. A., Macedo, E. A., et al., (2004). "Solubility of amino acids and diglycine in aqueous-alkanol solutions." Chemical Engineering Science, 59(15), 3117-3124.

Furst, W. and Renon, H. (1993). "Representation of Excess Properties of Electrolyte-Solutions Using a New Equation of State." American Institute of Chemical Engineers Journal, 39(2), 335-343.

Gibbins, J. and Chalmers, H., (2008). "Preparing for global rollout: A 'developed country first' demonstration programme for rapid CCS deployment." Energy Policy, 36(2), 501-507.

Goff, G. S. and Rochelle, G. T., (2006). "Oxidation inhibitors for copper and iron catalyzed degradation of monoethanolamine in CO_2 capture processes." Industrial & Engineering Chemistry Research, 45(8), 2513-2521.

Guggenheim, E. A., (1935). "The specific thermodynamic properties of aqueous solutions of strong electrolytes." Philosophical Magazine, 19(127), 588-643.

HajiSulaiman, M. Z., Aroua, M. K. and Pervez, M. I. (1996). "Equilibrium concentration profiles of species in CO_2-alkanolamine-water systems." Gas Separation & Purification, 10(1), 13-18.

Holst, J., Politiek, P. P., et al. (2006). "CO_2 capture from flue gas using amino acid salt solutions." GHGT-8, NTNU VIDERE, Pav. A, Dragvoll, NO-7491 Trondheim, Norway.

Hook, R. J., (1997). "An investigation of some sterically hindered amines as potential carbon dioxide scrubbing compounds." Industrial & Engineering Chemistry Research, 36(5), 1779-1790.

Huttenhuis, P. J. G., Agrawal, N. J., Solbraa, E. and Versteeg, G. F. (2008). "The solubility of carbon dioxide in aqueous N-methyldiethanolamine solutions." Fluid Phase Equilibria, 264(1-2), 99-112.

Idem, R. and Tontiwachwuthikul, P., (2006). "Preface for the special issue on the capture of carbon dioxide from industrial sources: Technological developments and future opportunities." Industrial & Engineering Chemistry Research, 45(8), 2413-2413.

IEA (2008). "International Energy Agency - http://www.iea.org/."

Jensen, A., Jensen, J. B., et al., (1952). "Studies on Carbamates .6. The Carbamate of Glycine." Acta Chemica Scandinavica, 6(3), 395-397.

Jones, J. H., Froning, H. R., et al., (1959). "Solubility of Acidic Gases in Aqueous Monoethanolamine." Journal of Chemical Engineering Data, 4(1), 85.

Kielland, J. (1937). "Individual activity coefficients of ions in aqueous solutions." Journal of the American Chemical Society, 59, 1675-1678.

Kent, R. L. and Eisenberg, B., (1976). "Better Data for Amine Treating." Hydrocarbon Processing, 55(2), 87-90.

Knowlton, A. E., (1941). "Standard handbook for electrical engineers" McGraw-Hill, New York.

Kumar, P., Hogendoorn, J., et al., (2002). "New absorption liquids for the removal of CO_2 from dilute gas streams using membrane contactors." Chemical Engineering Science, 57(9), 1639-1651.

Kumar, P., Hogendoorn, J., et al., (2003a). "Equilibrium solubility of CO_2 in aqueous potassium taurate solutions: Part 1. Crystallization in carbon dioxide loaded aqueous salt solutions of amino acids." Industrial & Engineering Chemistry Research, 42(12), 2832-2840.

Kumar, P., Hogendoorn, J., et al., (2003b). "Equilibrium solubility of CO_2 in aqueous potassium taurate solutions: Part 2. Experimental VLE data and model." Industrial & Engineering Chemistry Research, 42(12), 2841-2852.

Kumar, P., Hogendoorn, J., et al., (2003c). "Kinetics of the reaction of CO_2 with aqueous potassium salt of taurine and glycine." American Institute of Chemical Engineers Journal, 49(1), 203-213.

Lee, J. I., Otto, F. D., et al., (1974). "Solubility of Mixtures of Carbon-Dioxide and Hydrogen-Sulfide in Aqueous Diethanolamine Solutions." Canadian Journal of Chemical Engineering, 52(1), 125-127.

Lee, J. I., Otto, F. D., et al., (1976). "Equilibrium in Hydrogen Sulfide Monoethanolamine-Water System." Journal of Chemical and Engineering Data, 21(2), 207-208.

Li, C. X. and Furst, W. (2000). "Representation of CO_2 and H2S solubility in aqueous MDEA solutions using an electrolyte equation of state." Chemical Engineering Science, 55(15), 2975-2988.

Li, M. H. and Shen, K. P. (1993). "Calculation of Equilibrium Solubility of Carbon-Dioxide in Aqueous Mixtures of Monoethanolamine with Methyldiethanolamine." Fluid Phase Equilibria, 85, 129-140.

Li, M. H. and Chang, B. C. (1994). "Solubilities of Carbon-Dioxide in Water Plus Monoethanolamine Plus 2-Amino-2-Methyl-1-Propanol." Journal of Chemical and Engineering Data, 39(3), 448-452.

Liu, H. B., Zhang, C. F. and Xu, G. W. (1999). "A study on equilibrium solubility for carbon dioxide in methyldiethanolamine-piperazine-water solution." Industrial & Engineering Chemistry Research, 38(10), 4032-4036.

Ma'mun, S., Jakobsen, J. P., Svendsen, H. F. and Juliussen, O. (2006). "Experimental and modeling study of the solubility of carbon dioxide in aqueous 30 mass % 2-((2-aminoethyl)amino)ethanol solution." Industrial & Engineering Chemistry Research, 45(8), 2505-2512.

Metz, B., Davidson, O., et al. (2005). "IPCC Special Report on Carbon Dioxide Capture and Storage." C. U. Press. Cambridge, New York, Melbourne, Madrid, Cape Town, Singapore, São Paulo, Intergovernmental Panel on Climate Change.

Park, J. Y., Yoon, S. J. and Lee, H. (2003). "Effect of steric hindrance on carbon dioxide absorption into new amine solutions: Thermodynamic and spectroscopic verification through solubility and NMR analysis." Environmental Science & Technology, 37(8), 1670-1675.

Park, S. H., Lee, K. B., Hyun, J. C. and Kim, S. H. (2002). "Correlation and prediction of the solubility of carbon dioxide in aqueous alkanolamine and mixed alkanolamine solutions." Industrial & Engineering Chemistry Research, 41(6), 1658-1665.

Perrin, D. (1965). "Dissociation Constants of Organic Bases in Aqueous Solutions." Butterworth, London.

Portugal, A. F., Derks, P. W. J., et al., (2007). "Characterization of potassium glycinate for carbon dioxide absorption purposes." Chemical Engineering Science, 62(23), 6534-6547.

Portugal, A. F., Magalhães, F. D., et al., (2008). "Carbon dioxide absorption kinetics in potassium threonate." Chemical Engineering Science, 63(13), 3493-3503.

Rascol, E., Meyer, M. and Prevost, M. (1996). "Simulation and parameter sensitivity analysis of acid gas absorption into mixed alkanolamine solutions." Computers & Chemical Engineering, 20, S1401-S1406.

Sartori, G. and Savage, D. W. (1983). "Sterically Hindered Amines for CO_2 Removal from Gases." Industrial & Engineering Chemistry Fundamentals, 22(2), 239-249.

Seo, D. J. and Hong, W. H. (1996). "Solubilities of carbon dioxide in aqueous mixtures of diethanolamine and 2-amino-2-methyl-1-propanol." Journal of Chemical and Engineering Data, 41(2), 258-260.

Shen, K. P. and Li, M. H., (1992). "Solubility of Carbon-Dioxide in Aqueous Mixtures of Monoethanolamine with Methyldiethanolamine." Journal of Chemical and Engineering Data, 37(1), 96-100.

Smith, J. M., Ness, H. C. V., et al., (1996). "Introduction to chemical engineering thermodynamics." McGraw-Hill, Singapore.

Song, H. J., Lee, S., et al., (2006). "Solubilities of carbon dioxide in aqueous solutions of sodium glycinate." Fluid Phase Equilibria, 246(1-2), 1-5.

Supap, T., Idem, R., et al., (2006). "Analysis of monoethanolamine and its oxidative degradation products during CO_2 absorption from flue gases: A comparative study of GC-MS, HPLC-RID, and CE-DAD analytical techniques and possible optimum combinations." Industrial & Engineering Chemistry Research, 45(8), 2437-2451.

Tobiesen, F. A., Juliussen, O. and Svendsen, H. F. (2008). "Experimental validation of a rigorous desorber model for CO_2 post-combustion capture." Chemical Engineering Science, 63(10), 2641-2656.

Tontiwachwuthikul, P., Meisen, A. and Lim, C. J. (1991). "Solubility of CO_2 in 2-Amino-2-Methyl-1-Propanol Solutions." Journal of Chemical and Engineering Data, 36(1), 130-133.

UNFCCC (2008). "United Nations Framework Convention on Climate Change - http://unfccc.int. "

Vallee, G., Mougin, P., Jullian, S. and Furst, W. (1999). "Representation of CO_2 and H2S absorption by aqueous solutions of diethanolamine using an electrolyte equation of state." Industrial & Engineering Chemistry Research, 38(9), 3473-3480.

Versteeg, G. F. and Van Swaaij, W. P. M., (1988). "Solubility and Diffusivity of Acid Gases (CO_2, N_2O) in Aqueous Alkanolamine Solutions." Journal of Chemical and Engineering Data, 33(1), 29-34.

Weiland, R. H., Chakravarty, T., et al., (1993). "Solubility of Carbon-Dioxide and Hydrogen-Sulfide in Aqueous Alkanolamines. " Industrial & Engineering Chemistry Research, 32(7), 1419-1430.

Part IV

5. Carbon dioxide removal from anaesthetic gas circuits using hollow fiber membrane contactors with amino acid salt solutions[1]

Abstract

A novel technology, based on the use of hollow fiber membrane contactors with regenerable liquid absorbents is proposed for the carbon dioxide removal from anaesthetic closed breathing circuits. To analyse the performance of the contactor for this specific application and the influence of the system parameters, a 2 D numerical model was developed for the transport of CO_2 through the hollow fibers. The model considered potassium glycinate solutions as absorbents and a composite membrane, made of a porous support layer and a dense thin layer. Both co- and counter-current operations were studied. The model results were compared to results obtained with conventional mass transfer models, valid for limit conditions, and a good agreement was found. The analysis performed indicates that the use of hollow fiber membrane contactors with amino acid salt absorbent solutions is suitable for CO_2 removal from closed anaesthetic circuits. Contactor design and operating conditions are suggested.

[1] Portugal, A. F.; Magalhães, F. D.; Mendes, A., "Carbon dioxide removal from anaesthetic gas circuits using hollow fiber membrane contactors with amino acid salt solutions", submitted to J. Memb. Sci.

5.1. Introduction

Low flow or closed loop anaesthesia is a current clinical practice that consists in feeding back to the patient (in the subsequent inhalation) the unused anaesthetic gas stream (Baum and Woehlck, 2003). In such systems, CO_2 needs to be continuously removed from the breathing circuit. For this purpose, mixtures of alkali hydroxides are commonly used as absorbents (Baum and Woehlck, 2003). However, all halogenated volatile anaesthetics react with conventional CO_2 absorbents when these become accidentally desiccated, resulting in toxic compounds such as carbon monoxide and the so called compound A (Baum and Woehlck, 2003; Fan et al., 2008; Knolle and Gilly, 2000; Whalen et al., 2005). In addition, the spent absorbents are contaminated hospital waste, therefore requiring specific and expensive treatments (Mendes, 2000).

Hollow fiber membrane contactors with renewable liquid absorbents can be an attractive technology to perform the CO_2 removal from respiratory circuits in anaesthesia machines, as sketched in Figure 5.1 (Mendes, 2000; Portugal et al., 2007). Because of the absence of interpenetration of the gaseous and liquid phases, membrane contactors overcome a number of operational limitations, common in other sorts of contactors, and enable aseptic operation, making the process suitable for the required application (Gabelman and Hwang, 1999; Li and Chen, 2005).

In absorbent membrane contactors, the selectivity is mostly provided by the liquid and the driving force for the mass transfer is the concentration gradient between gas and liquid phases (Gabelman and Hwang, 1999; Li and Chen, 2005). Therefore, the membrane works as a phase separator and should impose the least possible resistance to mass transfer. Hence, porous membranes with gas filled pores are usually used (Boucif et al., 2008; Feron and Jansen, 2002; Sea et al., 2002; Zhang and Cussler, 1985). However, for the proposed application, the membranes must also block the possible passage of pathogenic microorganisms from the breathing circuit to the absorbent solution and the subsequent transmission to the next patient under surgery. A possible strategy to meet this demand is the use of supported dense polymer membranes as suggested by Kreulen et al. (1993b) for other applications. Although the dense coating

imposes an extra resistance to mass transfer, it also prevents the pores from wetting, independently of the liquid surface tension and contact angle (Kreulen et al., 1993b).

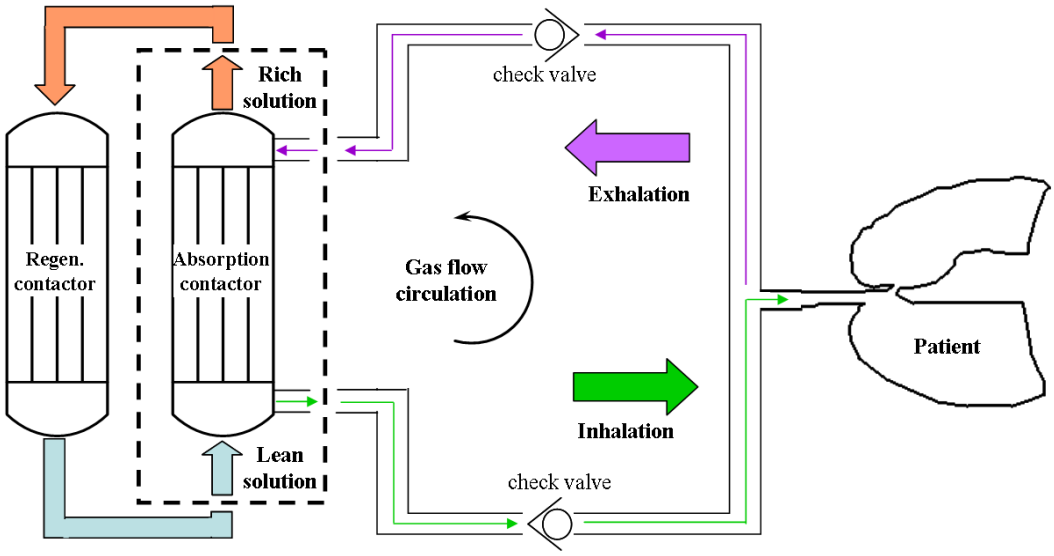

Figure 5.1 – Sketch of a closed anaesthetic breathing circuit using hollow fiber membrane contactors for CO_2 removal.

Chemical absorption in reactive liquids (usually aqueous solutions of alkanolamines) is an established technology to perform CO_2 separation from a variety of gas mixtures (Idem and Tontiwachwuthikul, 2006; Ma'mun et al., 2007). However, alkanolamines may undergo oxidation in environments with high oxygen concentrations (Goff and Rochelle, 2006; Hook, 1997; Supap et al., 2006). Therefore other absorbent systems are being developed, namely aqueous solutions of amino acid salts (Feron and Jansen, 2002; Hamborg et al., 2007; Kumar et al., 2002; Portugal et al., 2008; Song et al., 2006). These solutions are much more resistant to oxidative degradation, are more thermally stable, present lower volatilities and higher surface tensions and have densities and viscosities similar to water. Besides, when compared to alkanolamines, they present similar reaction equilibrium and kinetics (Feron and Jansen, 2002; Hamborg et al., 2007; Kumar et al., 2002; Portugal et al., 2008; Song et al., 2006). An important drawback may be related to precipitation of the reaction products, which has been reported for high amino acid salt concentrations and high loadings (Hook, 1997; Kumar et al., 2003c; Majchrowicz et al., 2006). This can result in the blockage of the

membrane pores (if porous membranes are to be used) and originate hydrodynamic problems when small fiber diameters are used.

In the present work, a 2D numerical model is developed to describe the CO_2 absorption in amino acid salt solutions. A membrane contactor is considered, with the absorbent flowing in the hollow fibers bore, and with the gas flowing in the shell side. Both co- and counter-current operations are considered. To validate the model, simulation results are compared to results obtained by conventional mass transfer models, at limit conditions where these are applicable.

For the anaesthetic closed loop simulations, the permeability properties of a composite PDMS (polydimethylsiloxane) membrane and of aqueous absorbent solutions of potassium glycinate were used. Specific aspects of this system such as the extra resistance imposed by the membrane coating, the reaction mechanism and the absorption equilibrium of CO_2 in potassium glycinate are taken into account in the simulations. The performance of the contactor is analysed and the influence of the packing density, fiber length, liquid flow rate and solution concentration on the separation achieved is evaluated.

5.2. Mass Transfer with Chemical Reaction

5.2.1. Chemical reaction

Alkali salts of primary amino acids present identical reactions towards CO_2 as primary alkanolamines (Kumar et al., 2003a). CO_2 reacts with aqueous solutions of primary alkanolamines forming carbamates, bicarbonates and carbonates (Caplow, 1968) and the first reaction taking place is the formation of the carbamate or an intermediate (Hook, 1997; Sartori and Savage, 1983):

$$2RNH_2 + CO_2 \rightleftarrows RNHCOO^- + RNH_3^+ \qquad (1)$$

It is generally accepted that reaction (1) occurs according to the zwitterion mechanism (Caplow, 1968). Zwitterion mechanism considers the following reaction steps:

Formation of the zwitterion

$$RNH_2 + CO_2 \underset{k_{-1}}{\overset{k_2}{\rightleftharpoons}} RNH_2^+COO^- \tag{2}$$

Deprotonation of the zwitterion by a base

$$RNH_2^+COO^- + B_i \underset{k_{-B}}{\overset{k_B}{\rightleftharpoons}} RNHCOO^- + B_iH^+ \tag{3}$$

where B_i are the bases present in solution able to deprotonate the zwitterion, which includes the amine itself (Blauwhoff et al., 1984; Portugal et al., 2007). Based on the quasi-steady-state condition for the zwitterion concentration, the following expression for the rate of CO_2 absorption can be written:

$$S_{CO_2} = \frac{C_{CO_2} C_{RNH_2} - C_{RNHCOO^-} \left(\frac{k_{-1}}{k_2}\right)\left(\frac{\sum_i k_{-B_i} C_{B_iH^+}}{\sum_i k_{B_i} C_{B_i}}\right)}{\frac{1}{k_2} + \frac{k_{-1}}{k_2 \sum_i k_{B_i} C_{B_i}}} \tag{4}$$

Considering that the amine is playing the main role on the zwitterion deprotonation, the kinetic constants of reactions (2) and (3) can be related to the equilibrium constant of reaction (1), K_{ov}, as follows:

$$K_{ov} = \frac{k_2}{k_{-1}} \frac{k_{B_i}}{k_{-B_i}} \tag{5}$$

Substituting equation (5) in (4) and since, for primary amines, the deprotonation of the zwiteterion is relatively fast when compared to the backward rate of reaction (2) ($\frac{k_{-1}}{\sum_i k_{B_i} c_{B_i}} << 1$), the following expression for the rate of CO_2 absorption results:

$$S_{CO_2} = k_2 C_{CO_2} C_{RNH_2} - \frac{k_2}{K_{ov}} \frac{C_{RNHCOO^-} C_{RNH_3^+}}{C_{RNH_2}} \tag{6}$$

And, according to reaction (1), the rate of consumption of the amino acid is given by:

$$S_{RNH_2} = 2S_{CO_2} \tag{7}$$

5.2.2. Analogy to conventional mass transfer models

The process of mass transfer of a gaseous solute A in a membrane contactor includes the following steps: diffusion from the gas bulk to the outer membrane surface, diffusion trough the membrane pores, diffusion and sorption in the dense layer (if coated membranes are used) and dissolution and diffusion in the liquid accompanied (or not) by chemical reaction (Li and Chen, 2005). Then, the local flux of A into the liquid, J_A, can be expressed by the following equation:

$$J_A = k_{ov}\Delta C_A \tag{8}$$

where ΔC_A is the concentration gradient between gas and liquid phases and k_{ov} is the overall mass transfer coefficient that, relating to the resistance in series model, is given as follows:

$$\frac{1}{k_{ov}} = \underbrace{\frac{1}{k_g}}_{\text{gas phase resistence}} + \underbrace{\frac{1}{k_m}}_{\text{membrane resistence}} + \underbrace{\frac{1}{mk_L E}}_{\text{liquid phase resistence}} \tag{9}$$

Usually, the gas phase mass transfer resistance needs to be obtained empirically and is very specific of the type of module used (Gabelman and Hwang, 1999). If porous non-wetted membranes are used, the mass transfer resistance due to the membrane is usually negligible. However, when using coated membranes, membrane resistance needs to be accounted for. Even in these cases, generally, the liquid phase mass transfer resistance controls the process.

There are a number of mass transfer models to describe the absorption of a gas into a liquid under well-mixed bulk conditions (Danckwerts, 1970). Since the flow along a hollow fiber is usually laminar (given its small diameter) there is a velocity profile across the entire fiber radius. Therefore, a well-mixed bulk cannot be considered (Dindore et al., 2005a; Kreulen et al., 1993b; Kumar, 2002). However, there are limiting situations where the analogy to conventional mass transfer models is possible (Elk et al., 2007; Knaap et al., 2000; Kreulen et al., 1993a; Kreulen et al., 1993b; Kumar et al., 2003d).

Concerning the physical absorption of a gas with constant composition into a liquid, the following applies (Dindore et al., 2005a):

$$J_A = k_L \left(C_{A,int} - C_{A,bulk} \right) \tag{10}$$

where $C_{A,int}$ is the interfacial concentration and, $C_{A,bulk}$ is the concentration of A in the liquid bulk.

Making the analogy to heat transfer models, Kreulen et al. (1993a) proposed an approximate solution to compute the mass transfer coefficient, k_L, when the liquid is flowing laminarly (with fully developed velocity profile) along the fiber lumen:

$$Sh = \sqrt[3]{3.67^3 + 1.62^3 Gz} \tag{11}$$

where Sh and Gz are the dimensionless Sherwood and Graetz numbers.

For the same flow conditions $C_{A,bulk}$ can be approximated by the average mixing cup concentration of A over the length of the fiber, $\bar{C}_{A,L}$. Considering a lean liquid entering a hollow fiber with diameter d, the mixing cup concentration at the axial distance z from the liquid inlet, $C_{A,z}$, is given by (Kreulen et al., 1993a):

$$C_{A,z} = C_{A,int} \left[1 - \exp\left(-\frac{4 k_L z}{v d} \right) \right] \tag{12}$$

Integrating $C_{A,z}$ over the fiber length, the average mixing cup concentration of A is obtained (Dindore et al., 2005a; Kumar, 2002):

$$\bar{C}_{A,L} = C_{A,int} + C_{A,int} \frac{v d}{4 L k_L} \left[\exp\left(-\frac{4 L k_L}{v d} \right) - 1 \right] \tag{13}$$

where L is the fiber length and v is the liquid velocity.

The approximation proposed by Kreulen et al. (1993a) was experimentally validated and shown to be applicable over the entire range of laminar flow.

In the case of plug flow, according to the penetration theory, the mass transfer coefficient is given by (Bird et al., 2002):

$$k_L = 2 \sqrt{\frac{D_A v}{\pi L}} \tag{14}$$

being D_A the diffusion coefficient of the absorbing gaseous component A.

When the gas absorption is accompanied by chemical reaction, an enhancement factor, E, is introduced in the calculation of the absorption flux (Dindore et al., 2005a):

$$J_A = E\, k_L \left(C_{A,int} - C_{A,bulk} \right) \tag{15}$$

Generally, the enhancement factor is a function of the dimensionless Hatta number, Ha, and the infinite enhancement factor, E_∞, which for a general reaction $\nu_A A + \nu_B B \rightarrow$ Products, with reaction rate expression $S_A = k_{m,n} C_A^m C_B^n$, are defined as:

$$Ha = \frac{\sqrt{k_{m,n}\, C_{B,bulk}^n C_{A,int}^{m-1} D_A}}{k_L} \tag{16}$$

$$E_\infty = \left(1 + \frac{C_{B,bulk} D_B}{\nu_B C_{A,int} D_A} \right) \left(\frac{D_A}{D_B} \right)^q \tag{17}$$

being $k_{m,n}$ the reaction kinetic constant, $C_{B,bulk}$ the reactant concentration in the liquid bulk and D_B the diffusion coefficient of reactant B in the liquid. The value of q depends on the mass transfer model chosen, being 0 for the film model, 1/2 for the penetration model and 1/3 for the Leveque model (which accounts for the presence of a velocity gradient in the mass transfer zone).

Based on the surface renewal theory, DeCoursey (1974) developed an explicit expression to calculate the enhancement factor of a second order irreversible reaction ($\nu_A A + \nu_B B \rightarrow$ Products with $S_A = k_2 C_A C_B$):

$$E = -\frac{Ha^2}{2\left(E_\infty - 1\right)} + \sqrt{\frac{Ha^4}{4\left(E_\infty - 1\right)^2} + \frac{E_\infty Ha^2}{E_\infty - 1} + 1} \tag{18}$$

The DeCoursey approximation proved to accurately predict the enhancement factors over a wide range of process conditions (Van Swaaij and Versteeg, 1992).

According to the film theory, Secor and Beutler (1967) derived an equation for the infinite enhancement factor, including reversibility, of the following general absorption reaction:

$$\nu_A A + \nu_B B \rightleftarrows \nu_C C + \nu_D D \tag{19}$$

The expression from Secor and Beutler (1967) was later adapted by Hogendoorn et al. (1997) to make it more compatible with the penetration and surface renewal theories (Derks et al., 2006):

$$E_\infty = 1 + \frac{\nu_A \left(C_{C,int} - C_{C,bulk} \right)}{\nu_C \left(C_{A,int} - C_{A,bulk} \right)} \sqrt{\frac{D_C}{D_A}} \tag{20}$$

The concentration of the product C at the interface, $C_{C,int}$ can be computed using the following equations (Derks et al., 2006):

$$C_{B,int} = C_{B,bulk} + \frac{\nu_B}{\nu_C} \frac{D_C}{D_B} \left(C_{C,bulk} - C_{C,int} \right) \tag{21}$$

$$C_{D,int} = C_{D,bulk} - \frac{\nu_D}{\nu_C} \frac{D_C}{D_D} \left(C_{C,bulk} - C_{C,int} \right) \tag{22}$$

$$K_{ov} = \frac{C_{C,int}^{\nu_C} C_{D,int}^{\nu_D}}{C_{A,int}^{\nu_A} C_{B,int}^{\nu_B}} \tag{23}$$

Equations (18) and (20) can then be combined to compute the enhancement factor for reversible reactions (Hogendoorn et al., 1997).

For short gas-liquid contact times, penetration depth of the gas into the liquid is smaller than the fiber radius and the liquid can be considered of infinite depth (Kumar et al., 2003b). For this situation, the centreline concentration of the liquid reactant remains essentially constant and the analogy to the reported models can be made based on the fiber inlet conditions (Kumar et al., 2003b), that is $C_{B,bulk} \approx C_{B,\,feed}$.

Although the applicability of the analogies to conventional mass transfer models covers a wide range of asymptotic conditions, for reactive absorption, small fiber diameters and large contact times, the depletion of the reactant along the fiber axis might become significant and a model based on first principles is required to accurately predict the absorption flux (Dindore et al., 2005a; Kreulen et al., 1993b; Kumar et al., 2003b; Kumar, 2002). Besides, for unequal diffusivities of the species involved in the reaction, the approximations tend to deviate from the real solution, even when a well-mixed bulk

is present (Hogendoorn et al., 1997). Finally, to assess axial gradients in gas phase velocity and composition, a coupled differential model for both gas and liquid phases must be solved.

5.2.3. Mathematical model

Numerous models for the mass transfer in hollow fiber absorbent membrane contactors, with the liquid flowing in the fibers lumen, have been proposed and solved. Among these, some consider the governing equations for both gas and liquid phases (Al-Marzouqi et al., 2008; Coker et al., 1998; Dindore et al., 2005b; Hoff et al., 2004; Keshavarz et al., 2008; Zhang et al., 2006). Other works, on the other hand, are focused on the liquid phase, assuming uniform gas velocity and concentration along the contactor's axial coordinate (Bao and Trachtenberg, 2005; Boucif et al., 2008; Chen et al., 2007; Kumar et al., 2002; Li and Chen, 2005; Paul et al., 2007; Wang et al., 2004). Since, in the present work, one is concerned with the CO_2 concentration in the outlet gas stream, and not just with the global amount of CO_2 removed, the model considered integrates both gas and liquid phases, being 1D for the gas and 2D for the liquid. The unsteady state model was developed with the following main assumptions: negligible temperature effects (Kumar, 2002), negligible pressure drop in both shell and lumen and applicability of the Henry law (Zhang et al., 2006).

Assuming plug flow, ideal gas behaviour and constant feed pressure in the gas phase, the following mass balances can be written:

Partial gas phase mass balance

$$C_{g,T}\frac{\partial y_i}{\partial t} = f\,C_{g,T}\frac{\partial (uy_i)}{\partial z} - 2\frac{\varepsilon}{1-\varepsilon}N_{i,m} \tag{24}$$

Total gas phase mass balance

$$\frac{\partial u}{\partial z} = 2f\frac{\varepsilon}{1-\varepsilon}\sum_i N_{i,m} \tag{25}$$

with initial and boundary conditions:

Initial condition

$t = 0,\ y_i = y_{i,0}$

Axial boundary condition

co-current: $z = 0,\quad y_i = y_{i,\,feed}$ and $u = u_{feed}$

counter-current: $z = L,\quad y_i = y_{i,\,feed}$ and $u = u_{feed}$

where y_i is the gas molar fraction of component i, $C_{g,T}$ is the total molar concentration, which, for ideal gas behaviour is given by $C_{g,T} = P/(RT)$, where P is the operation pressure, R is the ideal gas constant and T is the temperature; u is the gas velocity, ε is the module packing density, defined as $nR_{inner}^2 / R_{shell}^2$, being n the number of fibers, R_{inner} the fibber inner radius and R_{shell} the shell internal radius; f assumes the value of 1 or -1, respectively, for counter- or co-current operation. The flux of the gaseous component i across the membrane, $N_{i,m}$, is given by:

$$N_{i,m} = \frac{k_{i,ext}}{R_{inner}}\left(y_i C_{g,T} - \frac{C_{i,L}\big|_{R_{inner}}}{m_i} \right) \tag{26}$$

where and $k_{i,ext}$ is the external mass transfer coefficient, which takes into account the gas and membrane mass transfer resistances: $k_{i,ext} = \dfrac{1}{1/k_{i,g} + 1/k_{i,m}}$, $C_{i,L}\big|_{R_{inner}}$ is the concentration of i in the liquid, at the wall and m_i is the partition coefficient of i, which accounts for the physical solubility.

Concerning the liquid phase, axi-symmetry and negligible axial diffusion were assumed (Dindore et al., 2005a; Kumar, 2002). Both plug and laminar flows were considered in the axial direction and diffusive flow is assumed in the radial direction. Then, the differential mass balance of any absorbing species i present in the liquid phase and the reactant species B are given by:

Liquid phase mass balance to the absorbed component i

$$\frac{\partial C_{i,L}}{\partial t} = -v\frac{\partial C_{i,L}}{\partial z} + D_i\left[\frac{1}{r}\frac{\partial}{\partial r}\left(r\frac{\partial C_{i,L}}{\partial r} \right) \right] - S_i \tag{27}$$

Liquid phase mass balance to the reactive component B

$$\frac{\partial C_B}{\partial t} = -v\frac{\partial C_B}{\partial z} + D_B\left[\frac{1}{r}\frac{\partial}{\partial r}\left(r\frac{\partial C_B}{\partial r}\right)\right] - S_B \tag{28}$$

with the following initial and boundary conditions:

Initial condition

$t = 0$, $C_{i,L} = C_{i,L,0}$ and $C_B = C_{B,0}$

Axial boundary condition

$z = 0$, $C_{i,L} = C_{i,L,\,feed}$ and $C_B = C_{B,\,feed}$

Axi-symmetry condition

$r = 0$, $\frac{\partial C_{i,L}}{\partial r} = 0$ and $\frac{\partial C_B}{\partial r} = 0$

Mass transfer across the membrane

$r = R_{inner}$, $D_i\frac{\partial C_{i,L}}{\partial r} = k_{i,ext}\left(C_{i,g} - \frac{C_{i,L}\big|_{R_i}}{m_i}\right)$ (Absorbed gases)

$\frac{\partial C_B}{\partial r} = 0$ (Non-volatile reactant)

where $C_{i,L}$ is the concentration of specie i in the liquid, v is the liquid velocity: $v = 2\overline{v}\left[1-\left(\frac{r}{R_i}\right)^2\right]$ for laminar velocity profile and $v = \overline{v}$ for plug flow, being $\overline{v}$ the average liquid velocity; D_i and D_B are the diffusion coefficients of absorbed species i and reactant species B; S_i and S_B are the terms accounting for the chemical reaction.

To put in evidence the governing parameters of the process, model equations are also presented in their dimensionless form.

Partial gas phase mass balance

$$\frac{\partial y_i}{\partial \theta} = f\frac{\partial\left(u^* y_i\right)}{\partial x}R^{\tau}_{L/G} - 2\frac{\varepsilon}{1-\varepsilon}R^{\tau}_{L/M}N^*_{i,m} \tag{29}$$

Total gas phase mass balance

$$\frac{\partial u^*}{\partial x} = 2f\,\frac{\varepsilon}{1-\varepsilon}\,\frac{R^{\tau}_{L/M}}{R^{\tau}_{L/G}}\sum_i N^*_{i,m} \tag{30}$$

with initial and boundary conditions:

Initial condition

$\theta = 0,\ y_i = y_{i,0}$

Axial boundary condition

co-current: $x = 0,\quad y_i = y_{i,\,feed}$ and $u^* = 1$

counter-current: $x = 1,\quad y_i = y_{i,\,feed}$ and $u^* = 1$

where θ is the dimensionless time defined as t/τ_L and τ_L is the liquid phase residence time: $\tau_L = L/\overline{v}$; x is the dimensionless axial coordinate, z/L; u^* is the gas velocity normalized by the gas feed velocity: $u^* = u/u_{feed}$; $R^{\tau}_{L/G}$ is the ratio between liquid and gas residence times, τ_L/τ_g, being the gas phase residence time, τ_g, defined as L/u_{feed}; $R^{\tau}_{L/M}$ is the ratio between the liquid residence time and a membrane characteristic time, τ_m, defined as $R_i/k_{A,ext}$, where $k_{A,ext}$ is the external mass transfer coefficient for the reference component A. The dimensionless flux of the gaseous component i across the membrane, $N^*_{i,m}$, is given by:

$$N^*_{i,m} = k^*_{i,ext}\left(y_i - \frac{C^*_{i,L}\big|_{R_{inner}}}{m^*_i}\right) \tag{31}$$

where $k^*_{i,ext}$ and m^*_i are, respectively, the external mass transfer coefficient and the partition coefficient of i normalized by the reference component A.

Liquid phase mass balances can be written in the dimensionless form as follows:

Liquid phase mass balance to the absorbed component i

$$\frac{\partial C^*_{i,L}}{\partial \theta} = -v^*\,\frac{\partial C^*_{i,L}}{\partial x} + 4\frac{D^*_i}{Gz}\left[\frac{1}{\rho}\frac{\partial}{\partial \rho}\left(\rho\frac{\partial C^*_{i,L}}{\partial \rho}\right)\right] - Da\,S^*_i \tag{32}$$

Liquid phase mass balance to the reactive component B

$$\frac{\partial C_B^*}{\partial \theta} = -v^* \frac{\partial C_B^*}{\partial x} + 4\frac{D_B^*}{Gz}\left[\frac{1}{\rho}\frac{\partial}{\partial \rho}\left(\rho \frac{\partial C_B^*}{\partial \rho}\right)\right] - Da\frac{C_{L,ref}}{C_{B,\,feed}} S_B^* \tag{33}$$

with the following initial and boundary conditions:

Initial condition

$\theta = 0$, $C_{i,L}^* = C_{i,L,0}^*$ and $C_B^* = C_{B,0}^*$

Axial boundary condition

$x = 0$, $C_{i,L}^* = C_{i,L,\,feed}^*$ and $C_B^* = 1$

Axi-symmetry condition

$\rho = 0$, $\frac{\partial C_{i,L}^*}{\partial \rho} = 0$ and $\frac{\partial C_B^*}{\partial \rho} = 0$

Mass transfer across the membrane

$\rho = 1$, $\frac{\partial C_{i,L}^*}{\partial \rho} = \frac{1}{m_A}\frac{k_{i,ext}^*}{D_i^*}\frac{R_{L/M}^{\tau}\mathrm{Gz}}{4}\left(y_i - \frac{C_{i,L}^*\big|_{R_i}}{m_i^*}\right)$ (Absorbed gases)

$\frac{\partial C_B^*}{\partial \rho} = 0$ (Non-volatile reactant)

where $C_{i,L}^*$ is the dimensionless concentration of specie i in the liquid, $C_{i,L}^* = C_{i,L}/C_{L,ref}$, being the reference liquid concentration, $C_{L,ref}$, defined as $m_A C_{g,T}$; v^* is the dimensionless liquid velocity ($v^* = v/\overline{v}$); ρ is the dimensionless radial coordinate, r/R_{inner}; D_i^* is the diffusion coefficient of component i normalized by the reference component A: $D_i^* = D_i/D_A$. The Graetz dimensionless number, Gz, relates the convection and diffusion characteristic times and is given by: $Gz = \frac{\overline{v}d^2}{D_A L}$. The Damköhler dimensionless number, Da, which relates convection and reaction characteristic times, is defined here as $Da = \tau_L k_2 C_{B,\,feed}$, being $C_{B,\,feed}$ the concentration of the non-volatile reactant at the entrance of the contactor and k_2 the reaction kinetic constant; S_i^* is the dimensionless term accounting for the chemical reaction and is equal to zero for all non-reactive species in solution. For a second order irreversible reaction with $\nu_A = \nu_B = 1$: $S_A^* = S_B^* = C_{A,L}^* C_B^*$. If the absorption rate expression (6) applies:

$S_A^* = C_{A,L}^* C_B^* - \frac{1}{K_{ov} C_{L,ref}} \frac{\left(1 - C_B^*\right)^2}{4 C_B^*}$ and $S_B^* = 2 S_A^*$. C_B^* is the dimensionless concentration of reactant B in the liquid, normalized by the feed concentration: $C_B^* = C_B / C_{B,\,feed}$.

5.2.4. Numerical resolution strategy

Even though one is interested only on the steady state solution, the unsteady state model was solved in order to overcome numerical instability problems. These are likely to occur for conditions that lead to steep concentration profiles (high reactant concentrations and high liquid velocities) and for counter-current operation (Sousa and Mendes, 2003). The strategy used to solve the resulting system of partial differential equations, (29) to (33), consisted on the spatial discretization of each equation, using the finite volumes method (Cruz et al., 2005; Santos et al., 2007), and the subsequent time integration (method of lines).

Concerning the spatial discretization, both shell and fiber were divided in equally spaced intervals along the axial direction. The fiber lumen was also divided in the radial direction following a geometric progression, therefore providing a higher number of volumes next to the hollow fiber wall, where the concentration profiles are steepest. The concentrations in each cell face were calculated using a first-order upwind differencing scheme (Courant et al., 1952), for both axial and radial faces, and the radial derivatives were computed using a second order central differencing scheme (Santos et al., 2007). Details on this spatial discretization are presented in Appendix.

The resulting time dependent ordinary differential equations were then integrated using the time integration package LSODA (Petzold and Hindmarsh, 1997). This routine solves initial value problems, consisting on stiff or non-stiff systems of first order ordinary differential equations, with variable step size and convergence order.

The solution is considered to be in steady state when the time derivative of each dependent variable, for each spatial coordinate, is smaller than a pre-defined value.

5.3. Results and Discussion

5.3.1. Model validation

The results obtained with the model described above were compared to those from conventional mass transfer models, for the limiting situations where the analogy is valid. To keep the gas phase composition constant, pure CO_2 was considered for these simulations.

Physical absorption flux of CO_2 in water, under laminar and plug flow, are shown in Figure 5.2 as a function of Gz. The results from the conventional approach, were obtained from equations (10) to (13), for laminar flow, and equation (14), for plug flow. From this figure it can be seen that the numerical model matches closely with the simplified models for both flow patterns.

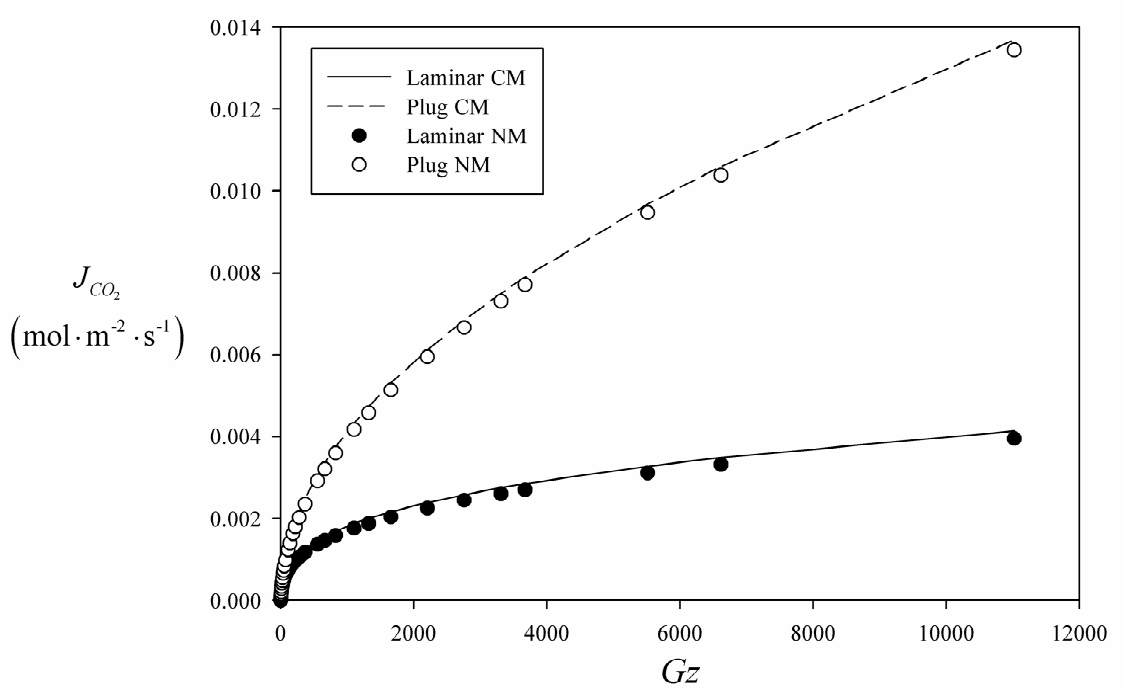

Figure 5.2 – Absorption flux of CO_2 in water as a function of Gz – numerical model (NM) and conventional model (CM) results. Simulation conditions: $\varepsilon = 0.196$, $Gz \cdot R^{\tau}_{L/M} = 5.818\times10^{7}$, $m_A = 0.833$, $C_{g,T} = 40.34\ \text{mol}\cdot\text{m}^{-3}$.

The absorption in the presence of chemical reaction was studied for the limiting condition where the depletion of the reactant at the fiber axis is negligible. Three typical reaction types were considered in the simulations:

$$A + B \xrightarrow{k_2} C + D \text{ with } S_A = k_2 C_A C_B \tag{34}$$

$$A + B \underset{k_{-1}}{\overset{k_2}{\rightleftharpoons}} C + D \text{ with } S_A = k_2 C_A C_B - k_{-1} C_C C_D, \; K_{ov} = \frac{k_2}{k_{-1}} = \frac{C_C C_D}{C_A C_B} \tag{35}$$

$$A + 2B \underset{k_{-1}}{\overset{k_2}{\rightleftharpoons}} C + D \text{ with } S_A = k_2 C_A C_B - k_{-1} \frac{C_C C_D}{C_B}, \; K_{ov} = \frac{k_2}{k_{-1}} = \frac{C_C C_D}{C_A C_B^2} \tag{36}$$

In Figure 5.3, the results from the numerical model (NM) and conventional model (CM) are plotted in terms of E as a function of Ha. Values of Ha were varied by changing the reaction kinetic constant, k_2. The conventional approach results were obtained using the DeCoursey equation (18). The physical mass transfer coefficients used to compute Ha - equation (16) - were obtained from equations (11) and (14), respectively for laminar and plug flow. The infinite enhancement factors, E_∞, used for reaction (34) was calculated using equation (17) and the enhanced factors of reactions (35) and (36) were computed using equations (20) to (23).

Figures 5.2 and 5.3 show that simulations results obtained with the model developed in this work are in agreement with results from conventional mass transfer models, with slight differences (especially in the intermediate regime), inherent to the approximations involved in the conventional models (Kumar et al., 2003b). This validates the developed model and the numerical strategy adopted.

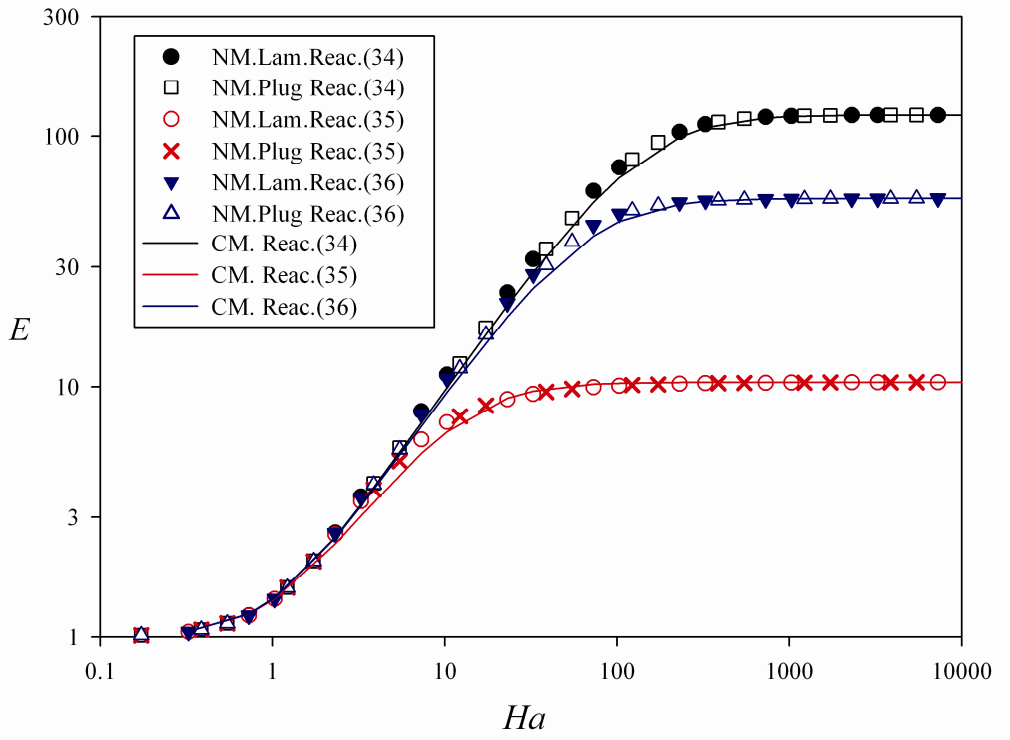

Figure 5.3 – E vs Ha plot for reactions (34), (35) and (36) – numerical (NM) and conventional (CM) models results. Simulation conditions: $Gz = 412.63$, $R^{\tau}_{L/G} = 19.795$, $R^{\tau}_{L/M} = 1.36\times10^{5}$, $\varepsilon = 0.196$, $m_A = 1$, $D^{*}_{B} = 1$, $C_{g,T} = 41.6\ \text{mol}\cdot\text{m}^{-3}$, $C_{B,\,feed} = 5\,\text{M}$ and $K = 0.8$.

Radial concentration profiles of the reactant and the absorbed gas at the exit of the contactor, obtained using the numerical model, are plotted in Figures 5.4 and 5.5 for $Ha = 3253$ and $Ha = 3.253$ for laminar flow - these conditions correspond, respectively to instantaneous (IR) and fast pseudo-first order reaction (PFO) regimes (Danckwerts, 1970). The profile for physical absorption in water is also shown for comparison. Figure 5.4 states for a direct reaction type (34) and Figure 5.5 for a reversible reaction type (35)

.

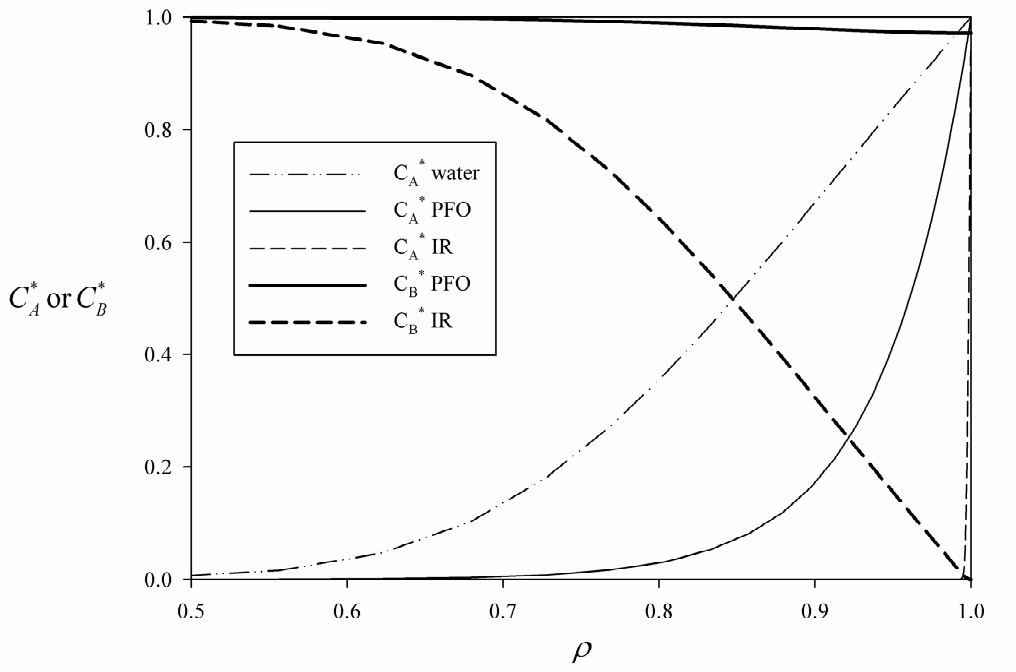

Figure 5.4 – Radial profiles at the fiber outlet for pseudo first order (PFO) and instantaneous reaction (IR) regimes, for a direct second order reaction – equation (34). Simulation conditions: Laminar flow, $Gz = 412.63$, $R_{L/G}^{\tau} = 19.795$, $R_{L/M}^{\tau} = 1.36 \times 10^5$, $\varepsilon = 0.196$, $m_A = 1$, $D_B^* = 1$, $C_{g,T} = 41.6\ \text{mol} \cdot \text{m}^{-3}$, $C_{B,\,feed} = 5\,\text{M}$.

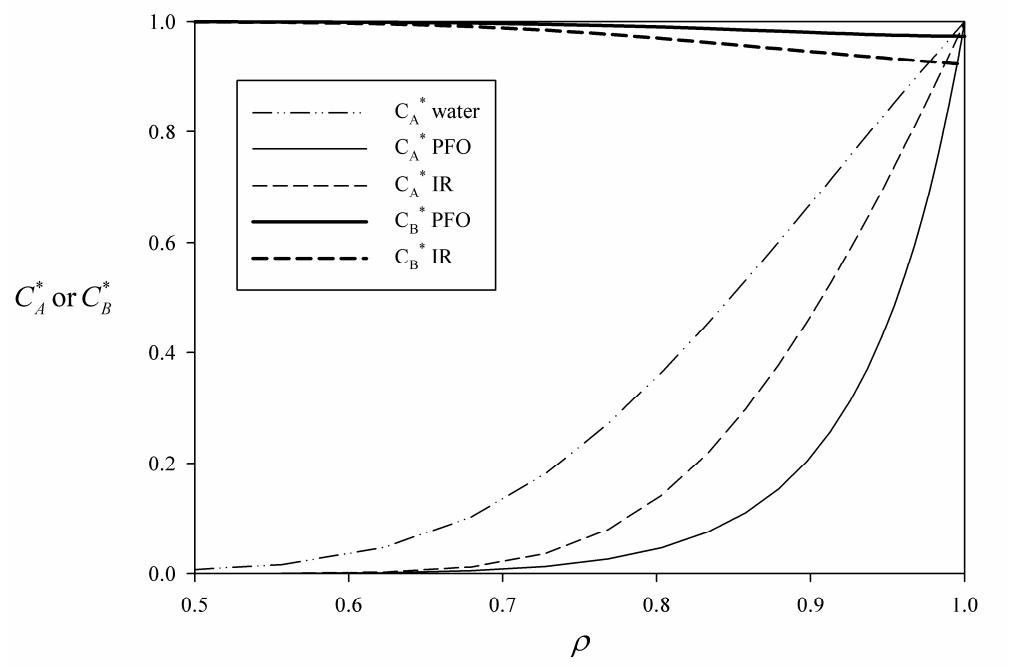

Figure 5.5 – Radial profiles at the fiber outlet for pseudo first order (PFO) and instantaneous reaction (IR) regimes, for a direct second order reaction – equation (35). Simulation conditions: Laminar flow, $Gz = 412.63$, $R_{L/G}^{\tau} = 19.795$, $R_{L/M}^{\tau} = 1.36 \times 10^5$, $\varepsilon = 0.196$, $m_A = 1$, $D_B^* = 1$, $C_{g,T} = 41.6\ \text{mol} \cdot \text{m}^{-3}$, $C_{B,\,feed} = 5\,\text{M}$ and $K = 0.8$.

Figures 5.4 and 5.5 make clear that, at these conditions, the concentrations of both reactant and absorbed gas stay practically unchanged along the fiber axis. Figure 5.4 also shows that, as expected, under pseudo first order reaction regime, the depletion of the reactant at the fiber wall in negligible, while under the instantaneous reaction regime, the absorption is controlled by the diffusion of the species to a reaction plane where their concentrations approach zero – the steepest profile of the absorbed gas is obtained for this regime. However, for reversible reaction (35) – see Figure 5.5, the concentration profile at the fiber outlet for IR is smoother than for PFO. This happens because, at high reaction rates, the reactant depletion becomes significant at a certain fiber length and the reverse reaction starts playing a role on the process. Close to the fiber inlet, the steepest concentration profile still corresponds to the IR and, therefore, the average absorption flux is still higher for this case.

5.3.2. Performance of a membrane contactor for CO_2 removal from anaesthesia breathing circuits

During anaesthesia, the gas flows from the patient at a flow rate, Q_g, of approximately 5 $\mathrm{L \cdot min^{-1}}$ and with a CO_2 concentration of about 5 % (Billiet and Burchill, 2008; Nguyen, 1996). This CO_2 composition must be reduced to a maximum value of 0.5 % before being recycled back to the patient (Lagorsse et al., 2007).

For this specific application, composite membranes made by a porous support (PEI), coated internally with a PDMS thin layer were considered. In such membranes, the main resistance to mass transfer is originated by the PDMS coating. The mass transfer coefficient of CO_2 in this layer, k_{m,CO_2}, is approximately 1.58×10^{-3} $\mathrm{m \cdot s^{-1}}$ (Rego and Mendes, 2004). The fibers internal and external diameters were assumed to be, respectively, 5.6×10^{-4} and 8.4×10^{-4} m.

Aqueous solutions of potassium glycinate were considered as absorbent. The physical and chemical parameters used to model the system CO_2 - potassium glycinate – water are given in Table 5.1, together with the respective literature sources. Portugal et al. (2007) derived an expression for the rate of absorption of CO_2 in solutions using

estimated values of the diffusion coefficients of CO_2 and potassium glycinate in solutions, $D_{CO_2,Sol}$ and $D_{RNH_2,Sol}$. Later, Hamborg et al. (2008) determined these diffusion coefficients experimentally. The work by Portugal et al. (2007) was re-analysed using these values and a new expression for the reaction rate was obtained – Table 5.1.

Given the above considerations, to meet the target of reducing the CO_2 concentration from 5 % to a maximum of 0.5 %, the following design and operation variables can still be adjusted: the contactor length and shell diameter, the packing density, the liquid flow-rate, Q_L, and the inlet amino acid salt concentration. The influence of these variables on the system behaviour will be further discussed. The gas phase mass transfer resistance was neglected and all simulations were performed for a temperature of 298 K and for fully developed laminar flow in the liquid. CO_2 was considered the only absorbing gas. The conditions studied in the simulations are summarized in Table 5.2.

Given the specificities of the problem under study, namely the fact that the known restrictions are defined in terms of flow rates rather than velocities – notice that $u = \frac{Q_g}{\pi R_{shell}^2 (1-\varepsilon)}$ and $v = \frac{Q_L}{\pi R_{shell}^2 \varepsilon}$ - equations (29) and (32) were re-written, for stationary state, as follows:

$$\frac{\partial \left(u^* y_i \right)}{\partial x} = 4 f \frac{k_{A,ext}}{d} \frac{\varepsilon \pi R_{shell}^2 L}{Q_g} N_{i,m}^* \tag{37}$$

$$v^* \frac{\partial C_{i,L}^*}{\partial x} = 4 D_i^* \frac{D_A}{d^2} \frac{\varepsilon \pi R_{shell}^2 L}{Q_L} \left[\frac{1}{\rho} \frac{\partial}{\partial \rho} \left(\rho \frac{\partial C_{i,L}^*}{\partial \rho} \right) \right] - k_2 C_{RNH_2,\,feed} \frac{\varepsilon \pi R_{shell}^2 L}{Q_L} S_i^* \tag{38}$$

Equations (30) and (33) can be re-written as well.

Table 5.1 - Physical and chemical parameters used to model the absorption of CO_2 in potassium glycinate aqueous solutions in a hollow fiber membrane contactor - liquid phase concentrations are expressed in molarity.

$\log\left(\frac{m_{CO_2,w}}{m_{CO_2,Sol}}\right) = KC_{RNH_2}$		
$K = (62.1831/T) - 0.1112$	(M^{-1})	(Portugal et al., 2007)
$m_{CO_2,w} = 3.54\times10^{-7} RT \exp(2044/T)$		(Versteeg and Van Swaaij, 1988)
$D_{RNH_2,Sol} = \left(\begin{array}{l}-2.412 - 9.403\times10^{-3}T + 7.110\times10^{-5}T^2 - 0.2177C_{RNH_2} - \\ -5.447\times10^{-2}C_{RNH_2}^2 + 1.296\times10^{-3}TC_{RNH_2}\end{array}\right)\times10^{-9}$	$(\mathrm{m}^2\cdot\mathrm{s}^{-1})$	(Hamborg et al., 2008)
$D_{CO_2,Sol} = D_{CO_2,w}(\eta_{Sol}/\eta_w)^{-0.48}$	$(\mathrm{m}^2\cdot\mathrm{s}^{-1})$	(Hamborg et al., 2008)
$D_{CO_2,w} = 2.35\times10^{-6}\exp(-2119/T)$	$(\mathrm{m}^2\cdot\mathrm{s}^{-1})$	(Versteeg and Van Swaaij, 1988)
$(\eta_{Sol}/\eta_w) = 1 + 0.2109C_{RNH_2} + 0.05124C_{RNH_2}^2$		(Portugal et al., 2007)
$k_2 = 3.28\times10^{16}\exp\left(\frac{-8636}{T}\right)\exp(0.36C_{RNH_2})$	$(\mathrm{M}^{-1}\cdot\mathrm{s}^{-1})$	(Portugal et al., 2007)
$K_{ov} = \frac{K_{CO_2}}{K_{AmA}K_{carb}}$	(M^{-1})	
$K_{AmA} = \exp(-0.000237956T^2 + 0.202203T - 61.6499)$	(M)	(Perrin, 1965)
$K_{CO_2} = \exp(-12092.1/T - 36.7816\ln T + 235.482)$	(M)	(Benamor and Aroua, 2005)
$K_{carb} = \exp(1792/T - 4.786)$	(M)	(Portugal et al., 2009)

Table 5.2 - Simulation conditions.

$T\,(\mathrm{K})$	298.15
$P\,(\mathrm{Pa})$	10^5
$Q_{g,\,feed}\,(\mathrm{L\cdot min^{-1}})$	5
$y_{CO_2,\,feed}$	0.05 (5 %)
$k_{m,CO_2}\times10^3\,(\mathrm{m\cdot s^{-1}})$	1.58
$R_{inner}\times10^4\,(\mathrm{m})$	2.8
ε	0.098 – 0.392
$R_{shell}\times10^2\,(\mathrm{m})$	2 – 4
$L\times10^2\,(\mathrm{m})$	5 – 50
$Q_L\,(\mathrm{mL\cdot min^{-1}})$	10 – 500
$C_{RNH_2,\,feed}\,(\mathrm{M})$	0.1 – 3

The influence of packing density, ε, contactor length, L, shell radius, R_{shell}, reactant feeding concentration, $C_{RNH_2,\,feed}$, and liquid flowrate, Q_L, on the CO_2 molar fraction exiting the contactor is discussed next.

Influence of the packing density, contactor length and shell diameter

The packing density and the contactor volume define the contact area - $A=\frac{2}{R_{inner}}\varepsilon R_{shell}^2 L$ - that is the area available for the mass transfer. Therefore, being Q_g and R_{inner} fixed, for a given Q_L and $C_{RNH_2,\,feed}$, the gas concentration exiting the contactor depends on the product $\varepsilon R_{shell}^2 L$, which is clear from equations (37) and (38) and was also verified by simulation. The contact area, *A*, is only limiting the separation process if it is smaller than the "effective area", commonly expressed in terms of the effective length at which the solution becomes saturated and no further separation is achieved. This concept is illustrated in Figure 5.6, where some representative examples of gaseous concentration profiles along the contactor are plotted for co- and counter-current operation.

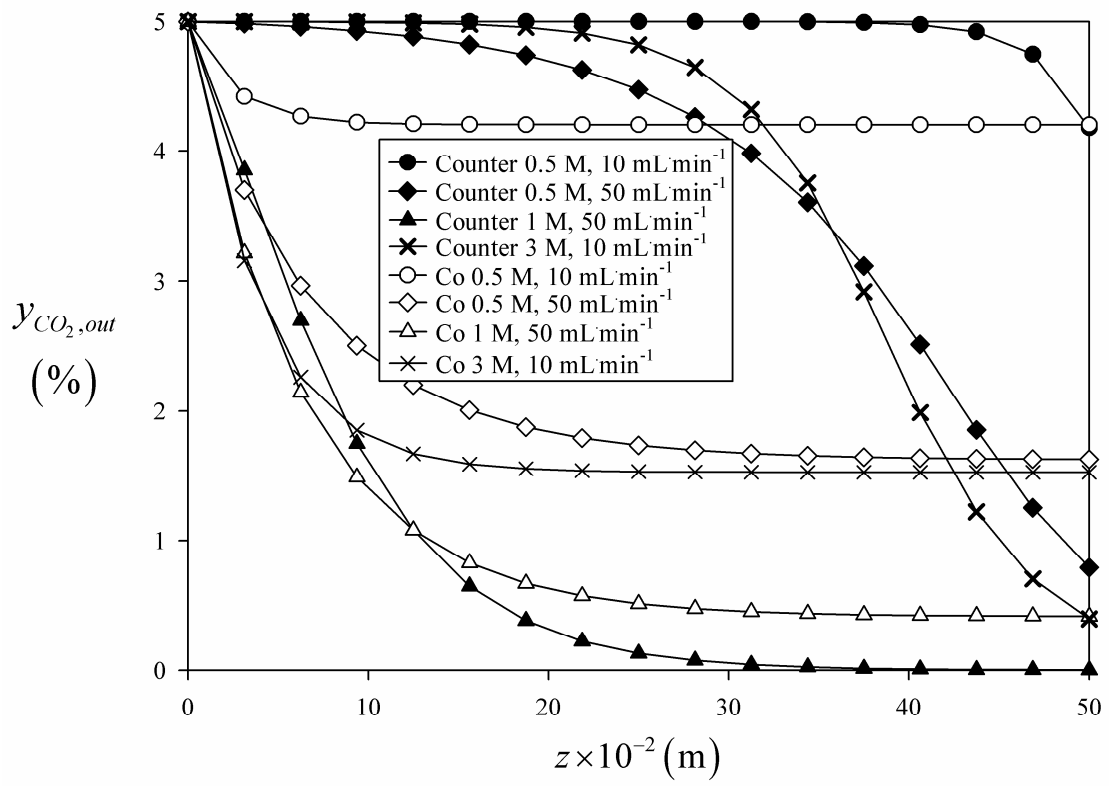

Figure 5.6 – Axial profiles along the contactor for co- and counter-current operation and for different Q_L and $C_{RNH_2,feed}$. Simulation conditions: $\varepsilon = 0.196$, $R_{shell} = 2 \times 10^{-2}$ m.

It can be seen from this figure that, for the case of a 0.5 M solution flowing at 10 $\text{mL} \cdot \text{min}^{-1}$, all the changes in the gas composition occur at a small fraction of the contactor length (approximately within 12×10^{-2} m) which is the portion effectively used for the separation. From that point on, increasing the contactor length won't bring any advantage for the separation, because the solution is already saturated and unable to absorb more CO_2. When a 3 M solution is used at the same flow rate, the effective length increases because this solution has a higher capacity and then saturates later. Observing this case, one can also notice that the effective length is larger for counter-current (around 35×10^{-2} m) than for co-current operation (around 29×10^{-2} m). For both 0.5 and 1 M solutions flowing at 50 $\text{mL} \cdot \text{min}^{-1}$, solution capacity is not reached within the available contact area (this is particularly visible for counter-current operation), which means that increasing the fiber length would further improve the separation. Figure 5.6 makes also clear the advantages of operating counter-currently. Counter-current operation not only enables a more effective use of the contactor area but leads to

lower CO_2 gas molar fractions exiting the contactor, for the same flow rates and reactant concentrations.

In Figure 5.7, the gas outlet composition is shown as a function of the contact area for counter-current operation.

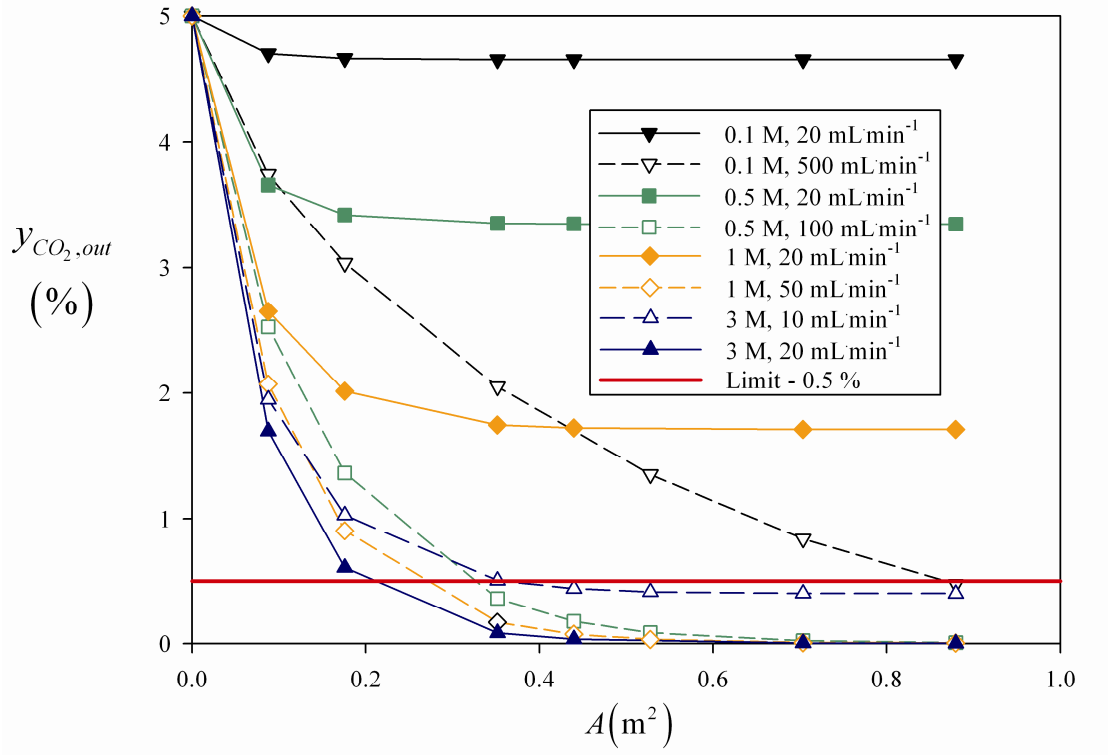

Figure 5.7 - Influence of the contact area on the CO_2 molar fraction at the contactor exit for different $C_{RNH_2,feed}$ and Q_L and for counter-current operation.

As already observed in Figure 5.6 for the 0.5 M solution, increasing the liquid flow rate increases the effective area. As a consequence, the separation becomes controlled by the contact area available – see for example the results for 0.1 M and 500 $\mathrm{mL \cdot min^{-1}}$ in Figure 5.7. Figure 5.7 illustrates more clearly the effect of increasing the amino acid salt concentration in the contactor effective area.

It can also be observed from Figure 5.7 that, for certain reactant concentrations and liquid flow rates, it is possible to get outlet CO_2 concentrations far below the minimum required (0.5 %) even when the separation is still limited by the available contact area. This might be relevant if volume constraints are imposed for the anaesthesia machine.

Concerning the contactor design, it must be kept in mind that the value of ε is constrained by the device geometry. For packing of circles in a plane, the highest possible packing is $\varepsilon = 0.907$ (Weisstein, 2008) which, taking into account the membrane thickness of 140 µm, corresponds to $\varepsilon = 0.403$, based on the fiber internal diameter. Due to manufacturing restraints, a reasonable maximum packing density for the type of contactor used should be about 0.3. Moreover, a final contactor design should consider an appropriate balance between shell diameter and length. A contactor with a large diameter and short fibers would lead to the presence of dead volumes or dominant cross flow operation, while a contactor with very long fibers and short diameter would imply a high pressure drop and would not fit in a common anaesthetic machine.

Influence of the amino acid salt concentration

As can be seen in Table 5.1, the potassium glycinate concentration influences the CO_2 physical solubility (represented by the partition factor), the CO_2 and the reactant diffusion coefficients and the reaction kinetic constant. The effect of $C_{RNH_2,\,feed}$ on the CO_2 molar fraction at the contactor exit is shown in Figure 5.8.

A maximum concentration of 3 M was considered for the simulations. Although in principle higher concentrations could enhance the separation (as Figure 5.8 indicates), enabling the use of smaller contactors and lower liquid flow rates, they would also increase the solution viscosity. Highly viscous solutions would carry hydrodynamic problems and pumping would become an issue. Precipitation would also become more likely for concentrated solutions.

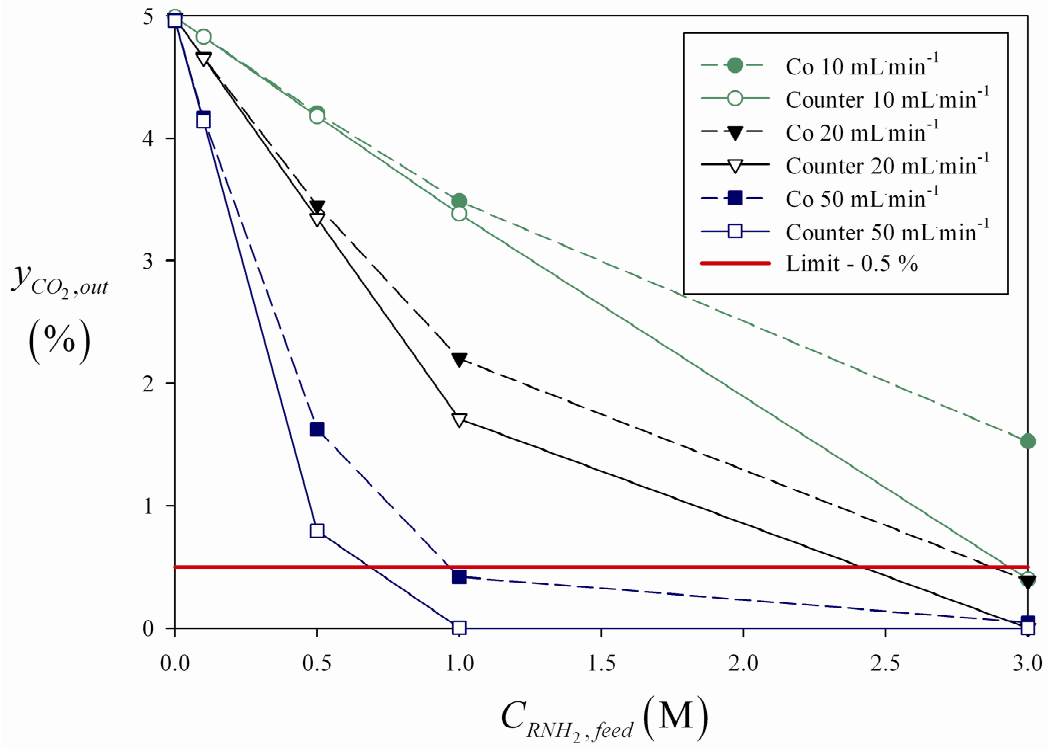

Figure 5.8 - Influence of the amino acid salt feed concentration liquid flow rate on the CO_2 concentration at the contactor exit for different Q_L and for co- and counter-current operations – $A = 0.8796$ m^2 . Lines are for improving the read.

Influence of the liquid flow rate

The influence of the liquid flow rate on the CO_2 molar fraction at the contactor exit is shown in Figure 5.9.

Increasing the liquid flow rate, Q_L, up to a certain value leads to an increase of the CO_2 removal and a consequent decrease on the CO_2 gas phase exit molar fraction. However, for sufficiently high liquid flow rates, other parameters such as the contact area and the membrane resistance are limiting the CO_2 removal. For the asymptotic situation where there is no depletion of the reactant in the fiber axis along the entire fiber length, the analogy to conventional mass transfer models is valid. If the conditions for PFO are fulfilled, the enhancement factor becomes equal to the Hatta number (Danckwerts, 1970) and therefore the absorption flux is independent of the mass transfer coefficient, k_L - see

equations (15) and (16). Since k_L is related to the liquid velocity, increasing Q_L in the PFO regime, for constant centreline reactant concentration, would bring no improvement for the separation achieved. This effect is visible in Figure 5.9, for counter-current and for Q_L higher than 250 $\text{mL}\cdot\text{min}^{-1}$, for concentrations above 0.5 M.

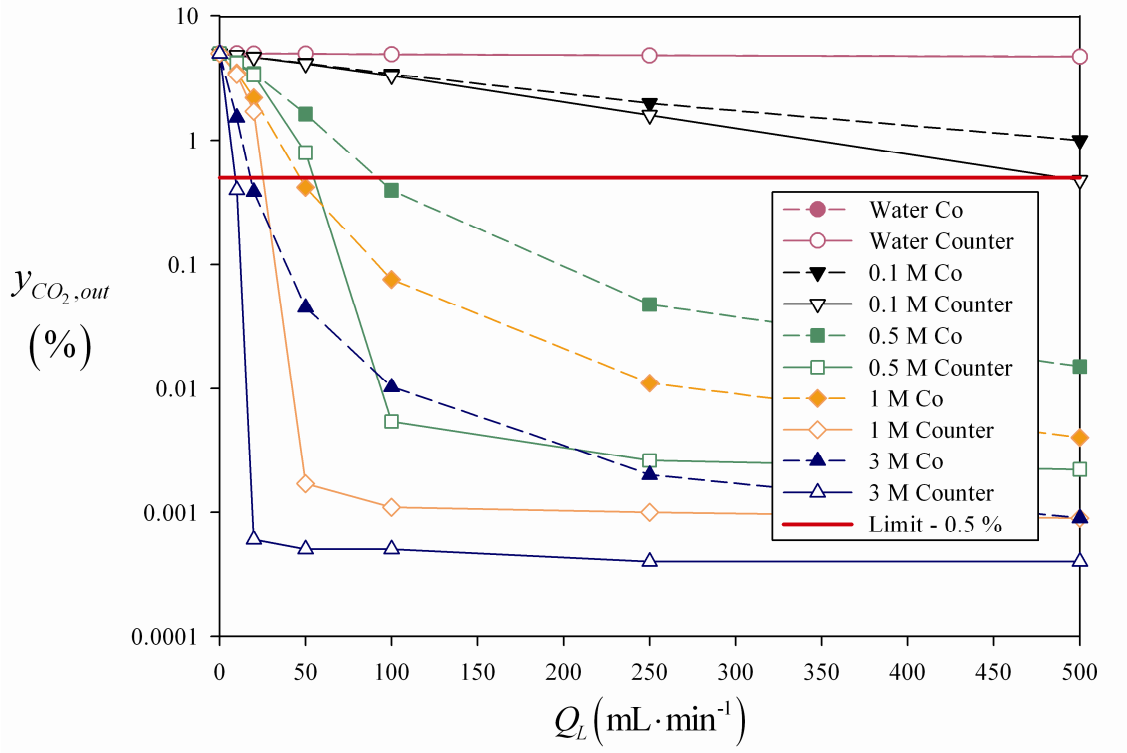

Figure 5.9 – Influence of the liquid flow rate on the CO_2 concentration at the contactor exit for different $C_{RNH_2,feed}$ and for co- and counter-current operations – $A = 0.8796$ m^2. Lines are for improving the read.

Figure 5.9 shows that, for a number of operating conditions, the CO_2 outlet concentration is well below the limit for anaesthesia purposes. One must keep in mind that, although this work is focused on the absorption step, the global process also comprises the continuous regeneration of the solution. Usually the CO_2 desorption is carried out upon heating the rich solutions, which makes the regeneration step critical in what concerns energy consumptions. Therefore, to minimize the energy requirements, the liquid flow rate should be the lowest possible. As a consequence, the reactant feed concentration should be the highest possible, which, given the above considerations corresponds to 3 M.

According to Figures 5.7 to 5.9, a contactor having 0.5 m^2 of contact area, with a 3 M aqueous solution of potassium glycinate, flowing at 10 $mL \cdot min^{-1}$ counter-currently with respect to the gas would be suitable to reduce the CO_2 molar fraction in anaesthesia closed loop from 5 % to less than 0.5 %. Considering a packing density of 0.3, a contactor for this application should have a volume of approximately 240 mL. Taking into consideration the dimensions of the usual alkali hydroxides canisters, a contactor with 5 cm shell diameter and 12.5 cm length would be easily retrofitted into a common anaesthesia machine.

5.4. Conclusions

A numerical model was developed to simulate the mass transfer accompanied by chemical reaction, occurring during the absorption of a gas into a liquid flowing through a hollow fiber membrane contactor. The model considers the liquid flowing in the fiber lumen and the gas in the shell side. Both co- and counter-current operations were analysed. Good agreement was found between the proposed numerical model results and results obtained with conventional mass transfer models, for the limit conditions where these are valid.

The performance of a hollow fiber membrane contactor with potassium glycinate absorbent solutions was studied for the purpose of carbon dioxide removal from anaesthesia closed-loops. The effect of the contact area on the CO_2 molar fraction exiting the contactor was analysed; the contact area is defined by the design parameters packing density, contactor length and shell diameter. The separation achieved increases by increasing the contact area until the liquid solution becomes saturated, which happens at the so-called effective area or effective length. The operation parameters liquid flow rate and reactant feed concentration determine the area effectively used for the mass transfer.

The effect of the reactant feed concentration on the separation was examined and, for the concentration range considered (0 to 3 M), the amount of CO_2 absorbed always increased with increasing concentration.

Generally, increasing the liquid flow rate increases the separation. However, when the contactor is working in the limit situation of PFO and no depletion of the reactant at the fiber axis, the liquid velocity has no effect on the absorption rate and consequently on the CO_2 molar fraction exiting the contactor. Concerning the application under study, to minimize energy requirements for the thermal desorption, one are interested on keeping the liquid flow rate the lowest possible.

Finally, based on practical considerations and restrictions, a set of operating conditions and design parameters were assumed for the contactor and its viability confirmed by simulation. These are a packing density of 0.3 and a volume of 240 mL (approximately 0.5 m^2 of contact area), with a 3 M solution of potassium glycinate flowing counter currently with respect to the gas, at a flow rate of 10 $mL \cdot min^{-1}$.

5.5. Nomenclature

A	Contact area, m^2
C	Concentration, M or $mol \cdot m^{-3}$
d	Fiber internal diameter, m
D	Diffusion coefficient, $m^2 \cdot s^{-1}$
Da	Damköhler number, dimensionless
E	Enhancement factor, dimensionless
E_∞	Infinite enhancement factor, dimensionless
f	Flag standing for co- or counter-current operation
Gz	Graetz number, dimensionless
Ha	Hatta number, dimensionless
IR	Instantaneous reaction regime
J	Absorption flux, $mol \cdot m^{-2} \cdot s^{-1}$
K_{ov}	Overall equilibrium constant
k_{-1}	Reverse reaction kinetic constant, s^{-1}
k_2	Second order reaction kinetic constant, $M^{-1} \cdot s^{-1}$
k_{ext}	External mass transfer coefficient, $m \cdot s^{-1}$

k_g	Gas phase mass transfer coefficient, $\mathrm{m \cdot s^{-1}}$
k_m	Membrane mass transfer coefficient, $\mathrm{m \cdot s^{-1}}$
k_L	Liquid phase physical mass transfer coefficient, $\mathrm{m \cdot s^{-1}}$
k_{ov}	Overall mass transfer coefficient, $\mathrm{m \cdot s^{-1}}$
L	Fiber length, m
m	Partition coefficient
n	Number of fibers
$N_{i,m}$	Flux across the membrane, $\mathrm{mol \cdot m^{-2} \cdot s^{-1}}$
nj	Number of discretization points in the axial direction
nk	Number of discretization points in the radial direction
PFO	Pseudo first order reaction regime
Q	Flow rate, $\mathrm{L \cdot min^{-1}}$ or $\mathrm{mL \cdot min^{-1}}$
r	Radial coordinate, m
R	Universal gas constant, 8.314 $\mathrm{J \cdot mol^{-1} \cdot K^{-1}}$
R_{inner}	Membrane internal radius, m
$R^{\tau}_{L/G}$	Ratio between liquid and gas residence times, dimensionless
$R^{\tau}_{L/M}$	Ratio liquid residence and membrane characteristic times, dimensionless
R_{shell}	Contactor shell inner radius, m
S	Rate of reaction, $\mathrm{mol \cdot m^{-3} \cdot s^{-1}}$
Sh	Sherwood number, $Sh = \frac{k_L d}{D_A}$, dimensionless
T	Temperature, K
u	Gas velocity, $\mathrm{m \cdot s^{-1}}$
v	Liquid velocity, $\mathrm{m \cdot s^{-1}}$
V	Volume, $\mathrm{m^3}$
x	Axial coordinate, dimensionless
z	Axial coordinate, m

Greek symbols

φ	Flux, $\mathrm{mol \cdot m^{-2} \cdot s^{-1}}$
ε	Packing density, dimensionless

ν	Stoichiometric coefficient
η	Solution viscosity, $kg \cdot m^{-1} \cdot s^{-1}$
ρ	Radial coordinate, dimensionless
θ	Time, dimensionless
τ	Residence time, s

Subscripts

0	Initial
∞	Infinite (instantaneous reaction regime)
A	Absorbed gas
B	Non-volatile reactant
C, D	Reaction products
F	Cell face
g	Gas phase
i	Gaseous component
int	Interface
L	Liquid phase
m	Membrane
ref	Reference
Sol	Solution
T	Total
w	Water

Superscripts

*	Dimensionless
z	Axial coordinate, m
r	Radial coordinate, m

5.6. References

Al-Marzouqi, M., El-Naas, M., Marzouk, S. and Abdullatiff, N. (2008). "Modeling of chemical absorption of CO2 in membrane contactors." Separation and Purification Technology, 62(3), 499-506.

Bao, L. H. and Trachtenberg, M. C. (2005). "Modeling CO2-facilitated transport across a diethanolamine liquid membrane." Chemical Engineering Science, 60(24), 6868-6875.

Baum, J. A. and Woehlck, H. J. (2003). "Interaction of inhalational anaesthetics with CO2 absorbents " Best Practice and Research Clinical Anaesthesiology, 17(1), 63-76.

Benamor, A. and Aroua, M. K. (2005). "Modeling of CO2 solubility and carbamate concentration in DEA, MDEA and their mixtures using the Deshmukh-Mather model." Fluid Phase Equilibria, 231(2), 150-162.

Billiet, P. and Burchill, S. (2008). "The Open Door Web Site - Breathing in the Air: The Lungs - http://www.saburchill.com." 2008.

Bird, R. B., Sewart, W. E. and Lightfoot, E. N. (2002). "Transport phenomena". New York, John Wiley and Sons, inc.

Blauwhoff, P. M. M., Versteeg, G. F. and Vanswaaij, W. P. M. (1984). "A Study on the Reaction between Co2 and Alkanolamines in Aqueous-Solutions." Chemical Engineering Science, 39(2), 207-225.

Boucif, N., Favre, E. and Roizard, D. (2008). "CO2 capture in HFMM contactor with typical amine solutions: A numerical analysis." Chemical Engineering Science, 63(22), 5375-5385.

Caplow, M. (1968). "Kinetics of carbamate formation and breakdown." Journal of the American Chemical Society, 90(24), 6795-6803.

Chen, G., Ren, Z. Q., Zhang, W. D. and Gao, J. (2007). "Modeling study of the influence of porosity on membrane absorption process." Separation Science and Technology, 42(15), 3289-3306.

Coker, D. T., Freeman, B. D. and Fleming, G. K. (1998). "Modeling multicomponent gas separation using hollow-fiber membrane contactors." American Institute of Chemical Engineers Journal, 44(6), 1289-1302.

Courant, R., Isaacson, E. and Rees, M. (1952). "On the Solution of Nonlinear Hyperbolic Differential Equations by Finite Differences." Communications on Pure and Applied Mathematics, 5(3), 243-255.

Cruz, P., Santos, J., Magalhaes, F. and Mendes, A. (2005). "Simulation of separation processes using finite volume method." Computers & Chemical Engineering, 30(1), 83-98.

Danckwerts, P. (1970). "Gas-Liquid Reactions", McGraw-Hill Book Company.

DeCoursey, W. J. (1974). "Absorption with Chemical-Reaction - Development of a New Relation for Danckwerts Model." Chemical Engineering Science, 29(9), 1867-1872.

Derks, P. W. J., Kleingeld, T., van Aken, C., Hogendoom, J. A. and Versteeg, G. F. (2006). "Kinetics of absorption of carbon dioxide in aqueous piperazine solutions." Chemical Engineering Science, 61(20), 6837-6854.

Dindore, V., Brilman, D. and Versteeg, G. (2005a). "Hollow fiber membrane contactor as a gas-liquid model contactor." Chemical Engineering Science, 60(2), 467-479.

Dindore, V., Brilman, D. and Versteeg, G. (2005b). "Modelling of cross-flow membrane contactors: Mass transfer with chemical reactions." Journal of Membrane Science, 255(1-2), 275-289.

Elk, E. P. V., Knaap, M. C. and Versteeg, G. F. (2007). "Application of the penetration theory for gas-liquid mass transfer without liquid bulk: Differences with systems with a bulk." Chemical Engineering Research & Design, 85(4), 516-524

Fan, S. Z., Lin, Y. W., Chang, W. S. and Tang, C. S. (2008). "An evaluation of the contributions by fresh gas flow rate, carbon dioxide concentration and desflurane partial pressure to carbon monoxide concentration during low fresh gas flows to a circle anaesthetic breathing system." European Journal of Anaesthesiology, 25(8), 620-626.

Feron, P. and Jansen, A. (2002). "CO2 separation with polyolefin membrane contactors and dedicated absorption liquids: performances and prospects." Separation and Purification Technology, 27(3), 231-242.

Gabelman, A. and Hwang, S. (1999). "Hollow fiber membrane contactors." Journal of Membrane Science, 159(1-2), 61-106.

Goff, G. S. and Rochelle, G. T. (2006). "Oxidation inhibitors for copper and iron catalyzed degradation of monoethanolamine in CO2 capture processes." Industrial & Engineering Chemistry Research, 45(8), 2513-2521.

Hamborg, E. S., Niederer, J. P. M. and Versteeg, G. F. (2007). "Dissociation constants and thermodynamic properties of amino acids used in CO2 absorption from (293 to 353) K." Journal of Chemical and Engineering Data, 52(6), 2491-2502.

Hamborg, E. S., van Swaaij, W. P. M. and Versteeg, G. F. (2008). "Diffusivities in aqueous solutions of the potassium salt of amino acids." Journal of Chemical and Engineering Data, 53(5), 1141-1145.

Hoff, K. A., Juliussen, O., Falk-Pedersen, O. and Svendsen, H. F. (2004). "Modeling and experimental study of carbon dioxide absorption in aqueous alkanolamine solutions using a membrane contactor." Industrial & Engineering Chemistry Research, 43(16), 4908-4921.

Hogendoorn, J. A., Vas Bhat, R. D., Kuipers, J. A. M., van Swaaij, W. P. M. and Versteeg, G. F. (1997). "Approximation for the enhancement factor applicable to reversible reactions of finite rate in chemically loaded solutions." Chemical Engineering Science, 52(24), 4547-4559.

Hook, R. J. (1997). "An investigation of some sterically hindered amines as potential carbon dioxide scrubbing compounds." Industrial & Engineering Chemistry Research, 36(5), 1779-1790.

Idem, R. and Tontiwachwuthikul, P. (2006). "Preface for the special issue on the capture of carbon dioxide from industrial sources: Technological developments and future opportunities." Industrial & Engineering Chemistry Research, 45(8), 2413-2413.

Keshavarz, P., Ayatollahi, S. and Fathikalajahi, J. (2008). "Mathematical modeling of gas–liquid membrane contactors using random distribution of fibers." Journal of Membrane Science, 325, 98–108.

Knaap, M. C., Lenferink, J. E. O., Versteeg, G. F. and van Elk, E. P. (2000). "Differences in local absorption rates of CO2 as observed in numerically comparing tray

columns and packed columns." 79th Annual Convention of the Gas Processors Association, Proceedings, 82-94

596.

Knolle, E. and Gilly, H. (2000). "Absorption of carbon dioxide by dry soda lime decreases carbon monoxide formation from isoflurane degradation." Anesthesia and Analgesia, 91(2), 446-451.

Kreulen, H., Smolders, C. A., Versteeg, G. F. and Vanswaaij, W. P. M. (1993a). "Microporous Hollow-Fiber Membrane Modules as Gas-Liquid Contactors .1. Physical Mass-Transfer Processes - a Specific Application - Mass-Transfer in Highly Viscous-Liquids." Journal of Membrane Science, 78(3), 197-216.

Kreulen, H., Smolders, C. A., Versteeg, G. F. and Vanswaaij, W. P. M. (1993b). "Microporous Hollow-Fiber Membrane Modules as Gas-Liquid Contactors .2. Mass-Transfer with Chemical-Reaction." Journal of Membrane Science, 78(3), 217-238.

Kumar, P., Hogendoorn, J., Versteeg, G. and Feron, P. (2003a). "Kinetics of the reaction of CO2 with aqueous potassium salt of taurine and glycine." American Institute of Chemical Engineers Journal, 49(1), 203-213.

Kumar, P., Hogendorn, J., Feron, P. and Versteeg, G. (2003b). "Approximate solution to predict the enhancement factor for the reactive absorption of a gas in a liquid flowing through a microporous membrane hollow fiber." Journal of Membrane Science, 213(1-2), 231-245.

Kumar, P. S. (2002). "Development and design of membrane gas absorption processes". Enschede, University of Twente.

Kumar, P. S., Hogendoorn, J. A., Feron, P. H. M. and Versteeg, G. F. (2002). "New absorption liquids for the removal of CO2 from dilute gas streams using membrane contactors." Chemical Engineering Science, 57(9), 1639-1651.

Kumar, P. S., Hogendoorn, J. A., Feron, P. H. M. and Versteeg, G. F. (2003c). "Equilibrium solubility of CO2 in aqueous potassium taurate solutions: Part 1. Crystallization in carbon dioxide loaded aqueous salt solutions of amino acids." Industrial & Engineering Chemistry Research, 42(12), 2832-2840.

Kumar, P. S., Hogendorn, J. A., Feron, P. H. M. and Versteeg, G. F. (2003d). "Approximate solution to predict the enhancement factor for the reactive absorption of a gas in a liquid flowing through a microporous membrane hollow fiber." Journal of Membrane Science, 213(1-2), 231-245.

Lagorsse, S., Magalhaes, F. D. and Mendes, A. (2007). "Xenon recycling in an anaesthetic closed-system using carbon molecular sieve membranes." Journal of Membrane Science, 301(1-2), 29-38.

Li, J. L. and Chen, B. H. (2005). "Review Of CO2 absorption using chemical solvents in hollow fiber membrane contactors." Separation and Purification Technology, 41(2), 109-122.

Ma'mun, S., Svendsen, H. F., Hoff, K. A. and Juliussen, O. (2007). "Selection of new absorbents for carbon dioxide capture." Energy Conversion and Management, 48(1), 251-258.

Majchrowicz, M., Niederer, J. P. M., Velders, A. H. and Versteeg, G. F. (2006). "Precipitation in amino acid salt CO2 absorption systems". GHGT-8 NTNU VIDERE, Pav. A, Dragvoll, NO-7491 Trondheim, Norway.

Mendes, A. M. M. (2000). "Development of an adsorption/membrane based system for carbon dioxide, nitrogen and spur gases removal from a nitrous oxide and xenon anaesthetic closed loop." Acp-Applied Cardiopulmonary Pathophysiology, 9(2), 156-163.

Nguyen, J. (1996). "End-tidal carbon dioxide monitoring during CPR: A predictor of outcome - http://enw.org/ETCO2inCPR.htm."

Paul, S., Ghoshal, A. K. and Mandal, B. (2007). "Removal of CO2 by single and blended aqueous alkanolamine solvents in hollow-fiber membrane contactor: Modeling and simulation." Industrial & Engineering Chemistry Research, 46(8), 2576-2588.

Perrin, D. (1965). "Dissociation Constants of Organic Bases in Aqueous Solutions". London, Butterworth.

Petzold, L. R. and Hindmarsh, A. C. (1997). LSODA, Computer and mathematics research division, Lawrence Livermore National Laboratory.

Portugal, A. F., Derks, P. W. J., Versteeg, G. F., Magalhães, F. D. and Mendes, A. (2007). "Characterization of potassium glycinate for carbon dioxide absorption purposes " Chemical Engineering Science, 62(23), 6534-6547

Portugal, A. F., Magalhaes, F. D. and Mendes, A. (2008). "Carbon dioxide absorption kinetics in potassium threonate." Chemical Engineering Science, 63(13), 3493-3503.

Portugal, A.F., Sousa, J.M., Magalhães, F. D. and Mendes A. (2009). "Solubility of carbon dioxide in aqueous solutions of amino acid salts", Chemical Engineering Science, 10.1016/j.ces.2009.01.036

Rego, R. and Mendes, A. (2004). "Carbon dioxide/methane gas sensor based on the permselectivity of polymeric membranes for biogas monitoring." Sensors and Actuators B-Chemical, 103(1-2), 2-6.

Santos, J. C., Cruz, P., Regala, T., Magalhaes, F. D. and Mendes, A. (2007). "High-purity oxygen production by pressure swing adsorption." Industrial & Engineering Chemistry Research, 46(2), 591-599.

Sartori, G. and Savage, D. W. (1983). "Sterically Hindered Amines for Co2 Removal from Gases." Industrial & Engineering Chemistry Fundamentals, 22(2), 239-249.

Sea, B., Park, Y. I. and Lee, K. H. (2002). "Comparison of porous hollow fibers as a membrane contactor for carbon dioxide absorption." Journal of Industrial and Engineering Chemistry, 8(3), 290-296.

Secor, R. M. and Beutler, J. A. (1967). "Penetration Theory for Diffusion Accompanied by a Reversible Chemical Reaction with Generalized Kinetics." American Institute of Chemical Engineers Journal, 13(2), 365-373.

Song, H. J., Lee, S., Maken, S., Park, J. J. and Park, J. W. (2006). "Solubilities of carbon dioxide in aqueous solutions of sodium glycinate." Fluid Phase Equilibria, 246(1-2), 1-5.

Sousa, J. M. and Mendes, A. (2003). "Simulation study of a dense polymeric catalytic membrane reactor with plug-flow pattern." Chemical Engineering Journal, 95(1-3), 67-81.

Supap, T., Idem, R., Tontiwachwuthikul, P. and Saiwan, C. (2006). "Analysis of monoethanolamine and its oxidative degradation products during CO2 absorption from flue gases: A comparative study of GC-MS, HPLC-RID, and CE-DAD analytical techniques and possible optimum combinations." Industrial & Engineering Chemistry Research, 45(8), 2437-2451.

Van Swaaij, W. P. M. and Versteeg, G. F. (1992). "Mass-Transfer Accompanied with Complex Reversible Chemical-Reactions in Gas-Liquid Systems - an Overview." Chemical Engineering Science, 47(13-14), 3181-3195.

Versteeg, G. F. and Van Swaaij, W. P. M. (1988). "Solubility and Diffusivity of Acid Gases (Co2, N2O) in Aqueous Alkanolamine Solutions." Journal of Chemical and Engineering Data, 33(1), 29-34.

Wang, R., Li, D. F. and Liang, D. T. (2004). "Modeling of CO2 capture by three typical amine solutions in hollow fiber membrane contactors." Chemical Engineering and Processing, 43(7), 849-856.

Weisstein, E. W. (2008). ""Circle Packing." From MathWorld-A Wolfram Web Resource - http://mathworld.wolfram.com/CirclePacking.htmlWeisstein." 2008.

Whalen, F. X., Bacon, D. R. and Smith, H. M. (2005). "Inhaled anesthetics: an historical overview." Best Practice Research Clinical Anaesthesiology, 19(3), 323-330.

Zhang, H. Y., Wang, R., Liang, D. T. and Tay, J. H. (2006). "Modeling and experimental study of CO2 absorption in a hollow fiber membrane contactor." Journal of Membrane Science, 279(1-2), 301-310.

Zhang, Q. and Cussler, E. L. (1985). "Microporous Hollow Fibers for Gas-Absorption .1. Mass-Transfer in the Liquid." Journal of Membrane Science, 23(3), 321-332.

5.A. Spatial discretization method

Equations in this appendix are written in their dimensional form to simplify understanding.

The hollow fiber membrane contactor was discretized as shown in Figure 5.A1 - both shell and fiber are divided in nj equally spaced intervals in the axial direction; the fiber lumen is also divided in the radial direction following a geometric progression:

$$r_k = \frac{1-0.85^{k-1}}{1-0.85^{nk-1}} R_{inner} \tag{B.1}$$

where nk is the number of finite volumes in the radial direction. It was found that 16 axial discretization points and 64 radial discretization points were sufficient to describe the problem.

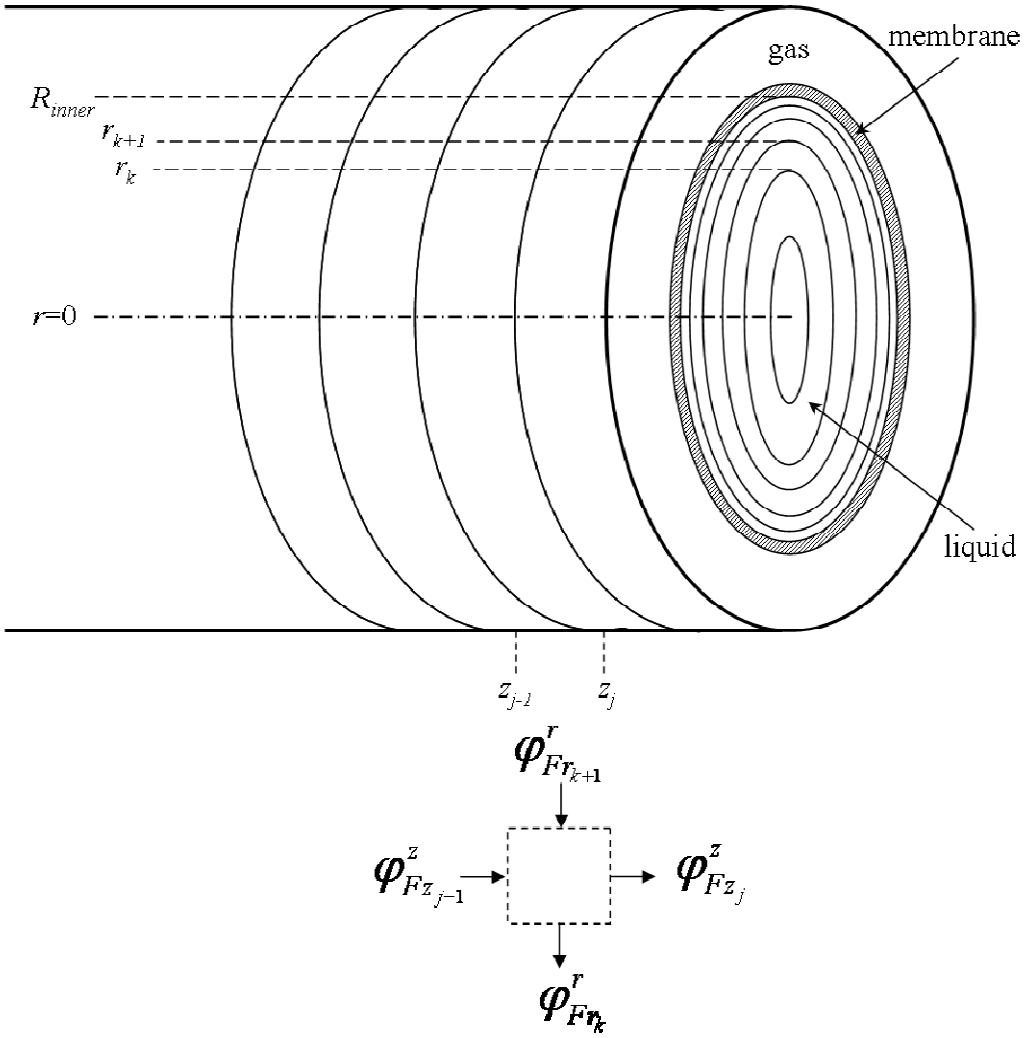

Figure 5.A1 – Schematic representation of the spatial discretization and cell mass balance.

For each cell and for each component i present in the system, the following mass balances can be written:

Liquid phase mass balance

$$\underbrace{\varphi^{z}_{Fz_{j-1}}\pi\left(r_{k+1}^{2}-r_{k}^{2}\right)}_{\text{what enters in axial direction}}+\underbrace{\varphi^{r}_{Fr_{k+1}}2\pi r_{k+1}\left(z_{j}-z_{j-1}\right)}_{\text{what enters in radial direction}}=$$

$$=\underbrace{\varphi^{z}_{Fz_{j}}\pi\left(r_{k+1}^{2}-r_{k}^{2}\right)}_{\text{what comes out in axial direction}}+\underbrace{\varphi^{r}_{Fr_{k}}2\pi r_{k}\left(z_{j}-z_{j-1}\right)}_{\text{what comes out in radial direction}}+ \qquad \text{(B.2)}$$

$$+\underbrace{\pi\left(r_{k+1}^{2}-r_{k}^{2}\right)\left(z_{j}-z_{j-1}\right)\frac{dC_{i,liq}}{dt}}_{\text{what accumulates in the element}}+\underbrace{\pi\left(r_{k+1}^{2}-r_{k}^{2}\right)\left(z_{j}-z_{j-1}\right)S_{i}}_{\text{what disapears upon reaction}}$$

According to the model assumptions, φ^{z}_{F} and φ^{r}_{F}, respectively, the axial and radial fluxes crossing the cell faces, are given by $\varphi^{z}_{F}=v_{F}C_{i,L,F}$ and $\varphi^{r}_{F}=D_{i}\left.\frac{dC_{i,L}}{dr}\right|_{F}$. Then, substituting in (B.2), the following equation results:

$$\frac{\partial C_{i,L}}{\partial t}=-\frac{v_{Fz_{j}}C_{i,L,Fz_{j}}-v_{Fz_{j-1}}C_{i,L,Fz_{j-1}}}{\left(z_{j}-z_{j-1}\right)}+2D_{i}\frac{r_{k+1}\left.\frac{\partial C_{i,L}}{\partial r}\right|_{Fr_{k+1}}-r_{k}\left.\frac{\partial C_{i,L}}{\partial r}\right|_{Fr_{k}}}{\left(r_{k+1}^{2}-r_{k}^{2}\right)}-S_{i} \qquad \text{(B.3)}$$

where $C_{i,L}$ is the concentration of i in the cell, $v_{Fz_{j-1}}$ and $v_{Fz_{j}}$ are the liquid velocities respectively in the upstream and downstream faces of the cell - in case of laminar flow $v_{Fz_{j}}=2\overline{v}\left(1-\frac{\left(r_{k+1}/R\right)^{2}+\left(r_{k}/R\right)^{2}}{2}\right)$, $C_{i,L,Fz_{j-1}}$ and $C_{i,L,Fz_{j}}$ are the concentrations of i respectively in the upstream and downstream faces of the cell and $\left.\frac{\partial C_{i,L}}{\partial r}\right|_{Fr_{k+1}}$ and $\left.\frac{\partial C_{i,L}}{\partial r}\right|_{Fr_{k}}$ are the concentration gradients, respectively in the outer and inner faces of the liquid cylindrical shell. Initial and axial boundary conditions of equation (B.3) are straightforwardly implemented: $t=0,\ C_{i,L}=C_{i,L,0}$ and $z=0,\ C_{i,L,Fz_{1}}=C_{i,L,\,feed}$. Concerning the radial boundary condition for the absorbing compounds, an infinitesimal volume, V_{inf}, with concentration $C_{i,m}$, was created in the fiber wall and a mass balance was performed in this volume:

$$\frac{\partial C_{i,m}}{\partial t}=\frac{2\pi R\left(z_{j}-z_{j-1}\right)}{V_{inf}}\left(N_{im}-D_{i}\left.\frac{\partial C_{i,L}}{\partial r}\right|_{Fr_{nk}}\right) \qquad \text{(B.4)}$$

where the flux through the membrane, $N_{i,m}$, is given by: $N_{i,m}=k_{i,ext}\left(C_{i,g}-C_{i,m}\right)$. The radial boundary condition of equation (B.3) then becomes: $r=R_{inner},\ C_{i,L,Fr_{nk}}=m_{i}C_{i,m}$

and the initial condition of equation (B.4) was set as: $t = 0,\ C_{i,m} = C_{i,L,0} / m_i$. This strategy considerably attenuates the numerical instability associated to the condition of fluxes equality in the interface.

Gas phase mass balances were computed equivalently, but only axial flux was considered $\left(\varphi_F^z = u_F C_{i,g,F}\right)$.

Part V

General Conclusions and Future Work

The present work aimed at studying the use of hollow fiber membrane contactors for CO_2 removal from anaesthetic gas streams by selective absorption.

The CO_2 removal from closed anaesthetic loops is currently achieved using mixtures of alkali hydroxides which, under desiccated conditions, react with the anaesthetic volatiles originating highly toxic compounds. In addition, this technique is associated to explosions due to the hydrogen formation and excessive heating during the reaction of these absorbents with CO_2. Furthermore, the exhaust containers of the absorbent mixtures are hospital solid waste. These reasons drive the need for replacing this absorption system with a safer and more environmentally friendly technology. The use of hollow fiber membrane contactors with renewable liquid absorbents is a possible strategy to overcome most of the pointed out drawbacks. Using dense and highly permeable membranes in such devices, the absorption system can be kept isolated from the anesthetic loop and aseptic operation is possible. The absorbent solution can be subsequently regenerated after contacting with CO_2.

Most of the present work was focussed on the study of absorbent solutions suitable for the intended application. Such solution must be biocompatible, chemically and thermally stable and have a low vapour pressure. Additionally, it must present high absorption and desorption kinetics and high absorption capacity and should be easy to regenerate. Aqueous solutions of alkali salts of amino acid are expected to fulfil these requirements and, therefore, two amino acid salts were characterized for CO_2 absorption: potassium glycinate (because glycine is the simplest amino acid, it has a relatively low cost and its molecular structure indicates high absorption kinetics) and potassium threonate (because its molecular structure envisioned better regeneration properties).

Following the absorbents characterization, the performance of the contactor for CO_2 removal from closed-loop anaesthesia was analysed by simulation, using the physico-chemical properties obtained for potassium glycinate. The use of hollow fiber absorbent

membrane contactors for the CO_2 removal from closed anaesthetic breathing circuits was proposed for the first time by our research group. The analysis performed in the present dissertation indicates that this technology is suitable. The absorbent regeneration process, however, still has to be studied in some detail.

Some relevant results obtained along the different phases of the work are described below.

Physical Properties Measurements

Densities and viscosities of potassium glycinate and potassium threonate aqueous solutions were measured for amino acid salt concentrations ranging from 0.1 to 3.0 M and temperatures from 293 to 313 K. For the concentration range analysed, the increase of density and viscosity are not likely to bring additional hydrodynamic concerns or pumping difficulties. However, for potassium threonate concentrations above 3.0 M and low temperatures, the solution viscosity might become too high for use in hollow fibre membrane modules.

Diffusion coefficients of N_2O and the amino acids salts in amino acid salts solutions were estimated using the modified Stokes Einstein relation. CO_2 diffusion coefficients were computed using the N_2O analogy.

To estimate the physical solubility of CO_2 in amino acid salts solutions, N_2O solubility was measured and the results interpreted using the Shumpe model. These measurements were performed for potassium glycinate and potassium threonate concentrations from 0.1 to 3.0 M and temperatures from 293 to 313 K.

Adsorption Kinetics Studies

The kinetics of the reactions of CO_2 with potassium glycinate and potassium threonate were determined using a stirred cell working semi-continuously with respect to the gas phase and batchwise with respect to the liquid phase. It was concluded that both amino

acid salts presented absorption rates towards CO_2 similar to alkanolamines. The results also indicate that the reaction rate significantly depends on the ionic strength of the solution. As expected, because of the molecular configuration, it was verified that potassium glycinate shows a faster absorption of CO_2 than potassium threonate.

The enhancement factor, and subsequently the overall kinetic constant, was computed using the DeCorsey equation. The apparent kinetic constant of potassium glycinate is in line with the Brønsted plot drawn for other amines, whereas the apparent kinetic constant for potassium threonate falls below the plot. This is likely to be due to the sterical hindrance of the amine group from threonate.

For potassium glycinate, the rate of absorption as a function of temperature and amino acid salt concentration, for the conditions studied, was found to be given by the following expression: $-r_{CO_2} = 2.42\times10^{16}\exp\left(\frac{-8544}{T}\right)\exp\left(0.44C_S\right)C_S C_{CO_2}$ $\mathrm{mol\cdot m^{-3}\cdot s^{-1}}$. Based on experimental diffusivity data recently published, this expression was later updated: $-r_{CO_2} = 3.28\times10^{16}\exp\left(\frac{-8636}{T}\right)\exp\left(0.36C_S\right)C_S C_{CO_2}$ $\mathrm{mol\cdot m^{-3}\cdot s^{-1}}$. The absorption rate as a function of the temperature and concentration found for potassium threonate was: $-r_{CO_2} = 4.13\times10^{8}\exp\left(\frac{-3580}{T}\right)\exp\left(0.90C_S\right)C_S\, C_{CO_2}$ $\mathrm{mol\cdot m^{-3}\cdot s^{-1}}$.

Adsorption Equilibrium Studies

CO_2 solubility in potassium glycinate aqueous solutions with concentrations from 0.1 to 3.0 M and temperatures from 293 to 351 K was determined in a stirred cell. CO_2 solubility in a 1.0 M solution of potassium threonate was also measured at 313 K.

Potassium glycinate showed absorption capacities towards CO_2 (expressed in terms of $\mathrm{mol_{CO_2}\cdot mol_{AmA}^{-1}}$) similar to monoethanolamine. On the other hand, potassium threonate showed a considerably lower CO_2 absorption capacity. This can be assigned to the

sterical hindrance of the threonate amine group (higher K_{carb}) along with the lower pK_A (then higher K_{AmA}).

Potassium glycinate did not show significant change on the CO_2 solubility for temperatures between 293 and 323 K. This result is somehow surprising and is a sign of potential problems in the regeneration of the absorbent solutions.

The Deshmukh-Mather and the Kent-Eisenberg models were used to interpret the equilibrium results. Although the predictions of both models significantly deviate from the experimental results, they prove to qualitatively describe the system. These models are particularly useful to provide the composition of the solutions (speciation) as a function of loading and temperature. Speciation enables the prediction of CO_2 absorption rates in partially loaded solutions likely to take place in absorption/desorption cycles.

No precipitation was observed for any of the solutions of potassium glycinate and potassium threonate studied, which indicates that these are suitable for hollow fiber membrane contactors, even if porous membranes are to be used.

Hollow Fiber Membrane Contactor Simulation

A coupled differential model for both gas and liquid phases was proposed to simulate the mass transfer accompanied by chemical reaction, occurring during the absorption of CO_2 into amino acid salt solutions flowing through a hollow fiber membrane contactor. The model considered the liquid flowing in the fiber lumen and the gas in the shell side. Both co- and counter-current operations were considered.

The developed model enables to assess the radial and axial concentration profiles in the liquid and the axial velocity and concentration profiles in the gas.

Model results were compared to results obtained with conventional mass transfer models valid for limit conditions and good agreement was found.

The performance of a hollow fiber membrane contactor for CO_2 removal from anaesthesia closed-loops was analysed. For this analysis, composite PDMS membranes were assumed and aqueous solutions of potassium glycinate were considered as absorbents. The physical, kinetic and equilibrium data experimentally obtained for potassium glycinate were used in the simulations.

The influence of the design parameters packing density, contactor length and shell diameter and of the operation parameters liquid flow rate and reactant feed concentration, on the CO_2 molar fraction exiting the contactor were studied. Based on this study, a contactor with 5 cm shell diameter and 12.5 cm length, with a 3 M solution of potassium glycinate flowing at 10 $mL \cdot min^{-1}$, counter-currently with respect to the gas was found to be suitable for the CO_2 removal from closed anaesthetic breathing circuits. A contactor with these dimensions would be easily retrofitted into a common anaesthesia machine (note that common soda lime canisters have 1.5 L).

Suggestions for Future Work

Literature information about amino acid salts as CO_2 absorbents is still scarce, although it keeps increasing due to their potential application to flue gas treatment. A more comprehensive data set is needed, namely concerning physical properties (such as diffusion coefficients and physical solubility) and equilibrium and kinetics data. This will allow for a more consistent implementation of the data analysis proposed in the present work. Furthermore, it may serve as a basis for more complex and accurate models.

In particular, there is a lack of information in the open literature concerning the regeneration of the absorbent solutions. After absorbing CO_2, the solution should be regenerated (possibly in another device) and used again for absorption. Therefore, it is the cyclic performance of the solution which will define the viability of the global process. Additionally, the regeneration is usually performed at high temperatures,

making this step critical in what concerns energy consumption. For these reasons, research on the regeneration subject is suggested for future work.

Pursuing this suggestion, measurements of all properties at higher temperatures are strongly recommended, since the studies of the CO_2 absorption in amino acid salts performed so far were limited to a relatively narrow temperature interval when compared to the conditions expected to be found in cyclic absorption/regeneration processes. Moreover, a method to determine the CO_2 desorption kinetics should be developed.

Concerning the specific application studied in the present work, CO_2 removal from anaesthetic gaseous circuits, it is suggested to perform multi component experiments with gaseous mixtures similar to the ones present in real anaesthesia. In particular, these mixtures should include the halogenated anaesthetics, in order to check the effect of these compounds in the absorbent solutions as well as in the membrane materials.

Finally, the complete cyclic process should be simulated, experimentally validated and further optimized for the required separations.

Appendix A

Details on the Experimental Setups Used

Details on the Experimental Setups Used

Some considerations on the setups used in the experimental work, which are not detailed in the papers, are presented next.

All the experiments concerning potassium glycinate (apart the viscosity measurements) were performed in the OOIP Group of the Department of Development and Design of Industrial Processes in the Twente University, Enschede, The Netherlands. The setup used for the physical solubility and kinetics measurements is presented in Figures A1 and A2. Descriptions of the experimental procedures are presented in Chapter 2.

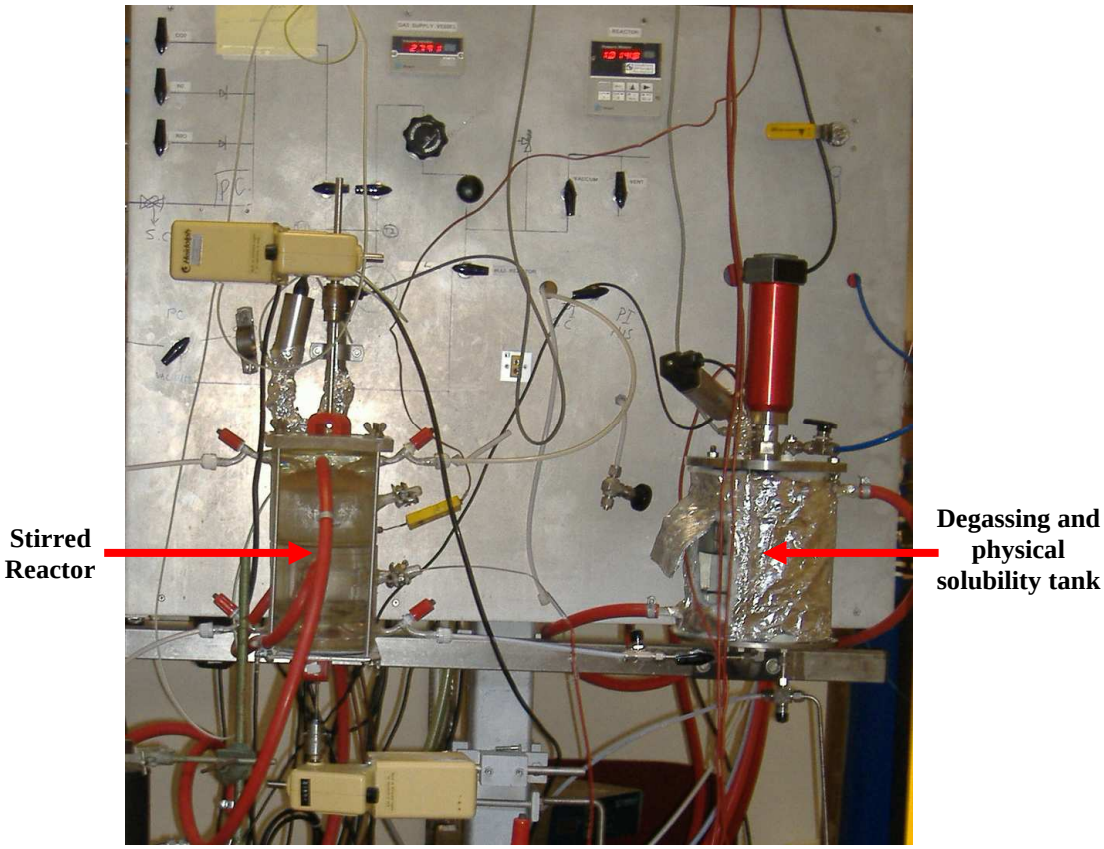

Figure A1 – Setup used for the physical absorption and kinetics measurements of CO_2 in potassium glycinate (Chapter 2) - the gas vessel and pressure controller are located behind the panel.

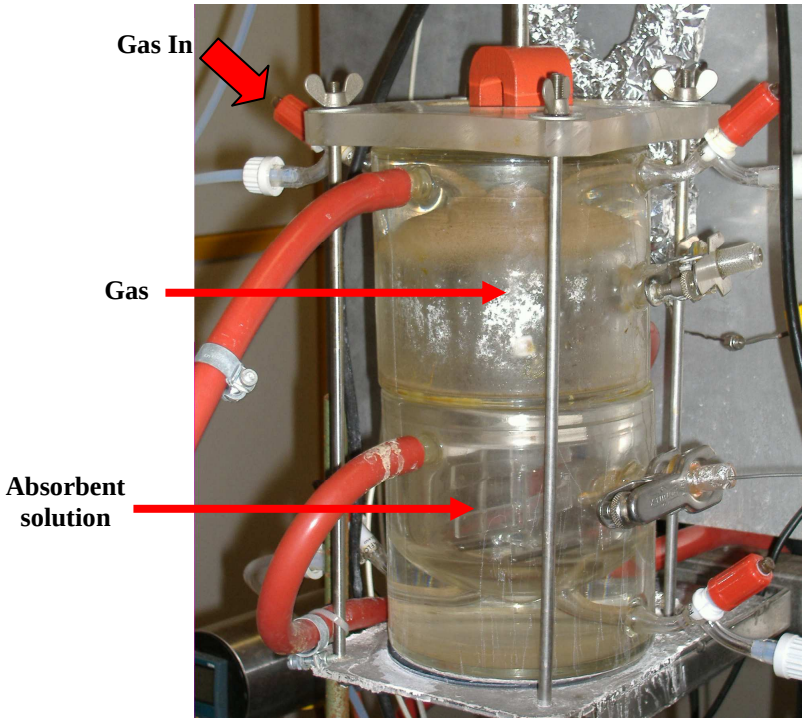

Figure A2 – Detail of the setup - stirred reactor (liquid volume: 600 cm^3, reactor diameter: 9.09 cm).

For the characterization of potassium threonate (Chapter 3), an apparatus with similar functioning but with smaller dimensions (about 12 times smaller than the one used for Chapter 2) was built in LEPAE - Laboratory for Process, Environmental and Energy, in the Department of Chemical Engineering from the University of Porto. The setup, designed and assembled by the author of this thesis, is shown in Figure A3.

The main advantage of using a reactor with smaller dimensions is that less reactant is necessary for the experimental measurements. This makes the characterization more economic and pursues the objective of characterizing non-commercially available absorbents (although around 1 kg of absorbent is still needed for a reasonable characterization). On the other hand, eventual experimental error sources (including leaking, dead volumes, presence of solution drops in the reactor walls, among others) have a much more noticeable effect on experimental results. To check the accuracy of the setup assembled, results obtained for a 1 M solution of potassium glycinate at 298 K were compared with these obtained with the setup used in Chapter 2. Figure A4 shows the absorption flux as a function of the CO_2 partial pressure obtained using the setups shown in Figures A1 and A3.

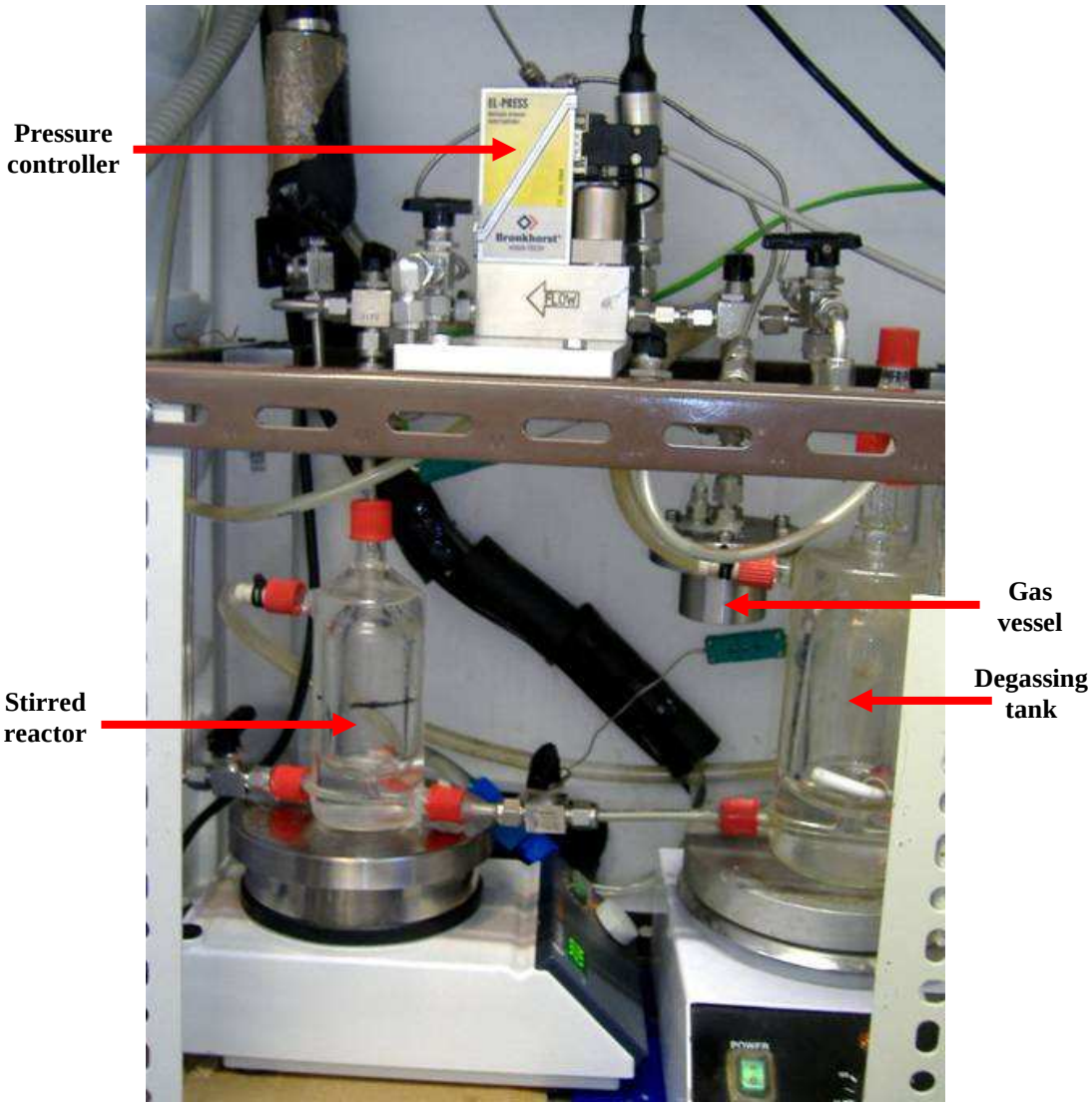

Figure A3 - Setup used for the determination of the physical absorption and reaction kinetics of CO_2 in potassium threonate (Chapter 3) and for the equilibrium measurements of CO_2 in potassium glycinate (Chapter 4) - liquid volume: 50 cm^3, reactor diameter: 3.87 cm.

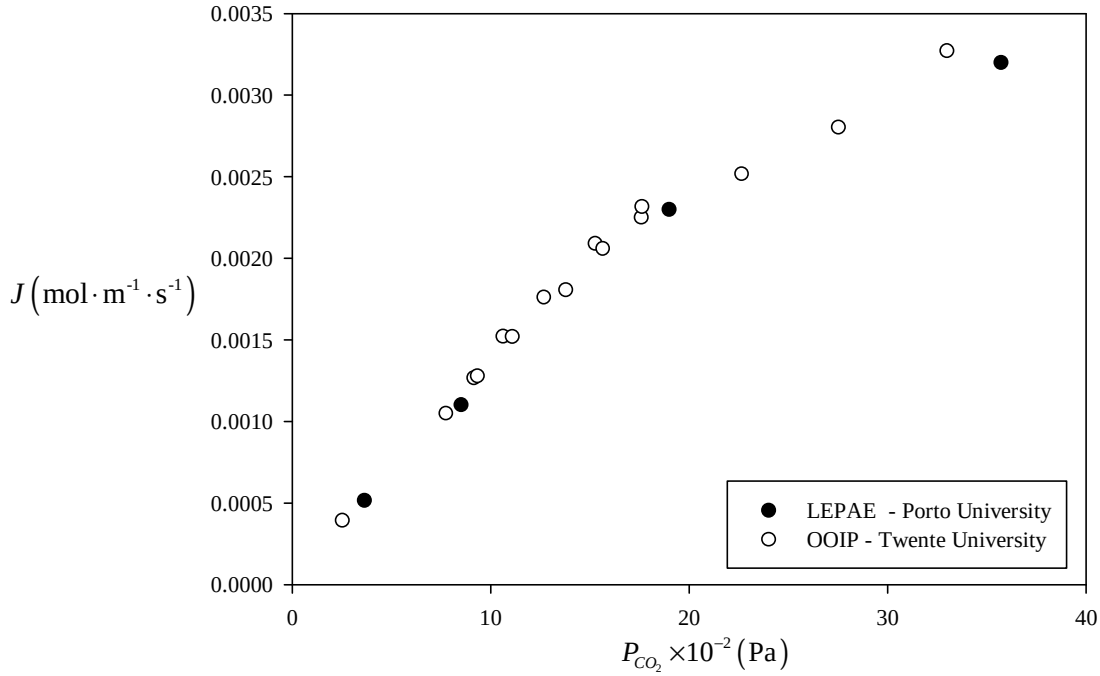

Figure A4 – Comparison of the experimental results obtained using the setup at Porto University and using the setup from Twente University.

The setup shown in Figure A3 was also used to perform the experiments presented in Part III (Chapter 4).